Towards better understanding of Respiratory Syncytial Virus (RSV) vaccine-induced enhanced disease

Abenaya Muralidharan

Thesis submitted to the Faculty of Graduate and Postdoctoral Studies

In partial fulfillment of the requirements for the degree of doctor of Philosophy

Department of Biochemistry, Microbiology, and Immunology

Faculty of Medicine

University of Ottawa

© Abenaya Muralidharan, Ottawa, Canada, 2019

ABSTRACT

Respiratory Syncytial Virus (RSV) infects almost all children under the age of one and is the leading cause of hospitalization among infants. Despite several decades of research, there is no licensed vaccine available to date whereas inactivated vaccines have been shown to induce severe adverse reaction in a clinical trial, with other forms of RSV vaccine also found to induce enhanced respiratory disease (ERD) in preclinical animal studies. Here, three novel facets of ERD were identified.

First, RSV fusion protein (F) was fused with CD40 ligand and delivered by an adenoviral vector into BALB/c mice. In contrast to an inactivated vaccine, the vectored vaccine effectively protected animals against RSV without inducing ERD. This protection involved a robust induction of neutralizing antibodies and memory CD8 T cells, which were not observed in the ERD-inducing inactivated vaccine group.

Second, the mRNA of programmed cell death-1 (PD-1) of *Sigmodon hispidus* or cotton rat was isolated, sequenced and the protein was characterized. *Sigmodon hispidus* is an excellent animal model for studying human infections of respiratory viruses including RSV. While arguably the cotton rat is the best small animal model for evaluation of RSV vaccine and antivirals, many important genes of the immune system remain to be isolated. Programmed cell death-1 (PD-1) plays an integral role in regulating many aspects of immunity by inducing suppressive signals. Using the isolated and characterized cotton rat PD-1 gene sequence, I observed decreased levels of PD-1 in cotton rats experiencing ERD induced by inactivated RSV vaccine, unraveling a new facet of vaccine-induced disease.

Third, chitosan, a polysaccharide capable of augmenting immune responses with a proven safety record in animals and humans, was investigated to determine whether chitosan alone could protect animals against RSV infection and whether it could alter immune responses or immunopathology induced by inactivated RSV vaccine. Chitosan alone was found to modestly protect animals against RSV infection, while, in conjunction with inactivated RSV vaccine, it could significantly reduce RSV infection in mice. Further mechanistic investigation revealed that chitosan enhanced inactivated RSV vaccine-elicited immune responses through augmenting the induction of regulatory T cells, lung resident T cells and neutralizing antibodies while reversing Th2-skewed immune responses induced by inactivated RSV vaccine. These finding indicate ERD development has a different functional pathway from chitosan-mediated immune protection.

ACKNOWLEDGEMENTS

First, I would like to express my sincere gratitude to my supervisor Dr. Sean Li for his guidance and encouragement. Without his mentorship and the scientific freedom he provided, I could not have realized my true potential for research. He was always there for me when I needed advice and support. I am truly privileged for the opportunity to learn from him and work with him. I could not have asked for a better supervisor! Hope our scientific discussions continue and we can work together again in the future.

I would like to extend my sincere thanks to my co-supervisor, Dr. Lisheng Wang and my thesis advisory committee, Dr. Jessie Lavoie, Dr. Terry Cyr and Dr. Aaron Farnsworth for their valuable suggestions, support and guidance. Their constructive criticism and discussions helped me stay on track in my research and achieve my end goal efficiently.

I am eternally grateful to my wonderful lab mates and friends, Caroline Gravel, Marsha Russell, Louise Larocque and Bozena Jaentschke for a stimulating environment and technical assistance. They were always there to help when I needed it. Their motivation, dedication and positivity are inspiring. My research would be incomplete without their invaluable help and input.

A special thank you to Dr. Martha Navarro and all the staff at the animal care facility at Health Canada for their excellent assistance with all the animal experiments. They were very accommodating and helpful. Thank you to Emily Dupuis for her help with flow cytometry.

I would like to acknowledge all the research collaborators whose experience and knowledge helped me fine-tune my work and publications. I would also like to thank everybody at the Centre for Biologics Evaluation at Health Canada for the stimulating discussions and contributions to my research. Not only did they advance my knowledge but their humor and warmth also made it a wonderful place to work.

Thank you to CIHR, OGS and University of Ottawa for granting me scholarships for pursuing my graduate studies.

I am forever grateful to my parents for their unwavering love, patience and support throughout my life. I am greatly indebted to them for all the sacrifices they have made to give me the future I desired. Their constant encouragement to pursue my dreams and always showing up when I need them is the true reason behind my success in every aspect of my life. They taught me that I can do anything I put my mind to and led by example with their hard work. I hope I have made them proud.

Last but not the least, I am extremely lucky to have my husband Arun in my life. Without his support and patience, the past few years would have been very difficult. He was there to patiently listen about my good and bad days. His strong yet calming presence makes tough days easier. Thank you for your unfaltering love and understanding.

DEDICATION

To my loving parents and husband, my strong pillars of support

I couldn't have done this without you.

TABLE OF CONTENTS

LIST OF ABBREVIATIONS

A	Adenine
aa	Amino acids
Ad-Empty	Recombinant adenovirus empty control vector
Ad-SF	Recombinant adenovirus expressing secreted RSV F protein
Ad-SF40L	Recombinant adenovirus expressing secreted RSV F-CD40L fusion protein
ANOVA	Analysis of Variance
APC	Antigen presenting cells
ATCC	American Type Culture Collection
bp	Base pairs
BSA	Bovine serum albumin
C terminal	Carboxyl-terminal
CD40L	CD40 ligand
cDNA	Complementary DNA
crPD-1	Cotton rat PD-1
DC	Dendritic cell
DMEM	Dulbecco's modified Eagle's medium
DNA	Deoxyribonucleic acid
eIF	Eukaryotic translation initiation factor
ELISA	Enzyme linked immunosorbent assay
ERD	Enhanced respiratory disease
F	RSV fusion protein
FACS	Fluorescence-activated cell sorting
FBS	Fetal bovine serum
FDA	Food and Drug Administration
FI-Mock	Formaldehyde-inactivated mock infection control
FIRSV	Formaldehyde-inactivated RSV
G	RSV attachment protein
GC	Germinal center
GFP	Green fluorescent protein
H&E	Hematoxylin and eosin
HEK-293	Human Embryonic Kidney-293 cells
HeLa	Human epithelial cells
Hep-2	Human epithelial type 2 cells
His	Histidine
HPE	Hematoxylin-Phloxine-Eosin stain
HRA	Heptad repeat connected to the fusion peptide of RSV F protein
HRB	Heptad repeat connected to the transmembrane domain of RSV F protein
ICAM	Intracellular adhesion molecule
IFN	Interferon

Ig	Immunoglobulin
IL	Interleukin
kb	Kilobases
kDa	Kilodalton
L	RSV polymerase protein
M	RSV matrix protein
M2-1	RSV transcription processivity factor
M2-2	RSV RNA transcription/replication regulating protein
ml	Millilitre
mRNA	Messenger RNA
N	RSV nucleoprotein
N terminal	Amino-terminal
nm	Nanometer
NS1 and NS2	RSV nonstructural proteins
nt	Nucleotide
P	RSV phosphoprotein
PAS	Periodic acid schiff stain
PBMC	Peripheral blood mononuclear cells
PBS	Phosphate buffered saline
PD-1	Programmed cell death receptor
PD-L	Programmed cell death ligand
PFU	Plaque forming units
PKR	Protein kinase R
RFP	Red fluorescent protein
rmPD-1	Recombinant mouse PD-1
RNA	Ribonucleic acid
RSV	Respiratory syncytial virus
SH	RSV small hydrophobic protein
SIGN	Specific intercellular adhesion molecule-3-grabbing non-integrin
Th	Helper T cells
TLR	Toll-like receptor
TNF	Tumor necrosis factor
Tregs	Regulatory T cells
TTP	Tristetraprolin
U	Uracil
USD	United States of America Dollars
WHO	World Heath Organization
µg	Microgram
µm	Micrometer

LIST OF FIGURES AND TABLES

Chapter 1: General Introduction

1. Respiratory Syncytial Virus (RSV)

1.1 Pathogenesis and Epidemiology

RSV was first isolated in 1955. It was found to cause disease that can be mild to lethal with a wide range of acute upper and lower respiratory tract disease manifestations such as mild rhinitis to bronchiolitis and pneumonia (1). Symptomatic RSV infection is most commonly observed in children under the age of 5, immunocompromised individuals, and the elderly. Approximately 33.1 million new RSV-associated lower respiratory tract infection cases were reported globally in children in 2015 (2). In the USA, up to 172,000 RSV-related hospitalizations and 2.1 million outpatient visits were reported annually among children under the age of 5 and an annual average of 36 RSV-related deaths among children less than 1 year of age (3–8). RSV accounts for 60-80% of bronchiolitis in USA, mainly for children less than 1 year old, and is the major cause of viral bronchiolitis and bronchopneumonia (9). Severe RSV disease at infancy can lead to airway hyperreactivity during childhood, which may last until adulthood, whereas in immunocompromised patients, severe disease leads to giant cell pneumonia and in the elderly, exacerbation of underlying conditions and death (1). Some factors that can affect the severity of RSV disease are premature birth, frail old age, chronic lung or heart disease, immunosuppression, and narrow or reactive airways.

A notable feature of RSV is its ability to repeatedly infect RSV-seropositive individuals. Reinfections have been documented in both children and adults; within 3 years, 30% of children are estimated to have RSV reinfections (10). Although relatively mild, repeated

RSV infections are also common in healthy adults (11). This suggests that natural infections give rise to insufficient immunity (12). Antibody levels induced by a primary infection has been observed to reduce to pre-infection levels after 3 to 6 months (13, 14).

1.2 Tropism

Humans and bovines are the only natural hosts of RSV and can be infected with human RSV and bovine RSV strains, respectively. However, there are many animal models such as mice, cotton rats, sheep and African green monkeys that are semi-permissive to human RSV strains but transmission within the same species does not occur (1). In these animals, RSV can be found in nasal secretions, nasopharyngeal swabs, lung washes and the sinuses, whereas humans and bovines infected with their natural strains have virus in the epithelial cells of the trachea, bronchi and bronchioles. Even though RSV RNA and antigens have been detected in the blood, circulating mononuclear leukocytes, and in few cases, in the cerebrospinal fluid of infected humans, infectious virus has rarely been found in extrapulmonary sites with the exception of immune suppressed individuals and animal models (15–17). Chimpanzees are the only animal hosts where human RSV can infect and replicate to levels allowing intra-species transmission and respiratory tract disease manifestations (1). Primates are also susceptible to bovine RSV but virus replication is severely restricted (18, 19).

1.3 Genome

RSV has a single-stranded nonsegmented negative sense RNA genome with size of 15 kb. This genome consists of 10 genes encoding 11 proteins: 3’-NS1-NS2-N-P-M-SH-G-F-M2-L-

5’ (20). The M2 gene has two separate overlapping ORFs and encodes M2-1 and M2-2 protein (21). NS1 and NS2 are nonstructural proteins and nucleoprotein (N), phosphoprotein (P), and transcription processivity factor (M2-1) serve as nucleocapsid proteins. L is the large polymerase protein, M is the matrix protein and M2-2 is a RNA transcription/replication regulating protein while fusion (F), attachment (G) and small hydrophobic (SH) are surface glycoproteins. These proteins are further discussed below. Viruses belonging to the same subfamily as RSV, *Paramyxoviridae*, have orthologs of N, P, M, F and L proteins conserving their order in the genome though counterparts of the other 6 proteins are not present (1).

In the genome structure, there is a 44-nucleotide (nt) leader region on the 3’ end before the NS1 gene and a 155 nt trailer region on the 5’ end following the L gene. The genome also possesses a highly conserved 9 nt gene start signal at the beginning of each gene and a moderately conserved 12-14 nt gene end signal at the end of each gene. The gene end signal contains 4-7 uracil (U) residues at the end encoding the poly A tail. Furthermore, there are intergenic regions separating the first 9 genes that can vary in length from 1 to 58 nt depending on the RSV strain (1). However, unlike the gene start and end signals, these regions are poorly conserved. The only known function of the intergenic regions is the importance of the first nucleotide in the region for mRNA termination. Apart from that role, these regions have been shown to have little effect on gene expression or viral replication (22, 23). In addition, there is no intergenic region between the M2 and L genes since the gene start of L is 68 nt upstream of the M2 gene resulting in a 68 nt overlap (24).

Remarkably, neither the genome nor the antigenome have a 5’ cap or 3’ poly A tail but their degradation is not quick. This is because the N protein coats the genome and antigenome

forming a nucleopcapsid protecting the RNA from degradation and recognition by the host cell pattern recognition receptors impeding the initiation of innate immune responses (1).

1.4 Classification and Homology

RSV belongs to the Genus *Pneumovirus*, subfamily *Pneumovirinae*, family *Paramyxoviridae*, and order *Mononegavirales*. Human RSV can be divided into two subgroups, RSV A and B that show divergence in the amino acid sequence of all the 11 encoded proteins. The two antigenic subgroups only share 53% homology within the surface G protein and therefore, are distinguished mainly by their G protein sequence (1). With the exception of the SH and M2-2 protein sharing 76% and 72% identity between the subgroups, respectively, the remaining 8 proteins encoded by the genome are about 90% conserved. Notably, bovine RSV also shares more than 80% identity with RSV A in all but 4 proteins, NS1, SH, G and M2-2 with 69%, 38%, 30% and 42% identity, respectively (1).

1.5 Structure and Morphology

RSV was difficult to characterize when it was first isolated due to its inefficient growth in cell culture, cell-associated nature and physical instability (1). However, with technological advancements, the structure and morphology of the virus has been deduced. RSV virions consist of a nucleocapsid in a lipid envelope that is derived from the host cell membrane. On the inner face of the envelope, the matrix M protein can be found. Surface glycoproteins, F, G and SH, form homo-oligomers forming short surface spikes that can be 11-16 nm in length

(1). In cell culture, RSV virions can either assume a spherical shape of 100-350 nm in diameter or be long filaments of 60-200 nm in diameter and 10 μm in length (25). Majority of the progeny virus remains cell-associated, which can look like the virus has failed to bud but this allows the virus to form its characteristic syncytia (1).

1.6 Viral Proteins and Functions

1.6.1 F Protein

The fusion (F) protein is a type I integral membrane protein that is 574 amino acids (aa) long (26). It directs viral penetration into the host cell and syncytium formation. It is synthesized as an inactive F0 precursor, which assembles into a trimer and passes through the golgi (1, 27, 28). The F0 is readily cleaved and activated by intracellular furin-like proteases in the golgi to yield F1, which is the larger C-terminal product, and F2, the N-terminal product, that are linked by two disulfide bond (1, 29, 30). Since the F has two cleavage sites, one after aa136 and one after aa109, there is a 27 aa segment in the middle called pep27 that dissociates after cleavage (31–33). The N-terminus of the F1 subunit is the fusion peptide that is a stretch of hydrophobic residues that insert into the target membrane (26). The accessible surface location, vital role in RSV entry, and high conservation rate among RSV isolates in both A and B subgroups make the F protein an ideal target for neutralizing antibodies (34, 35). Indeed, many neutralizing epitopes have been identified on F; it is the target for the only prophylactic treatment available for RSV named Palivizumab (discussed in detail below) (36, 37). Furthermore, the conformational changes it undergoes in order to

allow viral fusion with the host cell membrane also make F a great target for antiviral development (38).

In the prefusion form of the F protein, each monomer is divided into two lobes separated by a 7-strand anti-parallel barrel. Two of those strands connect through hydrogen bonds and make up portions of the two lobes and a central barrel. Each lobe contains the F2 and F1 subunits (39). The F2 subunit starts in the membrane-proximal lobe and then extends through the central barrel and into the membrane-distal lobe. The N-terminus of F1 that has the fusion peptide is buried in the central trimer cavity and is connected to two perpendicular helices followed by a β-hairpin and another helix. The fusion peptide along with these secondary structures undergoes dramatic conformational changes upon switch to postfusion state by refolding into a single α-helix (39). The C-terminus of F1 also undergoes a drastic conformational change that swings the heptad repeat connected to the transmembrane domain (HRB) around the molecule bringing it near the heptad repeat connected to the fusion peptide (HRA) to complete the 6-helix bundle observed in the postfusion state (39).

During the transition from the prefusion to the postfusion state, the F protein attains an intermediate structure, which is a fully extended unstable transient state. At this stage, the viral and cell membranes are parallel after the insertion of the F protein into both membranes. Then, the F folds at its centre and brings the viral membrane closer to the host membrane. The hairpin 6-helix bundle structure of the postfusion state forms, merging the membranes to initiate membrane fusion. Indeed, interfering with the formation of this helix bundle can inhibit viral fusion (39).

Following cleavage of F0 at the furin sites, F protein forms organized aggregates or "rosettes" (40). These rosettes are a direct result of aggregation of the exposed hydrophobic fusion peptide as deleting the first 10 aa in the fusion peptide prevented rosette formation (41). This form of F has a globular head with an extended stalk where the head contains both the F2 and F1 subunits along with a cysteine rich region and has both α-helices and β-sheets. The stalk region is composed of hairpin 6-helix bundle that is made of three heptad repeat coiled-coils in the center with another three anti-parallel heptad repeat helices on the outside. Folding to the postfusion conformation brings the N and C terminals of F1 close to each other forming a stable structure that brings the viral and host membranes together initiating a non-reversible fusion process (42, 43).

1.6.2 G Protein

The attachment (G) protein is 298 aa long RSV surface glycoprotein. It has a membrane anchor near the N-terminus and two-thirds of the C-terminal is external. Unlike the other RSV surface proteins, G is also produced as a secreted form, which accounts for 80% of released G (44). Translation of the G gene initiates at the second start codon in the ORF followed by proteolytic trimming forming the secreted G protein that lacks the membrane anchor (1). The ectodomain of G has two large divergent domains that have high variability in the aa sequence among RSV strains flanking a short conserved segment. Although highly conserved, deletion of the segment does not affect viral replication *in vitro* and in mice (45). Interestingly, studies have found that deletions in the G protein or its absence do not render the virus replication deficient (46, 47) but the G protein is required for efficient infection of primary well-differentiated human airway epithelial cultures (48).

Even though the G protein is not essential for infection, it plays many vital roles in helping the virus evade host immunity. The protein contains a CX3C motif for structural stability that happens to mimic the CX3C chemokine fractalkine that functions to reduce the influx of immune cells into the lungs of RSV-infected mice (49). Secondly, secreted G interferes with antibody-mediated and Fc receptor-bearing cells-mediated virus neutralization by tricking the immune system into neutralizing it instead of the virus (50). Antigen presentation can also be altered by the G protein through interaction with DC-SIGN on dendritic cells (DCs) (51). Finally, the central conserved regions in G inhibit the activation of several TLRs including TLR-4 counteracting its activation by the F protein (52).

1.6.3 SH Protein

The small hydrophobic (SH) protein is a transmembrane protein that is 64 aa long. It forms pentameric pore-like structures with cation selective channel like activity (53, 54). However, the importance of this activity for RSV infection and replication is unclear. Some studies postulate the role of the SH protein in affecting membrane permeability, virus budding and apoptosis but these were not confirmed. The SH protein has also been shown to inhibit TNF-α signalling (55). However, minimal attenuation of RSV *in vivo* and no effect *in vitro* were observed upon SH deletion (56).

1.6.4 M Protein

The 256 aa matrix (M) protein has been shown to have multiple functions. First, it is vital for RSV morphogenesis. As the virion goes from its spherical to filamentous form, which is thought to be the precursor to infectious virus, the M protein plays a key role in aiding the virion attaining its mature form. In fact, the absence of the M protein results in immature

viral filaments (57). Second, in the early stages of RSV infection, the M protein may modestly inhibit host transcription in the nucleus. Third, in the later stages of infection, the protein has been observed to associate with cytoplasmic viral inclusion bodies, which are the site of RNA synthesis, and the host plasma membrane, which is the site of virion formation (58). It was later found to be required for the transport of nucleocapsids from the viral inclusion bodies to the plasma membrane (57). The loss of this transport function may be the reason for the formation of immature viral filaments in an M deleted mutant RSV.

1.6.5 N Protein

The nucleoprotein (N) is 391 aa long and binds the genome and antigenome. This binding forms nucleocapsids and become templates for RNA synthesis (1). In addition to its function in promoting viral replication by creating stable templates for genome replication, the N protein also has an important role in suppressing host antiviral responses. RSV N protein binds double stranded RNA-regulating protein kinase R (PKR), which prevents PKR from phosphorylating its substrate, eIF-2a (59). PKR, upon activation, is known to inhibit cellular mRNA translation leading to loss of viral protein synthesis, activation of inflammatory pathways, increase in interferons and induction of cellular apoptosis. All of these downstream functions of PKR can impede viral replication but is inhibited by the N protein counteracting host innate immunity (59).

1.6.6 P Protein

The phosphoprotein (P), which is 241 aa long, is heavily phosphorylated. Its activities, therefore, depend on the dynamics of the amount and rate of phosphorylation (60–62). The P protein plays many roles during RSV replication. First, it is an essential co-factor for the

polymerase (L) acting as an adapter by binding the N, M2-1 and L proteins to mediate the interactions in the nucleocapsid/polymerase complex (63). Second, the P protein allows the N protein to bind specifically to viral RNA by binding free N and delivering it to nascent genomes and antigenomes. This not only prevents binding of non-viral RNA but prevents self-aggregation of N (63). Finally, during uncoating of the virion, P dissociates the M protein from the nucleocapsid allowing initiation of infection (62). In fact, knockdown of the phosphorylation of P reduced RSV replication (64).

1.6.7 L Protein

The polymerase (L) protein is the largest of protein encoded by the RSV genome with 2,165 aa length. Among the viruses belonging to the same order as RSV, *Mononegavirales*, segments in the L protein thought to be the catalytic domains for polymerization are well conserved (1). Although extensive characterization of this protein has not been done, preliminary findings show the presence of residues affecting the efficiency of gene end signal recognition (65), putative nucleotide-binding sites involved in capping (66), and polymerization domains (67).

1.6.8 M2-1 Protein

M2-1 is a 194 aa essential transcription processivity factor (68–70). It has been shown to bind RNA and also interact with the P protein, which are essential interactions for M2-1 to support RNA synthesis; P is displaced from the nucleocapsid once it delivers M2-1 (71–73). Furthermore, M2-1 binds the M protein and mediates its transport to the inclusion bodies and interaction with the nucleocapsid (74). Studies based on structural analysis of the protein suggest that the ability of M2-1 to bind RNA may not be preferential to viral RNA. M2-1 has

a zinc finger motif that resembles a family of cellular zinc finger proteins like tristetraprolin (TTP), which is known to bind host response mRNAs including cytokine mRNAs affecting their stability. Similarly, M2-1 was shown to associate with cell stress granules involved in translation regulation under stress but the significance of this is unclear (75).

1.6.9 M2-2 Protein

M2-2 protein of RSV has two start sites 2 aa apart resulting a protein that can be either 88 or 90 aa in length (76). It plays a role in regulating RNA synthesis during infection but is expressed at low levels in the infected cells. Deleting M2-2 resulted in a virus with delayed and reduced RNA replication accompanied by increase levels of RNA transcription (77). In later stages of infection, transcription must be downregulated to allow for RNA synthesis and packaging of the genome into progeny virions. Therefore, the increased transcription in M2-2 deleted mutants suggests that M2-2 plays a role in regulating RNA synthesis by reducing transcription. Indeed, the replication in M2-2 deleted RSV is restricted 500-1000 fold compared to wild type in mice and chimpanzees (77, 78).

1.6.10 NS1 and NS2 Proteins

NS1 and NS2 are nonstructural proteins of 139 aa and 124 aa length, respectively. They can function independent of each other but are commonly observed as complexes functioning synergistically. However, the synergistic effects are poorly understood (79, 80). NS1 and NS2 play roles in ensuring viral survival by evading host immune responses and inhibiting cell apoptosis (79–81). They prevent the accumulation of viral double stranded RNA by downregulating viral transcription and RNA replication preventing the activation of innate immune responses (82). Moreover, NS1 and NS2 have been shown to interfere with

interferon induction and signalling (79, 80). Indeed, NS1 and/or NS2 deleted RSV has increased sensitivity to interferon, increased cell apoptosis and reduced replication *in vitro* and *in vivo*, although deleting NS1 has greater effect (56, 78).

1.7 Viral Replication

RSV follows similar replication cycle as other viruses in its order *Mononegavirales* (1). First, entry occurs by fusion of the viral envelope with the cell plasma membrane following which genome transcription and replication occurs in the host cytoplasm. Looking at other viruses in its family, nucleocapsids then begin transcription using the preexisting polymerase (L). RNA replication products are coated with newly synthesized N and P proteins to promote elongation forming full-length encapsidated genomes and antigenomes. These genomes are then concurrently transcribed and replicated (1). Studies show detection of mRNAs and proteins 4 to 6 hours post infection, which reach peak accumulation by 15 to 20 hours. At this time, M2-2 mediated downregulation of transcription and increase of RNA replication occurs allowing genome production for packaging of progeny virions (77). In the meantime, at 10 to 12 hours post infection, release of progeny begins. This release peaks at 24 hours and continues until the cells deteriorate by 30 to 48 hours. Furthermore, at 12 hours post infection, large cytoplasmic inclusion bodies become evident in the infected cells (83, 84). Viral N, P, M2-1 and L proteins are present in the inclusion bodies, which are sites for RNA synthesis. In addition, these inclusion bodies seem to sequester key cell signalling components, thereby, inhibiting host cell responses such as pathways involved in interferon induction (84), stress responses, and stress granule formation (75). Lastly, RSV assembly

and budding occurs at the plasma membrane, the site of localization for the F, G, SH and M proteins (25, 85–88). Infected cells develop filamentous surface projections presenting the viral glycoproteins eventually developing syncytia, which is the hallmark sign of RSV induced cytopathic effect (89, 90).

1.8 Viral Mutations

Like other RNA viruses, RSV is prone to mutations. There are some common mutations observed *in vitro* and in nature. When passaged *in vitro*, the RSV genome can acquire uracil (U) residue insertions in the gene end signals or into untranslated regions. However, this mutation is not as common as the mutations observed in the G and SH proteins. Spontaneous deletion of G and SH have been observed *in vitro* whereas deletion of the majority of G has been noted *in vivo* (46). Furthermore, two different spontaneous intragenic duplications of a portion of the G gene have been documented in nature (91). One of these mutants has been recorded to spread worldwide and continue to evolve. Circulating strains of RSV seems to accumulate progressive changes in sequence and antigenicity in response to immune pressure, especially in the G protein. However, this process has been very slow (1).

1.9 Potential Receptors for F and G Proteins

Specific host cell receptors essential for RSV attachment, triggering conformational change of the F protein or that help explain tissue tropism have not yet been identified. Both RSV F and G have been shown to interact with heparan sulfate. They are also heavily glycosylated

allowing them to bind to proteoglycans and C-type lectins (1). Furthermore, bovine and human RSV infect their respective hosts preferentially and this specificity has been traced to F2/pep27 region of the F protein (92). Moreover, since G is nonessential for infection *in vitro*, F may have the specific receptor vital for RSV infection. Addition of nucleolin has been found to increase permissivity to RSV infection suggesting a role as a potential functional receptor for F (93). ICAM-1 (94) and TLR4 (95) have also been postulated to be F protein receptors. However, all of these molecules are expressed on cells that are not susceptible to RSV infection failing to shed light on RSV's preference for the respiratory epithelium (1, 39). It is possible that there may be tissue-specific co-receptors or post-translational modifications for these molecules or in their downstream pathway that have not yet been identified.

2. Vaccine-Induced Enhanced Respiratory Disease

2.1 First Observation

In a clinical trial conducted in the 1960s, formaldehyde inactivated RSV (FIRSV) vaccine was used to immunize children of different ages. Although preclinical studies showed induction of high antibody titers, upon subsequent infection from a natural RSV epidemic, the clinical trial participants vaccinated with FIRSV experienced enhanced respiratory disease (ERD) (96–99). Out of 31 infants immunized with FIRSV, 25 required hospitalization and two died following RSV infection (96). The severity of disease was inversely correlated with the vaccinee's age. Indeed, the youngest age group of less than 6

months of age experienced the most severe disease. As the children became older, the frequency of severe illness decreased; ERD was observed in children up to 37 months of age at the time of immunization (98).

2.2 Characteristics of ERD

Clinical symptoms of ERD observed in the FIRSV immunized clinical trial participants were similar to that of most severe disease observed during RSV epidemics. Lung pathology of the two deceased children showed peribronchiolar inflammation and fibrinous exudates composed of sloughed epithelial cells, mononuclear cells, neutrophils, and eosinophils obstructing small airways (96–100). The children experiencing ERD also has poorly neutralizing antibodies (101, 102). Similar to the atypical measles syndrome resulting from immunization with inactivated measles virus vaccine, FIRSV induced peripheral blood mononuclear cells (PBMC) showed delayed-type hypersensitivity and significant lymphoproliferative responses (103, 104). Notably, in nature, repeated exposure to RSV does not induce ERD leading to the conclusion that ERD is specific to RSV naïve vaccinees (105).

In animal models, FIRSV induced ERD involves a Th2-bias in the antibody- and cell-mediated immune response including the production of Th2 cytokines such as Il-4, IL-5 and IL-13 (106). Not only has ERD seen in animals immunized with FIRSV, but also with whole inactivated virus and purified proteins immunizations. Interestingly, neither wild type nor attenuated replication-competent RSV induced ERD in animals or human infants (107–109).

Mechanistic studies have shown that ERD may depend on mode of antigen presentation altering immunological priming, which may lead to poorly binding/neutralizing antibodies (107) and Th2-biased CD4 T cell responses (110). It is important to note that manifestations of ERD can vary from one animal model to another. For a detailed summary of the preclinical signs and symptoms of ERD, refer to 'Appendix A – Immunopathogenesis associated with formaldehyde-inactivated RSV vaccine in preclinical and clinical studies'.

With advancements in the immunological tools available, there is better general understanding of RSV immunopathology and immunoregulation. However, there are still uncertainties about the basis of FIRSV mediated ERD and all the factors involved. Better understanding of this phenomenon is crucial for effective preclinical assessment of new vaccine candidates, especially in their potential for inducing ERD.

3. Vaccines and Therapeutics

3.1 Current Treatment

The only treatment currently available for RSV is a humanized neutralizing monoclonal antibody called Palivizumab (Synagis) made by MedImmune. It was approved by the FDA in 1998 and is a prophylactic treatment for severe RSV infections. This antibody targets the postfusion F protein by binding the antigenic A site (36, 42, 111). In preclinical studies, Palivizumab showed reduction of RSV replication in the lower respiratory tract of cotton rats (112, 113) and in clinical trials, it showed reduction of RSV-related hospitalizations of at risk infants (36, 114). Studying the mechanism of action of Palivizumab showed that treatment

with the antibody does not inhibit viral attachment or the ability of the F protein to interact with the target cell membrane. It was also shown to have no effect on viral budding. However, viral transcription was absent following Palivizumab treatment, and cell-to-cell and virus-to-cell fusion was blocked (115). Together, these results suggest that Palivizumab may prevent conformational changes in the F protein for the fusion process (115).

Although many studies have attested to the effectiveness of Palivizumab in reducing hospitalization and protecting high-risk infants from severe RSV disease, it has few major drawbacks. First, is the frequency of administration; it has to be given once monthly during the RSV season, which is typically from November to March in the northern hemisphere, to high-risk infants (36, 116). Next, is the high cost associated with the treatment; the price in USD can range from $1500 to $4300 per dose leading to a total cost of $6000 to $20,000 per child per RSV season (117, 118). This cost has remained steady for the last 5 years reiterating the need for a less frequent more affordable treatment for RSV infections.

3.2 Experimental Antivirals

Some antiviral compounds targeting the RSV F protein have been found. Although none of them are available to the public, they have shown some promise in preclinical studies. Most of these compounds bind the RSV F Y198 residue in the heptad repeat domain connected to the fusion peptide (HRA) (119–121). BMS-433771 has been shown to inhibit both RSV A and B by binding a hydrophobic pocket in the HRA coiled coil and preventing HRB from binding properly in that region (119, 122). TMC353121 was another compound found to

bind similar to BMS-433771 (121). These molecules distort the 6-helix bundle of the postfusion state instead of preventing its formation, thus interfering with the RSV fusion process.

3.3 Clinical Trials and Vaccine Strategies

There are 94 clinical trials worldwide that have recently completed or are active or recruiting for investigating interventional vaccines/treatments for RSV, out of which 55 studies are in the USA, 9 in Canada and 40 in Europe (123, 124). Majority of the vaccines being tested target the pediatric populations with a few targeting the maternal and elderly populations. The studies have reached various phases of clinical trial but none of the vaccines have reached the market for public use thus far. The vaccines/therapeutics under investigation use a wide range of strategies. There are live-attenuated, live-vectored, whole-inactivated, particle-based, subunit antigen-based, nucleic acid based, gene-based vectors, and combination and immunoprophylaxis (123, 124).

4. Objectives and Hypothesis

The major objectives of the following studies were to gain further insight into the mechanisms underlying FIRSV-mediated ERD. In the first study, a vaccination strategy where CD40 ligand administered along with a RSV immunogen, mainly the F protein, was used (Chapter 2). We hypothesized that this CD40-targeting strategy could provide effective protection against RSV infection by: (i) creating a balance between Th1 and Th2 responses

reversing the Th2-skew observed with FIRSV, (ii) increasing CD8 T cell response and memory, and (iii) inducing neutralizing antibodies. As a result, this could reduce eosinophil/neutrophil infiltration in the lungs preventing the occurrence of ERD. Furthermore, using the experimental vaccine, we aimed to delineate the role of CD8 T cells in FIRSV-induced immune responses, which is a major knowledge gap with FIRSV. Next, due to the exaggerated stimulation of the immune system observed during FIRSV-induced ERD, we hypothesized that there may be alterations in immunosuppressive molecules such as PD-1 and aimed to study expression levels of PD-1 during FIRSV-induced ERD (Chapter 3). Finally, we aimed to use chitosan, a polysaccharide shown to protect against other respiratory viruses through the induction of Th1 responses and neutralizing antibodies, to explore its potential in protecting against RSV and reversing ERD. Moreover, the effect of FIRSV on regulatory T cells and lung resident T cells, which are vital for immune suppression and RSV clearance, respectively, and the role of chitosan in altering those responses were also explored.

As mentioned above, RSV causes severe disease in humans. Its infection is the leading cause of hospitalization in infants while in the elderly, it is as rampant as influenza. Notably, while flu vaccines first became available almost 80 years ago, no RSV vaccine is available up to date. In fact, early RSV vaccine clinical trial in the 1960s was catastrophic, resulting in hospitalization of 80% of vaccinated participants and 2 deaths. Since then, subsequent studies revealed that various vaccines either inadvertently induce disease or fail due to a lack of efficacy. The slow progress in RSV vaccine development over several decades is largely due to a lack of understanding of the RSV vaccine-induced disease and critical elements for

the evaluation of the efficacy and adverse reactions associated with the RSV vaccines. Because of the significantly negative impact on public health posed by RSV infections, RSV vaccine development has been deemed one of the highest priorities by the World Health Organization (WHO) and Canada. It is of critical importance to develop efficacious and safe vaccine against this serious infectious disease and gain in-depth insight into RSV vaccine-induced enhanced respiratory disease.

Chapter 2: Targeting CD40 enhances antibody- and CD8- mediated protection against respiratory syncytial virus infection

This manuscript was published on November 9, 2018 in the journal *Scientific Report*s 8(1). I contributed more than 50% to the manuscript. Xuguang (Sean) Li, Changgui Li, Wangxue Chen, Terry Cyr, Jessie R Lavoie, Aaron Farnsworth, Michael Rosu-Myles, Lisheng Wang and I conceived the overall study. I performed the experiments and analyzed the data with the help of Marsha Russell, Louise Larocque and Caroline Gravel. Xuguang (Sean) Li and I wrote the manuscript. All authors edited and approved the manuscript.

Emily Dupuis at Health Canada provided technical assistance with flow cytometry. Dr. Martha Navarro and the technicians at the Health Canada animal facility helped with the animal studies. Dr. Don Caldwell, veterinary pathologist at Health Canada, conducted expert analyses of the lung tissues. Finally, Drs Houman Ghasriani and Roger Tam critically reviewed the manuscript.

The major knowledge gap addressed in this manuscript is the role of CD8 T cells in ERD. An experimental adenovirally-vectored RSV vaccine was developed where the RSV F protein was the immunogen and CD40 ligand was used as an adjuvant. BALB/c mice immunized with the experimental vaccine, which were effectively protected without ERD, were compared to mice immunized with FIRSV. New facets of FIRSV-induced CD8 T cells were identified.

Targeting CD40 enhances antibody- and CD8-mediated protection against respiratory syncytial virus infection

Abenaya Muralidharan[1,3], Marsha Russell[1], Louise Larocque[1], Caroline Gravel[1], Changgui Li[2], Wangxue Chen[4], Terry Cyr[1], Jessie R. Lavoie[1], Aaron Farnsworth[1], Michael Rosu-Myles[1,3], Lisheng Wang[3], Xuguang Li[1,3,*]

[1]Centre for Biologics Evaluation, Biologics and Genetic Therapies Directorate, HPFB, Health Canada and WHO Collaborating Center for Standardization and Evaluation of Biologicals, Ottawa, ON, Canada.

[2]National Institute for Food and Drug Control and WHO Collaborating Center for Standardization and Evaluation of Biologicals, Beijing, China

[3]Department of Biochemistry, Microbiology and Immunology, Faculty of Medicine, University of Ottawa, Ottawa, ON, Canada

[4]Human Therapeutics Portfolio, National Research Council of Canada, Ottawa, ON, Canada

[*]Corresponding author:

Dr. Xuguang (Sean) Li
Centre for Biologics Evaluation,
Biologics and Genetic Therapies Directorate,
Health Canada
Sir Frederick G. Banting Research Centre, A/L 2201E
251 Sir Frederick Banting Driveway
Ottawa, ON K1A 0K9, Canada
Tel: 613 954 2383
Fax: 613 941 8933
E-mail: Sean.Li@hc-sc.gc.ca

Abstract

Respiratory Syncytial Virus (RSV) infects almost all children under the age of one and is the leading cause of hospitalization among infants. Despite several decades of research with dozens of candidate vaccines being vigorously evaluated in pre-clinical and clinical studies, there is no licensed vaccine available to date. Here, the RSV fusion protein (F) was fused with CD40 ligand and delivered by an adenoviral vector into BALB/c mice where the CD40 ligand serves two vital functions as a molecular adjuvant and an antigen-targeting molecule. In contrast to a formaldehyde-inactivated vaccine, the vectored vaccine effectively protected animals against RSV without inducing enhanced respiratory disease. This protection involved a robust induction of neutralizing antibodies and memory CD8 T cells, which were not observed in the inactivated vaccine group. Finally, the vectored vaccine was able to elicit long-lasting protection against RSV, one of the most challenging issues in RSV vaccine development. Further studies indicate that the long lasting protection elicited by the CD40 ligand targeted vaccine was mediated by increased levels of effector memory CD8 T cell 3 months post-vaccination.

Introduction

Respiratory Syncytial Virus (RSV) causes severe disease in young children, elderly and immunocompromised patients (7, 125–127). It is the leading cause of hospitalization in infants (5, 7, 125, 128) with approximately 50% of children being infected in their first year of life (129, 130). In the 1960s, a clinical trial involving formaldehyde-inactivated RSV (FIRSV) resulted in hospitalization of 80% of the vaccinees and 2 deaths following subsequent RSV infection (96–98, 131). Similar to the symptoms observed in the trial participants, FIRSV has been shown to induce a Th2-biased immune response leading to pulmonary inflammation, airway obstruction and mucus hypersecretion in many animal models, which are now deemed as the hallmarks of vaccine-induced enhanced respiratory disease (ERD) (100, 132–134). Moreover, non-neutralizing antibodies induced by FIRSV have been implicated in ERD development (135–137), while another major facet of immunity, subsets of CD4+ T cells, was implicated in mediating various parameters of FIRSV-induced ERD (138, 139). However, the contribution of memory CD8 T cells in providing protection against RSV re-infection remains to be fully understood in spite of their known importance in viral clearance (138, 140, 141). Indeed, eliciting a robust memory CD8 T cell response is thought to be the key in developing a vaccine that can promote long-lived immunity against RSV (140, 142).

CD40 and its ligand (CD40L) are a critical part of the adaptive immune system. In the adaptive immune response, antigen-presenting cells (APCs) must first be activated by an antigen with high affinity to MHC class I and/or II molecules on its surface. Next, the interaction of a receptor and its ligand occurs as a costimulatory signal necessary to initiate and regulate the response. Lastly, the activated APCs, CD8+ and CD4+ T cells activate

cytokine release to carry out effector functions (143–145). Interactions between CD40 and CD40L occur during the costimulation step and profoundly enhance the humoral and cell-mediated responses in addition to activating the APCs (146–148).

CD40, part of the TNF receptor superfamily, is constitutively expressed on all APCs, activated CD4 T cells, CD8 T cells, fibroblasts, endothelial and epithelial cells (146–148). CD40L, which is part of the TNF superfamily, is transiently expressed on activated CD4 T cells (146) and may also be expressed on activated B cells, some dendritic cell subsets, platelets and smooth muscle cells (148). Interactions between CD40 and CD40L have a considerable effect on promoting expansion and survival of APCs, T cells and B cells (147). Moreover, CD40-CD40L is a crucial signal in stimulating CD4 T cells and in the process of direct or indirect priming of cytotoxic T lymphocytes by dendritic cells (146). In B cells, engagement of the CD40 receptor improves antibody production, isotype switching, germinal center (GC) formation, and memory B cell maturation in addition to enhancing antigen presentation to T cells. Specifically, GC B cells undergo apoptosis after constant B cell receptor stimulation but T cell signals such as CD40L prevent this from happening, leading to longer antibody production (146, 147, 149).

Previously, studies have shed light on the profound impact of targeting CD40 during RSV immunization using an anti-CD40 antibody or CD40L (150), (151, 152). Nevertheless, separate administrations of the RSV antigen and CD40 targeting molecule were done and detailed mechanism of the immune responses, specifically cell-mediated responses, remain to be fully understood.

In this study, our goal was to develop and evaluate a vaccine expressing one protein consisting of both the RSV fusion (F) protein and CD40L. To the best of our knowledge, this

is the first report of CD40L being used not only as a molecular adjuvant to enhance RSV F-induced host immunity, but also as an antigen-targeting molecule. Compared with FIRSV vaccine, the targeted vaccine induced higher levels of neutralizing antibodies while no ERD pathology was observed in the lungs. Further mechanistic studies indicate that the protection was dependent on CD8 but not CD4 T cells. Importantly, our study also demonstrated for the first time that it is feasible to induce CD8 T cell-mediated long-lasting protection through CD40-targeting immunization.

Results

Recombinant adenovirus construction and in vitro protein expression

Our aim was to determine if using CD40L as a molecular adjuvant during immunization can improve effective protection of mice from RSV infection. To that end, recombinant replication-deficient adenovirus expressing the full length RSV F protein, the most immunogenic of all RSV surface proteins (129), fused to mouse CD40L were generated (Ad-SF40L) (Figure 2.1A). A secretion signal and a trimerization motif were added to help increase antigen load, and to maintain the expressed CD40L in its functional trimeric form, respectively. To deduce the contribution of the CD40L to the observed protection, adenovirus expressing RSV F but not CD40L was also generated (Ad-SF). An empty adenovirus control (Ad-Empty) and antigen-specificity control expressing influenza nucleoprotein fused to CD40L (Ad-SNP40L) (153) were also added to ensure that the protection detected was in fact due to the presence of both RSV F and CD40L.

Following the recombinant adenovirus construction, protein expression was tested *in vitro*. Immunofluorescence of HeLa cells infected with the adenoviruses confirmed the

expression of RSV F protein in both Ad-SF and Ad-SF40L infected cells, whereas the expression of CD40L was only seen with Ad-SF40L (Figure 2.1B). An image merging the fluorochromes attached to each antibody shows the co-expression of RSV F protein and CD40L by Ad-SF40L. Ad-Empty did not induce expression of either protein, as expected (data not shown).

Immunization with Ad-SF40L augments RSV clearance without ERD in BALB/c mice

The adenoviruses produced were then tested in BALB/c mice for their ability of inducing protection against RSV. RSV and FIRSV groups were added to serve as controls for outcomes of a secondary infection and vaccine-induced ERD, respectively. All vectored vaccines and live RSV-A2 were immunized intranasally while FIRSV was injected intramuscularly. A prime-boost regimen was followed for all vaccines tested. Boost immunization was given 28 days following the prime and all mice were challenged with live RSV-A2 intranasally 14 days after the boost. Necropsy for tissue collection was conducted 4 days post challenge, which is the peak of infection (Figure 2.2A).

Ad-SF40L immunization resulted in significantly higher lung viral clearance than all other immunization groups ($p=0.0045$) with an almost complete lung RSV clearance (Figure 2.2B). Most importantly, these mice did not display any signs of ERD, demonstrating a safe, non-toxic protection (Figure 2.2C-D). Clearly, the ERD pathology is only associated with FI-RSV vaccination. It is of note that even though Ad-SF immunization did not induce ERD, it failed to effectively clear the virus, similar to the two negative controls, i.e. Ad-Empty and Ad-SNP40L (influenza A NP construct control). These results collectively demonstrated the important role of CD40L in promoting RSV-specific immunity and robust viral clearance.

Moreover, RSV immunization also resulted in better viral clearance than FIRSV immunization ($p=0.044$) (Figure 2.2B).

Lungs were H&E and PAS stained for histopathological analysis of interstitial disease, edema, perivascular aggregates of leukocytes and mucus. Mice from all immunization groups except FIRSV showed minimal perivascular cell infiltration and mucus levels whereas FIRSV immunized mice exhibited severe ERD displaying significantly higher cellularity and epithelial mucinous hyperplasia with luminal mucus accumulation in airways ($p=0.016$) (Figure 2.2C-D, Supplementary Figure 2.1).

Ad-SF40L induces high levels of neutralizing antibodies with the absence of a Th2-bias

Antibody-mediated immune responses are vital for robust protection against RSV (136). The Th2-skewed nature of FIRSV-induced protection, especially in mice, has been well established (136, 154). This skew accompanied by the low levels of neutralizing antibodies detected post challenge has been shown in many studies as the major drawback associated with FIRSV-elicited immune responses (138, 154, 155).

In this study, we first confirmed these aspects of FIRSV-induced antibody responses where FIRSV-immunized mice had lower levels of RSV F protein-specific IgG than RSV, Ad-SF and Ad-SF40L immunized mice post challenge and highest Th2 subtypic profile, i.e. higher IgG1 to IgG2a ratio (Figure 2.3A-B). Furthermore, the antibodies in FIRSV-immunized mice had very low RSV neutralizing abilities, as expected (Figure 2.3C). Importantly, Ad-SF40L immunization induced high levels of F-specific IgG in the serum, even higher than live RSV immunization, without a Th2-bias. As there is no difference between Ad-SF and Ad-SF40L in terms of antigen specific IgG and IgG subtype, CD40L

does not have a significant effect in this regard. However, the addition of CD40L during immunization contributes to a significant increase in neutralizing antibodies ($p<0.01$) against RSV (Figure 2.3C). Overall, these data indicate that while Ad-SF and RSV immunization gave rise to similar levels of neutralizing antibodies, Ad-SF40L induced the highest levels of neutralizing antibody among the vaccines tested.

Increase in effector/effector memory CD8 T cells (TEM) following RSV challenge contributes to Ad-SF40L-induced protection

CD8 T cells play a critical role during infections and are sufficient to clear RSV (156, 157). Over time following infection or vaccination, as the antigen load decreases, the population of mature CD8 T cells contracts to form a stable memory CD8 T cell pool whose functional activities evolve with time (158). As is the role of immune memory, RSV-specific CD8 T cells expand in magnitude and effector functions following infection (159). However, FIRSV has been shown to elicit no memory CD8 T cell response in mice adding another facet to its ineffectiveness (160, 161).

To determine memory CD8 T cell-mediated immunity induced by Ad-SF40L and further characterize the CD8 population induced by FIRSV, we evaluated the CD8 T cell phenotype and functional changes that occur following RSV challenge. BALB/c mice were administered with the vaccines twice and euthanized either before or 4 days after challenge (Figure 2.4A). Spleens were analyzed using flow cytometry for markers distinguishing various CD8 T cell phenotypes (Supplementary Figure 2.2). The population of effector/effector memory CD8 T cells (TEM) after challenge significantly increased in mice immunized with Ad-SF40L ($p<0.05$) compared to before challenge; no change was observed

in Ad-SF, RSV and FIRSV immunization group post RSV challenge (Figure 2.4B). Moreover, an increase in F-specific TNF-α producing CD8+ cells was only observed following challenge in Ad-SF40L and RSV immunized mice (Figure 2.4C). The lack of increase in TEMs and TNF-α post-challenge in mice immunized with FIRSV may point to a defect in T cell memory maturation in FIRSV, which also occurs with Ad-SF, abrogating effective protection.

Following RSV infection, antigen-specific CD8 T cells exhibit an activated phenotype and gain effector functions (159) corroborating the common theory that inflammatory responses increase with antigen encounters (158). Notably, in humans, an increase in TEM population can be seen following resolution of infection (162). Here, we found, unlike the other vaccination groups, Ad-SF40L resulted in complete viral clearance 4 days post-challenge (Figure 2.2B), indicating that the resolution of infection was accompanied by an increase in TEMs. Additionally, following challenge, Ad-SF40L also increased expression of TNF-α, a potent inflammatory cytokine known to mediate RSV clearance (163, 164), confirming the presence of activated effector cells during the time of RSV resolution.

CD40L enhances antibody-induced protection but not CD4 T cell-induced response

Next we investigated the magnitude of protection afforded by antibodies derived from Ad-SF40L immunized mice in naïve mice. Figure 2.5A outlines the timeline followed for passive serum transfer where serum from immunized and challenged mice was transferred into naïve recipient mice that were subsequently challenged. As shown in Figure 2.5B, four days post-challenge, lung viral titer was the lowest in mice that received serum from Ad-SF40L

immunized donors compared to other groups, confirming the importance of the protective antibodies present in Ad-SF40L immunized donors (Figure 2.3C). Since FIRSV immunization induced low F-specific IgGs that did not possess sufficient neutralizing ability (Figure 2.3A, C), serum transfer expectedly failed to result in marked viral clearance in recipients (Figure 2.5B).

Next, we examined the ability of CD4 T cells derived from each immunization groups in protecting naïve mice against RSV (Supplementary Figure 2.4). No difference between Ad-SF and Ad-SF40L was found in viral clearance following adoptive CD4 T cell transfer even though Ad-SF40L resulted in better viral clearance than RSV ($p<0.01$) and FIRSV ($p<0.05$) groups. These results suggest that the protection induced by Ad-SF40L is CD4 T cell-independent.

Marked increase in CD8 T cell effector phenotype and function following Ad-SF40L immunization

We next set out to determine CD8 T cell functional activities in various immunization groups before and after RSV challenge. Figure 2.6A represents a schematic diagram of the adoptive transfer of CD8 T cells into naïve mice following immunization either before (BC) or after (AC) challenge. BC transfer from Ad-SF40L immunization led to an almost complete RSV clearance from the lungs of recipients, levels significantly lower than Ad-SF, RSV and FIRSV ($p=0.0165$) that had no differences among them (Figure 2.6B left). AC transfer, however, showed a spike in lung RSV titer when the CD8 T cells were isolated from FIRSV immunized donors whereas the other groups were not significantly different from the protection observed in BC transfer recipients (Figure 2.6B right), revealing a significant

deterioration of CD8 T cell function after challenge in the FIRSV group (see below for more discussion).

To analyze the effector response in the BC and AC transfer recipients, we measured the total RSV F-specific cytokine levels in the recipients. BC transfer resulted in significantly higher levels of IFN-γ (Figure 2.6C left) and TNF-α (Figure 2.6D left) in recipients of CD8 T cells from Ad-SF40L ($p<0.05$) immunized donors compared to Ad-SF and FIRSV. IFN-γ expression considerably increased in Ad-SF40L AC transfer recipients while levels induced by Ad-SF, RSV and FIRSV immunization decreased or remained unchanged (Figure 2.6C right). Importantly, IFN-γ and TNF-α were induced to barely detectable levels in AC transfer mice receiving CD8 T cells from FIRSV immunization (Figure 2.6C, D right). Overall, Ad-SF40L gives rise to CD8 T cells that improve with RSV challenge as demonstrated by increased effector functions and TEMs (Figure 2.4) whereas FIRSV induced CD8 T cells which are deficient in effector cytokine production, especially post RSV challenge, resulting in a substantial decrease of the capacity for viral clearance in CD8 T cell recipients.

Ad-SF40L invokes long-lasting protection against RSV infection accompanied by a durable CD8 T cell effector memory response

Finally, we determined if targeting CD40 could induce long-term protection. To this end, BALB/c mice were immunized with either Ad-SF or Ad-SF40L and challenged three months later with RSV (Figure 2.7A). As shown in Figure 2.7B, Ad-SF40L immunized mice were able to resolve the infection significantly better than Ad-SF ($p=0.0286$). Importantly, significantly higher levels of TEM cells was observed in Ad-SF40L immunized mice

(p=0.0014) following challenge (Figure 2.7C), which was comparable to the increase seen in short-term protection (Figure 2.4B, Supplementary Figure 2.3B). Taken together, Ad-SF40L effectively induces long-lasting protection in mice with a durable induction of TEMs.

Discussion

Decades of effort have not resulted in a licensed vaccine for RSV. In addition to the ERD observed in the early clinical trials, results from most vaccines evaluated in recent clinical trials show a lack of efficacy (124, 165, 166). Although a commercially-available monoclonal antibody against an epitope on the RSV F protein named palivizumab (Synagis®) could be administered to children with serious lower respiratory tract disease, it needs to be administered multiple times to reach therapeutic effects; in addition, this therapeutic antibody is costly and is also known to be ineffective in adults (36, 167). Clearly, vaccination is the most effective means of protecting children against RSV. Although there have been many recent studies exploring different modes of vaccination, antigen targets and animal models to gain further mechanistic insight (168–170), there are important questions yet to be answered, particularly with respect to long-lasting immune responses and the role of memory CD8 T cells. The aim of this study was to investigate if enhancing immune response by using CD40 ligand as both an antigen-targeting molecule and immune modulator could result in robust and long-lasting CD8 T cell memory responses. This strategy of administering one protein expressing both the RSV antigen and CD40 targeting molecule is different from previous work reported in the literature. Specifically, Lee et al. showed enhanced viral clearance and decreased lung pathology in mice immunized with the RSV M2 protein along with a TLR3 agonist and anti-CD40 antibody (150). Yet, while M2 is a potent antigen in

inducing cell-mediated immune responses, it may not be as immunogenic as the RSV F protein (129). In another study, Tripp et al used live wild-type RSV as the vaccine with a separate intraperitoneal inoculation of mice with adenovirus-vectored CD40L and observed increased levels of Th1 cytokines and antigen-specific antibody production during a short-term observation period (151). Another study involved a DNA vector expressing RSV F and/or G protein in conjunction with a separate DNA vector producing CD40L (152). They also observed complete viral clearance but the antigen-specific antibodies were very low before the actual viral challenge took place; it is also unclear as to whether those antibodies have neutralizing activities. In our study, the neutralizing antibodies were markedly higher than non-CD40L immunization, suggesting that both neutralizing antibodies and CD8 T cells significantly contributed to protection, which is also supported by our observations that serum transfer from Ad-SF40L immunized mice did not afford protection as effectively as the donor mice themselves (Figure 2.2B, Figure 2.5). Our findings also corroborate previous studies which revealed that TLR activation results in high avidity antigen-specific protective antibodies as the F protein employed in this study is a known TLR agonist (136). Moreover, it is also known that TLR agonists and CD40L could synergistically facilitate B cell development (171). Our findings together with these previous observations indicate that the selection of F protein as an antigen component in conjunction with CD40 stimulation could be a viable approach to maximize the protective potential of a candidate RSV vaccine.

Antibodies against the RSV F protein play an important role in the protection against RSV (136, 172). Analyses of human sera showed that majority of the RSV neutralizing antibodies target the F protein (173, 174). Structural analysis of antibodies raised from FIRSV immunization showed the exclusive induction of antibodies targeting poorly

neutralizing epitopes, even though neutralizing epitopes were not hidden (172). Moreover, low avidity of FIRSV-induced antibodies for protective epitopes on RSV has been attributed to the lack of protection. Indeed, lack of antibody affinity maturation due to poor toll-like receptor stimulation has been shown to result in non-protective antibodies (136). Although the vital role of neutralizing antibodies in protection against RSV has been established, the role of non-neutralizing antibodies remains to be fully understood. In other viral infection such as influenza, non-neutralizing antibodies have been shown to promote antigen presentation to FcR+ cells, such as macrophages and/or lung phagocytes, leading to activation of CD8 T cells (175, 176). In our study, FIRSV induced low levels of neutralizing antibodies (Figure 2.3C) but higher number of TEMs (Supplementary Figure 2.3) compared to Ad-SF40L even though the number of FIRSV-induced TEM did not increase post challenge (Figure 2.4B). Interestingly, while CD8 T cells contribute to viral clearance, they can also induce lethal immunopathology following RSV infection (140). As such, a balance might be needed to ensure effective viral elimination without inducing ERD.

We then characterized the T cell-mediated immunity induced by Ad-SF40L to show the production of a strong effector memory CD8 T cell response upon RSV challenge. CD40L had a profound effect on RSV clearance and F-specific cytokine production in recipients after CD8 T cell transfer (Figure 2.6). Ad-SF40L immunization elicited a CD8+ TEM population that increased in size upon encounter with the live virus indicating the presence of memory and antigen recognition capacity (Figure 2.4B); importantly, the fold increase of TEMs due to RSV challenge remained comparable between short- and long-term protection in terms of memory CD8 T cell response (Figure 2.7C), suggesting that the augmentation of CD8 T cell memory is long-lasting.

It is of note that following viral challenge the functional activities of CD8 T cells derived from FIRSV immunized animals significantly deteriorated (Figure 2.6). Moreover, it is known that patients with severe lower respiratory tract disease may have insufficient cell-mediated immunity (177). Clearly, the induction of memory CD8 T cells should be a vital element in evaluating the efficacy of RSV vaccines whereas the current RSV vaccine development like many other vaccines is focused on inducing a strong humoral response (178–180).

It is worth mentioning that targeting CD40L more effectively eliminated virus and afforded long lasting protection, there is still limitation in our current work. Specifically, as the study presented in this report was mostly aimed at comparing the vectored vaccines delivered intranasally with FIRSV injected intramuscularly, we did not investigate the changes of resident CD8 T cells in the lung tissues, given intranasal delivery of alum-adjuvanted FIRSV was unsuccessful due to the viscosity of the vaccine preparation, while previous studies have shown that route of injection plays a crucial role in determining the immune responses at the site of infection (181). Specifically, studies involving respiratory viruses have shown that intranasal administration results in robust pulmonary tissue-resident effector and memory CD8 T cells compared to intraperitoneal and intramuscular administration (181, 182). However, other studies have shown that both intranasal and intramuscular administration result in similar numbers of effector memory CD8 T cells in the spleen and lung vasculature (182). Nevertheless, more experiments should be conducted to better decipher the roles of RSV-specific CD8 T cells in the lung tissues, given its crucial role in protection (181), which is ongoing in our laboratories.

In summary, we present the first report on a fusion protein comprised of a RSV F

antigen and CD40L, in which CD40L functions as both antigen-targeting molecular and immunomodulator. Our studies help better understand the mechanisms underlying CD8 T cell mediated short- and long-term protection against RSV infection and FIRSV-induced ERD with regards to CD8 T cell induction.

Methods

Generation of recombinant adenovirus

Constructs were designed to express the full RSV-A2 F protein (GenBank accession # KJ155694.1) as a secreted form with the inclusion of 23 amino acids from the human tyrosinase signal peptide (MLLAVLYCLLWSFQTSAGHFPRA; GenBank accession # AH00 3020) at the N-terminus (Ad-SF) as previously described (153). A 27 amino acid fragment from the bacteriophage T4 fibritin trimerization motif (GYIPEAPRDGQAYVRKDGEWVLLSTFL) was added to the C-terminus of SF along with the complete mouse CD40L (GenBank accession # NM_011616) to form a trimeric, secreted protein, SF40L. Recombinant adenoviruses (Ad) were generated using the Directional TOPO® and the Gateway®-adapted ViraPower adenoviral expression vector system (Invitrogen) according to the manufacturer's instructions.

Briefly, SF40L was synthesized by Bio S&T (Montreal, QC, Canada) in pBluescript II SK+. All PCR reactions were done using High Fidelity Platinum Pfx PCR kits (Life Technologies). Using the primers listed in Supplementary Table 2.1, SF40L and SF were isolated from pBluescript containing SF40L. The PCR products were then cloned into pENTR/SD/D-TOPO (Invitrogen) as per manufacturer's instructions. Following transformation into *E. coli* and isolation of the plasmid, the sequence of the insert was confirmed. Next, a recombination reaction was done between the TOPO vector containing SF40L or SF and pAd/CMV/V5-DEST (Invitrogen). Once again, transformation, plasmid isolation and sequencing were conducted. Then, pAd-DEST vector was digested with *PacI* restriction enzyme to expose the viral inverted terminal repeats, phenol-chloroform extracted, ethanol-precipitated, and transfected into QBI-HEK 293A cells. Following 80% cytopathic

effect due to the production of adenoviruses, the cells and supernatant were harvested, lysed, and frozen at -80ºC. Purified stocks were made in QBI-HEK 293A cells for animal studies by ultracentrifugation with a sucrose cushion. Adeno-X Rapid Titer Kit (Clontech Laboratories Inc.) was used for titration of the adenoviruses.

Protein expression and immunofluorescence

HeLa cells were seeded at a density of 10,000 per well in growth media in a 96-well flat clear-bottom black plates and incubated overnight at 37ºC and 5% CO_2. Next day, the cells were infected at a MOI of 100 with purified adenovirus. On the following day, infected cells were fixed with cold cytofix/cytoperm (BD Biosciences) for 10min at 4ºC. After blocking with 3% IgG-free BSA diluted in wash buffer (1x PBS with 0.1% Tween 20) for 1 hour at 37ºC, the cells were stained with an unconjugated Rabbit RSV F monoclonal antibody (Sino Biological; clone #009) for 1 hour at 37ºC. Then, a mixture of Alexa Fluor 594-conjugated anti-rabbit IgG (Abcam) and FITC-conjugated anti-mouse CD40L (Invitrogen) was added for 1 hour at 37ºC. The cells were imaged using the EVOS FL microscope: Alexa Fluor 594 in the RFP and FITC in the GFP channel.

Cells, viruses and vaccines

HEp-2 (ATCC: CCL-23) and HeLa cells (ATCC: CCL-2) were grown in Dulbecco's Modified Eagle Medium (DMEM) supplemented with 1.5 g/l sodium bicarbonate, 2mM Glutamax, 1mM HEPES, 20 U/ml Penicillin, 0.02 mg/ml Streptomycin, and 10% FBS. Finally, QBI-HEK 293A were cultured in DMEM with 1.5 g/l sodium bicarbonate, 25mM

HEPES, 20 U/ml Penicillin, 0.02 mg/ml Streptomycin, and 10% FBS.

RSV-A2 (ATCC: VR-1540) was grown in HEp-2 cells according to supplier's instructions and sucrose-purified for animal studies. FIRSV was prepared with the RSV-A2 strain in HEp-2 cells as described elsewhere (135).

Animal studies

Six-week old female BALB/c mice (Charles River, Saint Constant, QC) were used for all animal studies. Ad-SF and Ad-SF40L were administered intranasally at 10^8 PFU per mouse, RSV at 10^5 PFU intranasally and FIRSV at 10^6 PFU intramuscularly. All mice were challenged intranasally with $5x10^5$ PFU of RSV-A2. Intranasal inoculations were given in 25µl per mouse and intramuscular in 50µl. Each immunization was administered twice at the same dose and route 28 days apart. Fourteen days after the second immunization, the mice were challenged and 4 days post challenge (peak of infection in mice) euthanized for blood and tissue collection. All animal experiments were reviewed and approved by Institutional Animal Care and Use Committee of Health Canada and were conducted in accordance with Institutional Animal Care and Use Committee of Health Canada guidelines and regulations.

Lung viral titer

Lungs were removed four days post RSV challenge and tittered as described elsewhere (135). Briefly, lungs were collected in serum free RPMI media and weighed prior to mechanical homogenization. The homogenates were clarified using centrifugation and the supernatants were frozen at -80ºC until further use. Serial dilutions of the supernatant were done and

incubated on HEp-2 cells for 2 hours at 37ºC. A 1:1 overlay of 2x DMEM media and 0.8% agarose was added. Following 6 days of incubation, the overlay was removed and the cell monolayer was stained with crystal violet before counting plaques. Results are expressed as PFU/g lung tissue.

Histopathology

Four days post RSV challenge, whole lungs were collected from the BALB/c mice and fixed in 10% neutral buffered formalin. They were then trimmed, processed and embedded into paraffin blocks. Five-micron Hematoxylin and Eosin (H&E) and Periodic Acid Schiff (PAS) stained slides were made for evaluation. Scoring was done by a veterinary pathologist who was blinded to the experimental design. The lesion assessment protocol outlined by Weiss et al. (183) was adopted. Perivascular leukocytic infiltration was evaluated where 1 means within normal parameters ; 2 means small numbers of solitary cells with uncommon aggregates; 3 means multifocal small to moderate aggregates; 4 means moderate to high cellularity with multifocal large cellular aggregates that may be expansive into adjacent tissues. Mucus was visualized with PAS stain and graded as follows: 1 means none; 2 means epithelial mucinous hyperplasia with none to rare luminal mucus accumulation in airways; 3 means epithelial mucinous hyperplasia with luminal mucus accumulation in airways; 4 means there is severe mucinous hyperplasia with airway obstruction by mucus. Total pathological score was calculated as the average of the individual scores.

ELISA

Serum from immunized and challenged mice was collected for determination of IgG, IgG1 and IgG2a titer. Ninety six-well plates were coated with recombinant RSV F protein (Sino Biological) overnight at 4ºC. Next day, the plates were washed and blocked with BSA in PBS containing 0.05% Tween 20 for 2 hours at 37ºC. Serial dilutions of the mouse serum in blocking buffer were then added for 1 hour at 37ºC. After washing, HRP-conjugated anti-mouse IgG (GE Healthcare Life Sciences), anti-mouse IgG1 or IgG2a (Jackson Immunoresearch Laboratories) were added for 1 hour at 37ºC. The plates were again washed and Tetramethylbenzidine substrate (Cell Signaling Technology) was added for 20 min at room temperature. The reaction was then stopped with 0.16 M sulfuric acid. The plates were read spectrophotometrically at 450nm.

Microneutralization

RSV-neutralizing ability of the serum from immunized and challenged mice was determined. Serial dilutions of the serum were incubated with 800 PFU of purified RSV-A2 for 1 hour at 37ºC, 5% CO_2. The virus-antibody mixture was added to HEp-2 cells seeded the previous day and incubated at 37ºC. After 3 days, the cells were fixed with ice-cold methanol for 10 min at room temperature, air-dried, and blocked with 5% non-fat dry milk in PBS containing 0.1% Tween 20 for 2 hours at 37ºC. Then, the plates were washed and a HRP-conjugated anti-RSV (Meridian Life Science) was added for 1 hour at 37ºC. The plates were again washed and Tetramethylbenzidine substrate (Cell Signaling Technology) was added for 20 min at room temperature. The reaction was then stopped with 0.16 M sulfuric acid. The plates were read spectrophotometrically at 450nm.

Flow cytometry for surface and intracellular markers

Cells from spleens were isolated from immunized mice before or 4 days after challenge. Single-cell suspensions were washed with PBS and first, stained with Fixable Viability Dye eFluor® 506 (eBioscience) for 30 min at 4ºC, then, with purified anti-mouse CD16/CD32 (eBioscience) as a Fc block for 5 min. Next, cells were washed with FACS wash buffer (PBS with 1% BSA and 0.05% sodium azide) and stained with PE-CF594-conjugated anti-mouse CD40 (clone 3/23) or a panel with BV786-conjugated anti-mouse CD3 (clone 145-2C11), FITC-conjugated anti-mouse CD8a (clone 53-6.7), BV421-conjugated anti-mouse CD44 (clone IM7), PE-Cy7-conjugated anti-mouse CD62L (clone MEL-14), and AF647-conjugated anti-mouse CD197 (clone 4B12). All antibodies were purchased from BD Biosciences. Stained samples were fixed with 1% paraformaldehyde.

For intracellular staining, splenocytes were stimulated with an immunodominant H-2K^{d}-restricted RSV F_{85-93} peptide (KYKNAVTEL; ProImmune) at 5µg/ml, along with GolgiPlug (BD Biosciences) for 4 hours at 37ºC, 5% CO_2. Stimulated cells were washed and stained sequentially with the viability dye, Fc block, FITC-conjugated anti-mouse CD8a (clone 53-6.7), and incubated with BD cytofix/cytoperm (BD Biosciences) for 20 min. The permeabilized cells were then washed with 1x perm wash (BD Biosciences) and stained with PE-conjugated anti-mouse TNF-α (clone MP6-XT22) for 30 min. For both surface and intracellular stained samples, using a BD LSRFortessa flow cytometer, 100,000 viable singlet events for spleen and 50,000 viable singlet events for lymph node were recorded. FMO controls and compensation beads were used where appropriate to correct for spectral overlap. Data analysis was completed using FACSDiva version 8.0.1.

Secreted cytokines

Splenocytes were stimulated with an immunodominant H-2K^d-restricted RSV F_{85-93} peptide (KYKNAVTEL; ProImmune) at 5µg/ml for 48 hours at 37ºC, 5% CO_2. Supernatants were collected following centrifugation and stored at -80ºC for later analysis. A ProcartaPlex Mouse Cytokine Panel (eBiosciences) was used to determine the levels of IFN-γ and TNF-α in the supernatants. The samples were read on a Luminex 200 System (xMAP Technology). Data analysis was performed using MILLIPLEX Analyst version 5.1 for determining the pg/ml of each cytokine.

Passive Serum Transfer

Serum was aseptically collected and pooled from 25 immunized BALB/c mice 4 days after challenge. Naïve 6-week-old BALB/c mice were intraperitoneally injected 4 times with 300µl of donor serum 3 days, 2 days, 1 day before RSV challenge and on the day of the challenge (153). Four days post-challenge, mice were euthanized for tissue collection (Figure 2.5A).

Adoptive T cell transfer

Spleens were aseptically extracted from 25 immunized BALB/c mice before or after RSV challenge. Splenocytes were isolated and pooled for CD8 and CD4 T cells extraction. Dynabeads® Untouched Mouse CD8 Cells Kit and CD4 Cells Kit (Life Technologies) were used according to manufacturer's instructions. Prior to transfer, flow cytometry staining was

done to determine purity of the resulting CD8 and CD4 T cells using PerCP-conjugated anti-mouse CD8a (clone 53-6.7; BD Biosciences), and FITC- conjugated anti-Mouse CD4 (clone RM4-4; eBiosciences). On the same day, 4.6 million CD8 or CD4 T cells at 80% and 87% purity, respectively, were injected intravenously, via the tail vein, into naïve 6-week-old BALB/c mice (153). Three days later, mice were challenged intranasally with RSV and euthanized 4 days post-challenge (Figure 2.6A, Supplementary Figure 2.4A).

Statistical Analysis

Analysis was conducted using unpaired Student's t-test, one-way or two-way ANOVA where appropriate. Bonferroni posttest was used to adjust for multiple comparisons between different test groups. Tests were done at a 5% significance level. All statistical analyses were performed using GraphPad Prism 6 software.

Figures

Figure 2.1

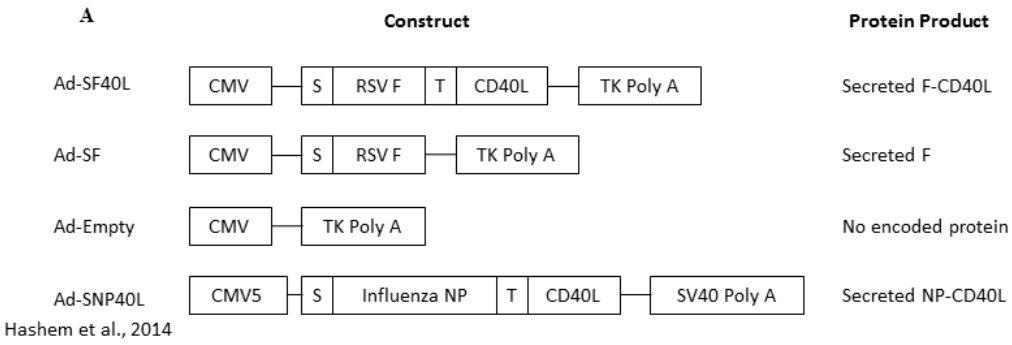

Hashem et al., 2014

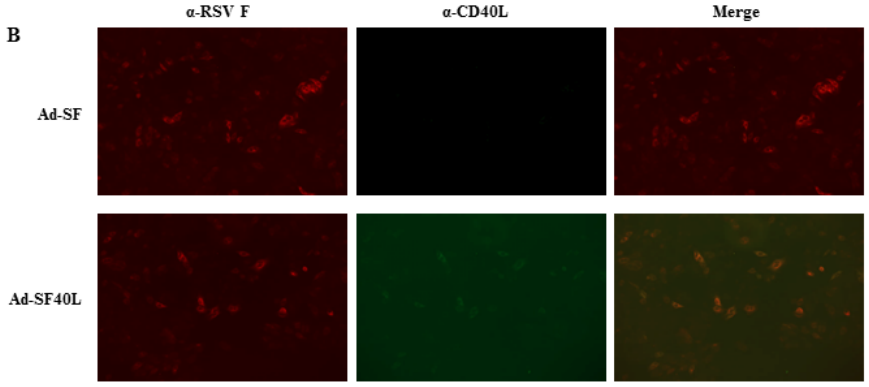

Figure 2. 1: Non-replicating mouse codon-optimized recombinant adenovirus vaccines construction and in vitro protein expression. (A) Schematic representation of the Ad constructs. Both Ad-SF and Ad-SF40L express the full length RSV F protein preceded by a secretion signal, S. Ad-SF40L also encodes the full length mouse CD40 ligand, CD40L, following a trimerization motif, T. Ad-Empty does not encode for RSV F or CD40L whereas Ad-SNP40L encodes the influenza A nucleoprotein (NP) followed by CD40L as previously described. (B) Representative images at 10x magnification of in vitro protein expression following an immunofluorescence assay with a rabbit RSV F antibody along with Alexa Fluor 594-conjugated anti-rabbit IgG and FITC-conjugated anti-mouse CD40L. A merge of the two fluorochromes show the co-expression of RSV F and CD40L. Data are representative of two experiments.

Figure 2.2

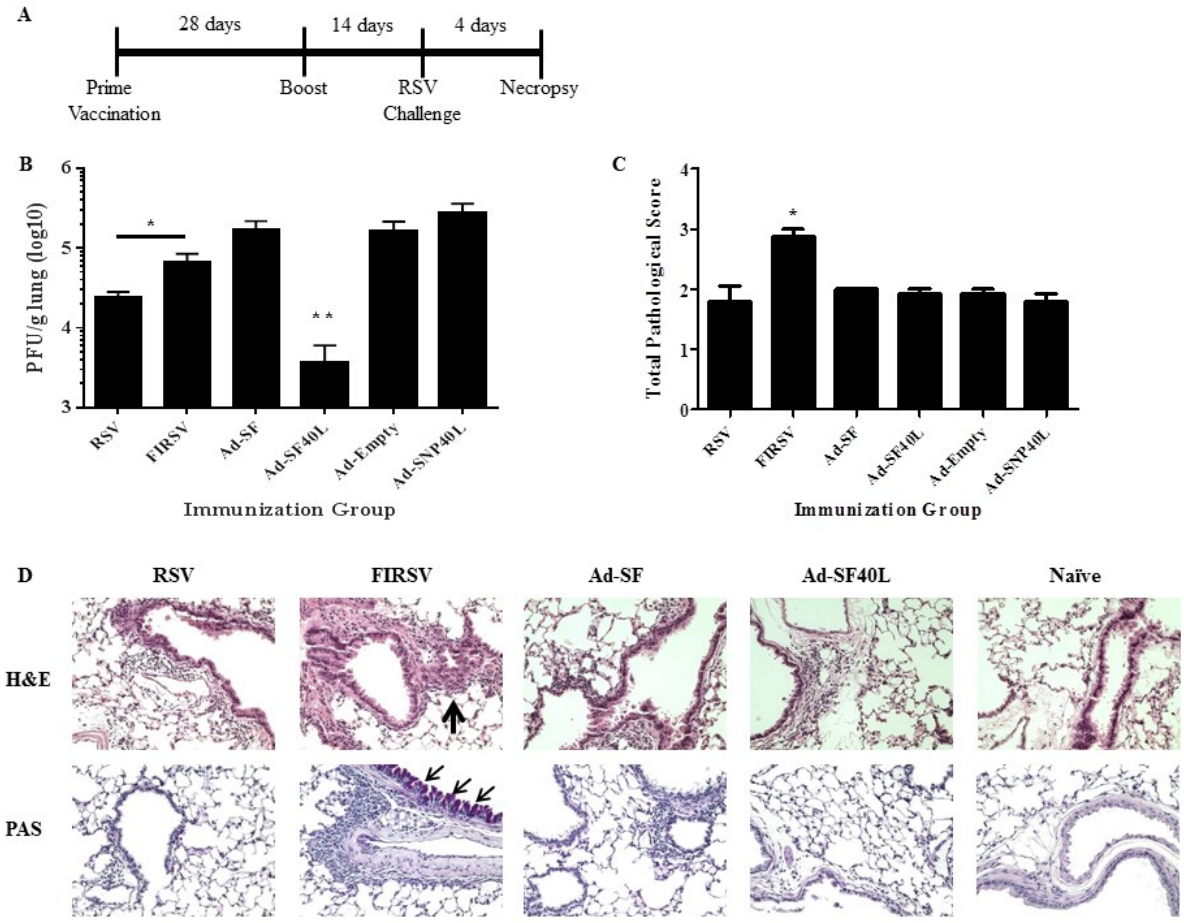
A
28 days
14 days
4 days
Prime Vaccination
Boost
RSV Challenge
Necropsy
B
PFU/g lung (log10)
RSV
FIRSV
Ad-SF
Ad-SF40L
Ad-Empty
Ad-SNP40L
Immunization Group
C
Total Pathological Score
Immunization Group
D
RSV
FIRSV
Ad-SF
Ad-SF40L
Naïve
H&E
PAS

Figure 2. 2: Immunization with Ad-SF40L augments RSV clearance without ERD in BALB/c mice. (A) Schematic diagram of the immunization, RSV challenge and necropsy timeline. (B) Lung viral titer determined using plaque assay 4 days post challenge. (C) Pathological scoring of lung tissue. Perivascular leukocyte infiltration and mucus were scored using H&E and PAS stained slides, respectively, 4 days following RSV challenge. An average of the two scores is shown. (D) Representative images of H&E and PAS stained immunized BALB/c mouse lungs post challenge at 40x magnification. The arrows point to the extensive cell infiltration in the H&E stained lungs and mucus-positive cells in the PAS stained lungs. Neutral mucins in airway epithelial cells are red when stained with a PAS stain. Data shown is mean ± SEM representative of 2 independent experiments; n = 4 per group in each experiment; *$p < 0.05$, **$p<0.01$ (one-way ANOVA with Bonferroni posttest). FIRSV: Formaldehyde-inactivated RSV.

Figure 2.3

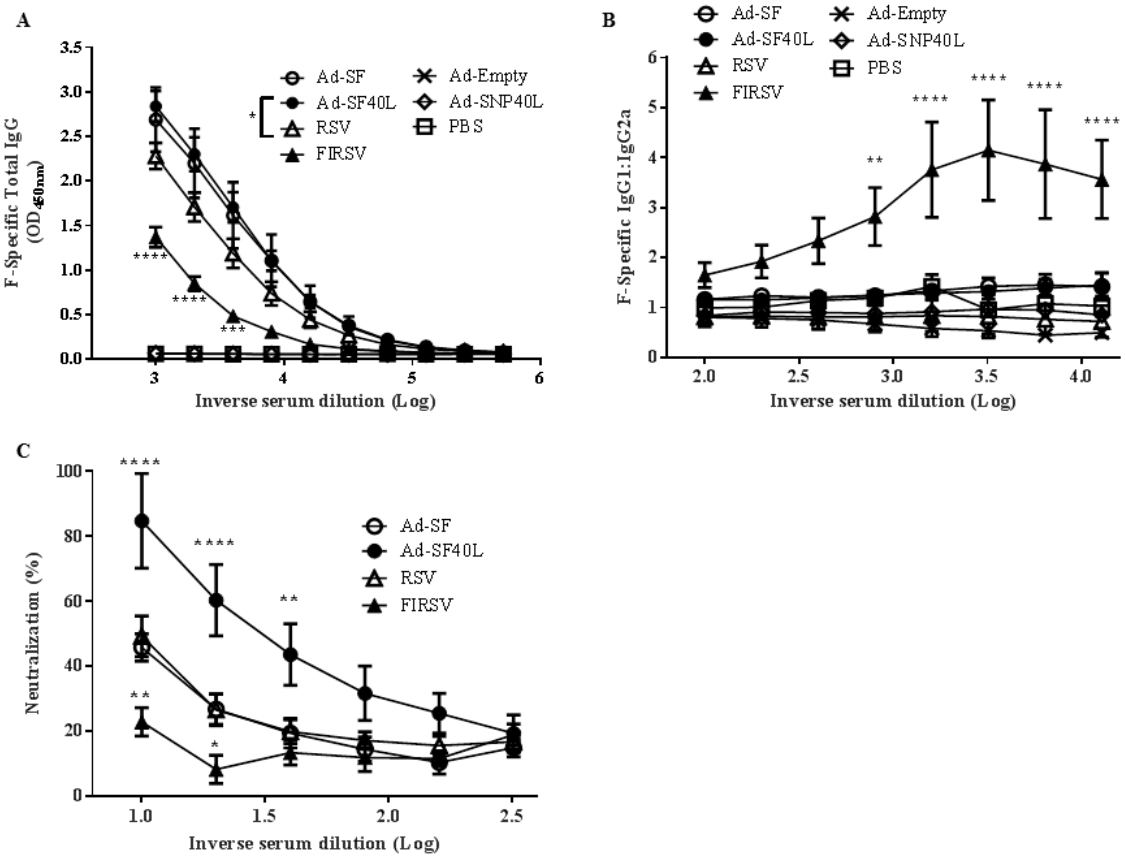
A
F-Specific Total IgG (OD450nm)
Inverse serum dilution (Log)
Ad-SF
Ad-SF40L
RSV
FIRSV
Ad-Empty
Ad-SNP40L
PBS
B
F-Specific IgG1:IgG2a
Inverse serum dilution (Log)
C
Neutralization (%)
Inverse serum dilution (Log)

Figure 2. 3: Ad-SF40L induces high levels of neutralizing antibodies. (A) F-specific total IgG in serum of primed/boosted mice 4 days post-challenge determined using ELISA (n=5). The * in the legend indicates a significant difference in F-specific total IgG between Ad-SF40L and RSV at dilutions 1/1000, 1/2000 and 1/4000. (B) F-specific IgG1/IgG2a ratio in mice serum to show the Th2 or Th1 nature of the immune response (n=5). (C) RSV neutralizing ability of the mice serum collected 4 days post-challenge (n=8). Data shown is mean ± SEM representative of 2 independent experiments; *$p < 0.05$, **$p<0.01$, ***$p<0.001$, ****$p<0.0001$ (two-way ANOVA with Bonferroni posttest).

Figure 2.4

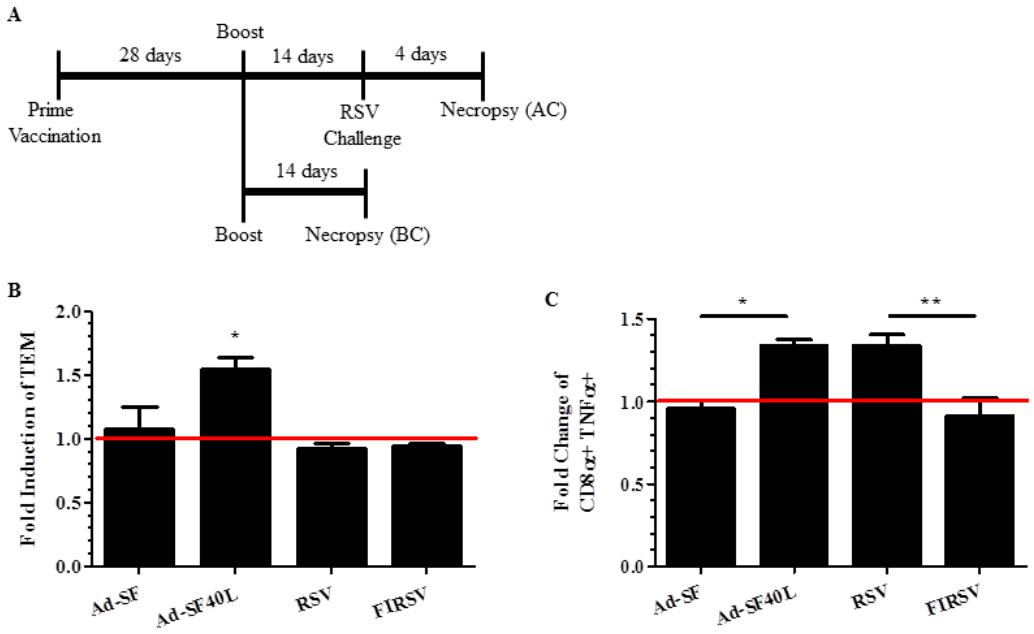
A
Boost
28 days
14 days
4 days
Prime
Vaccination
RSV
Challenge
Necropsy (AC)
14 days
Boost
Necropsy (BC)
B
Fold Induction of TEM
2.0
1.5
1.0
0.5
0.0
*
Ad-SF
Ad-SF40L
RSV
FIRSV
C
Fold Change of
CD8α+ TNFα+
1.5
1.0
0.5
0.0
*
**
Ad-SF
Ad-SF40L
RSV
FIRSV

Figure 2. 4: Increase in CD8 T cell effector phenotype and function following challenge is unique to Ad-SF40L immunization. (A) Schematic diagram of the animal study with BALB/c mice. Mice were necropsied for tissue collection before or after challenge. (B) Flow cytometry was used to determine the TEM population (CD3+ CD8a+ CD44+ CD62L- CCR7-) in the spleen. Induction of the TEM population as a result of the RSV challenge is shown as a ratio (TEM after challenge/TEM before challenge). A ratio of 1 indicates no change in the TEM population after challenge. (C) Intracellular cytokine staining was done following 4-hour ex-vivo stimulation with F85-93 peptide to analyze the number of CD8α+ TNF-α+ cells in the spleen using flow cytometry. Fold change of this population as a result of the challenge is shown (after challenge/before challenge). Data shown is mean ± SEM representative of 2 independent experiments; n = 4 per group; *$p < 0.05$, **$p<0.01$ (one-way ANOVA with Bonferroni posttest).

Figure 2.5

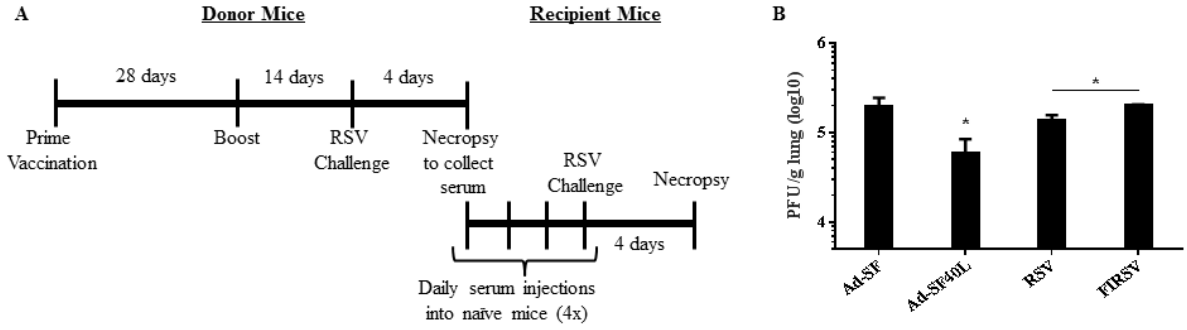
A
Donor Mice
Recipient Mice
28 days
14 days
4 days
Prime Vaccination
Boost
RSV Challenge
Necropsy to collect serum
RSV Challenge
Necropsy
4 days
Daily serum injections into naive mice (4x)
B
PFU/g lung (log10)
6
5
4
*
*
Ad-SF
Ad-SF40L
RSV
FIRSV

Figure 2. 5: CD40L enhances antibody-induced protection. (A) Schematic diagram of the animal study timeline. Passive serum transfer was done from immunized and challenged donor mice into naïve recipient mice. (B) Four days post-challenge, lungs from the recipient mice were collected for viral titer determination using plaque assay. Serum from Ad-SF40L immunized mice resulted in the highest lung viral clearance in recipients. Data shown is mean ± SEM representative of 2 independent experiments; n = 4 per group; *$p < 0.05$ (one-way ANOVA with Bonferroni posttest).

Figure 2.6

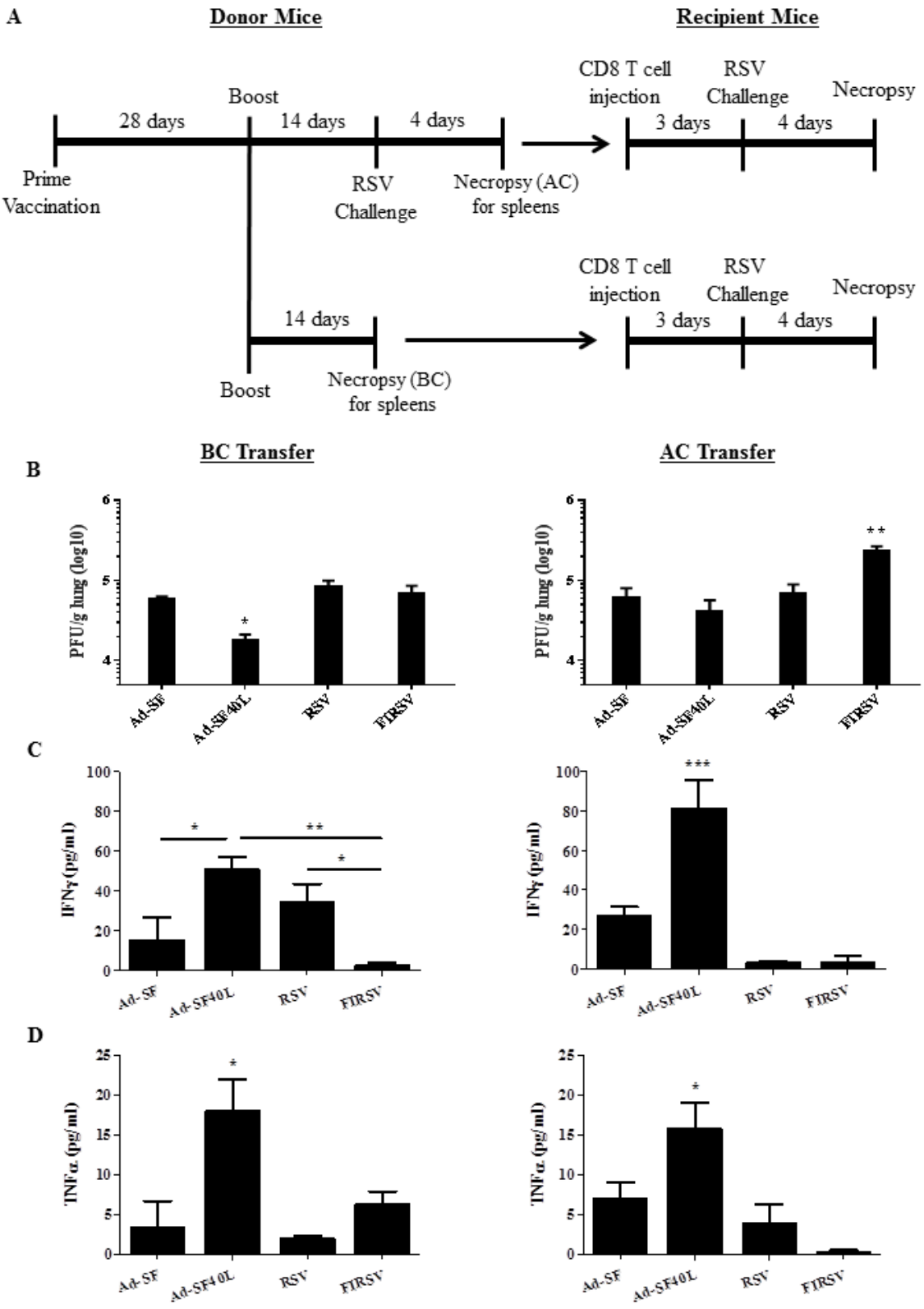
A
Donor Mice
Recipient Mice
28 days
Boost
14 days
4 days
Prime Vaccination
RSV Challenge
Necropsy (AC) for spleens
CD8 T cell injection
3 days
RSV Challenge
4 days
Necropsy
14 days
Boost
Necropsy (BC) for spleens
B
BC Transfer
AC Transfer
PFU/g lung (log10)
Ad-SF
Ad-SF40L
RSV
FIRSV
C
IFNγ (pg/ml)
D
TNFα (pg/ml)

Figure 2. 6: CD8 T cell effector function is altered following challenge of FIRSV-immunized mice unlike in Ad-SF40L immunization. (A) Schematic diagram of the animal study timeline. Adoptive CD8 T cell transfer was done from immunized donors either before (BC) or after (AC) challenge into naïve recipient mice. CD8 T cells were isolated from spleens of donor mice using a magnetic bead kit and checked for purity prior to transfer. (B) Four days post-challenge, lungs from the recipient mice from BC transfer (left) and AC transfer (right) were collected for viral titer determination using plaque assay. Ad-SF40L was compared to all groups (left) and FIRSV was compared to all groups (right). Comparisons between other groups showed no statistically significant differences. Secreted levels of IFN-γ (C) and TNF-α (D) were determined, using the Luminex system, in spleens of recipient mice from BC transfer (left) and AC transfer (right) following 48-hour ex-vivo stimulation with F85-93 peptide. Ad-SF40L was statistically different from all groups for both cytokines. Data shown is mean ± SEM representative of 2 independent experiments; n = 4 per group; *$p < 0.05$, **$p<0.01$, ***$p<0.001$ (one-way ANOVA with Bonferroni posttest).

Figure 2.7

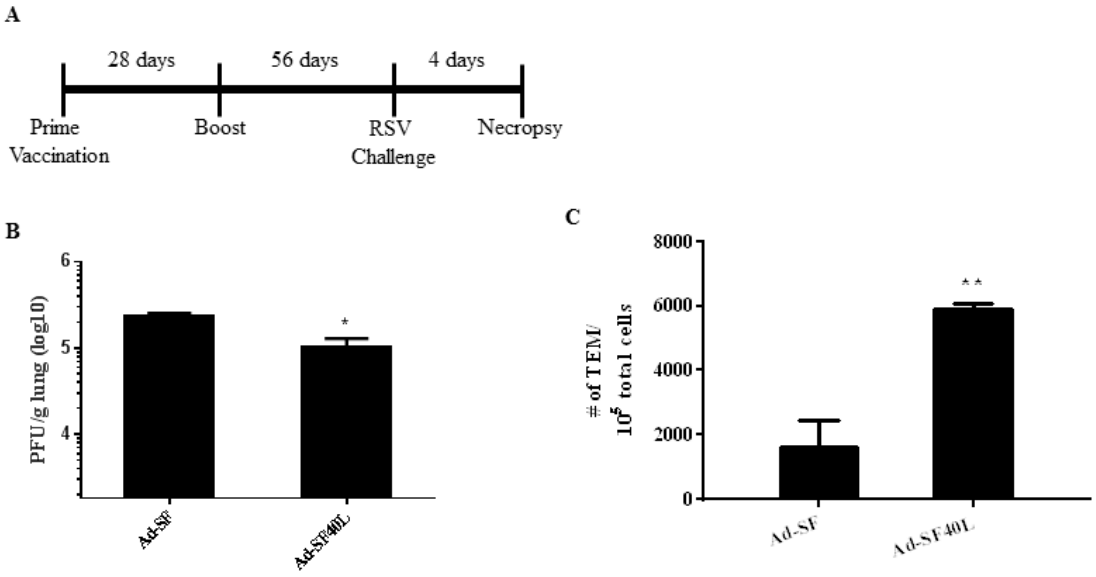
A
28 days
56 days
4 days
Prime Vaccination
Boost
RSV Challenge
Necropsy
B
PFU/g lung (log10)
6
5
4
*
Ad-SF
Ad-SF40L
C
# of TEM/ 10^5 total cells
8000
6000
4000
2000
0
**
Ad-SF
Ad-SF40L

Figure 2. 7: Ad-SF40L gives long-lasting protection from RSV infection accompanied by a durable CD8 T cell effector memory response. (A) Schematic diagram of the animal study with BALB/c mice. Mice were challenged 56 days after boost vaccination and necropsied 4 days after challenge. (B) Lung viral titer determined using plaque assay at necropsy. (C) Flow cytometry was used to determine the total number of TEMs (CD3+ CD8a+ CD44+ CD62L- CCR7-) in the spleen. Data shown is mean ± SEM; n = 4 per group; *$p<0.05$, **$p<0.01$ (unpaired Student's t-test).

Supplementary Information

Targeting CD40 enhances antibody- and CD8-mediated protection against respiratory syncytial virus infection

Abenaya Muralidharan[1,3], Marsha Russell[1], Louise Larocque[1], Caroline Gravel[1], Changgui Li[2], Wangxue Chen[4], Terry Cyr[1], Jessie R. Lavoie[1], Aaron Farnsworth[1], Michael Rosu-Myles[1,3], Lisheng Wang[3], Xuguang Li[1,3,*]

[1]Centre for Biologics Evaluation, Biologics and Genetic Therapies Directorate, HPFB, Health Canada and WHO Collaborating Center for Standardization and Evaluation of Biologicals, Ottawa, ON, Canada.

[2]National Institute for Food and Drug Control and WHO Collaborating Center for Standardization and Evaluation of Biologicals, Beijing, China

[3]Department of Biochemistry, Microbiology and Immunology, Faculty of Medicine, University of Ottawa, Ottawa, ON, Canada

[4]Human Therapeutics Portfolio, National Research Council of Canada, Ottawa, ON, Canada

[*]Corresponding author

Supplementary Table 2. 1: Primers used for cloning and sequencing of Ad-SF and Ad-SF40L constructs.

Name	Forward Primer (5’ – 3’)	Reverse Primer (5’ – 3’)
Primers for Cloning:		
Ad-SF40L	CACCGCCGCCACCATGCT	TCACAATTTCAACAAGCCAAA
Ad-SF	CACCGCCGCCACCATGCT	TCAATTGCTAAAGGCAATATTATTAATGCCGCTC
Primers for sequencing:		
SF40L-1F	CGCCGCCACCATGCTGCT	
SF40L-2F	AAAGGTAAAGCTCATCAAGCAGGAGC	
SF40L-3F	CAACAAGGCAGTAGTTTCCC	
SF40L-4F	GAGCAACAACGTCCAGATCGTGA	
SF40L-5F	TCTGCCTTCTGAAGTCAACTTGTGCA	
SF40L-6F	TATTAATTTCTATGACCCCCTGG	
SF40L-7F	TGGCTATATACCTGAGGCCCCCA	
SF40L-8F	CAAAGGCGAGGGGTCTCTGT	
SF40L-9F	GGTGACATTTTGCTCAAATCGCG	

Supplementary Figure 2.1

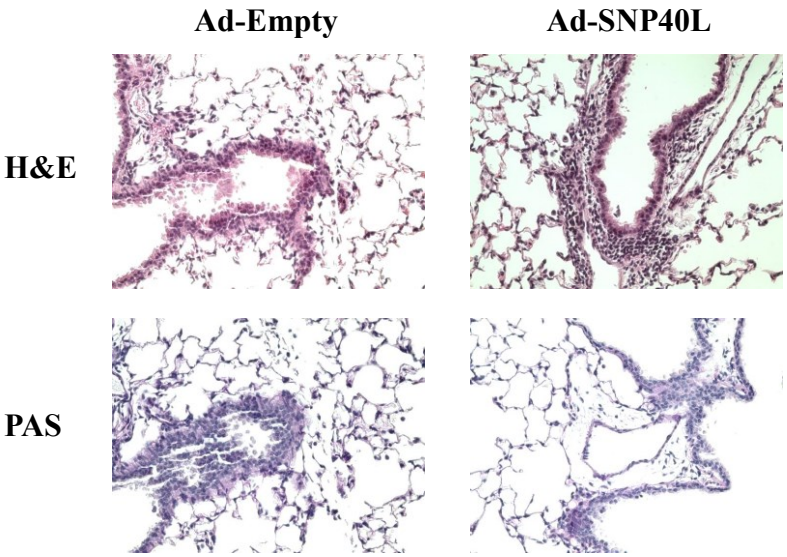

Supplementary Figure 2. 1: Representative image of H&E and PAS stained lungs of mice post-challenge. BALB/c mice were intranasally immunized twice with control vaccines, Ad-Empty or Ad-SNP40L, to determine the antigen specificity of the observed protection. Lungs were H&E and PAS stained 4 days post challenge for perivascular leukocyte infiltrate and mucus scoring, respectively. Representative images at 40x magnification are shown.

Supplementary Figure 2.2

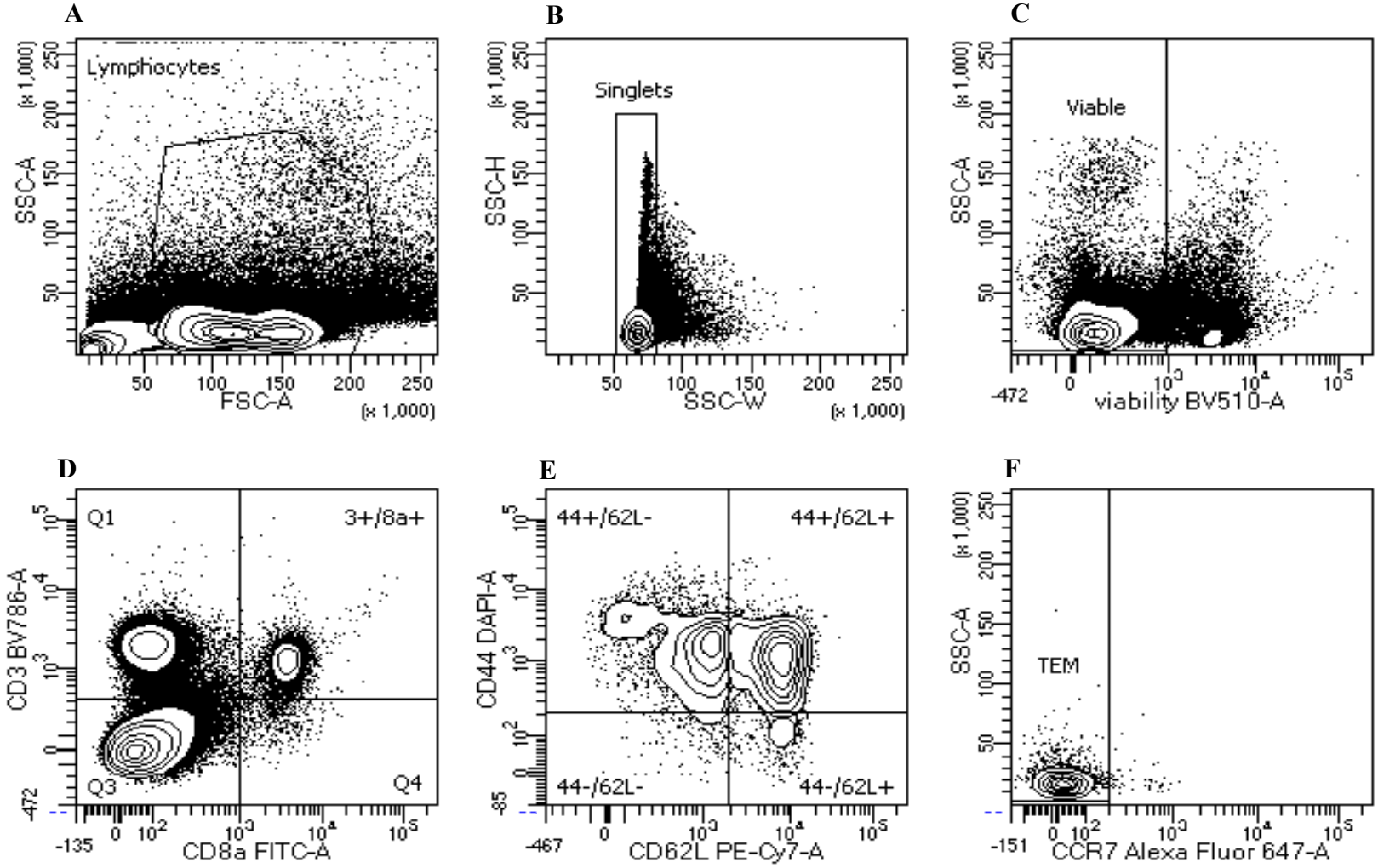

Supplementary Figure 2. 2: TEM gating strategy. Splenocytes were isolated from immunized BALB/c mice before or after challenge and stained for flow cytometry analysis. A FSC/SSC plot was done to gate for lymphocytes (A). Singlets were selected from the lymphocytes (B) and further gated for viable cells (C). The viable cells were then gated for CD3+CD8α+ (D). Next, the CD3+CD8α+ cells were analyzed for CD44+CD62L- (E), which were finally gated for CCR7- population (F). This CD3+ CD8a+ CD44+ CD62L- CCR7- is denoted as effector/effector memory CD8 T cells or TEM.

Supplementary Figure 2.3

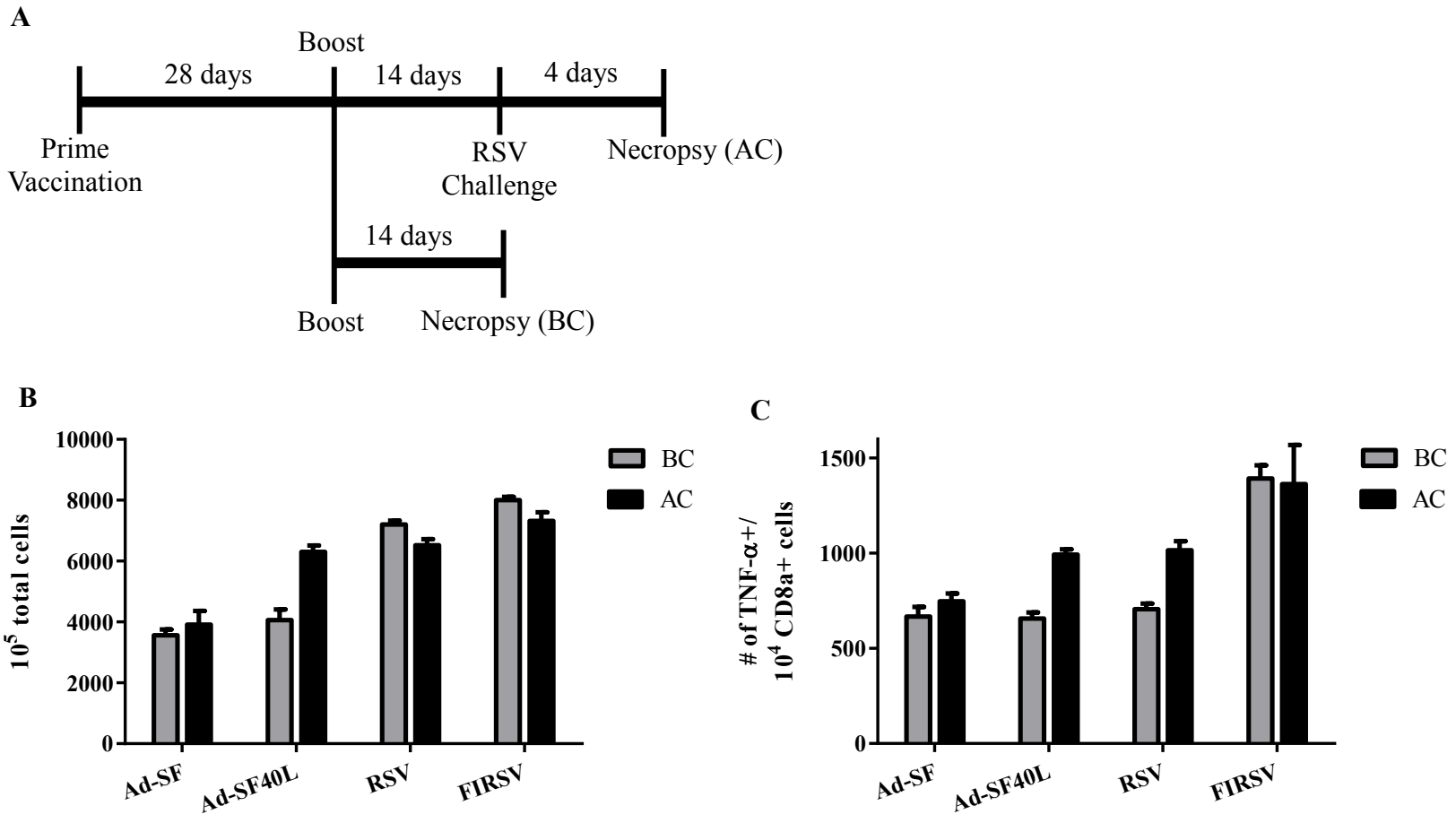

Supplementary Figure 2. 3: Increase in CD8 T cell effector phenotype and function following challenge is unique to Ad-SF40L immunization. (A) Schematic diagram of the animal study with BALB/c mice. Mice were necropsied for tissue collection before or after challenge. (B) Flow cytometry was used to determine the TEM population (CD3+ CD8a+ CD44+ CD62L- CCR7-) in the spleen. (C) Intracellular cytokine staining was done following 4-hour ex-vivo stimulation with F85-93 peptide to analyze the number of CD8α+ TNF-α+ cells in the spleen using flow cytometry. Data shown is mean ± SEM; n = 4 per group representative of 2 separate experiments; *$p < 0.05$, **$p<0.01$ (one-way ANOVA with Bonferroni posttest).

Supplementary Figure 2.4

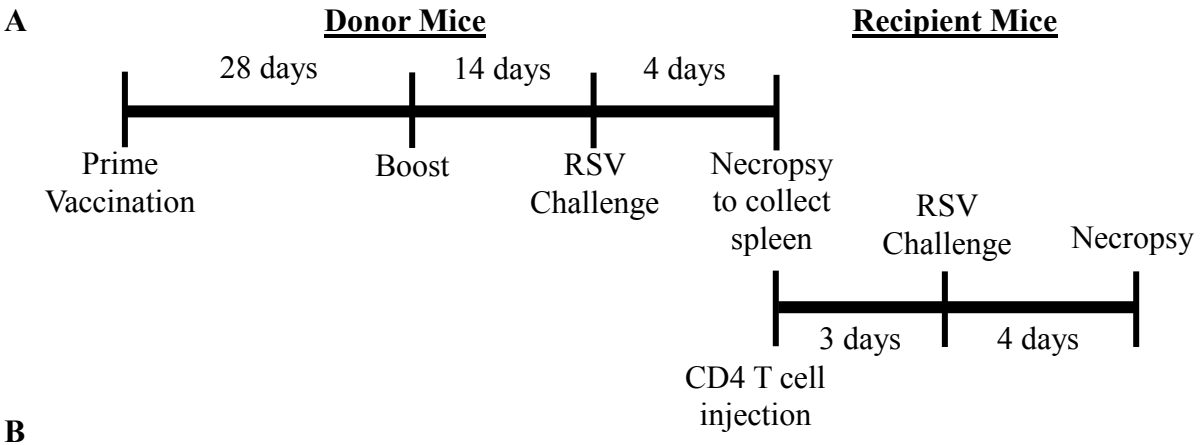

B

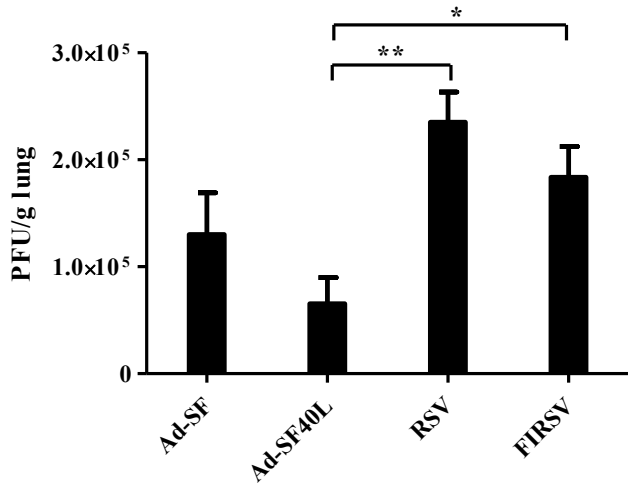

Supplementary Figure 2. 4: CD40L does not enhance CD4 T cell-induced protection. (A) Schematic diagram of the animal study timeline. Adoptive CD4 T cell transfer was done from immunized and challenged donor mice into naïve recipient mice. CD4 T cells were isolated from spleens of donor mice using a magnetic bead kit and checked for purity prior to transfer. (B) Four days post-challenge, lungs from the recipient mice were collected for viral titer determination using plaque assay. There were no significant differences between Ad-SF and Ad-SF40L group. Data shown is mean ± SEM; n = 4 per group; *$p < 0.05$, **$p<0.01$ (one-way ANOVA with Bonferroni posttest).

Chapter 3: PD-1 of *Sigmodon hispidus*: Gene identification, characterization and expression in inactivated RSV vaccine-induced enhanced respiratory disease

This manuscript is under review by the journal *Scientific Reports*. I contributed more than 50% to the manuscript. Xuguang (Sean) Li, Changgui Li, Wangxue Chen, Gary Van Domselaar, Terry Cyr, Lisheng Wang and I conceived the overall study. I performed the experiments and analyzed the data with the help of Louise Larocque, Marsha Russell and Marybeth Creskey. Xuguang (Sean) Li and I wrote the manuscript. All authors edited and approved the manuscript.

Emily Dupuis at Health Canada provided technical assistance with flow cytometry. Dr. Martha Navarro and the technicians at the Health Canada animal facility helped with the animal studies. Dr. Don Caldwell, veterinary pathologist at Health Canada, conducted expert analyses of the lung tissues. Finally, Drs Jessie Lavoie and Aaron Farnsworth critically reviewed the manuscript.

This manuscript sheds light on the role of programmed cell death-1 (PD-1) in FIRSV-induced ERD in cotton rats. Cotton rats may be the best model for development and evaluation of RSV vaccines and antivirals. However, the availability of immunological tools is limited for this animal model due to the lack of identification and characterization of important genes, mainly in the immune system. PD-1 is important for immune suppression and since there is exaggerated stimulation of the immune system during FIRSV-induced ERD, the PD-1 gene in cotton rats was sequenced and characterized.

PD-1 of *Sigmodon hispidus*: Gene identification, characterization and expression in inactivated RSV vaccine-induced enhanced respiratory disease

Abenaya Muralidharan[1,3], Louise Larocque[1], Marsha Russell[1], Marybeth Creskey[1], Changgui Li[2], Wangxue Chen[4], Gary Van Domselaar[5], Terry Cyr[1], Lisheng Wang[3], Xuguang Li[1,3,*]

[1]Centre for Biologics Evaluation, Biologics and Genetic Therapies Directorate, HPFB, Health Canada and WHO Collaborating Center for Standardization and Evaluation of Biologicals, Ottawa, ON, Canada.

[2]National Institute for Food and Drug Control and WHO Collaborating Center for Standardization and Evaluation of Biologicals, Beijing, China

[3]Department of Biochemistry, Microbiology and Immunology, Faculty of Medicine, University of Ottawa, Ottawa, ON, Canada

[4]Human Therapeutics Portfolio, National Research Council of Canada, Ottawa, ON, Canada

[5]National Microbiology Laboratory, Public Health Agency of Canada, Winnipeg, MB, Canada

[*]Corresponding author:

Dr. Xuguang (Sean) Li
Centre for Biologics Evaluation,
Biologics and Genetic Therapies Directorate,
Health Canada
Sir Frederick G. Banting Research Centre, A/L 2201E
251 Sir Frederick Banting Driveway
Ottawa, ON K1A 0K9, Canada
Tel: 613 954 2383
Fax: 613 941 8933
E-mail: Sean.Li@canada.ca

Abstract

Sigmodon hispidus or cotton rat is an excellent animal model for studying human infections of respiratory viruses including respiratory syncytial virus (RSV), which is the leading cause of hospitalization in infants and causes high rates of infection in the elderly and immunocompromised patient populations. Despite several decades of research, no vaccine has been licensed whereas inactivated vaccines have been shown to induce severe adverse reaction in a clinical trial, with other forms of RSV vaccine also found to induce enhanced disease in preclinical animal studies. While arguably the cotton rat is best small animal model for evaluation of RSV vaccine and antivirals, many important genes of the immune system remain to be isolated. Programmed cell death-1 (PD-1) plays an integral role in regulating many aspects of immunity by inducing suppressive signals. In this study, we report the isolation of mRNA encoding the cotton rat PD-1 (crPD-1) and characterization of the PD-1 protein. crPD-1 bound to its cognate ligand on dendritic cells and effectively suppressed cytokine secretion. Moreover, using the newly acquired gene sequence, we observed a decreased level of crPD-1 levels in cotton rats with enhanced respiratory disease induced by inactivated RSV vaccine, unraveling a new facet of vaccine-induced disease.

Introduction

Programmed cell death-1 (PD-1) is a receptor that belongs to the CD28 superfamily (184). It is a type I transmembrane glycoprotein composed of an IgV domain that exists as a monomer on the cell (185). Upon engagement of one of its two ligands, PD-L1 and PD-L2, it delivers negative signals in the immune system (184). When induced, PD-1 pathways play crucial roles in regulation of autoimmunity, transplantation immunity, infectious immunity and tumor immunity (184).

PD-1 expression is tightly regulated. Low basal levels are maintained on resting naïve T cells and some developing thymocytes which creates immune tolerance preventing autoimmunity (186–189). Following activation, PD-1 is transiently expressed on multiple immune cells such as CD4 and CD8 T cells, B cells, macrophages, natural killer cells and dendritic cells (187, 190–196). High expression is vital for regulatory T cell development while follicular helper T cells constitutively express high PD-1 (197–200).

The role of PD-1 in regulating T cell exhaustion during cancer and chronic infection is well established (189, 201). Specifically, PD-1 expression is upregulated on virus-specific T cells during chronic viral infections (184). The constant antigen exposure and prolonged T cell receptor stimulation leads to high levels of PD-1 and therefore, T cell exhaustion (202). Several studies involving a wide range of animal models and virus infections have demonstrated the importance of the PD-1 pathway. In non-human primates, blocking PD-1 resulted in rapid expansion of SIV-specific T cells drastically decreasing plasma viral load (203). Moreover, in mice, blocking the PD-1 pathway restored cytokine production, increased the number of lymphocytic choriomeningitis virus (LCMV)-specific T cells and enhanced viral clearance (204). In contrast, blocking PD-1 pathway during a respiratory

syncytial virus (RSV) infection in mice enhanced pulmonary inflammation and lung injury with modest effects on viral clearance (205).

RSV is the leading cause of hospitalization in infants (5, 7, 125, 128) with about 50% of children being infected in their first year of life (129, 130). RSV also causes severe disease in the elderly and immune-compromised patients (7, 125–127). In the 1960s, a clinical trial involving formaldehyde-inactivated RSV (FI-RSV) resulted in hospitalization of 80% of the participants and 2 deaths following a RSV infection (97–99, 206). This severe adverse reaction, commonly known as vaccine-induced enhanced respiratory disease (ERD), is yet to be fully understood but might be linked to the induction of a Th2-biased immune response leading to pulmonary inflammation, airway obstruction and mucus hypersecretion as observed in the trial participants and some animal models (100, 133, 134, 207).

Sigmodon hispidus (cotton rats) share many similarities in pathology with humans when infected by RSV. Notably, most findings in relation to FI-RSV induced ERD have been replicated in the cotton rats, making them one of the ideal animal models for RSV infection (208–211). Indeed, cotton rats have proven very useful in the study of human respiratory virus infections including the development and testing of antiviral drugs and vaccines for RSV, measles, influenza, human parainfluenza and human metapneumovirus (212). However, one of the major drawbacks with this animal model is the availability of research reagents because the genome has not been fully sequenced. As of today, approximately 300 genes have been sequenced in cotton rats that show 75-95% identity to mice and about 50% to humans (213), while few genes of the immune system have been sequenced. With increasing number of vaccines and therapeutics being evaluated in cotton rats prior to clinical trials, it would be important to better understand the immune system of this animal model (214–216).

It has been shown that PD1-PDL1 activation is vital for limiting immunopathology in

the context of a primary RSV infection in mice (205, 217). However, there have been no studies on the levels of PD-1 in cotton rats experiencing vaccine-induced ERD. Here, we report the isolation of cotton rat PD-1 (crPD-1) gene and characterization of the putative PD-1 protein. Using the newly identified gene sequence as a probe, we found significantly decreased levels of the PD-1 gene in ERD cotton rats following vaccination with FI-RSV, suggesting that downregulation of PD-1 could be associated with excessive pulmonary inflammation.

Results

Identification of cotton rat PD-1 sequence, species alignment and putative domains

The mRNA sequence of cotton rat programmed cell death receptor-1 (crPD-1) was isolated from cotton rat spleens (Figure 3.1). A 3' RACE strategy was applied, as previously described (218), using total RNA extracted from spleens as the starting material. Following isolation of mRNA from the total RNA using an oligo dT, primers designed from rodent consensus sequences were used to sequence from the 3' end to the 5' end in a stepwise fashion. The ORF was found to be 858 bp in length encoding 285 amino acids (aa) followed by a stop codon and 1027 bp 3' un-translated region.

Alignment of the crPD-1 protein sequence with other species revealed an 88% identity with Chinese hamster, 87% with prairie vole, 84% with brown rat, 82% with mouse, and 59% with human PD-1 (Figure 3.2A). Phylogenetic tree analysis showed a shared homology of crPD-1 with other members of the Cricetidae family (Figure 3.2B).

Next, we mapped the structure and functional domains of crPD-1 by comparing to other well-characterized PD-1. In Figure 3.3, various putative domains on crPD-1 are

annotated. The putative ectodomain spanning amino acid 30 to 147 consists of a single extracellular IgV domain of PD-1 (aa 35-144), which is common to members of the CD28 family (184). Within the putative IgV domain are the residues involved in the binding of the two ligands of PD-1, PD-L1 and PD-L2. Residues S73, N74, L86, P130 and K131 are involved in PD-L1 binding whereas residues V77, P89, A125, I126, P129 and Q133 bind PD-L2. Amino acids M64, N66, Y68, Q75, T76, K78, C83, K84, Q88, V90, L122, G124, L128, T132, I134 and E136 on PD-1 are involved in both PD-L1 and PD-L2 binding. The structure of the putative ectodomain of crPD-1 was visualized using EZmol software and is shown in Figure 3.3B (219).

In vitro expression of recombinant cotton rat PD-1

For further validation, the sequenced crPD-1 gene was synthesized and cloned into a pcDNA3.1(+) vector. The synthesized gene also consisted of rat codon optimized secretion signal and ten histidine residues at the 5'-end. Expression of this recombinant crPD-1 was conducted in 293T cells. Following his-tag purification, protein expression was confirmed using western blot with anti-his antibody (Figure 3.4A), mass spectrometry (Figure 3.4B) and immunofluorescence staining of transfected cells with both anti-PD1 and anti-his antibodies (Figure 3.4C). Under reducing conditions, the western blot showed a band at 37 kDa for the crPD-1 whereas this band was absent in the lipofectamine control (no plasmid). A band seen at approximately 60 kDa in both crPD-1 and lipofectamine control is likely to be cross-reaction of the antibody with proteins in the media, likely albumin. To serve as a positive control, a mouse recombinant PD-1 (rmPD-1) containing a his-tag was run alongside (Figure 3.4A).

Next, mass spectrometry analysis of the purified samples and rmPD-1 against the newly obtained crPD-1 sequence revealed a match of seven peptides in the crPD-1 sample found at high abundance and two peptides at low abundance with total sequence coverage of 41% (Figure 3.4B). No peptides from the crPD-1 sequence were found in the lipofectamine control and two peptides were found in the rmPD-1 sample. Comparing the rmPD-1 against the mouse PD-1 sequence resulted in sequence coverage of 33% (Figure 3.4B).

Since the commercial anti-human/mouse/rat PD-1 antibody could not detect the rmPD-1 under reducing conditions during western blotting, immunofluorescence was used to confirm co-expression of crPD-1 and the his-tag. While the lipofectamine control showed no fluorescence, crPD-1 transfected 293T cells showed fluorescence with both antibodies (Figure 3.4C). Co-expression is shown by merging the two fluorochromes.

Characterization of crPD-1 functional activity in vitro

As crPD-1 and mouse PD-1 share 82% protein identity with similar functional domains, we used mouse bone marrow derived dendritic cells (DCs) expressing PD-L1 to evaluate the functional activity of crPD-1. To this end, DCs were incubated with purified crPD-1 or rmPD-1 for 4 hours. Following incubation, the DCs were stained with a viability dye and an anti-human/mouse PD-L1 blocking antibody for flow cytometry analysis. A competitive binding strategy summarized in Figure 3.5 (left) was applied, i.e. if the added PD-1 protein was in its functional conformation, it would bind to PD-L1 expressed on the DCs preventing the PD-L1 blocking antibody from binding to the ligand resulting in lower fluorescence than cells not treated with a PD-1 receptor. However, if PD-1 cannot bind PD-L1 or binds with low affinity, the PD-L1 antibody would bind its epitope and, as a result, fluorescence would

be quantitatively detected. Our results show that among viable cells, the detected mean fluorescence intensity (MFI) of PD-L1 significantly decreased with the addition of crPD-1 ($p = 0.039$) and rmPD-1 ($p = 0.04$) compared to no treatment control (Figure 3.5). This result confirmed that expressed crPD-1 protein is capable of binding to its cognate ligand.

We next investigated whether crPD-1 could reduce IL-6 and TNF-α secretion by activated DCs, given interaction between PD-1 and its ligands is known to induce immunosuppressive pathways leading to decreased pro-inflammatory cytokine production (184, 205, 220). To this end, mouse DCs were stimulated with LPS along with crPD-1 or rmPD-1 for 24 hours prior to ELISA quantitation of IL-6 and TNF-α. Compared to the control group treated with LPS only, both crPD-1 and rmPD-1 treatment resulted in considerable decrease of IL-6 and TNF-α expression (Table 3.1). While magnitude of decreased IL-6 levels was comparable between crPD-1 and rmPD-1, rmPD-1 is slightly more effective in reducing TNF-α expression by mouse DCs, an observation likely due to imperfect match between the two species. Nonetheless, these results indicate that crPD-1 could effective suppress proinflammatory cytokine production, consistent with functional roles played by PD-1 derived from other species including human and mouse.

Downregulation of crPD-1 in ERD cotton rats

Having confirmed the functional activity of isolated crPD-1 *in vitro*, we set out to investigate whether crPD-1 could be downregulated in cotton rats suffering enhanced respiratory disease (ERD) as a result of inactivated RSV vaccination, given exacerbated pulmonary inflammation is one of the well-documented pathological findings (133, 212). To this end, we first established the ERD model based on previously reports (100, 133). Cotton rats were

immunized twice with formaldehyde-inactivated RSV (FI-RSV), formaldehyde-mock control (FI-Mock), live wild-type RSV-A2, or saline (PBS), followed by viral challenge with RSV-A2 four weeks after second immunization. The animals were euthanized 5 days post-challenge for lung viral titer and pathological analysis. Unlike FI-Mock and PBS-immunized rats, immunization with wild-type RSV resulted in effective clearance of virus in the lungs (Figure 3.6A); FI-RSV immunization also effectively reduced virus replication albeit less effectively than RSV immunization ($p = 0.015$).

Next, we examined hematoxylin and eosin (H&E) stained lung tissues post-challenge to confirm the extensive tissue damage that accompanies FI-RSV induced ERD, as observed in previous studies (221). Prominent alveolitis with infiltrating neutrophils, macrophages and lymphocytes along with a few eosinophils in alveolar spaces were clearly observed in the FI-RSV immunized cotton rats, whereas other immunization groups did not display similar pathological presentations (Figure 3.6B). Moreover, peribronchiolitis had a similar pattern of cellular infiltration as alveolitis as well as marked perivascular leukocyte infiltrates throughout the lung sections, which were absent or very mild in other groups (Figure 3.6B).

Having observed pathological presentations of ERD in FI-RSV immunized cotton rats, we next investigated the PD-1 mRNA expression in the lung tissue using primers and probes designed from the newly acquired gene sequence. Using quantitative real-time PCR, C_T values were collected and first, normalized to β-actin for each cotton rat, then, analyzed for fold change over the respective controls: FI-RSV over FI-Mock and RSV over PBS. FI-RSV immunized rats showed a 50% decrease in pulmonary PD-1 expression compared to FI-Mock, whereas RSV immunized rats had a fold change of 1 compared to the PBS group (Figure 3.7). Moreover, FI-RSV induced a significant downregulation of PD-1 in the lung tissues compared to live RSV immunization ($p = 0.025$). Taken together, these results

revealed that decreased levels of pulmonary PD-1 was associated with ERD in animals vaccinated with inactivated RSV vaccine upon subsequent viral infection.

Discussion

Sigmodon hispidus or cotton rats are an excellent animal model for studying human respiratory virus infections (133, 212). For RSV infections, cotton rats are considered the gold standard for development of antivirals, vaccines and biotherapeutics (214–216). While this animal model was successfully used to determine the dosing, safety and efficacy of the only licensed therapeutic antibody against RSV (214–216), very few genes of cotton rats have been cloned and characterized, substantially limiting this model's wider applications, particularly for mechanistic investigation of virus-induced pathogenesis and immune responses. Here, we report, for the first time, the mRNA sequence of cotton rat PD-1 and its expression in inactivated RSV vaccine-induced ERD.

Similar to other genes sequenced in the cotton rats (213), crPD-1 shares 75-95% homology to mice and rats, and about 50% homology to humans (Figure 3.2); phylogenetic analysis showed higher amino acid identity to its own family, Cricetidae, and distant relationship to primates, as expected. Moreover, structural mapping of the putative functional domains revealed high conservation rates among rodents, especially for residues involved in PD-L1 and PD-L2 binding (Figure 3.3).

Recombinant crPD-1 protein produced by cells transfected with the newly-isolated gene was found to effectively bind PD-L1 (Figure 3.5) on DCs; it could also suppress cytokine production by activated DCs (Table 3.1), confirming the functional activity of crPD-1. With the newly isolated crPD-1 gene as a molecular probe, we determined the

expression of crPD-1 in the lungs of wild-type RSV and FI-RSV immunized cotton rats following RSV challenge. As previously reported (100, 221), cotton rats twice-vaccinated and challenged with live RSV were able to effectively clear the virus from their lungs and had mild pulmonary inflammation accompanied by cellular infiltration, while FI-RSV immunized rats had moderate viral clearance and exacerbated pulmonary inflammation (Figure 3.6). Importantly, we found significant downregulation of PD-1 in the FI-RSV group, whereas the level of PD-1 remained unchanged in other groups including live RSV vaccination and primary infection controls, PBS and FI-Mock (Figure 3.7). Indeed, increased production of proinflammatory cytokines is one of several significant immunological deregulations in ERD cotton rats vaccinated with inactivated RSV followed by virus infection (222–224). Taken together, these observations indicate that PD-1, while not implicated in viral clearance, may have significantly contributed to exaggerated pulmonary pathology and ERD.

While this is the first report of PD-1 expression levels evaluated in the context of RSV vaccine-induced ERD, the relationship of reduced levels of PD-1 and enhanced pulmonary pathology could also be corroborated by findings from the mouse model of severe RSV infection. Specifically, following high dose of RSV infection, exacerbated pulmonary inflammatory response was characterized with over production of pro-inflammatory cytokines and increased infiltration of inflammatory cells similar to that of vaccine-induced ERD (225–227), while blockade of PD1-PD-L1 pathways at the time of T cell infiltration into the lungs resulted in augmentation of pulmonary inflammation and tissue injury with minimal effects on viral clearance (205). Indeed, the engagement of PD-1 with inflammatory DC-derived PD-L1 is crucial for regulation of pro-inflammatory cytokine release by effector CD4 and CD8 T cells, resulting in control of effector T cell activities in the lungs. In addition,

they showed that blocking PD-L1 following RSV infection enhanced weight loss and lung histopathology in mice (159, 205). Taken together, our observations are in good agreement with severe RSV infection in the murine model where low levels of PD-1 induction accompany enhanced respiratory disease.

In short, the gene encoding crPD-1 is 858 bp in length encoding 285 amino acids followed by a stop codon and 1027 bp 3' un-translated region. The protein shares homology of 82-88% with other small rodents and 59% with its human counterpart. Functional characterization revealed that the crPD-1 protein bound to its ligand expressed on dendritic cells and effectively suppressed IL-6 and TNF-α secretion. Moreover, PD-1 gene expression was substantially downregulated in the lung tissues of the cotton rats with ERD, suggesting its possible involvement in exacerbated pulmonary inflammation in the diseased animals. The availability of the PD-1 gene and protein could facilitate future studies of vaccine-induced protection or -associated disease enhancement in addition to other immunological investigations in the cotton rat model.

Methods

Animals and Ethics Statement

Six to seven week old cotton rats were obtained from Envigo, Somerset, N.J., USA. All animal experiments were reviewed and approved by Institutional Animal Care and Use Committee of Health Canada and were conducted in accordance with Institutional Animal Care and Use Committee of Health Canada guidelines and regulations.

Cells, Viruses and Vaccines

293T (ATCC: CRL-3216) were grown in Dulbecco's Modified Eagle Medium (DMEM) supplemented with sodium bicarbonate, HEPES, Penicillin, Streptomycin, and 10% FBS. Primary bone marrow derived dendritic cells from C57BL/6 mice were cultured in media from manufacturer (Cell Biologics) supplemented with 10% FBS, 2-mercaptoethanol, L-Glutamine, Penicillin and Streptomycin. HEp-2 (ATCC: CCL-23) were grown in DMEM supplemented with sodium bicarbonate, Glutamax, HEPES, Penicillin, Streptomycin, and 10% FBS.

RSV-A2 (ATCC: VR-1540) was grown in HEp-2 cells according to supplier's instructions and sucrose-purified for animal studies. FI-RSV was prepared with the RSV-A2 strain in HEp-2 cells as described elsewhere (135). FI-Mock was made with uninfected HEp-2 cells using the same procedure as FI-RSV.

Isolation and Sequence Determination of Cotton Rat PD-1 cDNA

Total RNA was isolated and 3' RACE was conducted as previously described (218). Briefly, spleens from naïve cotton rats were removed aseptically and frozen. An eighth of the spleens

were cut and homogenized with a TissueLyser II (Qiagen). Total RNA was extracted using the RNeasy Mini kit (Qiagen) with on-column DNase digestion according to the manufacturer's instructions. The 3' RACE system (Life Technologies) was then used to amplify the 3' portion of the cotton rat PD-1 from the total RNA according to the user's manual. Following first strand cDNA synthesis using an oligo dT adapter primer, the 3' portion of the cotton rat PD-1 mRNA was PCR amplified using the abridged universal amplification primer and consensus sequences derived gene specific primer (5'–GGAGTCCGGTTCTGTGTACCT–3') at an annealing temperature at 55˚C. The gene specific primer was determined by aligning the PD-1 sequences of *Microtus ochragaster* (NCBI Reference Sequence: XP_005361412.1), *Cricetulus griseus* (NCBI Reference Sequence: XP_003499314.1), *Mus musculus* (NCBI Reference Sequence: NP_032824.1) and *Rattus norvegicus* (NCBI Reference Sequence: XP_017451871.1). The PCR products obtained were run on a DNA gel and excised using a Qiagen QIAquick Gel Extraction kit as per manufacturer's procedure. All amplified fragments were sequenced with BigDye Terminator v.3.1 Cycle Sequencing kit (ThermoFisher) using a 3130xl Genetic Analyzer (Applied Biosystems) following amplification in a PTC-200 thermal cycler (MJ Research). Raw sequencing data was edited using 3130xl Genetic Analyzer Data Collection Software v3.0 (Thermo Fisher), and then imported into GeneCodes Sequencher v4.6.1 sequencing analysis software for further editing. The final sequenced contigs were then imported to NCBI BLAST (https://blast.ncbi.nlm.nih.gov/Blast.cgi) to confirm the identity. Reverse primers were designed as fragments of the gene were sequenced until the gene encoding the complete PD-1 protein (determined by aligning against other species) was found.

Sequence and Phylogenetic Analysis

Putative functional domains, intracellular and extracellular domains, and ligand binding sites were determined using a standard protein BLAST (https://blast.ncbi.nlm.nih.gov). Sequences with significant alignments were imported into Geneious Pro version 5.6.7 (Auckland, New Zealand) for phylogenetic analysis. Multiple alignment was conducted using the Clustal Omega tool from EMBL-EBI.

crPD-1 Gene Synthesis, Protein Expression and Purification

After confirmation of the full mRNA sequence, the gene was synthesized and cloned into a pcDNA3.1(+) vector (GenScript). The synthesized gene began with a kozak sequence (5'-GCCGCCACC-3') followed by a 23-amino acid secretion signal (MLLAVLYCLLWSFQTSAGHFPRA) from the human tyrosinase signal peptide as previously shown (228). Following the secretion signal, ten histidine residues were added to facilitate protein purification, followed by the complete 1885 bp crPD-1. Rat-codon optimized sequences were used for gene synthesis.

293T cells were transiently transfected with the pcDNA vector containing the recombinant crPD-1 for 5 hours with Lipofectamine® 2000 (Invitrogen). After the 5-hour incubation, the lipofectamine-DNA containing media was removed, growth media was added and cells were incubated overnight at 37ºC. The next day, cells were washed, scraped and lysed with a standard RIPA cell lysis buffer. Following sonication of the lysed cells, the samples were his-tag purified using a His Mag Sepharose^{TM} excel kit (GE Healthcare) according to manufacturer's instructions. The samples were then dialyzed in PBS for functional studies.

Western Blot, Mass Spectrometry and Immunofluorescence

Samples resulting from his-tag purification were used for western blotting and mass spectrometry for confirmation of protein expression. A recombinant mouse PD-1 protein with a his-tag at the C-terminus (Abcam) was used alongside. Western blotting was performed using 4 to 15% TGX gel and Tris/Glycine/SDS running buffer (Bio-Rad Laboratories Inc.). The protein samples were then transferred to PVDF membranes (Millipore) and detected with mouse tetra-His antibody (Qiagen) and goat anti-mouse IRDye-800CW (LiCor). Membranes were visualized using the Odyssey system (LiCor).

Mass spectrometry was performed after the samples were cysteine-reduced, alkylated, and then digested on filter with trypsin. Resulting peptides were injected onto an Easy-nLC 1000 for reversed phase separation and analyzed with an Orbitrap Fusion Tribrid Mass Spectrometer operating in DDA mode with HCD fragmentation. The data was processed with Proteome Discoverer 2.2 software searching databases of rat proteins, common laboratory contaminants, and crPD-1.

Immunofluorescence was used for further confirmation of protein expression. 293T cells were seeded at a density of 30,000 per well in growth media in a 96-well flat clear bottom black plates. Next day, the cells were transfected with 1µg crPD-1 in pcDNA vector for 24 hours. On the following day, transfected cells were fixed with cold cytofix/cytoperm (BD Biosciences). After blocking with 3% IgG-free BSA diluted in wash buffer (1x PBS with 0.1% Tween 20) for 1 hour at 37ºC, the cells were stained with a mixture of unconjugated rabbit anti-human/mouse/rat PD-1 antibody (Abcam) and mouse tetra-His antibody (Qiagen) for 1 hour at 37ºC. Then, a mixture of Alexa Fluor 555-conjugated anti-

mouse IgG (Invitrogen) and Cy2-conjugated anti-rabbit IgG (Jackson Immunoresearch) was added for 1 hour at 37ºC. The cells were imaged using the EVOS FL microscope: Alexa Fluor 555 in the RFP and Cy2 in the GFP channel.

Flow Cytometry

Dendritic cells were seeded at 300,000 per well in growth media in a 96-well round bottom plate. Seeded cells were incubated with 30 µg/ml purified and dialyzed crPD-1 or recombinant mouse PD-1 (Abcam) for 4 hours at 37ºC. Following the incubation, the plate was centrifuged, supernatant was removed and the cells were stained for flow cytometry analysis. Cell suspensions were washed with PBS and first, stained with Fixable Viability Dye eFluor® 506 (eBioscience) for 30 min, then, with purified anti-mouse CD16/CD32 (eBioscience) as a Fc block for 5 min. Next, cells were washed with FACS wash buffer (PBS with 1% BSA and 0.05% sodium azide) and stained with PE-conjugated anti-human/mouse PD-L1 antibody (CD274; eBioscience, clone MIH1). Stained samples were run on the same day on a BD LSRFortessa flow cytometer. Data analysis was completed using FACSDiva version 8.0.1.

Quantitation of Cytokines

Dendritic cells were seeded in growth media containing 0.02 µg/ml LPS. The cells were incubated with or without 20 µg/ml crPD-1 or recombinant mouse PD-1 (Abcam) for 24 hours at 37ºC. The next day, the plates were centrifuged and supernatant was collected for cytokine quantitation using ELISA. Mouse DuoSet® ELISA Kits (R&D Systems) for IL-6 and TNF-α were used as per manufacturer's procedure. The absorbance was read on a

BioTek Synergy 2 plate reader.

Animal Studies

On day 0 and day 21, 6 to 7-week old cotton rats were intramuscularly vaccinated with $1x10^6$ PFU FI-RSV, FI-Mock or PBS buffer. The RSV group was intranasally vaccinated at $1x10^6$ PFU. On day 49, all animals were challenged intranasally with $1x10^6$ PFU of RSV-A2. Five days post-challenge, the animals were euthanized. The lungs were removed and one lobe was used for virus titration while the other lobe was fixed in 10% neutral buffered formalin (Sigma) under 25cm of water pressure. Lungs for RNA isolation were snap frozen in liquid nitrogen.

Lung Viral Titration

Lungs were removed 5 days post RSV challenge and tittered as described elsewhere (135). Briefly, half the lungs were collected in serum free RPMI media and weighed prior to mechanical homogenization. The homogenates were clarified using centrifugation and the supernatants were serially diluted and incubated on HEp-2 cells for 2 hours at 37ºC. A 1:1 overlay of 2x DMEM media and 0.8% agarose was added. Following 6 days of incubation, the overlay was removed and the cell monolayer was stained with crystal violet before counting plaques. Results are expressed as PFU/g lung tissue.

Lung Histology

Half the lung fixed in 10% formalin 5 days following RSV challenge were trimmed, processed and embedded into paraffin blocks. Five-micron H&E stained slides were made

for evaluation by a certified veterinary pathologist who was blinded to the experimental design. Each sample was assessed for peribronchiolitis and alveolitis.

Real-Time Quantitative PCR

Frozen lungs from PBS, RSV, FI-RSV and FI-Mock immunized cotton rats were cut, homogenized and total RNA was extracted as described above for spleens. Superscript III First Strand Synthesis System (Invitrogen) was used to generate cDNA according to manufacturer's instructions. The cDNA was then used for quantitative PCR using TaqMan® Fast Advanced Master Mix (Applied Biosystems) as per the manufacturer's procedure. A forward primer (5'-CACTGTAACCTATGACCTCTGG-3'), a reverse primer (5'-CCTTTTCCCTCTTTTGATGCTG-3') and a TaqMan® probe (5'-TTGCCTCTCCCTACTCTTCCCCT-3') with a MGBNFQ 3' quencher and 6FAM 5'dye were designed to target crPD-1. β-actin was used as the reference gene and was targeted using a primer-probe set described elsewhere (229). Quantitative real-time PCR was conducted on an ABI Prism 7500 Fast Sequence detection system (Applied Biosystems) and C_T values were obtained. Fold change over control immunization groups was calculated using the ΔC_T method using β-actin as the reference gene (230).

Statistical Analysis

Analysis was conducted using unpaired Student's t-test, one-way ANOVA where appropriate. Bonferroni posttest was used to adjust for multiple comparisons between different test groups. Tests were done at a 5% significance level. All statistical analyses were performed using GraphPad Prism 7 software.

Data availability: The datasets generated during and/or analyzed during the current study are available from the corresponding author on reasonable request. The mRNA and amino acid sequence of crPD-1 can be found in GenBank: Accession # MK040464.

Figures and Tables

Figure 3.1

5’ –
ATGTGGGTCCAGCAGGTGCCCTGGCCACTCACTTGGGCTGTGCTACAGTTGAGCTGGCAAGCAGGGT
GGCTTCTAGAGATCCCCAACGGGCCCTGGAGGCCCCTCACCTTCTCCCCAGCCTGGCTCACAGTGGC
AGAGGGAGAAAATGCCACCTTCACCTGCAGTTTTTCCAACTGGTCTGAGGACCTTATGCTGAACTGGT
ACCGCCTGAGCCCCAGCAACCAGACTGTGAAACAAGCCGCTTTCTGCAAAGGTCTCAGCCAGCCTGT
CCAGGACAAACGCTTCCAGATCACACAGCTGCCCAATGGGCATGACTTCCACATGAACATCCTTGCCG
CTAGGCGCAATGACAGTGGCATCTACCTCTGTGGGGCCATCTCCCTGCCCCCCAAGACACAAATCAAG
GAGAGTCCTGGAGCAGAGCTTGTGGTAACAGAGAGAATCCTGGAGACCTCAACAAGATACTCCAGTC
CCTCACCCAGACCAGCAGGCCAGTTTCAAGGCTTGGTCATTGGTATCATGAGCATCCTAGTGGGGGTC
CCTGTGTTGCTTCTGCTGGCCTGGGTCCTAGCTGCCTTCTGCTCAACAGAAACCAGAAGAGTTGAAA
GCAAGGAACAGCCTCAGGAAGACAACCACTCAGCAGCACCTGTCTTCAGTGTGGCCTACGAAGAGT
TGGATTTCCATGGACGAGAGAAGACTCCAGAGCTCCCCACCTCCTGTGTACACACAGAGTATGCCACT
ATTGTCTTCACAGAAGGGCTGGGTGCCTCATCCTTAGGACGAAGGGGCTCAGCTGATGACCTTCAAG
GTCCTCGACCTCCAAGGCATGAGGATGGACACTGCTCTTGGCCCCTTTGACCAGATGCTTTAGCCAGT
CACATCCTGCAGACTCTCCACTGAGAGCACCGGTGCATTCCTCCATCAGGAGTAAGGTGCAGGCTATA
CTGCAGCAAAGGCTCCCAGGGTCTGAGCTACACAGAGTGACAGCCTAGCAGTTGTATCGATTCCAAC
ACATGTGTTGTTGAGTGACAGATCTCTTAATGTTTACCACAAGCTGGAAGCAGCAGGCATCCCTGTTC
CCTGTGTCACAAAGTGCAGAGCTGGCCTGAGCATAGGTCTCCTGAGTCTGCTGCTGGGTCCTGCTAG
GGGCTTGAGTCACTGTAACCTATGACCTCTGGGGCCTGGAAATGGGGGAACCTCATTAGAGGTGCCT
GTGGGGTACCCCCATAACAAGAGGCTCCAAGTAACAGTAGACAGAGCACCTAAAGCTGCCCTTGAGA
GATACTCAGGAAATTCATAGACTGGGGAACGTAGGGACTCTGAACTAATCTCAGGGCCTGGAGAGAT
TCTGGTGAAAACTAGAAAAATCCCTAGCTTCAGGGGTCTGGGGAAGCATGAATACTCAGCAGACAAA
GGCTCTGCAAGGGTCTTTGCTGTTCTTCTGCATGCACAGGTACCTCAGCTCTTTCTACAGCTGGGAAA
CTGAGGCAGTGAAGGAAACGAAAAGATCTAGAGGCCTACCCACACCTCCAGTGAGGCACTTGCCTCT
CCCTACTCTTCCCCTGGGGACCAAAAGGACAGGTCCCATGTCAGCATCAAAAGAGGGAAAAGGGAG
ACCCAATTTGACTTGCCCCAACTGTGGCCATCTTGAATAGGGATCTGGTTGTTGAGGTCTCTCCATTCA
TCGTCTCTCTCCTGGAGTCCGGTTCTGTGTACCTTCACACTGTGGCCGTGAAGTGGACAAAGGGTTTT
TAGGCATCCCCTTGGCACTTCAGACAGGCAAGGTAGCACGAGCCTAGCTGTCTGGTGGGCACCCAGA
TGGCCAGTGCTCAGAATCCTTCCCCTTGGTTCCAGCCTATTATAATTAAATGGTAACAAAAACTTTAAAA
AAA – 3’

Figure 3. 1: Cotton rat (Sigmodon hispidus) PD-1 mRNA sequence. 3' RACE strategy was used on total RNA extracted from the spleen of a naïve cotton rat to determine the mRNA sequence. The predicted start and stop codon are underlined.

Figure 3.2

A)

```
CLUSTAL O(1.2.4) multiple sequence alignment

Human              MQIPQAPWPVVWAVLQLGWRPGWFLDSPDRPWNPPTFFPALLVVTEGDNATFTCSFSNTS      60
CottonRat          MWVQQVPWPLTWAVLQLSWQAGWLLEIPNGPWRPLTFSPAWLTVAEGENATFTCSFSNWS      60
PrairieVole        MWVRQVPWPLTWAVLQLSWQTGWLLEVSSGSWRPLTFSPAWLTVSEGANATFTCSFSNWT      60
ChineseHamster     MWVPQVPWPLTWAVLQLSWHAGWLLEVSSGPWRPLTFSPAWLTVSEGANATFTCSFSNWS      60
Mouse              MWVRQVPWSFTWAVLQLSWQSGWLLEVPNGPWRSLTFYPAWLTVSEGANATFTCSLSNWS      60
BrownRat           MWVQQVPWSFTWAVLQLSWQSGWLLEVLNKPWRPLTFSPTWLTVSEGANATFTCSFSNWS      60
                   * : *.** ..******.*: **:*:  .  *.  ** *: *.*:** *******:** :

Human              ESFVLNWYRMSPSNQTDKLAAFPEDRSQPGQDCRFRVTQLPNGRDFHMSVVRARRNDSGT      120
CottonRat          EDLMLNWYRLSPSNQTVKQAAFCKGLSQPVQDKRFQITQLPNGHDFHMNILAARRNDSGI      120
PrairieVole        EDLKLNWYRLSPSNQTEKQAAFCNGFSQPVRDKRFQITQLPNGHDFHMNILATRRNDSGI      120
ChineseHamster     EDLMLNWYRLSPSNQTEKQAAFCKGLSQPVRDSRFQITQLANGHDFHMNILATRRNDSGI      120
Mouse              EDLMLNWWRLSPSNQTEKQAAFCNGLSQPVQDARFQIIQLPNRHDFHMNILDTRRNDSGI      120
BrownRat           EDLKLNWYRLSPSNQTEKQAAFCNGYSQPVRDARFQIVQLPNGHDFHMNILDARRNDSGI      120
                   *.: *** *:****** * *** :. *** :* **:: ** * :****.:: :******

Human              YLCGAISLAPKAQIKESLRAELRVTERRAEVPTAHPS-PSPRPAGQFQTLVVGVVGGLLG      179
CottonRat          YLCGAISLPPKTQIKESPGAELVVTERILETSTRYSS-PSPRPAGQFQGLVIGIMSILVG      179
PrairieVole        YLCGAISLPPKPQIKESPGAELVVTERILETSTRYPSSSSPRPAGQFQGLVIGIMSVLVG      180
ChineseHamster     YLCGAISLPPKTQIKESPGAELVVTERILETSTRYPSP-SPRPASQFQGLVIGIMSVLVG      179
Mouse              YLCGAISLHPKAKIEESPGAELVVTERILETSTRYPS-PSPKPEGRFQGMVIGIMSALVG      179
BrownRat           YLCGAISLPPKAQIKESPGAELVVTERILETPTRYPR-PSPKPEGQFQGLVIVIMSVLVG      179
                   ******** ** :*:**  *** ****  *. * :    **:* .:** .*: ::. *:*

Human              S--LVLLVWVLAVICSRAARGTIGARRTGQPLKEDPSAVPVFSVDYGELDFQWREKTPEP      237
CottonRat          VPVLLLLAWVLAAFCSTE---TRRVESKEQPQEDNHSAAPVFSVAYEELDFHGREKTPEL      236
PrairieVole        VPVLLLLTWVLAAFCSTAKSEARRTGRKEQPLKEDASAAPVFSVAYEELDFQGRQKTPEL      240
ChineseHamster     VPVLLLLAWVLAAFCSTGVSEARRARRKEQPLKGGPSAAPIFSVAYEELDFQGREKTPEP      239
Mouse              IPVLLLLAWALAVFCSTSMSEARGAGSKDDTLKEEPSAAPVPSVAYEELDFQGREKTPEL      239
BrownRat           IPVLLLLAWALAAFCSTEARE---AGRKED-PPEAHAAAPVPSVAYEELDFQGREKTPE-      234
                     *:**.*.**.:**       .  . :     :*.*: ** * ****: *:****

Human              PVPCVPEQTEYATIVFPSGMGTSSPARRGSADGPRSAQPLRPEDGHCSWPL 288
CottonRat          PTSCVH--TEYATIVFTEGLGASSLGRRGSADDLQGPRPPRHEDGHCSWPL 285
PrairieVole        PTPCVH--TEYATIVFTEGLGASSLGRRGSADVPQGPRPPRHEDGHCSWPL 289
ChineseHamster     PTPCIH--TEYATIVFSEGLGASSLGRRGSADGPQGPRPPRHEDGHCSWPL 288
Mouse              PTACVH--TEYATIVFTEGLGASAMGRRGSADGLQGPRPPRHEDGHCSWPL 288
BrownRat           PAPCVH--TEYATIVFTEGLDASAIGRRGSADGPQGPRPPRHEDGHCSWPL 283
                   *. *:   ******** .*:.:*: .******  :. :* * *********
```

B)

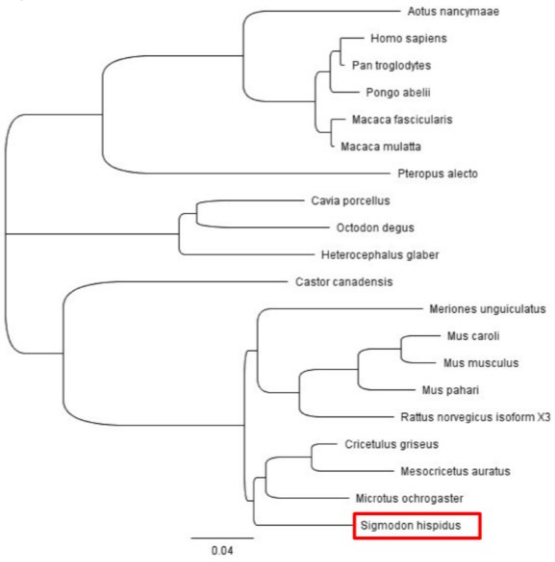

Figure 3. 2: Protein sequence alignment of the cotton rat PD-1. (A) Protein sequence of closely related species and human were aligned with crPD-1 using the Clustal Omega tool from EMBL-EBI. Human (Homo sapiens NCBI Reference Sequence: AAC51773.1), Prairie Vole (Microtus ochrogaster NCBI Reference Sequence: XP_005361412.1), Chinese Hamster (Cricetulus griseus NCBI Reference Sequence: XP_003499314.1), Mouse (Mus musculus NCBI Reference Sequence: NP_032824.1), and Brown Rat (Rattus norvegicus NCBI Reference Sequence: XP_017451871.1). An asterisk (*) indicates positions which have a single, fully conserved residue. A colon (:) indicates conservation between groups of strongly similar properties, scoring >0.5 in the Gonnet PAM 250 matrix. A period (.) indicates conservation between groups of weakly similar properties, scoring =<0.5 in the Gonnet PAM 250 matrix. (B) A phylogenetic tree was produced using Geneious software.

Figure 3.3

A)

MWVQQVPWPLTWAVLQLSWQAGWLLEIPNGPWRPLTFSPAWLTVAEGENATFTCSFSNWSEDLMLNWYRLSPS

NQTVKQAAFCKGLSQPVQDKRFQITQLPNGHDFHMNILAARRNDSGIYLCGAISLPPKTQIKESPGAELVVTERILETS

TRYSSPSPRPAGQFQGLVIGIMSILVGVPVLLLLAWVLAAFCSTETRRVESKEQPQEDNHSAAPVFSVAYEELDFHGRE

KTPELPTSCVHTEYATIVFTEGLGASSLGRRGSADDLQGPRPPRHEDGHCSWPL

B)

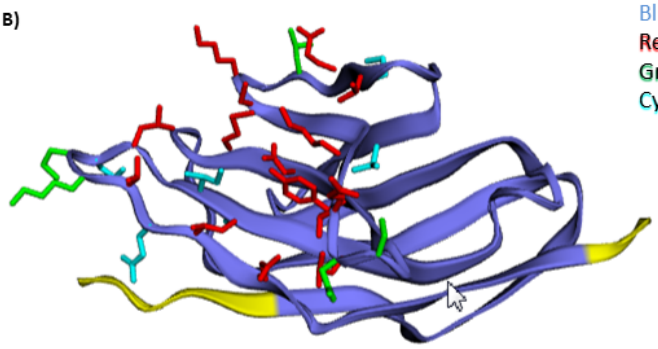

Underlined: Ectodomain
Blue: Extracellular IgV domain of PD-1
Red: Residues involved in both PD-L1 and PD-L2 binding
Green: Residues involved in PD-L1 binding
Cyan: Residues involved in PD-L2 binding

Figure 3. 3: Identification of putative conserved domains in the cotton rat PD-1. (A) The underlined sequence indicates the putative ectodomain of PD-1; amino acids in blue are the putative extracellular IgV domain of PD-1; putative residues involved in both PD-L1 and PD-L2 binding are highlighted in red; putative residues involved in PD-L1 binding only are highlighted in green and residues involved in PD-L2 binding only in cyan. (B) Predicted structure of the putative ectodomain of the cotton rat PD-1 monomer shown in blue and yellow where the blue region is the putative extracellular IgV domain, residues in red are involved in both PD-L1 and PD-L2 binding, residues in green are involved in PD-L1 binding only and residues in cyan are involved in PD-L2 binding only.

Figure 3.4


A)
1
2
3
4
150 kDa
75 kDa
50 kDa
37 kDa
25 kDa
15 kDa
Lane 1: Mouse recombinant PD -1 with a his tag
Lane 2: His -tag purified crPD -1
Lane 3: His -tag purified lipofectamine control
Lane 4: Protein ladder
B)
Coverage for crPD-1:
Coverage: 41.05%
Programmed Cell Death Protein 1 OS=Sigmodon hispidus OX=42415 GN=Pdcd1 PE=1 SV=1
Coverage for rmPD-1:
Coverage: 33.33%
Programmed cell death protein 1 OS=Mus musculus OX=10090 GN=Pdcd1 PE=1 SV=1
C)
a-PD-1
a-His
Merge
Lipofectamine control
crPD-1 transfected

Figure 3. 4: Cotton rat PD-1 protein expression. crPD-1 gene also encoding rat codon optimized secretion signal and ten histidine residues at the 5'-end was synthesized and cloned into pcDNA3.1(+) vector. 293T cells were then transfected for 24 hours, the lysate was collected and his-tag purified. (A) Protein expression was confirmed with western blot using a mouse anti-histidine antibody. The expected size of crPD-1 is 36.4 kDa. A his-tag conjugated recombinant mouse PD-1 (rmPD-1) was used as a positive control and, as expected, migrated from 25 to 45 kDa due to different glycosylation and may have aggregates depending on the reducing conditions. Different lanes of the same blot were cropped and merged to show the lanes of interest only. A full-length blot is shown as Supplementary Fig. S3.1. (B) Mass spectrometry was performed with his-tag purified lipofectamine control and crPD-1 along with rmPD-1. Seven peptides in the newly found sequence were found in the crPD-1 sample at high abundance and two peptides were found at low abundance with total sequence coverage of 41%. No peptides were found in the lipofectamine control, as expected and two peptides were found in the rmPD-1 sample. Mouse PD-1 sequence coverage for the positive control sample (rmPD-1) was 33.33%. (C) Immunofluorescence was also used for protein expression. Cells were permeabilized and stained 24 hours post-transfection. A rabbit anti-mouse PD-1 with Cy2-conjugated anti-rabbit IgG and mouse anti-his tag with Alexa Fluor 555 anti-mouse IgG were used. Representative image of the stained cells at 20X magnification is shown. A merge of the two fluorochromes shows the co-expression of PD-1 and the his-tag, as expected.

Figure 3.5

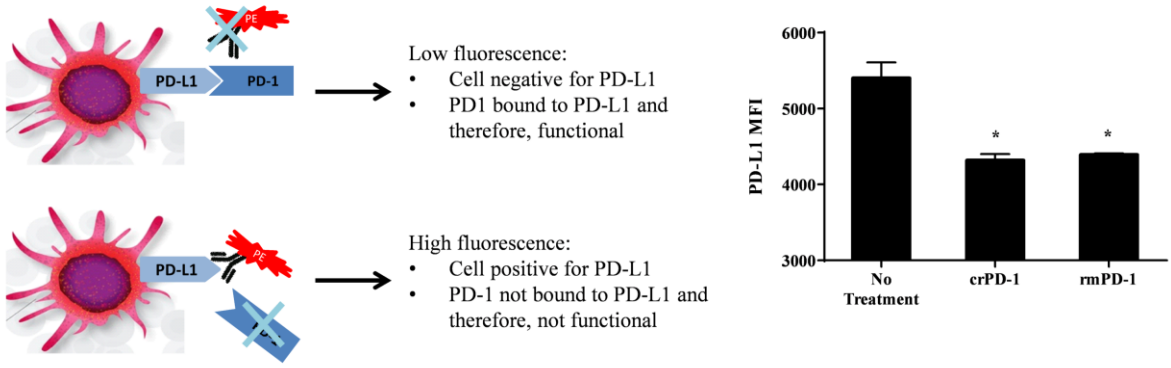
PE
PD-L1
PD-1
Low fluorescence:
• Cell negative for PD-L1
• PD1 bound to PD-L1 and therefore, functional
PD-L1
PE
High fluorescence:
• Cell positive for PD-L1
• PD-1 not bound to PD-L1 and therefore, not functional
PD-L1 MFI
6000
5000
4000
3000
*
*
No Treatment
crPD-1
rmPD-1

Figure 3. 5: crPD-1 binds PD-L1 on dendritic cells *in vitro*. Purified crPD-1 was added to mouse dendritic cells for 4 hours. Recombinant mouse PD-1 (rmPD-1) and no treatment controls were used. The cells were then stained with a fixable viability dye and PE-conjugated anti-human/mouse PD-L1 blocking antibody for flow cytometry analysis. The schematic displays the strategy used (left). The mean fluorescence intensity (MFI) of PD-L1 among viable cells is shown (right). Statistical difference between PD-1 treated and no treatment group is indicated. Data shown is mean ± SEM representative of 2 independent experiments; n = 3 per treatment in each experiment; *$p < 0.05$ (one-way ANOVA with Bonferroni posttest).

Figure 3.6

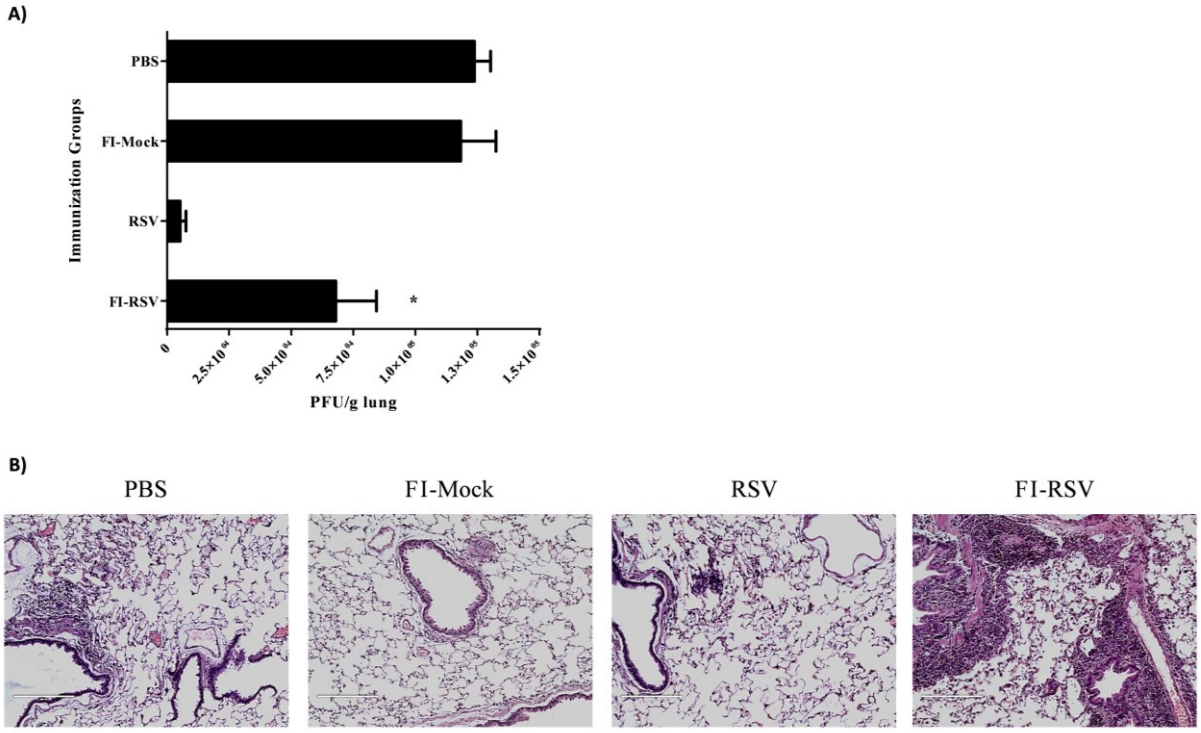
A)
PBS
FI-Mock
RSV
FI-RSV
Immunization Groups
*
0
2.5×10^04
5.0×10^04
7.5×10^04
1.0×10^05
1.3×10^05
1.5×10^05
PFU/g lung
B)
PBS
FI-Mock
RSV
FI-RSV

Figure 3. 6: FI-RSV immunization of cotton rats results in ineffective viral clearance with pronounced ERD. Cotton rats were immunized twice 21 days apart with FI-RSV, FI-Mock or PBS intramuscularly or wild-type RSV-A2 intranasally. Four weeks following second immunization, the animals were challenged with RSV-A2 intranasally and euthanized 5 days post-challenge for collection of lungs. (A) Lung viral titer determined using plaque assay post challenge. (B) Representative images of H&E stained cotton rat lungs post challenge at 20X magnification. Data shown is mean ± SEM representative of 2 independent experiments; n = 3 per group in each experiment; *$p < 0.05$ (one-way ANOVA with Bonferroni posttest). FI-RSV: Formaldehyde-inactivated RSV; FI-Mock: Formaldehyde-inactivated cell control; PBS: Phosphate-buffered saline.

Figure 3.7

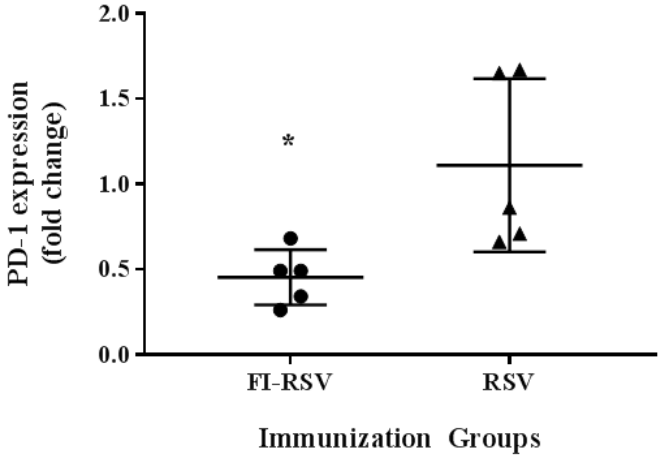
2.0
1.5
1.0
0.5
0.0
PD-1 expression
(fold change)
*
FI-RSV
RSV
Immunization Groups

Figure 3. 7: PD-1 gene expression is downregulated in FI-RSV immunized cotton rats experiencing ERD. RNA isolated from lungs collected from twice-immunized and challenged cotton rats were analyzed for PD-1 gene expression using quantitative real-time PCR. CT values were first normalized to β-actin, then, presented as fold change over the respective immunization control groups, i.e., FI-RSV over FI-Mock and RSV over PBS. Data shown is mean ± SEM; n = 5 per group; *$p < 0.05$ (Student's t-test). FI-RSV: Formaldehyde-inactivated RSV; FI-Mock: Formaldehyde-inactivated cell control; PBS: Phosphate-buffered saline.

Table 3. 1: crPD-1 downregulates expression of cytokines by dendritic cells *in vitro*. Mouse dendritic cells were stimulated with LPS along with purified crPD-1 for 24 hours. No treatment control containing LPS only and rmPD-1 control containing LPS and rmPD-1 were used. The supernatant was collected for cytokine quantitation using ELISA. Data shown is representative of 2 independent experiments; n = 3 per treatment in each experiment.

	IL-6 (pg/ml)		**TNF-α (pg/ml)**	
	Mean	**95% CI**	**Mean**	**95% CI**
No Treatment	3118	2839 to 3459	3762	3422 to 4128
crPD-1	2636	2400 to 2924	3214	2885 to 3558
rmPD-1	2666	2427 to 2958	3189	2861 to 3532

crPD-1: cotton rat PD-1; rmPD-1: recombinant mouse PD-1; CI: confidence interval

Supplementary Information

PD-1 of *Sigmodon hispidus*: Gene identification, characterization and expression in inactivated RSV vaccine-induced enhanced respiratory disease

Abenaya Muralidharan[1,3], Louise Larocque[1], Marsha Russell[1], Marybeth Creskey[1], Changgui Li[2], Wangxue Chen[4], Gary Van Domselaar[5], Terry Cyr[1], Lisheng Wang[3], Xuguang Li[1,3,*]

[1]Centre for Biologics Evaluation, Biologics and Genetic Therapies Directorate, HPFB, Health Canada and WHO Collaborating Center for Standardization and Evaluation of Biologicals, Ottawa, ON, Canada.

[2]National Institute for Food and Drug Control and WHO Collaborating Center for Standardization and Evaluation of Biologicals, Beijing, China

[3]Department of Biochemistry, Microbiology and Immunology, Faculty of Medicine, University of Ottawa, Ottawa, ON, Canada

[4]Human Therapeutics Portfolio, National Research Council of Canada, Ottawa, ON, Canada

[5]National Microbiology Laboratory, Public Health Agency of Canada, Winnipeg, MB, Canada

[*]Corresponding author

Supplementary Figure S3.1

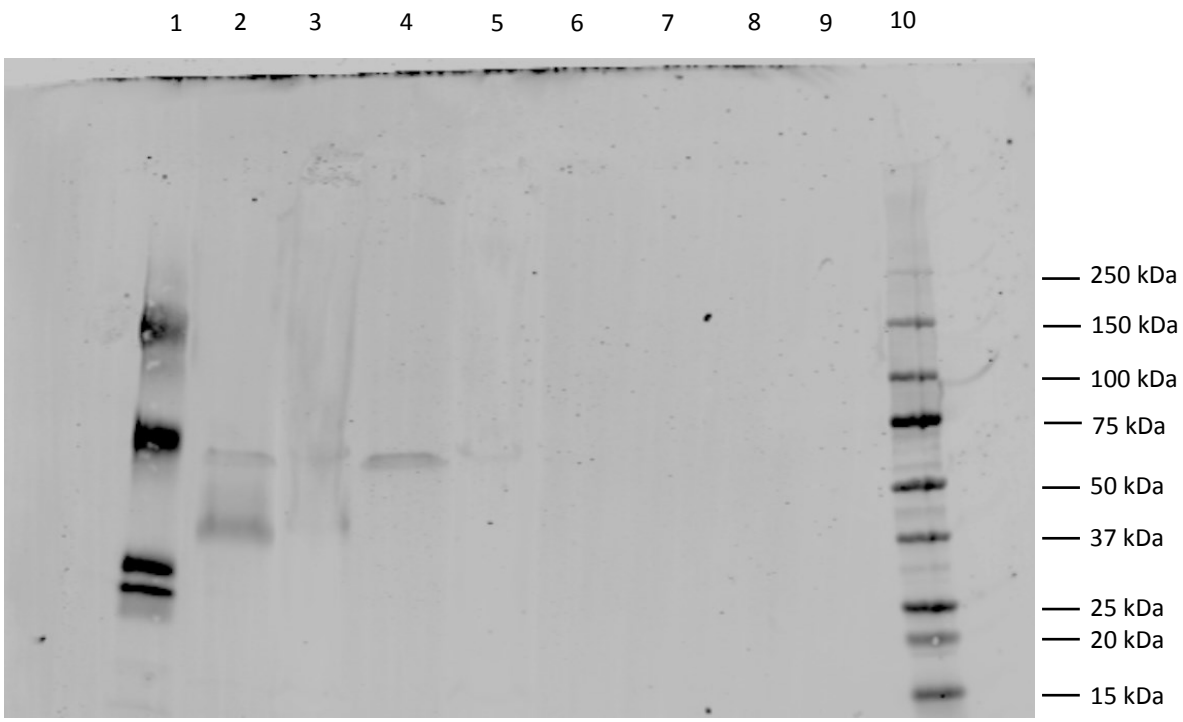

Lane 1: Mouse recombinant PD-1 with a his tag
Lane 2: His-tag purified crPD-1 from lysate
Lane 3: crPD-1 lysate (unpurified)
Lane 4: His-tag purified lipofectamine control from lysate
Lane 5: Lipofectamine control lysate (unpurified)
Lane 6: His-tag purified crPD-1 from supernatant
Lane 7: crPD-1 supernatant (unpurified)
Lane 8: His-tag purified lipofectamine control from supernatant
Lane 9: Lipofectamine control supernatant (unpurified)
Lane 10: Protein ladder

Supplementary Figure S3. 1: Cotton rat PD-1 protein expression. crPD-1 gene also encoding rat codon optimized secretion signal and ten histidine residues at the 5'-end was synthesized and cloned into pcDNA3.1(+) vector. 293T cells were then transfected for 24 hours, the lysate and supernatant were collected and his-tag purified. Protein expression was confirmed with western blot using a mouse anti-histidine antibody. The expected size of crPD-1 is 36.4 kDa and was only observed in his-tag purified lysate.

Chapter 4: Chitosan enhances inactivated vaccine elicited protection against respiratory syncytial virus

This manuscript is under review by the journal *Vaccine*. I contributed more than 50% to the manuscript. Xuguang (Sean) Li, Changgui Li, Wangxue Chen, Simon Sauvé, Ze Chen, Terry Cyr, Michael Rosu-Myles, Lisheng Wang and I conceived the overall study. I performed the experiments and analyzed the data with the help of Louise Larocque, Marsha Russell and Caroline Gravel. Xuguang (Sean) Li and I wrote the manuscript. All authors edited and approved the manuscript.

Emily Dupuis at Health Canada provided technical assistance with flow cytometry. Dr. Martha Navarro and the technicians at the Health Canada animal facility helped with the animal studies. Dr. Don Caldwell, veterinary pathologist at Health Canada, conducted expert analyses of the lung tissues. Finally, Drs Roger Tam and Michael Johnston critically reviewed the manuscript.

Using chitosan as an immune enhancer, this manuscript further reveals the mechanism underlying FIRSV-mediated ERD. It also sheds light on mechanisms involved in chitosan-elicited immune enhancement. Since chitosan has previously been used to protect against other respiratory viruses through induction of Th1 responses and neutralizing antibodies, both of which are not induced by FIRSV, the potential of chitosan to protect against RSV and reverse ERD was explored. Moreover, role of chitosan in augmenting the induction of regulatory T cells and lung resident T cells was observed.

Chitosan enhances inactivated vaccine elicited protection against respiratory syncytial virus

Abenaya Muralidharan[a,e], Marsha S. Russell[a], Louise Larocque[a], Caroline Gravel[a], Simon Sauvé[a], Ze Chen[b], Changgui Li[c], Wangxue Chen[d], Terry Cyr[a], Michael Rosu-Myles[a,e], Lisheng Wang[e], Xuguang Li[a,e,*]

[a]Centre for Biologics Evaluation, Biologics and Genetic Therapies Directorate, HPFB, Health Canada and WHO Collaborating Center for Standardization and Evaluation of Biologicals, Ottawa, ON, Canada.

[b]Shanghai Institute of Biological Products, Shanghai, China

[c]National Institute for Food and Drug Control and WHO Collaborating Center for Standardization and Evaluation of Biologicals, Beijing, China

[d]Human Therapeutics Portfolio, National Research Council of Canada, Ottawa, ON, Canada

[e]Department of Biochemistry, Microbiology and Immunology, Faculty of Medicine, University of Ottawa, Ottawa, ON, Canada

Abstract

Chitosan is a polysaccharide capable of augmenting immune responses with a proven safety record in animals and humans. These properties make it a potentially attractive agent for the prevention and treatment of infectious disease. Infection by respiratory syncytial virus (RSV) is the leading cause of serious lower respiratory disease in young children throughout the world. There is no licensed vaccine available against RSV whereas inactivated vaccine is known to cause enhanced respiratory disease instead of protection. Here, we investigated whether chitosan alone could protect animals against RSV infection and whether it could alter immune responses or immunopathology induced by inactivated RSV vaccine. We found chitosan alone could modestly protect animals against RSV infection, while, in conjunction with inactivated RSV vaccine, it could significantly reduce RSV infection in mice. Further mechanistic investigation revealed that chitosan enhanced inactivated RSV vaccine-elicited immune responses through augmenting the induction of regulatory T cells, lung resident T cells and neutralizing antibodies while reversing Th2-skewed immune responses induced by inactivated RSV vaccine.

Keywords

Respiratory syncytial virus; Vaccine; Immunopathology; Vaccine safety

1. Introduction

Chitosan is a generic term for a family of linear polysaccharides that is commercially available as a partially deacetylated α-chitin produced from the exoskeletons of crustacean or the cell walls of fungi (231–233). It is a biocompatible, non-toxic and non-allergenic material that has been tested for safety and toxicity in a variety of animal species for various applications through various routes of administration (234–236). In solution, the positive charge of chitosan confers it with mucoadhesive properties, which are crucial for its use in intranasal applications (237, 238). When nasally administered with an antigen, it has been shown to augment antigen-specific immune responses in many animal models (239–242) and in human subjects (239, 243–246). Interestingly, chitosan alone is also able to enhance the immune responses against some viral infections (240–242). While its activities of immune enhancement have been well documented, the molecular mechanisms remain to be fully understood. It would be of interest to investigate whether chitosan could alter immune responses induced by a vaccine known to be generally less effective or even induce severe adverse reactions.

Formaldehyde-inactivated respiratory syncytial virus (FIRSV) vaccine was initially developed to protect humans against RSV infection known to cause severe disease in young children, elderly and immunocompromised patients (7, 125–127). However, instead of protection, the vaccine was found to be associated with severe vaccine-induced enhanced respiratory disease (ERD), with 80% of the participants hospitalized and 2 deaths following subsequent RSV infection (97, 98, 131, 206). It has been shown that Th2-skewed immune responses and poorly neutralizing antibodies lead to pulmonary inflammation, airway obstruction, and mucus hypersecretion (100, 133, 135–137). Moreover, cell-mediated

immune responses could also be involved in the development of ERD (138, 140, 247). It is noted that there are studies showing the use of adjuvants to enhance FIRSV-induced protection (248), here, we investigated the mechanisms underlying chitosan-mediated immune enhancement using FIRSV as a model vaccine, specifically its role in inducing regulatory and tissue resident T cells which are known to be critically important in inducing a well-balanced and robust immune responses against microbial infections.

2. Materials and methods

2.1 Cells, virus and vaccines

HEp-2 (ATCC: CCL-23) were grown in Dulbecco's Modified Eagle Medium (DMEM) supplemented with 1.5 g/l sodium bicarbonate, 2mM Glutamax, 1mM HEPES, 20 U/ml Penicillin, 0.02 mg/ml Streptomycin, and 10% FBS.

RSV-A2 (ATCC: VR-1540) was grown in HEp-2 cells according to supplier's instructions and sucrose-purified for animal studies. FIRSV was prepared with the RSV-A2 strain in HEp-2 cells as described elsewhere (135).

2.2 Animal studies

Six-week old female Balb/c mice (Charles River, Saint Constant, QC) were used for all animal studies. For a primary infection, mice were infected intranasally with $5x10^5$ PFU of RSV-A2 in 25µl per mouse. Chitosan (Sigma) was dissolved in 25 mM sodium acetate solution (pH 5.0) to a concentration of 4 mg/ml (241, 242) and 25µl was administered intranasally per mouse either one day or three days post RSV infection. Mice were euthanized four days post-infection for lung collection.

FIRSV and formaldehyde-inactivated cell control (FI-Mock) were administered at 10^6 PFU intramuscularly in 50µl volume per mouse. Each immunization was administered twice at the same dose and route 28 days apart. On days 39 and 41, some mice were given 25µl chitosan at 4 mg/ml intranasally. On day 42, half the mice were euthanized while others were challenged intranasally with $5x10^5$ PFU of RSV-A2 in 25µl per mouse. Four days post-challenge, mice were euthanized for blood and tissue collection.

In all animal studies, mice were intravenously injected with 1.5µg of BV510-conjugated anti-mouse CD3 (clone 145-2C11; BD Biosciences) in 200µl PBS 5 minutes before being euthanized. During flow cytometry analysis of the lungs, the cells that appear negative for the injected CD3 antibody will be considered tissue-resident (249).

All animal experiments were reviewed and approved by Institutional Animal Care and Use Committee of Health Canada and were conducted in accordance with Institutional Animal Care and Use Committee of Health Canada guidelines and regulations.

2.3 Lung viral titer

Lungs were removed four days post RSV challenge and tittered as described elsewhere (135). Briefly, lungs were collected and weighed prior to mechanical homogenization. The homogenates were clarified using centrifugation and the supernatants were frozen at -80ºC until further use. Serial dilutions of the supernatant were done and incubated on HEp-2 cells for 2 hours at 37ºC. A 1:1 overlay of 2x DMEM media and 0.8% agarose was added. Following 6 days of incubation, the overlay was removed and the cell monolayer was stained with crystal violet before counting plaques. Results are expressed as PFU/g lung tissue.

2.4 Histopathology

Four days post RSV challenge, whole lungs were collected from the Balb/c mice and fixed in 10% neutral buffered formalin. They were then trimmed, processed and embedded into paraffin blocks. Four-micron Hematoxylin-Phloxine-Eosin (HPE) and Periodic Acid Schiff (PAS) stained slides were made for evaluation. Scoring was done by a veterinary pathologist who was blinded to the experimental design. The lesion assessment protocol outlined by Weiss et al. was adopted (183). Perivascular leukocytic infiltration was evaluated where 1 means within normal parameters; 2 means small numbers of solitary cells with uncommon aggregates; 3 means multifocal small to moderate aggregates; 4 means moderate to high cellularity with multifocal large cellular aggregates that may be expansive into adjacent tissues. Mucus was visualized with PAS stain and graded as follows: 1 means none; 2 means epithelial mucinous hyperplasia with none to rare luminal mucus accumulation in airways; 3 means epithelial mucinous hyperplasia with luminal mucus accumulation in airways; 4 means there is severe mucinous hyperplasia with airway obstruction by mucus. Total pathological score was calculated as the average of the individual scores.

2.5 ELISA

Serum from immunized mice was collected for determination of IgG1 and IgG2a titer. Ninety six-well plates were coated with recombinant RSV fusion (F) protein (Sino Biological) overnight at 4ºC. Next day, the plates were washed and blocked with BSA in PBS containing 0.05% Tween 20 for 2 hours at 37ºC. Serial dilutions of the mouse serum in blocking buffer were then added for 1 hour at 37ºC. After washing, HRP-conjugated anti-

mouse IgG1 or IgG2a (Jackson Immunoresearch Laboratories) were added for 1 hour at 37ºC. The plates were again washed and Tetramethylbenzidine substrate (Cell Signaling Technology) was added for 20 min at room temperature. The reaction was then stopped with 0.16 M sulfuric acid. The plates were read spectrophotometrically at 450nm.

2.6 Microneutralization

RSV-neutralizing ability of the serum from immunized mice was determined. Serial dilutions of the serum were incubated with 800 PFU of purified RSV-A2 for 1 hour at 37ºC, 5% CO_2. The virus-antibody mixture was added to HEp-2 cells seeded the previous day and incubated at 37ºC. After 3 days, the cells were fixed with ice-cold methanol for 10 min at room temperature, air-dried, and blocked with 5% non-fat dry milk in PBS containing 0.1% Tween 20 for 2 hours at 37ºC. Then, the plates were washed and a HRP-conjugated anti-RSV (Meridian Life Science) was added for 1 hour at 37ºC. The plates were again washed and Tetramethylbenzidine substrate (Cell Signaling Technology) was added for 20 min at room temperature. The reaction was then stopped with 0.16 M sulfuric acid. The plates were read spectrophotometrically at 450nm.

2.7 Flow cytometry

Cells were isolated from lungs of immunized mice using a lung dissociation kit (Miltenyi Biotec) and a mechanical tissue homogenizer. Single-cell suspensions were washed with PBS and first, stained with Fixable Viability Stain 700 (BD Biosciences) for 30 min at 4ºC, then, with purified anti-mouse CD16/CD32 (eBioscience) as a Fc block for 5 min. Next, cells were washed with FACS wash buffer (PBS with 1% BSA and 0.05% sodium azide) and

stained for 30 min at 4ºC with a panel containing BV711-conjugated anti-mouse CD127 (clone SB/199), BV650-conjugated anti-mouse CD25 (clone PC61), BV421-conjugated anti-mouse CD44 (clone IM7), PE-Cy7-conjugated anti-mouse CD62L (clone MEL-14), PE-CF594-conjugated anti-mouse CD103 (clone M290), FITC-conjugated anti-mouse CD8a (clone 53-6.7), APC-H7-conjugated anti-mouse CD4 (clone GK1.5), and AF647-conjugated CCR7 (CD197; clone 4B12). After washing the stained cells, BD Pharmingen™ Transcription Factor Buffer Set (BD Biosciences) was used as per manufacturer's instructions to stain with PE-conjugated anti-mouse Foxp3 (clone MF23). All antibodies were purchased from BD Biosciences. Using a BD LSRFortessa flow cytometer, 50,000 singlet events were recorded. FMO controls and compensation beads were used where appropriate to correct for spectral overlap. Data analysis was completed using FlowJo X 10.0. Gating strategy is outlined in Figure S4.1.

2.8 Secreted cytokines

Cells were isolated from lungs using a lung dissociation kit (Miltenyi Biotec) and a mechanical tissue homogenizer. The cells were then stimulated with an immunodominant H-2K^{d}-restricted RSV F_{85-93} peptide (KYKNAVTEL; ProImmune) at 5µg/ml for 48 hours at 37ºC, 5% CO_2. Supernatants were collected following centrifugation and stored at -80ºC for later analysis. A ProcartaPlex Mouse Cytokine Panel (eBiosciences) was used to determine the levels of IL-5 and IL-13 in the supernatants. The samples were read on a Luminex 200 System (xMAP Technology). Data analysis was performed using MILLIPLEX Analyst version 5.1 for determining the pg/ml of each cytokine.

2.9 Statistical Analysis

Analysis was conducted using one-way or two-way ANOVA where appropriate. Bonferroni posttest was used to adjust for multiple comparisons between different test groups. Tests were done at a 5% significance level. All statistical analyses were performed using GraphPad Prism 7 software.

3. Results

3.1 Chitosan enhances induction of resident effector T cells and regulatory T cells following RSV infection

We first investigated whether chitosan alone could afford protection against RSV and the underlying mechanism. To that end, Balb/c mice were infected with RSV-A2 and intranasally inoculated with chitosan either one day or three days post-infection. A 'no chitosan' control was included where mice were infected with RSV but did not receive any chitosan. Four days post-infection, all mice were injected with a fluorophore-conjugated anti-mouse CD3 antibody (249) and euthanized five minutes later for lung collection (Figure 4.1A). Minimally lower RSV titer, albeit statistically significant, was observed in mice given chitosan one day post-infection (Figure 4.1B), while chitosan treatment on day 3 failed to significantly inhibit viral replication. Notably, we found that the decreased levels of viral replication in chitosan treated mice was accompanied by significantly increased T cell populations known to be crucial for protection against RSV (247, 250–253). Specifically, treating with chitosan one-day post RSV infection significantly increased the number of lung-resident CD8+ and CD4+ effector T cells compared to day 3 and no treatment groups (Figure 4.1C, D). In addition, the population of CD4+ regulatory T cells (Tregs) expressing

transcription factor box P3 (Foxp3) also increased considerably in mice treated with chitosan one day post-infection compared to day 3 and no chitosan treatment groups (Figure 4.1E). Collectively, these results show that chitosan augments the induction of tissue-resident effector T cells and Tregs, and the timing of chitosan administration following infection has a profound effect on T cell activation.

3.2 Chitosan augments viral clearance elicited by inactivated RSV vaccine

Previous studies have demonstrated the use of chitosan in increasing neutralizing antibody levels and promoting a balance between Th1 and Th2 responses during viral infections when used as a vaccine adjuvant or a therapeutic treatment (239, 254–257). FIRSV, however, has been shown to induce skewed immune responses with high levels of Th2 antibodies with poor RSV neutralizing ability (136). Therefore, we investigated if chitosan treatment of FIRSV-immunized mice prior to RSV challenge may enhance FIRSV-induced protection. To that end, Balb/c mice were twice immunized with FIRSV or formaldehyde-inactivated cell control (FI-Mock) and given chitosan intranasally twice before RSV challenge (Figure 4.2A). Four days post-challenge, lung viral titre was significantly lower in FIRSV-immunized mice treated with chitosan compared all other treatment groups (Figure 4.2B). It is interesting to note that chitosan treatment prior to RSV challenge did not reduce virus replication (FI-Mock + Chitosan; Figure 4.2B), an observation different from that with treatment one day after RSV challenge (Figure 4.1B). These results collectively suggest that chitosan, when used alone or in the absence of antigen administration, has a small time window to effectively inhibit RSV replication, whereas FIRSV itself shows minimal inhibition of virus but FIRSV in conjunction with chitosan can significantly suppress virus

replication.

As FIRSV can induce exacerbated lung inflammatory reaction, we investigated whether chitosan treatment could reduce lung pathology. To this end, lung tissues from the animals were HPE and PAS stained for histopathological analysis of interstitial disease, edema, perivascular aggregates of leukocytes and mucus, respectively. All FIRSV-immunized mice despite chitosan treatment exhibited severe ERD as demonstrated by significantly higher perivascular cell infiltration and mucus cell hyperplasia with mucus in the bronchiolar lumen (Figure 4.2C, D), while vaccination with FI-Mock resulted in minimal cellularity and mucus irrespective of the chitosan treatment. These findings suggest that the exacerbated pulmonary inflammation is unrelated to virus replication but is greatly influenced by other immunopathological mechanisms (see below for more discussion).

3.3 The effect of chitosan on specific anti-RSV antibody responses

Having observed chitosan in conjunction with FIRSV significantly reduced viral loads in the lung, we set out to determine the antibody responses in these animals. As shown in Figure 4.3A, a high RSV F-specific IgG1 to IgG2a ratio indicative of a Th2 skew, and a hallmark of FIRSV (136), was observed exclusively in the FIRSV group without chitosan treatment (Figure 4.3B), whereas chitosan was able to restore the balance between IgG1 and IgG2a in FIRSV-immunized mice. As expected, a 1:1 ratio between IgG1 and IgG2a was observed in the other two control groups. Importantly, neutralizing antibody levels were significantly higher in the FIRSV group with chitosan treatment compared to other groups (Figure 4.3C). It is understood that chitosan itself would not change the structure of the viral antigens in the FIRSV preparation; it would be worthy studying its adjuvant effects on native

RSV antigens which have not been inactivated (more in discussion). Overall, chitosan treatment improved the neutralizing ability of FIRSV-induced antibodies and restored the balance between Th1 and Th2 antibody responses.

3.4 Chitosan increases FIRSV-elicited Tregs

Next, we examined the cell-mediated responses in the lungs of immunized/chitosan-treated mice. The number of total lung-resident CD4+ T cells was drastically increased in FIRSV-vaccinated mice following chitosan treatment compared to other groups (Figure 4.4A), while the highest levels of CD4+ Tregs were observed following FIRSV vaccination in conjunction with chitosan treatment (Figure 4.4B). It is of note that FIRSV immunization alone significantly decreased total tissue-resident CD4+ T cells and CD4+ Tregs compared to FI-Mock immunization (Figure 4.4A, B), accompanied by a significant increase in RSV F protein specific Th2 cytokines, IL-5 (Figure 4.4C) and IL-13 (Figure 4.4D). These FIRSV-induced pulmonary T cells responses were altered with chitosan treatment as demonstrated by the significant increase in the number of tissue-resident CD4+ T cells and Tregs compared to the other treatment groups as well as decreased levels of IL-5 and IL-13, similar to that of the FI-Mock control group. Taken together, chitosan exerts its adjuvant activity by increasing pulmonary resident CD4+ T cells and Tregs (Figure 4.4) and inducing higher levels of neutralizing antibody (Figure 4.3C).

4. Discussion

Because of its proven safety record and a variety of immunomodulatory properties, chitosan has been extensively studied for its potential as a vaccine adjuvant. Not only does it

have a profound effect on humoral immunity (239, 257), it also affects cell-mediated immunity (258). Several lines of evidence prompted us to conduct the current study in which FIRSV vaccine was used as a model vaccine to study the mechanisms of chitosan as a therapeutic. First, although the role of chitosan in stimulating NK cells and macrophages is well established (240, 258), its effect on tissue-resident T cells still remains to be understood. This is an important issue as tissue resident effector/memory T cells play a vital role in tissue-specific protection. By secreting cytokines and chemokines, these cells recruit innate and adaptive immune cells into the infected tissue (259, 260). Indeed, these cells are believed to be the first line of defense against infection mainly due to their ability to proliferate rapidly and kill infected cells directly as well as through immune cell recruitment (261–264). Secondly, the effect of chitosan on regulatory T cells (Tregs) remains unknown. These cells play important roles in regulating the balance between effective antimicrobial immune responses and excessive effector T cell activation or antigen-presenting cell maturation and functionality (265–269) during immune response against infections. Third, by employing FIRSV vaccine as an model antigen to study the adjuvant activity of chitosan, we could gain better insight into chitosan-mediated immune enhancement, given FIRSV is known to induce skewed immune responses and poorly neutralizing antibodies, and that lung resident T cells are critical for robust RSV virus clearance and early establishment of cell-mediated responses (247). Moreover, following RSV infection, Tregs have been shown to accumulate in the lungs and mediastinal lymph nodes in mice and recruit RSV-specific CD8+ cytotoxic T cells to the lungs thereby facilitating viral clearance (250, 252, 253). Given these considerations, we conducted animal studies to investigate how chitosan could alter immune responses in the RSV vaccine model.

We report for the first time the effect of chitosan on Tregs and tissue-resident T cells

following a RSV infection and FIRSV immunization. Specifically, we found that chitosan alone resulted in a significant increase in pulmonary resident CD8+, CD4+ T effector cells and Tregs. Furthermore, the reversal of FIRSV-induced Th2-skewed immune responses by chitosan could be mediated by elevated levels of resident CD4+ T cells and CD4+ Tregs, leading to a decrease in Th2 cytokines (Figure 4.4). These functional activities of chitosan, along with the capacity of substantially facilitating antigen-specific neutralizing antibodies (Figure 4.3C), could have contributed to the significant inhibition of RSV replication (Figure 4.2B).

While we are able to gain some insight into the mechanisms relating to the adjuvant activity of chitosan, it remains to be understood as to why chitosan failed to reduce exacerbated pulmonary inflammatory reactions or ERD in animals following FIRSV vaccination even if diminished Treg responses and increased Th2 responses have been implicated in ERD development (136, 138, 270). However, it is unlikely that the development of ERD was correlated to the level of viral replication, as the viral loads were the lowest in FIRSV/chitosan group.

Our findings provide some mechanistic insight into chitosan-induced balanced host responses between Th1 and Th2. In agreement with studies that have shown that Tregs could downregulate Th2 responses (271, 272), we show that chitosan upregulates Tregs, resulting in decreased levels of pulmonary Th2 cytokine production. In conclusion, through this study, we have gained some mechanistic insight into the functional activities of chitosan as a potential treatment/adjuvant. In addition to some well-characterized functional pathways reported by others, we show that chitosan can substantially augment antigen-specific immune responses through upregulating critical tissue-specific resident T cells and Tregs while significantly stimulating generation of neutralizing antibodies. Nonetheless, the exact

molecular mechanisms remains to be elucidated; further studies are necessary to delineate the definitive roles of Tregs and resident T cells induced by chitosan with respect to protection against RSV infection.

Figures

Figure 4.1

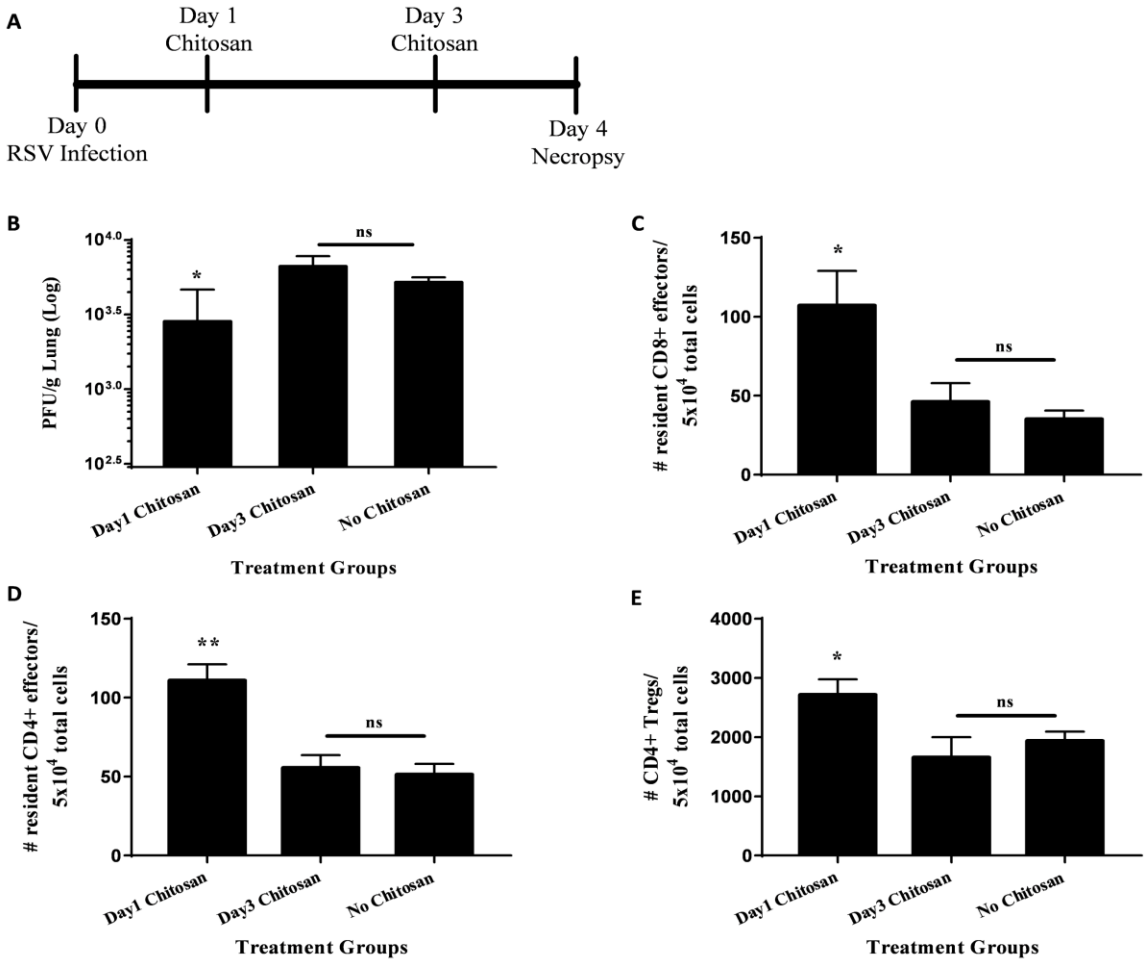

Figure 4. 1: Chitosan treatment following RSV infection leads to enhanced induction of resident T cells and Tregs. (A) Schematic diagram of the RSV infection and chitosan treatment timeline. (B) Lung viral titer determined using plaque assay 4 days post infection (n = 5). Flow cytometry was used to determine the number of lung resident T effector cells and Tregs. (C) Resident CD8+ T effector cells are CD3- CD8+ CD44+ CD62L- CCR7- CD103+, (D) resident CD4+ T effector cells are CD3- CD4+ CD44+ CD62L- CCR7- CD103+, and (E) Tregs are CD3- CD4+ CD127- CD25+ Foxp3+ in mice that were intravenously injected with BV510-conjugated anti-mouse CD3 prior to necropsy. Data shown is mean ± SEM; n = 7 per group; *$p < 0.05$, **$p < 0.01$ (one-way ANOVA with Bonferroni posttest). PFU: Plaque forming units

Figure 4.2

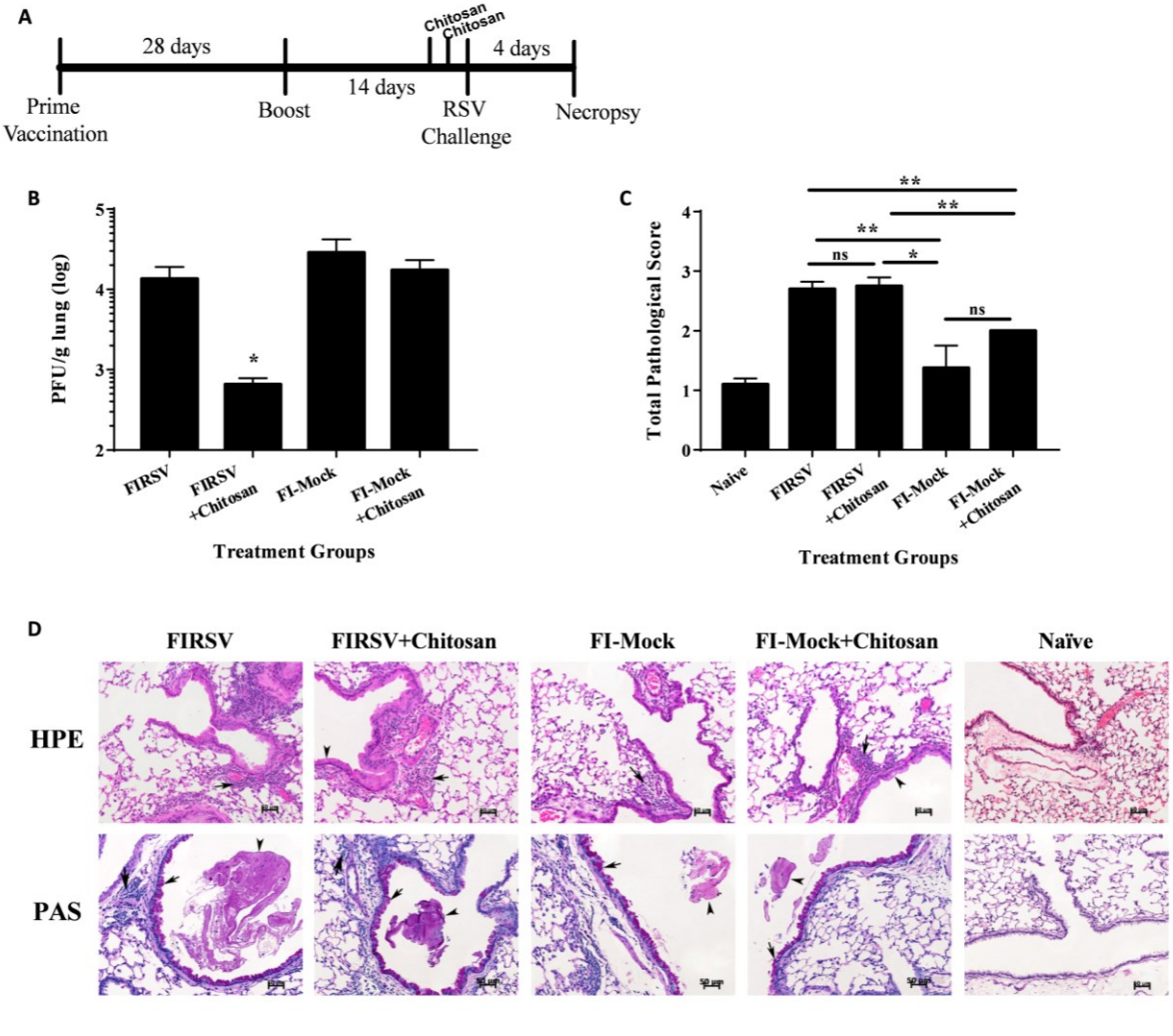
A
28 days
14 days
4 days
Chitosan
Chitosan
Prime Vaccination
Boost
RSV Challenge
Necropsy
B
PFU/g lung (log)
FIRSV
FIRSV +Chitosan
FI-Mock
FI-Mock +Chitosan
Treatment Groups
C
Total Pathological Score
ns
*
**
**
**
ns
Naïve
FIRSV
FIRSV +Chitosan
FI-Mock
FI-Mock +Chitosan
Treatment Groups
D
FIRSV
FIRSV+Chitosan
FI-Mock
FI-Mock+Chitosan
Naïve
HPE
PAS

Figure 4. 2: Chitosan enhances FIRSV-induced viral clearance without reversal of ERD. (A) Schematic diagram of the immunization, chitosan treatment, RSV challenge and necropsy timeline. (B) Lung viral titer determined using plaque assay 4 days post infection. (C) Pathological scoring of lung tissue. Perivascular leukocyte infiltration and mucus were scored using HPE and PAS stained slides, respectively, 4 days post-challenge. An average of the two scores is shown. (D) Representative images of HPE and PAS stained mouse lungs post-challenge at 20X magnification. In the HPE slides, the arrows point to the extensive cell infiltration and in the PAS stained slides, the arrows point to the mucus-positive cells and mucus in the bronchiolar lumen. Data shown is mean ± SEM; n = 5 per group; *$p < 0.05$, **$p < 0.01$ (one-way ANOVA with Bonferroni posttest). FIRSV: Formaldehyde-inactivated RSV, FI-Mock: Formaldehyde-inactivated cell control, PFU: Plaque forming units

Figure 4.3

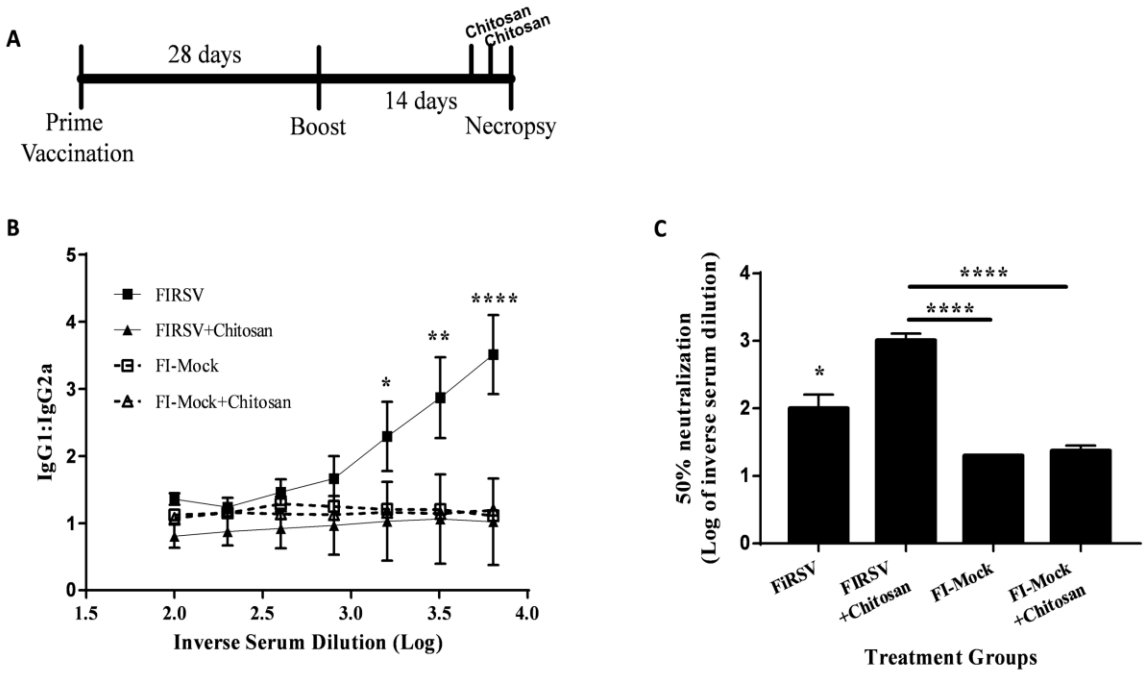
A
28 days
14 days
Chitosan
Chitosan
Prime
Vaccination
Boost
Necropsy
B
FIRSV
FIRSV+Chitosan
FI-Mock
FI-Mock+Chitosan
IgG1:IgG2a
Inverse Serum Dilution (Log)
C
50% neutralization
(Log of inverse serum dilution)
FiRSV
FIRSV
+Chitosan
FI-Mock
FI-Mock
+Chitosan
Treatment Groups

Figure 4. 3: FIRSV-induced antibodies are significantly enhanced with chitosan treatment. (A) Schematic diagram of the immunization, chitosan treatment and necropsy timeline. (B) RSV F-specific IgG1/IgG2a ratio in the serum before challenge was determined using ELISA. (C) RSV neutralizing ability of the mice serum pre-challenge. The serum dilution at which 50% neutralization is achieved is shown. Data shown is mean ± SEM; n = 5 per group; *$p < 0.05$, **$p < 0.01$, ****$p < 0.0001$ (two-way ANOVA (B) or one-way ANOVA (C) with Bonferroni posttest).

Figure 4.4

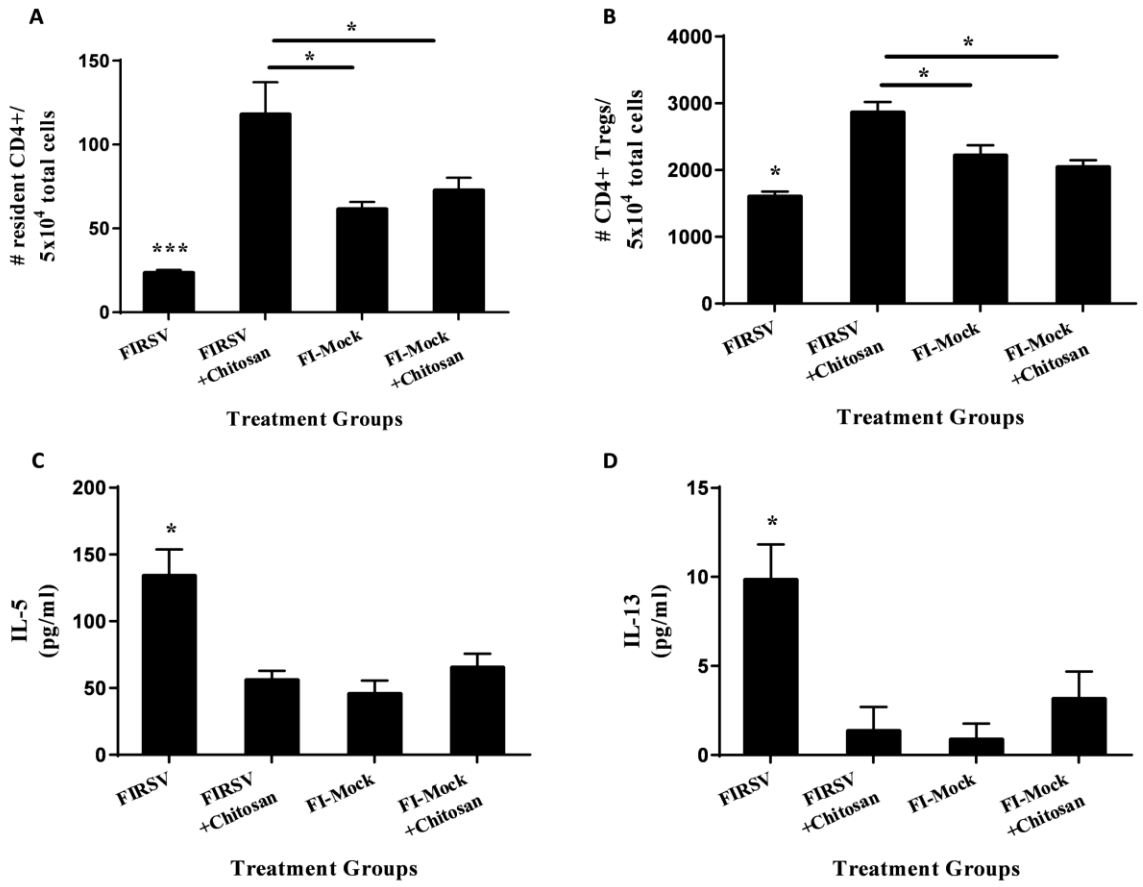
A
resident CD4+/ 5x10^4 total cells
150
100
50
0
***
*
*
FIRSV
FIRSV +Chitosan
FI-Mock
FI-Mock +Chitosan
Treatment Groups
B
CD4+ Tregs/ 5x10^4 total cells
4000
3000
2000
1000
0
*
*
*
FIRSV
FIRSV +Chitosan
FI-Mock
FI-Mock +Chitosan
Treatment Groups
C
IL-5 (pg/ml)
200
150
100
50
0
*
FIRSV
FIRSV +Chitosan
FI-Mock
FI-Mock +Chitosan
Treatment Groups
D
IL-13 (pg/ml)
15
10
5
0
*
FIRSV
FIRSV +Chitosan
FI-Mock
FI-Mock +Chitosan
Treatment Groups

Figure 4. 4: FIRSV-elicited Tregs are improved with chitosan treatment leading to a decrease in Th2 cytokines. Flow cytometry was used to determine the number of lung resident CD4+ T cells and Tregs before RSV challenge. (A) Resident CD4+ T cells are CD3- CD4+ CD103+, and (B) Tregs are CD3- CD4+ CD127- CD25+ Foxp3+ in mice that were intravenously injected with BV510-conjugated anti-mouse CD3 prior to necropsy. Secreted levels of IL-5 (C) and IL-13 (D) were determined using the Luminex system in the lungs of mice collected before challenge following 48-hour ex-vivo stimulation with RSV F85-93 peptide. Data shown is mean ± SEM; n = 5 per group; *$p < 0.05$ (one-way ANOVA with Bonferroni posttest).

Supplementary Information

Chitosan enhances inactivated vaccine elicited protection against respiratory syncytial virus

Abenaya Muralidharan[a,e], Marsha S. Russell[a], Louise Larocque[a], Caroline Gravel[a], Simon Sauvé[a], Ze Chen[b], Changgui Li[c], Wangxue Chen[d], Terry Cyr[a], Michael Rosu-Myles[a,e], Lisheng Wang[e], Xuguang Li[a,e,*]

[a]Centre for Biologics Evaluation, Biologics and Genetic Therapies Directorate, HPFB, Health Canada and WHO Collaborating Center for Standardization and Evaluation of Biologicals, Ottawa, ON, Canada.

[b]Shanghai Institute of Biological Products, Shanghai, China

[c]National Institute for Food and Drug Control and WHO Collaborating Center for Standardization and Evaluation of Biologicals, Beijing, China

[d]Human Therapeutics Portfolio, National Research Council of Canada, Ottawa, ON, Canada

[e]Department of Biochemistry, Microbiology and Immunology, Faculty of Medicine, University of Ottawa, Ottawa, ON, Canada

Figure S4.1

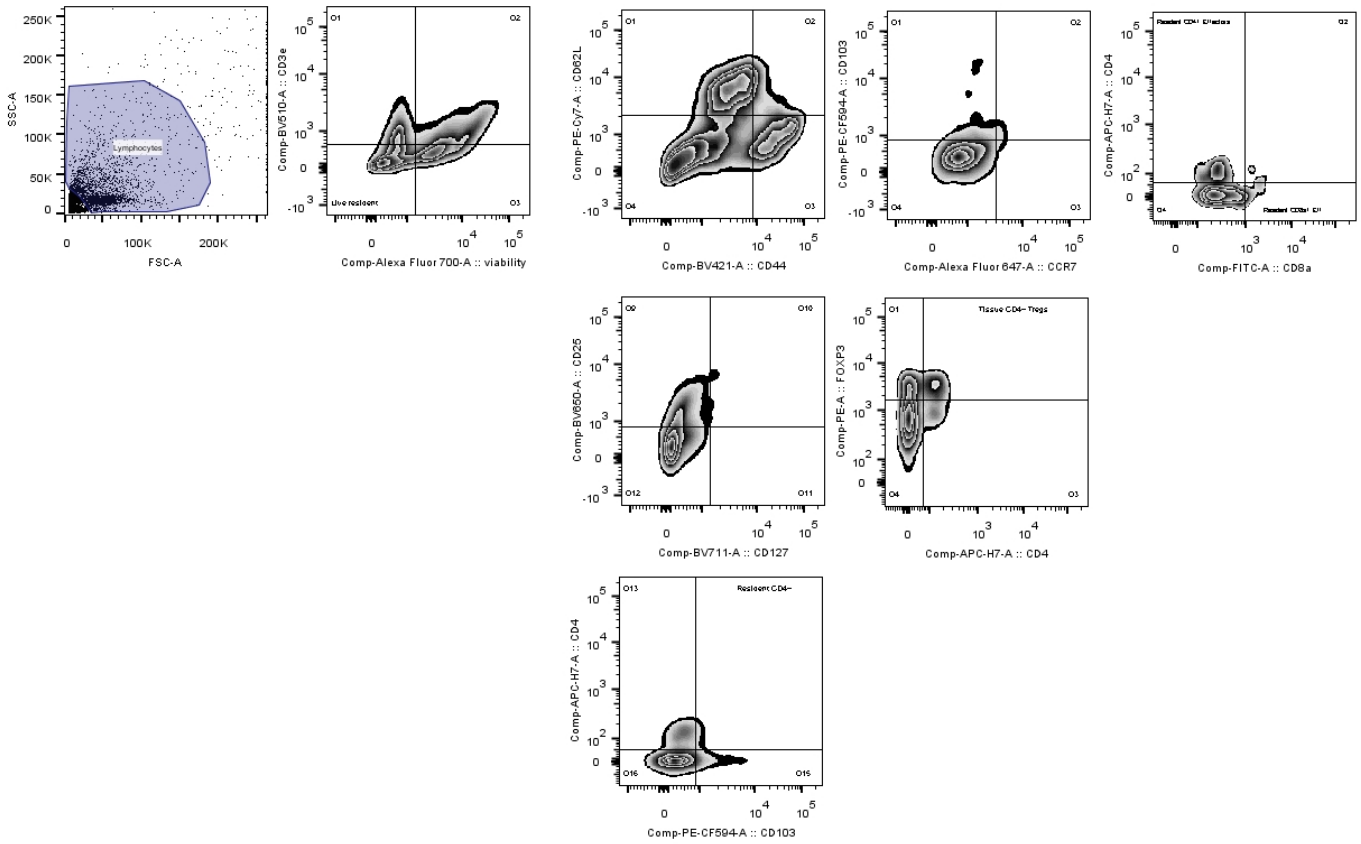
SSC-A
FSC-A
Lymphocytes
Comp-BV510-A :: CD3e
Comp-Alexa Fluor 700-A :: viability
Live resident
Comp-PE-Cy7-A :: CD62L
Comp-BV421-A :: CD44
Comp-PE-CF594-A :: CD103
Comp-Alexa Fluor 647-A :: CCR7
Comp-APC-H7-A :: CD4
Comp-FITC-A :: CD8a
Comp-BV650-A :: CD25
Comp-BV711-A :: CD127
Comp-PE-A :: FOXP3
Tissue CD4+ Tregs
Comp-APC-H7-A :: CD4
Resident CD4+
Comp-PE-CF594-A :: CD103

Figure S4. 1: Gating strategy for flow cytometry data. Lung cells were isolated from Balb/c mice intravenously injected with BV510-conjugated anti-mouse CD3 prior to necropsy and stained for flow cytometry analysis. (A) A FSC/SSC plot was done to gate for lymphocytes which were further gated for (B) viable CD3- cells. (C) These cells were then gated for CD44+ CD62L- followed by (D) CCR7- CD103+ cells and finally, (E) CD4+ or CD8+ to determine the number of lung resident CD4+ or CD8+ T effector cells. To analyze Tregs, viable CD3- cells were gated for (F) CD127- CD25+, which were further gated for (G) Foxp3+ CD4+ cells. Finally, to analyze lung resident CD4+ T cells, viable CD3- cells were gated for CD103+ CD4+ cells.

Chapter 5: General Discussion

After decades of effort towards finding an effective vaccine against RSV, there is still no licensed vaccine available on the market. A major impediment to this development process is the lack of complete understanding of vaccine-induced ERD associated with some types of RSV vaccines, preventing the reliable preclinical assessment of vaccine candidates. As observed in the clinical trial in the 1960s, FIRSV has been shown to induce a Th2-skew in the immune response leading to pulmonary inflammation, airway obstruction and mucus hypersecretion in many animal models (100, 132–134). Moreover, FIRSV induced non-neutralizing antibodies that have also been implicated in ERD development (135–137), while CD4+ T cell subsets were implicated in mediating various parameters of ERD (110, 139). Furthermore, adding to its ineffectiveness, FIRSV has been shown to elicit no memory CD8 T cell responses in mice (160, 161). However, in spite of the known importance of CD8+ T cells in RSV clearance (110, 140, 141), their contribution to effective protection or ERD development remains to be fully understood. Clearly, RSV vaccine candidates should be evaluated for their induction of memory CD8 T cells in addition to the current focus of inducing strong humoral responses (140, 179, 180). Together, eliciting a robust memory CD8 T cell response could be the key in developing a vaccine that can promote long-lived immunity against RSV (140, 142).

RSV F protein has been shown to bind TLR-4 initiating innate immune responses (95). Previous studies have also revealed that TLR activation results in high avidity antigen-specific protective antibodies (136). Moreover, TLR agonists and CD40L could function synergistically to facilitate B cell development (171). Therefore, we employed the RSV F protein, which is a known TLR agonist, along with CD40L as a vaccine. The aim of the

study was to investigate if using CD40L as both an antigen-targeting molecule and immune modulator could result in robust and long-lasting CD8 T cell memory responses.

Unlike FIRSV, Ad-SF40L protected mice effectively against RSV without inducing ERD. This protection involved neutralizing antibodies and memory CD8 T cells, which were not observed with FIRSV immunization. Furthermore, Ad-SF40L was able to elicit effector memory CD8 T cell mediated long-lasting protection against RSV. Our study showed that the protection was CD8 T cell dependent and CD4 T cell independent. Importantly, for the first time, we demonstrated that CD8 T cell mediated long-lasting protection could be achieved through CD40-targeting immunization (Chapter 2).

There are some limitations to this work that are mainly due to the route of administration of the vaccines tested in the study. Since the study aimed at comparing the vectored vaccines delivered intranasally with FIRSV injected intramuscularly, investigation of the alterations in resident T cell populations in the lung tissues was not conducted, given that the viscosity of alum-adjuvanted FIRSV made it difficult to administer intranasally. Previous studies have shown that the route of immunization plays a crucial role in determining tissue-specific immune responses at the site of infection (181). Specifically, protection against respiratory pathogens is best achieved through intranasal vaccination compared to intraperitoneal and intramuscular adminsitration due to the robust induction of pulmonary tissue-resident effector and memory CD8 T cells (181, 182). However, since other studies have shown that both intranasal and intramuscular immunization result in similar numbers of effector memory CD8 T cells in the spleen and lung vasculature (182), we examined the spleen for changes in CD8 T cell populations. Overall, our studies added to better understanding of the

mechanisms underlying CD8 T cell mediated protection against RSV and FIRSV-induced ERD with regards to CD8 T cell induction.

It is of note that the functional activities of CD8 T cells derived from FIRSV immunized animals significantly deteriorated following viral challenge, i.e. the number of CD8 T cells is high but these cells are non-protective. This could be suggestive of T cell exhaustion due to low PD-1 expression, which was investigated in my next study.

Programmed cell death-1 (PD-1) plays an integral role in inducing suppressive signals to regulate autoimmunity, transplantation immunity, infectious immunity and tumour immunity (184). Following activation, PD-1 is transiently expressed on multiple immune cells such as CD4 and CD8 T cells, B cells, macrophages, natural killer cells and dendritic cells (187, 190–196). High expression is vital for regulatory T cell development while follicular helper T cells constitutively express high PD-1 (197–200).

Cotton rats are one of the ideal animal models for RSV infection since most findings in relation to FIRSV-induced ERD have been replicated in this model (208–211). Increasing number of vaccines and therapeutics are being evaluated in cotton rats prior to clinical trials (113, 214, 215). While they were used successfully to determine the dosing, safety and efficacy of Palivizumab, the only licensed therapeutic antibody against RSV (113, 213, 215), very few cotton rat genes have been cloned and characterized limiting the use of this model for mechanistic investigation of pathogenesis and immune responses.

In the context of primary RSV infection in mice, PD1-PDL1 activation has been shown to be vital for limiting immunopathology (205, 217). However, the levels of PD-1 in cotton rats experiencing FIRSV-induced ERD have not been studied, mainly because the PD-1 gene in

cotton rats has not been sequenced. In our study, for the first time, we reported the mRNA sequence of cotton rat PD-1 (crPD-1) and its expression in ERD. Characterization of crPD-1 showed binding to its cognate ligand on dendritic cells and suppression of cytokine secretion. Moreover, we unraveled a new facet of vaccine-induced ERD by showing the downregulation of PD-1 in cotton rats experiencing FIRSV mediated excessive pulmonary inflammation (Chapter 3).

In contrast to other infections where blocking PD-1 improves viral clearance and expansion of virus-specific T cells (203, 204), blocking PD-1 pathway during a RSV infection in mice enhanced pulmonary inflammation and lung injury with minimal effects on viral clearance (205). Similarly, we observed moderate viral clearance and exacerbated pulmonary inflammation in FIRSV immunized cotton rats, which is in good agreement with severe RSV infection where low levels of PD-1 accompany respiratory disease. Further investigations could include antibody design and production against crPD-1 that can be used to block PD-1 pathway in cotton rats helping determine the causative role of PD-1 in ERD development.

High expression of PD-1 is vital for regulatory T cell development (197–200) and Tregs have been shown to accumulate in the lungs and mediastinal lymph nodes of mice infected with RSV recruiting CD8 T cells to the lungs facilitating viral clearance (250, 252, 253). Therefore, since FIRSV immunized animals were found to have poor CD8 T cell function (Chapter 2) and low expression of PD-1 (Chapter 3), we investigated the levels of Tregs in mouse lungs. In addition, we evaluated the use of chitosan in altering FIRSV-mediated immune responses.

Chitosan, in solution, has a positive charge that confers it with mucoadhesive properties that are crucial for its use in intranasal applications (237, 238). It has been shown to enhance antigen-specific immune responses when administered intranasally with an antigen in many animal models (239–242) and in humans (239, 243–246) having a profound effect on humoral (239, 257) and cell-mediated immunity (258). Interestingly, chitosan alone is also able to augment immune responses against some viral infections (240–242). Even though its activities of immune enhancement have been well documented, the molecular mechanisms remain to be fully understood. It would be of interest to investigate whether chitosan could alter immune responses induced by a vaccine known to be less effective and induce severe adverse reactions such as FIRSV.

The role of chitosan in stimulating NK cells and macrophages is well established (240, 258). However, its effect on tissue-resident T cells and Tregs remains to be understood. Given FIRSV is known to induce skewed immune responses and poorly neutralizing antibodies, by employing FIRSV vaccine as a model antigen to study the effects of chitosan, we aimed at gaining better insight into chitosan-mediated immune enhancement. Moreover, given that lung resident T cells are critical for robust RSV clearance and early establishment of cell-mediated responses (181) and Tregs play important roles in regulating the balance between effective immune activation and excessive stimulation during infections (265–269), we focused on these aspects of chitosan-induced immunity.

In our study, we found that chitosan alone could modestly protect animals against RSV infection, while it could significantly reduce RSV infection in mice when used in conjunction with FIRSV. However, chitosan was not able to reverse the ERD induced by FIRSV. Further mechanistic investigation revealed that chitosan enhanced antigen-specific

immune responses, contributing to significant inhibition of RSV replication, through augmentation of Tregs, lung resident T cells and neutralizing antibodies while reversing FIRSV-induced Th2-skewed immune responses. The reversal of FIRSV-induced Th2 responses by chitosan could be mediated by elevated levels of resident CD4+ T cells and CD4+ Tregs leading to a decrease in Th2 cytokines. This is the first report, to the best of our knowledge, showing the effect of chitosan on Tregs and tissue-resident T cells following RSV infection and FIRSV immunization (Chapter 4).

It remains to be understood as to why chitosan failed to reduce exacerbated pulmonary inflammation indicative of ERD in animals following FIRSV vaccination even though it was able to improve the diminished Treg responses and increased Th2 responses implicated in ERD development (110, 136, 270). Further studies are necessary to delineate the definitive roles of Tregs and resident T cells induced by chitosan with respect to protection against RSV infection. Additional studies administering chitosan at the same time as FIRSV, albeit through different routes, could be conducted to test if altering the initial priming with FIRSV has an effect on ERD development.

Together, the studies indicate that FIRSV-induced ERD development could be due to low PD-1 expression resulting in T cell exhaustion and/or curtailed Treg development, which in turn, could lead to diminished recruitment of CD8 T cells for viral clearance preventing effective protection against RSV infection.

References

1. Collins PL, Fearns R, Graham BS. 2013. Respiratory Syncytial Virus: Virology, Reverse Genetics, and Pathogenesis of Disease, p. 3–38. *In* Current topics in microbiology and immunology.
2. Shi T, McAllister DA, O'Brien KL, Simoes EAF, Madhi SA, Gessner BD, Polack FP, Balsells E, Acacio S, Aguayo C, Alassani I, Ali A, Antonio M, Awasthi S, Awori JO, Azziz-Baumgartner E, Baggett HC, Baillie VL, Balmaseda A, Barahona A, Basnet S, Bassat Q, Basualdo W, Bigogo G, Bont L, Breiman RF, Brooks WA, Broor S, Bruce N, Bruden D, Buchy P, Campbell S, Carosone-Link P, Chadha M, Chipeta J, Chou M, Clara W, Cohen C, de Cuellar E, Dang D-A, Dash-yandag B, Deloria-Knoll M, Dherani M, Eap T, Ebruke BE, Echavarria M, de Freitas Lázaro Emediato CC, Fasce RA, Feikin DR, Feng L, Gentile A, Gordon A, Goswami D, Goyet S, Groome M, Halasa N, Hirve S, Homaira N, Howie SRC, Jara J, Jroundi I, Kartasasmita CB, Khuri-Bulos N, Kotloff KL, Krishnan A, Libster R, Lopez O, Lucero MG, Lucion F, Lupisan SP, Marcone DN, McCracken JP, Mejia M, Moisi JC, Montgomery JM, Moore DP, Moraleda C, Moyes J, Munywoki P, Mutyara K, Nicol MP, Nokes DJ, Nymadawa P, da Costa Oliveira MT, Oshitani H, Pandey N, Paranhos-Baccalà G, Phillips LN, Picot VS, Rahman M, Rakoto-Andrianarivelo M, Rasmussen ZA, Rath BA, Robinson A, Romero C, Russomando G, Salimi V, Sawatwong P, Scheltema N, Schweiger B, Scott JAG, Seidenberg P, Shen K, Singleton R, Sotomayor V, Strand TA, Sutanto A, Sylla M, Tapia MD, Thamthitiwat S, Thomas ED, Tokarz R, Turner C, Venter M, Waicharoen S, Wang J, Watthanaworawit W, Yoshida L-M, Yu H, Zar HJ, Campbell H, Nair H, RSV Global Epidemiology Network. 2017. Global, regional, and national disease burden estimates of acute lower respiratory infections due to respiratory syncytial virus in young children in 2015: a systematic review and modelling study. Lancet 390:946–958.
3. Barbato G, Bianchi E, Ingallinella P, Hurni WH, Miller MD, Ciliberto G, Cortese R, Bazzo R, Shiver JW, Pessi A. 2003. Structural analysis of the epitope of the anti-HIV antibody 2F5 sheds light into its mechanism of neutralization and HIV fusion. J Mol Biol 330:1101–15.
4. Weinberger DM, Klugman KP, Steiner CA, Simonsen L, Viboud C. 2015. Association between Respiratory Syncytial Virus Activity and Pneumococcal Disease in Infants: A Time Series Analysis of US Hospitalization Data. PLoS Med 12:e1001776.
5. Stang P, Brandenburg N, Carter B. 2001. The economic burden of respiratory syncytial virus-associated bronchiolitis hospitalizations. Arch Pediatr Adolesc Med 155:95–6.
6. Stockman LJ, Curns AT, Anderson LJ, Fischer-Langley G. 2012. Respiratory Syncytial Virus-associated Hospitalizations Among Infants and Young Children in the United States, 1997–2006. Pediatr Infect Dis J 31:5–9.
7. Hall CB, Weinberg GA, Blumkin AK, Edwards KM, Staat MA, Schultz AF, Poehling KA, Szilagyi PG, Griffin MR, Williams J V., Zhu Y, Grijalva CG, Prill MM, Iwane MK. 2013. Respiratory Syncytial Virus-Associated Hospitalizations Among Children Less Than 24 Months of Age. Pediatrics 132:e341–e348.
8. Prill MM, Iwane MK, Little D, Gerber SI. 2016. Investigation of Respiratory

Syncytial Virus–Associated Deaths Among US Children Aged <2 Years, 2004–2007: Table 1. J Pediatric Infect Dis Soc 5:333–336.
9. Meissner HC. 2016. Viral Bronchiolitis in Children. N Engl J Med 374:62–72.
10. KUTSAYA A, TEROS-JAAKKOLA T, KAKKOLA L, TOIVONEN L, PELTOLA V, WARIS M, JULKUNEN I. 2016. Prospective clinical and serological follow-up in early childhood reveals a high rate of subclinical RSV infection and a relatively high reinfection rate within the first 3 years of life. Epidemiol Infect 144:1622–1633.
11. Hall CB, Long CE, Schnabel KC. 2001. Respiratory Syncytial Virus Infections in Previously Healthy Working Adults. Clin Infect Dis 33:792–796.
12. Hall CB, Walsh EE, Long CE, Schnabel KC. 1991. Immunity to and frequency of reinfection with respiratory syncytial virus. J Infect Dis 163:693–8.
13. Sande CJ, Mutunga MN, Okiro EA, Medley GF, Cane PA, Nokes DJ. 2013. Kinetics of the Neutralizing Antibody Response to Respiratory Syncytial Virus Infections in a Birth Cohort. J Med Virol 85:2020–2025.
14. Ohuma EO, Okiro EA, Ochola R, Sande CJ, Cane PA, Medley GF, Bottomley C, Nokes DJ. 2012. The Natural History of Respiratory Syncytial Virus in a Birth Cohort: The Influence of Age and Previous Infection on Reinfection and Disease. Am J Epidemiol 176:794–802.
15. Eisenhut M. 2006. Extrapulmonary manifestations of severe respiratory syncytial virus infection--a systematic review. Crit Care 10:R107.
16. Rohwedder A, Keminer O, Forster J, Schneider K, Schneider E, Werchau H. 1998. Detection of respiratory syncytial virus RNA in blood of neonates by polymerase chain reaction. J Med Virol 54:320–7.
17. Johnson RA, Prince GA, Suffin SC, Horswood RL, Chanock RM. 1982. Respiratory syncytial virus infection in cyclophosphamide-treated cotton rats. Infect Immun 37:369–73.
18. Brock LG, Karron RA, Krempl CD, Collins PL, Buchholz UJ. 2012. Evaluation of Pneumonia Virus of Mice as a Possible Human Pathogen. J Virol 86:5829–5843.
19. Buchholz UJ, Granzow H, Schuldt K, Whitehead SS, Murphy BR, Collins PL. 2000. Chimeric bovine respiratory syncytial virus with glycoprotein gene substitutions from human respiratory syncytial virus (HRSV): effects on host range and evaluation as a live-attenuated HRSV vaccine. J Virol 74:1187–99.
20. Collins PL, Dickens LE, Buckler-White A, Olmsted RA, Spriggs MK, Camargo E, Coelingh K V. 1986. Nucleotide sequences for the gene junctions of human respiratory syncytial virus reveal distinctive features of intergenic structure and gene order. Proc Natl Acad Sci U S A 83:4594–8.
21. Gould PS, Easton AJ. 2007. Coupled Translation of the Second Open Reading Frame of M2 mRNA Is Sequence Dependent and Differs Significantly within the Subfamily Pneumovirinae. J Virol 81:8488–8496.
22. Bukreyev A, Murphy BR, Collins PL. 2000. Respiratory syncytial virus can tolerate an intergenic sequence of at least 160 nucleotides with little effect on transcription or replication in vitro and in vivo. J Virol 74:11017–26.
23. Harmon SB, Wertz GW. 2002. Transcriptional termination modulated by nucleotides outside the characterized gene end sequence of respiratory syncytial virus. Virology 300:304–15.
24. Collins PL, Olmsted RA, Spriggs MK, Johnson PR, Buckler-White AJ. 1987. Gene overlap and site-specific attenuation of transcription of the viral polymerase L gene of

human respiratory syncytial virus. Proc Natl Acad Sci U S A 84:5134–8.
25. Jeffree CE, Rixon HWM, Brown G, Aitken J, Sugrue RJ. 2003. Distribution of the attachment (G) glycoprotein and GM1 within the envelope of mature respiratory syncytial virus filaments revealed using field emission scanning electron microscopy. Virology 306:254–67.
26. Collins PL, Huang YT, Wertz GW. 1984. Nucleotide sequence of the gene encoding the fusion (F) glycoprotein of human respiratory syncytial virus. Proc Natl Acad Sci U S A 81:7683–7.
27. Bolt G, Pedersen LO, Birkeslund HH. 2000. Cleavage of the respiratory syncytial virus fusion protein is required for its surface expression: role of furin. Virus Res 68:25–33.
28. Collins PL, Mottet G. 1991. Post-translational Processing and Oligomerization of the Fusion Glycoprotein of Human Respiratory Syncytial Virus. J Gen Virol 72:3095–3101.
29. Gruber C, Levine S. 1983. Respiratory Syncytial Virus Polypeptides. III. The Envelope-associated Proteins. J Gen Virol 64:825–832.
30. Day ND, Branigan PJ, Liu C, Gutshall LL, Luo J, Melero JA, Sarisky RT, Del Vecchio AM. 2006. Contribution of cysteine residues in the extracellular domain of the F protein of human respiratory syncytial virus to its function. Virol J 3:34.
31. Gonzalez-Reyes L, Ruiz-Arguello MB, Garcia-Barreno B, Calder L, Lopez JA, Albar JP, Skehel JJ, Wiley DC, Melero JA. 2001. Cleavage of the human respiratory syncytial virus fusion protein at two distinct sites is required for activation of membrane fusion. Proc Natl Acad Sci 98:9859–9864.
32. Zimmer G, Budz L, Herrler G. 2001. Proteolytic Activation of Respiratory Syncytial Virus Fusion Protein. J Biol Chem 276:31642–31650.
33. Begoña Ruiz-Argüello M, González-Reyes L, Calder LJ, Palomo C, Martín D, Saíz MJ, García-Barreno B, Skehel JJ, Melero JA. 2002. Effect of proteolytic processing at two distinct sites on shape and aggregation of an anchorless fusion protein of human respiratory syncytial virus and fate of the intervening segment. Virology 298:317–26.
34. Anderson LJ, Bingham P, Hierholzer JC. 1988. Neutralization of respiratory syncytial virus by individual and mixtures of F and G protein monoclonal antibodies. J Virol 62:4232–8.
35. Walsh EE, Hruska J. 1983. Monoclonal antibodies to respiratory syncytial virus proteins: identification of the fusion protein. J Virol 47:171–7.
36. The IMpact-RSV Study Group. 1998. Palivizumab, a humanized respiratory syncytial virus monoclonal antibody, reduces hospitalization from re- spiratory syncytial virus infection in high risk infants. Pediatrics 102.
37. Wu S-J, Schmidt A, Beil EJ, Day ND, Branigan PJ, Liu C, Gutshall LL, Palomo C, Furze J, Taylor G, Melero JA, Tsui P, Del Vecchio AM, Kruszynski M. 2007. Characterization of the epitope for anti-human respiratory syncytial virus F protein monoclonal antibody 101F using synthetic peptides and genetic approaches. J Gen Virol 88:2719–2723.
38. Costello HM, Ray WC, Chaiwatpongsakorn S, Peeples ME. 2012. Targeting RSV with vaccines and small molecule drugs. Infect Disord Drug Targets 12:110–28.
39. McLellan JS, Ray WC, Peeples ME. 2013. Structure and Function of Respiratory Syncytial Virus Surface Glycoproteins, p. 83–104. *In* Current topics in microbiology and immunology.

40. Calder LJ, González-Reyes L, García-Barreno B, Wharton SA, Skehel JJ, Wiley DC, Melero JA. 2000. Electron Microscopy of the Human Respiratory Syncytial Virus Fusion Protein and Complexes That It Forms with Monoclonal Antibodies. Virology 271:122–131.
41. Ruiz-Arguello MB, Martín D, Wharton SA, Calder LJ, Martín SR, Cano O, Calero M, García-Barreno B, Skehel JJ, Melero JA. 2004. Thermostability of the human respiratory syncytial virus fusion protein before and after activation: implications for the membrane-fusion mechanism. J Gen Virol 85:3677–3687.
42. McLellan JS, Yang Y, Graham BS, Kwong PD. 2011. Structure of Respiratory Syncytial Virus Fusion Glycoprotein in the Postfusion Conformation Reveals Preservation of Neutralizing Epitopes. J Virol 85:7788–7796.
43. Swanson KA, Settembre EC, Shaw CA, Dey AK, Rappuoli R, Mandl CW, Dormitzer PR, Carfi A. 2011. Structural basis for immunization with postfusion respiratory syncytial virus fusion F glycoprotein (RSV F) to elicit high neutralizing antibody titers. Proc Natl Acad Sci 108:9619–9624.
44. Hendricks DA, McIntosh K, Patterson JL. 1988. Further characterization of the soluble form of the G glycoprotein of respiratory syncytial virus. J Virol 62:2228–33.
45. Teng MN, Collins PL. 2002. The central conserved cystine noose of the attachment G protein of human respiratory syncytial virus is not required for efficient viral infection in vitro or in vivo. J Virol 76:6164–71.
46. Venter M, van Niekerk S, Rakgantso A, Bent N. 2011. Identification of Deletion Mutant Respiratory Syncytial Virus Strains Lacking Most of the G Protein in Immunocompromised Children with Pneumonia in South Africa. J Virol 85:8453–8457.
47. Karron RA, Buonagurio DA, Georgiu AF, Whitehead SS, Adamus JE, Clements-Mann ML, Harris DO, Randolph VB, Udem SA, Murphy BR, Sidhu MS. 1997. Respiratory syncytial virus (RSV) SH and G proteins are not essential for viral replication in vitro: clinical evaluation and molecular characterization of a cold-passaged, attenuated RSV subgroup B mutant. Proc Natl Acad Sci U S A 94:13961–6.
48. Kwilas S, Liesman RM, Zhang L, Walsh E, Pickles RJ, Peeples ME. 2009. Respiratory Syncytial Virus Grown in Vero Cells Contains a Truncated Attachment Protein That Alters Its Infectivity and Dependence on Glycosaminoglycans. J Virol 83:10710–10718.
49. Tripp RA, Jones LP, Haynes LM, Zheng H, Murphy PM, Anderson LJ. 2001. CX3C chemokine mimicry by respiratory syncytial virus G glycoprotein. Nat Immunol 2:732–738.
50. Bukreyev A, Yang L, Fricke J, Cheng L, Ward JM, Murphy BR, Collins PL. 2008. The Secreted Form of Respiratory Syncytial Virus G Glycoprotein Helps the Virus Evade Antibody-Mediated Restriction of Replication by Acting as an Antigen Decoy and through Effects on Fc Receptor-Bearing Leukocytes. J Virol 82:12191–12204.
51. Johnson TR, McLellan JS, Graham BS. 2012. Respiratory Syncytial Virus Glycoprotein G Interacts with DC-SIGN and L-SIGN To Activate ERK1 and ERK2. J Virol 86:1339–1347.
52. Polack FP, Irusta PM, Hoffman SJ, Schiatti MP, Melendi GA, Delgado MF, Laham FR, Thumar B, Hendry RM, Melero JA, Karron RA, Collins PL, Kleeberger SR. 2005. The cysteine-rich region of respiratory syncytial virus attachment protein inhibits innate immunity elicited by the virus and endotoxin. Proc Natl Acad Sci 102:8996–

9001.
53. Carter SD, Dent KC, Atkins E, Foster TL, Verow M, Gorny P, Harris M, Hiscox JA, Ranson NA, Griffin S, Barr JN. 2010. Direct visualization of the small hydrophobic protein of human respiratory syncytial virus reveals the structural basis for membrane permeability. FEBS Lett 584:2786–2790.
54. Gan S-W, Tan E, Lin X, Yu D, Wang J, Tan GM-Y, Vararattanavech A, Yeo CY, Soon CH, Soong TW, Pervushin K, Torres J. 2012. The Small Hydrophobic Protein of the Human Respiratory Syncytial Virus Forms Pentameric Ion Channels. J Biol Chem 287:24671–24689.
55. Fuentes S, Tran KC, Luthra P, Teng MN, He B. 2007. Function of the Respiratory Syncytial Virus Small Hydrophobic Protein. J Virol 81:8361–8366.
56. Whitehead SS, Bukreyev A, Teng MN, Firestone CY, St Claire M, Elkins WR, Collins PL, Murphy BR. 1999. Recombinant respiratory syncytial virus bearing a deletion of either the NS2 or SH gene is attenuated in chimpanzees. J Virol 73:3438–42.
57. Mitra R, Baviskar P, Duncan-Decocq RR, Patel D, Oomens AGP. 2012. The Human Respiratory Syncytial Virus Matrix Protein Is Required for Maturation of Viral Filaments. J Virol 86:4432–4443.
58. Ghildyal R, Ho A, Jans DA. 2006. Central role of the respiratory syncytial virus matrix protein in infection. FEMS Microbiol Rev 30:692–705.
59. Groskreutz DJ, Babor EC, Monick MM, Varga SM, Hunninghake GW. 2010. Respiratory Syncytial Virus Limits α Subunit of Eukaryotic Translation Initiation Factor 2 (eIF2α) Phosphorylation to Maintain Translation and Viral Replication. J Biol Chem 285:24023–24031.
60. Asenjo A, Rodríguez L, Villanueva N. 2005. Determination of phosphorylated residues from human respiratory syncytial virus P protein that are dynamically dephosphorylated by cellular phosphatases: a possible role for serine 54. J Gen Virol 86:1109–1120.
61. Asenjo A, Calvo E, Villanueva N. 2006. Phosphorylation of human respiratory syncytial virus P protein at threonine 108 controls its interaction with the M2-1 protein in the viral RNA polymerase complex. J Gen Virol 87:3637–3642.
62. Asenjo A, González-Armas JC, Villanueva N. 2008. Phosphorylation of human respiratory syncytial virus P protein at serine 54 regulates viral uncoating. Virology 380:26–33.
63. Castagne N, Barbier A, Bernard J, Rezaei H, Huet J-C, Henry C, Da Costa B, Eléouët J-F. 2004. Biochemical characterization of the respiratory syncytial virus P-P and P-N protein complexes and localization of the P protein oligomerization domain. J Gen Virol 85:1643–1653.
64. Lu B, Ma C-H, Brazas R, Jin H. 2002. The major phosphorylation sites of the respiratory syncytial virus phosphoprotein are dispensable for virus replication in vitro. J Virol 76:10776–84.
65. Cartee TL, Megaw AG, Oomens AGP, Wertz GW. 2003. Identification of a single amino acid change in the human respiratory syncytial virus L protein that affects transcriptional termination. J Virol 77:7352–60.
66. Liuzzi M, Mason SW, Cartier M, Lawetz C, McCollum RS, Dansereau N, Bolger G, Lapeyre N, Gaudette Y, Lagace L, Massariol M-J, Do F, Whitehead P, Lamarre L, Scouten E, Bordeleau J, Landry S, Rancourt J, Fazal G, Simoneau B. 2005. Inhibitors of Respiratory Syncytial Virus Replication Target Cotranscriptional mRNA

Guanylylation by Viral RNA-Dependent RNA Polymerase. J Virol 79:13105–13115.
67. Fix J, Galloux M, Blondot M-L, Eléouët J-F. 2011. The Insertion of Fluorescent Proteins in a Variable Region of Respiratory Syncytial Virus L Polymerase Results in Fluorescent and Functional Enzymes But with Reduced Activities. Open Virol J 5:103–108.
68. Fearns R, Collins PL. 1999. Role of the M2-1 transcription antitermination protein of respiratory syncytial virus in sequential transcription. J Virol 73:5852–64.
69. Collins PL, Hill MG, Cristina J, Grosfeld H. 1996. Transcription elongation factor of respiratory syncytial virus, a nonsegmented negative-strand RNA virus. Proc Natl Acad Sci U S A 93:81–5.
70. Collins PL, Camargo E, Hill MG. 1999. Support Plasmids and Support Proteins Required for Recovery of Recombinant Respiratory Syncytial Virus. Virology 259:251–255.
71. Cartee TL, Wertz GW. 2001. Respiratory Syncytial Virus M2-1 Protein Requires Phosphorylation for Efficient Function and Binds Viral RNA during Infection. J Virol 75:12188–12197.
72. Tran T-L, Castagne N, Dubosclard V, Noinville S, Koch E, Moudjou M, Henry C, Bernard J, Yeo RP, Eleouet J-F. 2009. The Respiratory Syncytial Virus M2-1 Protein Forms Tetramers and Interacts with RNA and P in a Competitive Manner. J Virol 83:6363–6374.
73. Blondot M-L, Dubosclard V, Fix J, Lassoued S, Aumont-Nicaise M, Bontems F, Eléouët J-F, Sizun C. 2012. Structure and Functional Analysis of the RNA- and Viral Phosphoprotein-Binding Domain of Respiratory Syncytial Virus M2-1 Protein. PLoS Pathog 8:e1002734.
74. Li D, Jans DA, Bardin PG, Meanger J, Mills J, Ghildyal R. 2008. Association of Respiratory Syncytial Virus M Protein with Viral Nucleocapsids Is Mediated by the M2-1 Protein. J Virol 82:8863–8870.
75. Fricke J, Koo LY, Brown CR, Collins PL. 2013. p38 and OGT Sequestration into Viral Inclusion Bodies in Cells Infected with Human Respiratory Syncytial Virus Suppresses MK2 Activities and Stress Granule Assembly. J Virol 87:1333–1347.
76. Cheng X, Park H, Zhou H, Jin H. 2005. Overexpression of the M2-2 Protein of Respiratory Syncytial Virus Inhibits Viral Replication. J Virol 79:13943–13952.
77. Bermingham A, Collins PL. 1999. The M2-2 protein of human respiratory syncytial virus is a regulatory factor involved in the balance between RNA replication and transcription. Proc Natl Acad Sci U S A 96:11259–64.
78. Teng MN, Whitehead SS, Bermingham A, St Claire M, Elkins WR, Murphy BR, Collins PL. 2000. Recombinant respiratory syncytial virus that does not express the NS1 or M2-2 protein is highly attenuated and immunogenic in chimpanzees. J Virol 74:9317–21.
79. Spann KM, Tran KC, Collins PL. 2005. Effects of Nonstructural Proteins NS1 and NS2 of Human Respiratory Syncytial Virus on Interferon Regulatory Factor 3, NF- B, and Proinflammatory Cytokines. J Virol 79:5353–5362.
80. Swedan S, Andrews J, Majumdar T, Musiyenko A, Barik S. 2011. Multiple Functional Domains and Complexes of the Two Nonstructural Proteins of Human Respiratory Syncytial Virus Contribute to Interferon Suppression and Cellular Location. J Virol 85:10090–10100.
81. Bitko V, Shulyayeva O, Mazumder B, Musiyenko A, Ramaswamy M, Look DC, Barik

S. 2007. Nonstructural Proteins of Respiratory Syncytial Virus Suppress Premature Apoptosis by an NF- B-Dependent, Interferon-Independent Mechanism and Facilitate Virus Growth. J Virol 81:1786–1795.
82. Atreya PL, Peeples ME, Collins PL. 1998. The NS1 protein of human respiratory syncytial virus is a potent inhibitor of minigenome transcription and RNA replication. J Virol 72:1452–61.
83. Lindquist ME, Mainou BA, Dermody TS, Crowe JE. 2011. Activation of protein kinase R is required for induction of stress granules by respiratory syncytial virus but dispensable for viral replication. Virology 413:103–110.
84. Lifland AW, Jung J, Alonas E, Zurla C, Crowe JE, Santangelo PJ. 2012. Human Respiratory Syncytial Virus Nucleoprotein and Inclusion Bodies Antagonize the Innate Immune Response Mediated by MDA5 and MAVS. J Virol 86:8245–8258.
85. McDonald TP, Pitt AR, Brown G, Rixon HWM, Sugrue RJ. 2004. Evidence that the respiratory syncytial virus polymerase complex associates with lipid rafts in virus-infected cells: a proteomic analysis. Virology 330:147–157.
86. McCurdy LH, Graham BS. 2003. Role of plasma membrane lipid microdomains in respiratory syncytial virus filament formation. J Virol 77:1747–56.
87. Yeo DS-Y, Chan R, Brown G, Ying L, Sutejo R, Aitken J, Tan B-H, Wenk MR, Sugrue RJ. 2009. Evidence that selective changes in the lipid composition of raft-membranes occur during respiratory syncytial virus infection. Virology 386:168–182.
88. Henderson G, Murray J, Yeo RP. 2002. Sorting of the respiratory syncytial virus matrix protein into detergent-resistant structures is dependent on cell-surface expression of the glycoproteins. Virology 300:244–54.
89. Johnson JE, Gonzales RA, Olson SJ, Wright PF, Graham BS. 2007. The histopathology of fatal untreated human respiratory syncytial virus infection. Mod Pathol 20:108–119.
90. Zhang L, Peeples ME, Boucher RC, Collins PL, Pickles RJ. 2002. Respiratory syncytial virus infection of human airway epithelial cells is polarized, specific to ciliated cells, and without obvious cytopathology. J Virol 76:5654–66.
91. Eshaghi A, Duvvuri VR, Lai R, Nadarajah JT, Li A, Patel SN, Low DE, Gubbay JB. 2012. Genetic Variability of Human Respiratory Syncytial Virus A Strains Circulating in Ontario: A Novel Genotype with a 72 Nucleotide G Gene Duplication. PLoS One 7:e32807.
92. Schlender J, Zimmer G, Herrler G, Conzelmann K-K. 2003. Respiratory syncytial virus (RSV) fusion protein subunit F2, not attachment protein G, determines the specificity of RSV infection. J Virol 77:4609–16.
93. Tayyari F, Marchant D, Moraes TJ, Duan W, Mastrangelo P, Hegele RG. 2011. Identification of nucleolin as a cellular receptor for human respiratory syncytial virus. Nat Med 17:1132–1135.
94. Behera AK, Matsuse H, Kumar M, Kong X, Lockey RF, Mohapatra SS. 2001. Blocking Intercellular Adhesion Molecule-1 on Human Epithelial Cells Decreases Respiratory Syncytial Virus Infection. Biochem Biophys Res Commun 280:188–195.
95. Haynes LM, Moore DD, Kurt-Jones EA, Finberg RW, Anderson LJ, Tripp RA. 2001. Involvement of Toll-Like Receptor 4 in Innate Immunity to Respiratory Syncytial Virus. J Virol 75:10730–10737.
96. Kim HW, Canchola JG, Brandt CD, Pyles G, Chanock RM, Jensen K, Parrott RH. 1969. Respiratory syncytial virus disease in infants despite prior administration of

antigenic inactivated vaccine. Am J Epidemiol 89:422–34.
97. Kapikian AZ, Mitchell RH, Chanock RM, Shvedoff RA, Stewart CE. 1969. Epidemiologic Study Of Altered Clinical Reactivity To Respiratory Syncytial (RS) Virus Infection In Children Previously Vaccinated With An Inactivated Rs Virus Vaccine. Am J Epidemiol 88:405–421.
98. Fulginiti VA, Eller JJ, Sieber OF, Joyner JW, Minamitani M, Meiklejohn G. 1969. Respiratory virus immunization. I. A field trial of two inactivated respiratory virus vaccines; an aqueous trivalent parainfluenza virus vaccine and an alum-precipitated respiratory syncytial virus vaccine. Am J Epidemiol 89:435–48.
99. Chin J, Magoeetn RL, Shearer L a NN, Schleble JH, Lennette EH. 1969. Field Evaluation of a Respiratory Syncytial Virus Vaccine and a Trivalent Parainfluenza Virus Vaccine in a Pediatric Population. Am J Epidemiol 89:449–463.
100. Prince GA, Curtis SJ, Yim KC, Porter DD. 2001. Vaccine-enhanced respiratory syncytial virus disease in cotton rats following immunization with Lot 100 or a newly prepared reference vaccine. J Gen Virol 82:2881–2888.
101. Murphy BR, Prince GA, Walsh EE, Kim HW, Parrott RH, Hemming VG, Rodriguez WJ, Chanock RM. 1986. Dissociation between serum neutralizing and glycoprotein antibody responses of infants and children who received inactivated respiratory syncytial virus vaccine. J Clin Microbiol 24:197–202.
102. Murphy BR, Walsh EE. 1988. Formalin-inactivated respiratory syncytial virus vaccine induces antibodies to the fusion glycoprotein that are deficient in fusion-inhibiting activity. J Clin Microbiol 26:1595–1597.
103. Kim HW, Leikin SL, Arrobio J, Brandt CD, Chanock RM, Parrott RH. 1976. Cell-mediated immunity to respiratory syncytial virus induced by inactivated vaccine or by infection. Pediatr Res 10:75–78.
104. Lennon RG, Isacson P, Rosales T, Elsea WR, Karzon DT, Winkelstein W. 1967. Skin tests with measles and poliomyelitis vaccines in recipients of inactivated measles virus vaccine. Delayed dermal hypersensitivity. JAMA 200:275–80.
105. Anderson LJ, Dormitzer PR, Nokes DJ, Rappuoli R, Roca A, Graham BS. 2013. Strategic priorities for respiratory syncytial virus (RSV) vaccine development. Vaccine 31:B209–B215.
106. Graham BS, Henderson GS, Tang YW, Lu X, Neuzil KM, Colley DG. 1993. Priming immunization determines T helper cytokine mRNA expression patterns in lungs of mice challenged with respiratory syncytial virus. J Immunol 151:2032–40.
107. Delgado MF, Coviello S, Monsalvo AC, Melendi GA, Hernandez JZ, Batalle JP, Diaz L, Trento A, Chang H-Y, Mitzner W, Ravetch J, Melero JA, Irusta PM, Polack FP. 2009. Lack of antibody affinity maturation due to poor Toll-like receptor stimulation leads to enhanced respiratory syncytial virus disease. Nat Med 15:34–41.
108. Wright PF, Karron RA, Belshe RB, Shi JR, Randolph VB, Collins PL, O'Shea AF, Gruber WC, Murphy BR. 2007. The absence of enhanced disease with wild type respiratory syncytial virus infection occurring after receipt of live, attenuated, respiratory syncytial virus vaccines. Vaccine 25:7372–7378.
109. Belshe RB, Van Voris LP, Mufson MA. 1982. Parenteral administration of live respiratory syncytial virus vaccine: results of a field trial. J Infect Dis 145:311–9.
110. Knudson CJ, Hartwig SM, Meyerholz DK, Varga SM. 2015. RSV Vaccine-Enhanced Disease Is Orchestrated by the Combined Actions of Distinct CD4 T Cell Subsets. PLoS Pathog 11:1–23.

111. Beeler JA, van Wyke Coelingh K. 1989. Neutralization epitopes of the F glycoprotein of respiratory syncytial virus: effect of mutation upon fusion function. J Virol 63:2941–50.
112. Johnson S, Oliver C, Prince GA, Hemming VG, Pfarr DS, Wang SC, Dormitzer M, O'Grady J, Koenig S, Tamura JK, Woods R, Bansal G, Couchenour D, Tsao E, Hall WC, Young JF. 1997. Development of a humanized monoclonal antibody (MEDI-493) with potent in vitro and in vivo activity against respiratory syncytial virus. J Infect Dis 176:1215–24.
113. Wu H, Pfarr DS, Johnson S, Brewah YA, Woods RM, Patel NK, White WI, Young JF, Kiener PA. 2007. Development of Motavizumab, an Ultra-potent Antibody for the Prevention of Respiratory Syncytial Virus Infection in the Upper and Lower Respiratory Tract. J Mol Biol 368:652–665.
114. Simoes, E., X. Carbonell, G. Losonsky, M. Hultquist, B. Harris and EC. 2007. Phase III trial of motavizumab, an enhanced potency respiratory syncytial virus (RSV)-specific monoclonal antibody for the prevention of serious RSV disease in high risk infants. Abstr 48th Annu Meet Eur Soc Paediatr Res.
115. Huang K, Incognito L, Cheng X, Ulbrandt ND, Wu H. 2010. Respiratory Syncytial Virus-Neutralizing Monoclonal Antibodies Motavizumab and Palivizumab Inhibit Fusion. J Virol 84:8132–8140.
116. Neuzil KM. 2016. Progress toward a Respiratory Syncytial Virus Vaccine. Clin Vaccine Immunol 23:186–188.
117. Haynes LM. 2013. Progress and Challenges in RSV Prophylaxis and Vaccine Development. J Infect Dis 208:S177–S183.
118. McLaurin KK, Farr AM, Wade SW, Diakun DR, Stewart DL. 2016. Respiratory syncytial virus hospitalization outcomes and costs of full-term and preterm infants. J Perinatol 36:990–996.
119. Cianci C, Yu K-L, Combrink K, Sin N, Pearce B, Wang A, Civiello R, Voss S, Luo G, Kadow K, Genovesi E V, Venables B, Gulgeze H, Trehan A, James J, Lamb L, Medina I, Roach J, Yang Z, Zadjura L, Colonno R, Clark J, Meanwell N, Krystal M. 2004. Orally active fusion inhibitor of respiratory syncytial virus. Antimicrob Agents Chemother 48:413–22.
120. Douglas JL, Panis ML, Ho E, Lin K-Y, Krawczyk SH, Grant DM, Cai R, Swaminathan S, Cihlar T. 2003. Inhibition of respiratory syncytial virus fusion by the small molecule VP-14637 via specific interactions with F protein. J Virol 77:5054–64.
121. Roymans D, De Bondt HL, Arnoult E, Geluykens P, Gevers T, Van Ginderen M, Verheyen N, Kim H, Willebrords R, Bonfanti J-F, Bruinzeel W, Cummings MD, van Vlijmen H, Andries K. 2010. Binding of a potent small-molecule inhibitor of six-helix bundle formation requires interactions with both heptad-repeats of the RSV fusion protein. Proc Natl Acad Sci 107:308–313.
122. Cianci C, Langley DR, Dischino DD, Sun Y, Yu K-L, Stanley A, Roach J, Li Z, Dalterio R, Colonno R, Meanwell NA, Krystal M. 2004. Targeting a binding pocket within the trimer-of-hairpins: Small-molecule inhibition of viral fusion. Proc Natl Acad Sci 101:15046–15051.
123. Search of: RSV Infection - List Results - ClinicalTrials.gov.
124. Higgins D, Trujillo C, Keech C. 2016. Advances in RSV Vaccine Research and Development - A Global AgendaWHO.
125. Calvo C, García-García ML, Blanco C, Pozo F, Flecha IC, Pérez-Breña P. 2007. Role

of Rhinovirus in Hospitalized Infants With Respiratory Tract Infections in Spain. Pediatr Infect Dis J 26:904–908.
126. Falsey AR. 2005. Respiratory syncytial virus infection in elderly and high-risk adults. Exp Lung Res 31 Suppl 1:77.
127. Nair H, Nokes DJ, Gessner BD, Dherani M, Madhi SA, Singleton RJ, O'Brien KL, Roca A, Wright PF, Bruce N, Chandran A, Theodoratou E, Sutanto A, Sedyaningsih ER, Ngama M, Munywoki PK, Kartasasmita C, Simões EA, Rudan I, Weber MW, Campbell H. 2010. Global burden of acute lower respiratory infections due to respiratory syncytial virus in young children: a systematic review and meta-analysis. Lancet 375:1545–1555.
128. Ehlken B, Ihorst G, Lippert B, Rohwedder A, Petersen G, Schumacher M, Forster J, PRIDE Study Group. 2005. Economic impact of community-acquired and nosocomial lower respiratory tract infections in young children in Germany. Eur J Pediatr 164:607–615.
129. Collins PL. 2001. Fields Virology, p. 1443–1486. *In* Knipe, D, PM, H (eds.), . Raven Press, New York.
130. Glezen WP, Taber LH, Frank AL, Kasel JA. 1986. Risk of primary infection and reinfection with respiratory syncytial virus. Am J Dis Child 140:543–6.
131. Chin J, Magoffin RL, Shearer LA, Schieble JH, Lennette EH. 1969. Field evaluation of a respiratory syncytial virus vaccine and a trivalent parainfluenza virus vaccine in a pediatric population. Am J Epidemiol 89:449–63.
132. Johnson T, Graham B. 1999. Secreted respiratory syncytial virus G glycoprotein induces interleukin-5 (IL-5), IL-13, and eosinophilia by an IL-4-independent mechanism. J Virol 73:8485–8495.
133. Muralidharan A, Li C, Wang L, Li X. 2017. Immunopathogenesis associated with formaldehyde-inactivated RSV vaccine in preclinical and clinical studies. Expert Rev Vaccines.
134. Deng Y, Herbert JA, Smith CM, Smyth RL. 2018. An in vitro transepithelial migration assay to evaluate the role of neutrophils in Respiratory Syncytial Virus (RSV) induced epithelial damage. Sci Rep 8:6777.
135. Polack FP, Teng MN, Collins PL, Prince GA, Exner M, Regele H, Lirman DD, Rabold R, Hoffman SJ, Karp CL, Kleeberger SR, Wills-Karp M, Karron RA. 2002. A role for immune complexes in enhanced respiratory syncytial virus disease. J Exp Med 196:859–65.
136. Delgado MF, Coviello S, Monsalvo AC, Melendi GA, Hernandez JZ, Batalle JP, Diaz L, Trento A, Chang H-Y, Mitzner W, Ravetch J, Melero JA, Irusta PM, Polack FP. 2009. Lack of antibody affinity maturation due to poor Toll-like receptor stimulation leads to enhanced respiratory syncytial virus disease. Nat Med 15:34–41.
137. Jaberolansar N, Chappell KJ, Watterson D, Bermingham IM, Toth I, Young PR, Skwarczynski M. 2017. Induction of high titred, non-neutralising antibodies by self-adjuvanting peptide epitopes derived from the respiratory syncytial virus fusion protein. Sci Rep 7:11130.
138. Knudson CJ, Hartwig SM, Meyerholz DK, Varga SM. 2015. RSV Vaccine-Enhanced Disease Is Orchestrated by the Combined Actions of Distinct CD4 T Cell Subsets. PLoS Pathog.
139. Hu X, Li X, Hu C, Qin L, He R, Luo L, Tang W, Feng J. 2017. Respiratory Syncytial Virus Exacerbates OVA-mediated asthma in mice through C5a-C5aR regulating

CD4+T cells Immune Responses. Sci Rep 7:15207.
140. Schmidt ME, Knudson CJ, Hartwig SM, Pewe LL, Meyerholz DK, Langlois RA, Harty JT, Varga SM. 2018. Memory CD8 T cells mediate severe immunopathology following respiratory syncytial virus infection. PLOS Pathog 14:e1006810.
141. Graham BS, Bunton LA, Wright PF, Karzon DT. 1991. Role of T lymphocyte subsets in the pathogenesis of primary infection and rechallenge with respiratory syncytial virus in mice. J Clin Invest 88:1026–1033.
142. Stoley ME, Knudson CJ, Pewe LL, Meyerholz DK, Langlois RA, TenOever BR, Harty JT, Varga SM. 2016. Memory CD8 T cells in RSV infection: friend or foe? J Immunol 196.
143. Kovacsovics-Bankowski M, Clark K, Benacerraf B, Rock KL. 1993. Efficient major histocompatibility complex class I presentation of exogenous antigen upon phagocytosis by macrophages. Proc Natl Acad Sci U S A 90:4942–6.
144. Guermonprez P, Valladeau J, Zitvogel L, Théry C, Amigorena S. 2002. ANTIGEN PRESENTATION AND T CELL STIMULATION BY DENDRITIC CELLS. Annu Rev Immunol 20:621–667.
145. Whitmire JK, Ahmed R. 2000. Costimulation in antiviral immunity: differential requirements for CD4(+) and CD8(+) T cell responses. Curr Opin Immunol 12:448–55.
146. van Kooten C, Banchereau J. 2000. CD40-CD40 ligand. J Leukoc Biol.
147. Bishop GA, Hostager BS. 2003. The CD40-CD154 interaction in B cell-T cell liaisons. Cytokine Growth Factor Rev 14:297–309.
148. Ma DY, Clark EA. 2009. The role of CD40 and CD154/CD40L in dendritic cells. Semin Immunol 21:265–272.
149. Lapointe R, Bellemare-Pelletier A, Housseau F, Thibodeau J, Hwu P. 2003. CD40-stimulated B lymphocytes pulsed with tumor antigens are effective antigen-presenting cells that can generate specific T cells. Cancer Res 63:2836–43.
150. Lee S, Stokes KL, Currier MG, Sakamoto K, Lukacs NW, Celis E, Moore ML. 2012. Vaccine-Elicited CD8+ T Cells Protect against Respiratory Syncytial Virus Strain A2-Line19F-Induced Pathogenesis in BALB/c Mice. J Virol 86:13016–13024.
151. Tripp RA, Jones L, Anderson LJ, Brown MP. 2000. CD40 Ligand (CD154) Enhances the Th1 and Antibody Responses to Respiratory Syncytial Virus in the BALB/c Mouse. J Immunol 164:5913–5921.
152. Harcourt JL, Brown MP, Anderson LJ, Tripp RA. 2003. CD40 ligand (CD154) improves the durability of respiratory syncytial virus DNA vaccination in BALB/c mice. Vaccine.
153. Hashem AM, Gravel C, Chen Z, Yi Y, Tocchi M, Jaentschke B, Fan X, Li C, Rosu-Myles M, Pereboev A, He R, Wang J, Li X. 2014. CD40 Ligand Preferentially Modulates Immune Response and Enhances Protection against Influenza Virus. J Immunol.
154. Moghaddam A, Olszewska W, Wang B, Tregoning JS, Helson R, Sattentau QJ, Openshaw PJM. 2006. A potential molecular mechanism for hypersensitivity caused by formalin-inactivated vaccines. Nat Med 12:905–907.
155. Openshaw PJ, Culley FJ, Olszewska W. 2002. Immunopathogenesis of vaccine-enhanced RSV disease. Vaccine 20:S27–S31.
156. Cannon MJ, Stott EJ, Taylor G, Askonas BA. 1987. Clearance of persistent respiratory syncytial virus infections in immunodeficient mice following transfer of primed T

cells. Immunology 62:133–8.
157. Taylor G, Stott EJ, Hayle AJ. 1985. Cytotoxic Lymphocytes in the Lungs of Mice Infected with Respiratory Syncytial Virus. J Gen Virol 66:2533–2538.
158. Martin MD, Kim MT, Shan Q, Sompallae R, Xue HH, Harty JT, Badovinac VP. 2015. Phenotypic and Functional Alterations in Circulating Memory CD8 T Cells with Time after Primary Infection. PLoS Pathog.
159. Knudson CJ, Varga SM. 2015. CD8 T-cell response to respiratory syncytial virus infection. Future Virol 10:779–794.
160. Acosta PL, Caballero MT, Polack FP. 2016. Brief History and Characterization of Enhanced Respiratory Syncytial Virus Disease. Clin Vaccine Immunol.
161. Olson MR, Varga SM. 2007. CD8 T cells inhibit respiratory syncytial virus (RSV) vaccine-enhanced disease. J Immunol 179:5415–24.
162. Heidema J, Lukens M V, van Maren WWC, van Dijk MEA, Otten HG, van Vught AJ, van der Werff DBM, van Gestel SJP, Semple MG, Smyth RL, Kimpen JLL, van Bleek GM. 2007. CD8+ T cell responses in bronchoalveolar lavage fluid and peripheral blood mononuclear cells of infants with severe primary respiratory syncytial virus infections. J Immunol 179:8410–7.
163. Rutigliano JA, Graham BS. 2004. Prolonged production of TNF-alpha exacerbates illness during respiratory syncytial virus infection. J Immunol 173:3408–17.
164. Aung S, Rutigliano JA, Graham BS. 2001. Alternative Mechanisms of Respiratory Syncytial Virus Clearance in Perforin Knockout Mice Lead to Enhanced Disease. J Virol 75:9918–9924.
165. Novavax. Clinical Stage Pipeline.
166. WHO. 2014. Status of vaccine research and development of vaccines for RSVWHO PD-VAC.
167. Young J. 2002. Development of a potent respiratory syncytial virus specific monoclonal antibody for the prevention of serious lower respiratory tract disease in infants. Respir Med 96:S31–S35.
168. McGill JL, Kelly SM, Kumar P, Speckhart S, Haughney SL, Henningson J, Narasimhan B, Sacco RE. 2018. Efficacy of mucosal polyanhydride nanovaccine against respiratory syncytial virus infection in the neonatal calf. Sci Rep 8:3021.
169. Fuentes S, Klenow L, Golding H, Khurana S. 2017. Preclinical evaluation of bacterially produced RSV-G protein vaccine: Strong protection against RSV challenge in cotton rat model. Sci Rep 7:42428.
170. Robitaille AC, Caron E, Zucchini N, Mukawera E, Adam D, Mariani MK, Gélinas A, Fortin A, Brochiero E, Grandvaux N. 2017. DUSP1 regulates apoptosis and cell migration, but not the JIP1-protected cytokine response, during Respiratory Syncytial Virus and Sendai Virus infection. Sci Rep 7:17388.
171. Boeglin E, Smulski CR, Brun S, Milosevic S, Schneider P, Fournel S. 2011. Toll-Like receptor agonists synergize with CD40L to induce either proliferation or plasma cell differentiation of mouse B cells. PLoS One.
172. Widjaja I, Wicht O, Luytjes W, Leenhouts K, Rottier PJM, van Kuppeveld FJM, Haijema BJ, de Haan CAM. 2016. Characterization of Epitope-Specific Anti-Respiratory Syncytial Virus (Anti-RSV) Antibody Responses after Natural Infection and after Vaccination with Formalin-Inactivated RSV. J Virol 90:5965–5977.
173. Magro M, Mas V, Chappell K, Vazquez M, Cano O, Luque D, Terron MC, Melero JA, Palomo C. 2012. Neutralizing antibodies against the preactive form of respiratory

syncytial virus fusion protein offer unique possibilities for clinical intervention. Proc Natl Acad Sci 109:3089–3094.
174. Ngwuta JO, Chen M, Modjarrad K, Joyce MG, Kanekiyo M, Kumar A, Yassine HM, Moin SM, Killikelly AM, Chuang G-Y, Druz A, Georgiev IS, Rundlet EJ, Sastry M, Stewart-Jones GBE, Yang Y, Zhang B, Nason MC, Capella C, Peeples ME, Ledgerwood JE, McLellan JS, Kwong PD, Graham BS. 2015. Prefusion F–specific antibodies determine the magnitude of RSV neutralizing activity in human sera. Sci Transl Med 7:309ra162-309ra162.
175. Laidlaw BJ, Decman V, Ali M-AA, Abt MC, Wolf AI, Monticelli LA, Mozdzanowska K, Angelosanto JM, Artis D, Erikson J, Wherry EJ. 2013. Cooperativity Between CD8+ T Cells, Non-Neutralizing Antibodies, and Alveolar Macrophages Is Important for Heterosubtypic Influenza Virus Immunity. PLoS Pathog 9:e1003207.
176. Kim JH, Reber AJ, Kumar A, Ramos P, Sica G, Music N, Guo Z, Mishina M, Stevens J, York IA, Jacob J, Sambhara S. 2016. Non-neutralizing antibodies induced by seasonal influenza vaccine prevent, not exacerbate A(H1N1)pdm09 disease. Sci Rep 6:1–13.
177. Welliver TP, Garofalo RP, Hosakote Y, Hintz KH, Avendano L, Sanchez K, Velozo L, Jafri H, Chavez-Bueno S, Ogra PL, McKinney L, Reed JL, Welliver, Sr. RC. 2007. Severe Human Lower Respiratory Tract Illness Caused by Respiratory Syncytial Virus and Influenza Virus Is Characterized by the Absence of Pulmonary Cytotoxic Lymphocyte Responses. J Infect Dis 195:1126–1136.
178. Schmidt ME, Varga SM. 2018. The CD8 T cell response to respiratory virus infections. Front Immunol.
179. Graham BS, Modjarrad K, McLellan JS. 2015. Novel antigens for RSV vaccines. Curr Opin Immunol 35:30–38.
180. Piedra PA, Jewell AM, Cron SG, Atmar RL, Glezen WP. 2003. Correlates of immunity to respiratory syncytial virus (RSV) associated-hospitalization: establishment of minimum protective threshold levels of serum neutralizing antibodies. Vaccine 21:3479–82.
181. Morabito KM, Ruckwardt TR, Redwood AJ, Moin SM, Price DA, Graham BS. 2017. Intranasal administration of RSV antigen-expressing MCMV elicits robust tissue-resident effector and effector memory CD8+ T cells in the lung. Mucosal Immunol 10:545–554.
182. McMaster SR, Wein AN, Dunbar PR, Hayward SL, Cartwright EK, Denning TL, Kohlmeier JE. 2018. Pulmonary antigen encounter regulates the establishment of tissue-resident CD8 memory T cells in the lung airways and parenchyma. Mucosal Immunol 11:1071–1078.
183. Weiss KA, Christiaansen AF, Fulton RB, Meyerholz DK, Varga SM. 2011. Multiple CD4+ T Cell Subsets Produce Immunomodulatory IL-10 During Respiratory Syncytial Virus Infection. J Immunol 187:3145–3154.
184. Jin H-T, Ahmed R, Okazaki T. 2010. Role of PD-1 in Regulating T-Cell Immunity 350:17–37.
185. Zhang X, Schwartz J-CD, Guo X, Bhatia S, Cao E, Lorenz M, Cammer M, Chen L, Zhang Z-Y, Edidin MA, Nathenson SG, Almo SC. 2004. Structural and functional analysis of the costimulatory receptor programmed death-1. Immunity 20:337–47.
186. Nishimura H, Honjo T, Minato N. 2000. Facilitation of beta selection and modification of positive selection in the thymus of PD-1-deficient mice. J Exp Med 191:891–8.

187. Agata Y, Kawasaki A, Nishimura H, Ishida Y, Tsubata T, Yagita H, Honjo T. 1996. Expression of the PD-1 antigen on the surface of stimulated mouse T and B lymphocytes. Int Immunol 8:765–72.
188. Nishimura H, Agata Y, Kawasaki A, Sato M, Imamura S, Minato N, Yagita H, Nakano T, Honjo T. 1996. Developmentally regulated expression of the PD-1 protein on the surface of double-negative (CD4-CD8-) thymocytes. Int Immunol 8:773–80.
189. Wherry EJ, Ha S-J, Kaech SM, Haining WN, Sarkar S, Kalia V, Subramaniam S, Blattman JN, Barber DL, Ahmed R. 2007. Molecular Signature of CD8+ T Cell Exhaustion during Chronic Viral Infection. Immunity 27:670–684.
190. Haynes NM, Allen CDC, Lesley R, Ansel KM, Killeen N, Cyster JG. 2007. Role of CXCR5 and CCR7 in follicular Th cell positioning and appearance of a programmed cell death gene-1high germinal center-associated subpopulation. J Immunol 179:5099–108.
191. Yao S, Wang S, Zhu Y, Luo L, Zhu G, Flies S, Xu H, Ruff W, Broadwater M, Choi I-H, Tamada K, Chen L. 2009. PD-1 on dendritic cells impedes innate immunity against bacterial infection. Blood 113:5811–5818.
192. Zhang Y, Ma CJ, Ni L, Zhang CL, Wu XY, Kumaraguru U, Li CF, Moorman JP, Yao ZQ. 2011. Cross-Talk between Programmed Death-1 and Suppressor of Cytokine Signaling-1 in Inhibition of IL-12 Production by Monocytes/Macrophages in Hepatitis C Virus Infection. J Immunol 186:3093–3103.
193. Okazaki T, Maeda A, Nishimura H, Kurosaki T, Honjo T. 2001. PD-1 immunoreceptor inhibits B cell receptor-mediated signaling by recruiting src homology 2-domain-containing tyrosine phosphatase 2 to phosphotyrosine. Proc Natl Acad Sci 98:13866–13871.
194. Bally APR, Lu P, Tang Y, Austin JW, Scharer CD, Ahmed R, Boss JM. 2015. NF-κB Regulates PD-1 Expression in Macrophages. J Immunol 194:4545–4554.
195. Honda T, Egen JG, Lämmermann T, Kastenmüller W, Torabi-Parizi P, Germain RN. 2014. Tuning of Antigen Sensitivity by T Cell Receptor-Dependent Negative Feedback Controls T Cell Effector Function in Inflamed Tissues. Immunity 40:235–247.
196. Costa PAC, Leoratti FMS, Figueiredo MM, Tada MS, Pereira DB, Junqueira C, Soares IS, Barber DL, Gazzinelli RT, Antonelli LR V. 2015. Induction of Inhibitory Receptors on T Cells During Plasmodium vivax Malaria Impairs Cytokine Production. J Infect Dis 212:1999–2010.
197. Francisco LM, Sage PT, Sharpe AH. 2010. The PD-1 pathway in tolerance and autoimmunity. Immunol Rev 236:219–242.
198. Boussiotis VA, Chatterjee P, Li L. 2014. Biochemical Signaling of PD-1 on T Cells and Its Functional Implications. Cancer J 20:265–271.
199. Johnston RJ, Poholek AC, DiToro D, Yusuf I, Eto D, Barnett B, Dent AL, Craft J, Crotty S. 2009. Bcl6 and Blimp-1 Are Reciprocal and Antagonistic Regulators of T Follicular Helper Cell Differentiation. Science (80-) 325:1006–1010.
200. Crotty S. 2011. Follicular Helper CD4 T Cells (TFH). Annu Rev Immunol 29:621–663.
201. Hashimoto M, Kamphorst AO, Im SJ, Kissick HT, Pillai RN, Ramalingam SS, Araki K, Ahmed R. 2018. CD8 T Cell Exhaustion in Chronic Infection and Cancer: Opportunities for Interventions. Annu Rev Med 69:301–318.
202. Bally APR, Austin JW, Boss JM. 2016. Genetic and Epigenetic Regulation of PD-1 Expression. J Immunol 196:2431–2437.

203. Velu V, Titanji K, Zhu B, Husain S, Pladevega A, Lai L, Vanderford TH, Chennareddi L, Silvestri G, Freeman GJ, Ahmed R, Amara RR. 2009. Enhancing SIV-specific immunity in vivo by PD-1 blockade. Nature 458:206–210.
204. Barber DL, Wherry EJ, Masopust D, Zhu B, Allison JP, Sharpe AH, Freeman GJ, Ahmed R. 2006. Restoring function in exhausted CD8 T cells during chronic viral infection. Nature 439:682–687.
205. Yao S, Jiang L, Moser EK, Jewett LB, Wright J, Du J, Zhou B, Davis SD, Krupp NL, Braciale TJ, Sun J. 2015. Control of pathogenic effector T-cell activities in situ by PD-L1 expression on respiratory inflammatory dendritic cells during respiratory syncytial virus infection. Mucosal Immunol 8:746–759.
206. Kim HW, Canchola JG, Brandt CD, Pyles G, Chanock RM, Jensen K, Parrott RH. 1969. Respiratory Syncytial Virus Disease in Infants Despite Prior Administration of Antigenic Inactivated Vaccine. Am J Epidemiol 89:422–434.
207. Johnson TR, Graham BS. 1999. Secreted respiratory syncytial virus G glycoprotein induces interleukin-5 (IL-5), IL-13, and eosinophilia by an IL-4-independent mechanism. J Virol 73:8485–95.
208. Prince GA, Jenson AB, Hemming VG, Murphy BR, Walsh EE, Horswood RL, Chanock RM. 1986. Enhancement of respiratory syncytial virus pulmonary pathology in cotton rats by prior intramuscular inoculation of formalin-inactivated virus. J Virol 57:721–8.
209. Prince GA, Horswood RL, Camargo E, Koenig D, Chanock RM. 1983. Mechanisms of immunity to respiratory syncytial virus in cotton rats. Infect Immun 42:81–7.
210. Curtis SJ, Ottolini MG, Porter DD, Prince GA. 2002. Age-dependent replication of respiratory syncytial virus in the cotton rat. Exp Biol Med (Maywood) 227:799–802.
211. Boukhvalova MS, Yim KC, Kuhn KH, Hemming JP, Prince GA, Porter DD, Blanco JCG. 2007. Age-Related Differences in Pulmonary Cytokine Response to Respiratory Syncytial Virus Infection: Modulation by Anti-inflammatory and Antiviral Treatment. J Infect Dis 195:511–518.
212. Green MG, Huey D, Niewiesk S. 2013. The cotton rat (Sigmodon hispidus) as an animal model for respiratory tract infections with human pathogens. Lab Anim (NY) 42:170–176.
213. Niewiesk S. 2009. Current animal models: cotton rat animal model. Curr Top Microbiol Immunol 330:89–110.
214. Niewiesk S, Prince G. 2002. Diversifying animal models: the use of hispid cotton rats (*Sigmodon hispidus*) in infectious diseases. Lab Anim 36:357–372.
215. Prince GA. 1994. The cotton rat in biomedical research. AWIC Newsl 5:3–5.
216. Wu H, Pfarr DS, Johnson S, Brewah YA, Woods RM, Patel NK, White WI, Young JF, Kiener PA. 2007. Development of Motavizumab, an Ultra-potent Antibody for the Prevention of Respiratory Syncytial Virus Infection in the Upper and Lower Respiratory Tract. J Mol Biol 368:652–665.
217. Erickson JJ, Gilchuk P, Hastings AK, Tollefson SJ, Johnson M, Downing MB, Boyd KL, Johnson JE, Kim AS, Joyce S, Williams J V. 2012. Viral acute lower respiratory infections impair CD8+ T cells through PD-1. J Clin Invest 122:2967–2982.
218. Russell MS, Muralidharan A, Larocque L, Cao J, Deschambault Y, Varga J, Thulasi Raman SN, Li X. 2018. Identification and characterisation of the CD40-ligand of Sigmodon hispidus. PLoS One 13:e0199067.
219. Reynolds CR, Islam SA, Sternberg MJE. 2018. EzMol: A Web Server Wizard for the

Rapid Visualization and Image Production of Protein and Nucleic Acid Structures. J Mol Biol 430:2244–2248.
220. Telcian AG, Laza-Stanca V, Edwards MR, Harker JA, Wang H, Bartlett NW, Mallia P, Zdrenghea MT, Kebadze T, Coyle AJ, Openshaw PJM, Stanciu LA, Johnston SL. 2011. RSV-induced bronchial epithelial cell PD-L1 expression inhibits CD8+ T cell nonspecific antiviral activity. J Infect Dis 203:85–94.
221. Prince GA, Prieels JP, Slaoui M, Porter DD. 1999. Pulmonary lesions in primary respiratory syncytial virus infection, reinfection, and vaccine-enhanced disease in the cotton rat (Sigmodon hispidus). Lab Invest 79:1385–92.
222. Sawada A, Nakayama T. 2016. Experimental animal model for analyzing immunobiological responses following vaccination with formalin-inactivated respiratory syncytial virus. Microbiol Immunol 60:234–242.
223. Boukhvalova MS, Prince GA, Blanco JCG. 2009. The cotton rat model of respiratory viral infections. Biologicals 37:152–159.
224. Boukhvalova MS, Prince GA, Soroush L, Harrigan DC, Vogel SN, Blanco JCG. 2006. The TLR4 agonist, monophosphoryl lipid A, attenuates the cytokine storm associated with respiratory syncytial virus vaccine-enhanced disease. Vaccine 24:5027–5035.
225. Peebles RS, Graham BS. 2005. Pathogenesis of Respiratory Syncytial Virus Infection in the Murine Model. Proc Am Thorac Soc 2:110–115.
226. Oshansky CM, Zhang W, Moore E, Tripp RA. 2009. The host response and molecular pathogenesis associated with respiratory syncytial virus infection. Future Microbiol 4:279–297.
227. Collins PL, Graham BS. 2008. Viral and Host Factors in Human Respiratory Syncytial Virus Pathogenesis. J Virol 82:2040–2055.
228. Hauser H, Shen L, Gu Q-L, Krueger S, Chen S-Y. 2004. Secretory heat-shock protein as a dendritic cell-targeting molecule: a new strategy to enhance the potency of genetic vaccines. Gene Ther 11:924–932.
229. Blanco JCG, Richardson JY, Darnell MER, Rowzee A, Pletneva L, Porter DD, Prince GA. 2002. Cytokine and Chemokine Gene Expression after Primary and Secondary Respiratory Syncytial Virus Infection in Cotton Rats. J Infect Dis 185:1780–1785.
230. Bio Rad Laboratories. Applications Guide Real-Time PCR Applications Guide.
231. Brück WM, Slater JW CB. 2011. Chitin and chitosan from marine organisms, p. 11–23. *In* Kim S.-K, E (ed.), Chitin, Chitosan, Oligosaccharides and Their Derivatives. CRC Press, New York.
232. Knezevic-Jugovic Z, Petronijevic Z SA. 2011. Chitin and chitosan from microorganisms, p. 25–36. *In* Kim S.-K, E (ed.), Chitin, Chitosan, Oligosaccharides and Their Derivatives. CRC Press, New York.
233. Nwe N, Furuike T TH. 2011. Chitin and chitosan from terrestrial organisms, p. 3–10. *In* Kim S.-K, E (ed.), Chitin, Chitosan, Oligosaccharides and Their Derivatives. CRC Press, New York.
234. Dornish M, Hagen A, Hansson E, Pecheur C, Verdier F, Skaugrud Ø. 1997. Safety of Protasan^{TM}: ultrapure chitosan salts for biomedical and pharmaceutical use., p. 664–670. *In* Advances in Chitin Science, Vol II. Andre Publisher, Lyon, France.
235. Arca HÇ, Günbeyaz M, Şenel S. 2009. Chitosan-based systems for the delivery of vaccine antigens. Expert Rev Vaccines 8:937–953.
236. Kean T, Thanou M. 2010. Biodegradation, biodistribution and toxicity of chitosan. Adv Drug Deliv Rev 62:3–11.

237. Harding S. 1997. Characterisation of chitosan-mucin complexes by sedimentation velocity analytical ultracentrifugation, p. 457–466. *In* Muzzarelli RAA, PM eds (ed.), Chitin Handbook. European Chitin Society.
238. Morris G, Kök S, Harding S, Adams G. 2010. Polysaccharide drug delivery systems based on pectin and chitosan. Biotechnol Genet Eng Rev 27:257–84.
239. Smith A, Perelman M, Hinchcliffe M. 2014. Chitosan: a promising safe and immune-enhancing adjuvant for intranasal vaccines. Hum Vaccin Immunother 10:797–807.
240. Zheng M, Qu D, Wang H, Sun Z, Liu X, Chen J, Li C, Li X, Chen Z. 2016. Intranasal Administration of Chitosan Against Influenza A (H7N9) Virus Infection in a Mouse Model. Sci Rep 6:28729.
241. Sui Z, Chen Q, Fang F, Zheng M, Chen Z. 2010. Cross-protection against influenza virus infection by intranasal administration of M1-based vaccine with chitosan as an adjuvant. Vaccine 28:7690–7698.
242. Sui Z, Chen Q, Wu R, Zhang H, Zheng M, Wang H, Chen Z. 2010. Cross-protection against influenza virus infection by intranasal administration of M2-based vaccine with chitosan as an adjuvant. Arch Virol 155:535–544.
243. Roon KI, Soons PA, Uitendaal MP, de Beukelaar F, Ferrari MD. 1999. Pharmacokinetic profile of alniditan nasal spray during and outside migraine attacks. Br J Clin Pharmacol 47:285–90.
244. Stoker DG, Reber KR, Waltzman LS, Ernst C, Hamilton D, Gawarecki D, Mermelstein F, McNicol E, Wright C, Carr DB. 2008. Analgesic Efficacy and Safety of Morphine-Chitosan Nasal Solution in Patients with Moderate to Severe Pain Following Orthopedic Surgery. Pain Med 9:3–12.
245. Newman SP, Simpson M, Fisher T IK. 2004. Quantification of lung deposition and nasal mucociliary clearance for a nasally administered drug formulation containing chitosan, p. 617–619. *In* Dalby RN, Byron PR, Peart J, SJ and FS eds. (ed.), Respiratory Drug Delivery IX, Virginia Commonwealth University. Virginia.
246. Aspden TJ, Mason JDT, Jones NS, Lowe J, Skaugrud Ø, Illum L. 1997. Chitosan as a Nasal Delivery System: The Effect of Chitosan Solutions on in Vitro and in Vivo Mucociliary Transport Rates in Human Turbinates and Volunteers. J Pharm Sci 86:509–513.
247. Morabito KM, Ruckwardt TR, Redwood AJ, Moin SM, Price DA, Graham BS. 2017. Intranasal administration of RSV antigen-expressing MCMV elicits robust tissue-resident effector and effector memory CD8+ T cells in the lung. Mucosal Immunol 10:545–554.
248. Park S, Lee Y, Kwon Y-M, Lee Y-T, Kim K-H, Ko E-J, Jung JH, Song M, Graham B, Prausnitz MR, Kang S-M. 2018. Vaccination by microneedle patch with inactivated respiratory syncytial virus and monophosphoryl lipid A enhances the protective efficacy and diminishes inflammatory disease after challenge. PLoS One 13:e0205071.
249. Anderson KG, Mayer-Barber K, Sung H, Beura L, James BR, Taylor JJ, Qunaj L, Griffith TS, Vezys V, Barber DL, Masopust D. 2014. Intravascular staining for discrimination of vascular and tissue leukocytes. Nat Protoc 9:209–222.
250. Fulton RB, Meyerholz DK, Varga SM. 2010. Foxp3+ CD4 Regulatory T Cells Limit Pulmonary Immunopathology by Modulating the CD8 T Cell Response during Respiratory Syncytial Virus Infection. J Immunol 185:2382–2392.
251. Raiden S, Pandolfi J, Payasliàn F, Anderson M, Rivarola N, Ferrero F, Urtasun M, Fainboim L, Geffner J, Arruvito L. 2014. Depletion of Circulating Regulatory T Cells

during Severe Respiratory Syncytial Virus Infection in Young Children. Am J Respir Crit Care Med 189:865–868.
252. Lee DCP, Harker JAE, Tregoning JS, Atabani SF, Johansson C, Schwarze J, Openshaw PJM. 2010. CD25+ Natural Regulatory T Cells Are Critical in Limiting Innate and Adaptive Immunity and Resolving Disease following Respiratory Syncytial Virus Infection. J Virol 84:8790–8798.
253. Ruckwardt TJ, Bonaparte KL, Nason MC, Graham BS. 2009. Regulatory T Cells Promote Early Influx of CD8+ T Cells in the Lungs of Respiratory Syncytial Virus-Infected Mice and Diminish Immunodominance Disparities. J Virol 83:3019–3028.
254. Atmar RL, Bernstein DI, Harro CD, Al-Ibrahim MS, Chen WH, Ferreira J, Estes MK, Graham DY, Opekun AR, Richardson C, Mendelman PM. 2011. Norovirus Vaccine against Experimental Human Norwalk Virus Illness. N Engl J Med 365:2178–2187.
255. El-Kamary SS, Pasetti MF, Mendelman PM, Frey SE, Bernstein DI, Treanor JJ, Ferreira J, Chen WH, Sublett R, Richardson C, Bargatze RF, Sztein MB, Tacket CO. 2010. Adjuvanted Intranasal Norwalk Virus-Like Particle Vaccine Elicits Antibodies and Antibody-Secreting Cells That Express Homing Receptors for Mucosal and Peripheral Lymphoid Tissues. J Infect Dis 202:1649–1658.
256. Mann AJ, Noulin N, Catchpole A, Stittelaar KJ, de Waal L, Veldhuis Kroeze EJB, Hinchcliffe M, Smith A, Montomoli E, Piccirella S, Osterhaus ADME, Knight A, Oxford JS, Lapini G, Cox R, Lambkin-Williams R. 2014. Intranasal H5N1 Vaccines, Adjuvanted with Chitosan Derivatives, Protect Ferrets against Highly Pathogenic Influenza Intranasal and Intratracheal Challenge. PLoS One 9:e93761.
257. Wen Z-S, Xu Y-L, Zou X-T, Xu Z-R. 2011. Chitosan Nanoparticles Act as an Adjuvant to Promote both Th1 and Th2 Immune Responses Induced by Ovalbumin in Mice. Mar Drugs 9:1038–1055.
258. Zaharoff DA, Rogers CJ, Hance KW, Schlom J, Greiner JW. 2007. Chitosan solution enhances both humoral and cell-mediated immune responses to subcutaneous vaccination. Vaccine 25:2085–2094.
259. Schenkel JM, Fraser KA, Beura LK, Pauken KE, Vezys V, Masopust D. 2014. Resident memory CD8 T cells trigger protective innate and adaptive immune responses. Science (80-) 346:98–101.
260. McMaster SR, Wilson JJ, Wang H, Kohlmeier JE. 2015. Airway-Resident Memory CD8 T Cells Provide Antigen-Specific Protection against Respiratory Virus Challenge through Rapid IFN-γ Production. J Immunol 195:203–209.
261. Gebhardt T, Wakim LM, Eidsmo L, Reading PC, Heath WR, Carbone FR. 2009. Memory T cells in nonlymphoid tissue that provide enhanced local immunity during infection with herpes simplex virus. Nat Immunol 10:524–530.
262. Ariotti S, Hogenbirk MA, Dijkgraaf FE, Visser LL, Hoekstra ME, Song J-Y, Jacobs H, Haanen JB, Schumacher TN. 2014. Skin-resident memory CD8+ T cells trigger a state of tissue-wide pathogen alert. Science (80-) 346:101–105.
263. Schenkel JM, Masopust D. 2014. Tissue-Resident Memory T Cells. Immunity 41:886–897.
264. Jiang X, Clark RA, Liu L, Wagers AJ, Fuhlbrigge RC, Kupper TS. 2012. Skin infection generates non-migratory memory CD8+ TRM cells providing global skin immunity. Nature 483:227–231.
265. Shalev I, Schmelzle M, Robson SC, Levy G. 2011. Making sense of regulatory T cell suppressive function. Semin Immunol 23:282–292.

266. Afzali B, Mitchell P, Lechler RI, John S, Lombardi G. 2010. Translational Mini-Review Series on Th17 Cells: Induction of interleukin-17 production by regulatory T cells. Clin Exp Immunol 159:120–130.
267. O'Connor RA, Taams LS, Anderton SM. 2010. Translational Mini-Review Series on Th17 Cells: CD4 $^{+}$ T helper cells: functional plasticity and differential sensitivity to regulatory T cell-mediated regulation. Clin Exp Immunol 159:137–147.
268. Miyara M, Sakaguchi S. 2007. Natural regulatory T cells: mechanisms of suppression. Trends Mol Med 13:108–116.
269. Huang C-T, Workman CJ, Flies D, Pan X, Marson AL, Zhou G, Hipkiss EL, Ravi S, Kowalski J, Levitsky HI, Powell JD, Pardoll DM, Drake CG, Vignali DAA. 2004. Role of LAG-3 in Regulatory T Cells. Immunity 21:503–513.
270. Liu J, Cao S, Peppers G, Kim S-H, Graham BS. 2014. Clonotype-specific avidity influences the dynamics and hierarchy of virus-specific regulatory and effector CD4 $^{+}$ T-cell responses. Eur J Immunol 44:1058–1068.
271. Durant LR, Makris S, Voorburg CM, Loebbermann J, Johansson C, Openshaw PJM. 2013. Regulatory T Cells Prevent Th2 Immune Responses and Pulmonary Eosinophilia during Respiratory Syncytial Virus Infection in Mice. J Virol 87:10946–10954.
272. Kearley J, Barker JE, Robinson DS, Lloyd CM. 2005. Resolution of airway inflammation and hyperreactivity after in vivo transfer of CD4+ CD25+ regulatory T cells is interleukin 10 dependent. J Exp Med 202:1539–1547.

Appendix A

Immunopathogenesis Associated with Formaldehyde-Inactivated RSV Vaccine in Preclinical and Clinical Studies

Abenaya Muralidharan[a,c], Changgui Li[b] Lisheng Wang[c] and Xuguang Li[a,c]

Published: ***Expert Rev Vaccines,*** **2017 Apr; 16(4):351-360**

[a]Centre for Biologics Evaluation, Biologics and Genetic Therapies Directorate, Health Canada and WHO Collaborating Center for Standardization and Evaluation of Biologics, Ottawa, ON, Canada

[b]National Institutes for Food and Drug Control and WHO Collaborating Center for Standardization and Evaluation of Biologicals, No.2 ; Tiantan Xili, Beijing , PR China, Beijing, China.

[c]Department of Biochemistry, Microbiology and Immunology, University of Ottawa, Ottawa, ON, Canada

*Corresponding author (XL): sean.li@hc-sc.gc.ca

Summary

Introduction: Respiratory syncytial virus (RSV) infection is responsible for one-third of deaths of acute lower respiratory infection in children less than one year old. The formaldehyde-inactivated RSV vaccine trial conducted in the 1960s predisposed the vaccinees to more serious RSV infection instead of protection. Better understanding of the underlying mechanism is of critical importance for better designing of safe and effective RSV vaccines.

Areas covered: PubMed was searched to review immunopathology induced by RSV vaccines**.** We intend to dissect the differences in clinical and pathological manifestations of enhanced respiratory disease (ERD) in different animal models in comparison with humans. Formaldehyde-inactivated RSV vaccine causes ERD in both humans and animals, while RSV vaccine without formaldehyde treatment could also induce similar disease in animals, suggesting multiple pathways may be involved.

Expert commentary: Identification of biomarkers pertinent to clinical evaluation should be further explored for safety assessment of RSV vaccines in human trials.

Keywords: formaldehyde-inactivated vaccine, RSV, animal models, vaccine enhanced disease, immunopathogenesis

Introduction

Approximately 33.8 million children under the age of 5 worldwide are reported to be afflicted with respiratory syncytial virus (RSV) related acute lower respiratory tract infection. While humans infected by the virus often present symptoms related to respiratory infections, the immuno-pathological effects of RSV infection remains to be clearly determined. At least 3.4 million hospital admissions associated with severe RSV disease are reported globally [1]. Most of the RSV-related mortality occurs in developing countries with the number of deaths estimated to be about 250,000. However, the number of RSV infection cases is believed to be grossly under-reported [1–3]. Like any other vaccines against infectious diseases, a vaccine against RSV should be one of the most effective means to prevent or contain RSV viral infection. However, challenges towards RSV vaccine development have been tremendous. Specifically, a RSV vaccine clinical trial in the 1960s failed, with the formaldehyde-inactivated RSV vaccine (FIRSV) causing enhanced respiratory disease (ERD) rather than protection upon subsequent RSV infection. The majority (80%) of the participants were hospitalized in addition to 2 deaths although no significant toxicity was observed in preclinical animal studies where the animals were immunized but not infected [4–6]. This failed clinical trial underscores the vital need in RSV vaccine development for a robust animal model that can predict severe adverse reactions such as ERD. However, the pathogenesis of FIRSV-induced ERD can vary amongst different animals and may not be the same as that observed in humans [7,8]. In this review, we attempt to dissect pathological findings of ERD in both animals and humans in addition to the underlying immunological mechanisms.

Results from the Human Trial

The human clinical trial on Lot 100 formaldehyde-inactivated RSV vaccine (made with the Bernett strain) revealed great challenges in vaccine development. This trial was conducted from December 1965 to May 1967 during which time there were two RSV epidemics. The subjects were infants between 2 and 7 months of age [5,6]. Prior to injecting the infants with Lot 100, it was tested in guinea pigs and cynomolgus monkeys for complement-fixing and neutralizing antibody. Safety of the vaccine was also tested in cynomolgus monkeys, guinea pigs, rabbits and mice [5,6]. The problems arose when the infants, who had received two intramuscular injections of FIRSV one month apart and a third injection 3 months after the second injection, were subsequently infected by RSV during the epidemics. Although no toxic effects were observed prior to RSV infection and highly virus-specific antibody titers were recorded 3 weeks after the third FIRSV injection, 80% of the vaccinees became severely ill following the RSV infection compared to only 5% of the parainfluenza control vaccinees [4–6, 9]. Longer persistence of pneumonia, mild rhinitis, pharyngitis and bronchitis was observed in the FIRSV immunized group. Interestingly, following FIRSV immunization, ERD occurrence was more frequent in infants aged between 1 to 6 months than those who were older than 6 months. While the exact immunological mechanisms remain to be completely understood, frequent outbreaks of RSV during that time period might have exposed the older infants to RSV viruses prior to FIRSV immunization, thereby reducing the occurrence of ERD. Two infants died, two and five months after the first FIRSV injection, respectively [4–6]. Autopsy results conducted at that time showed that there was extensive bronchopneumonia and patchy atelectasis with emphysema and pneumothorax. Pathological examination showed peribronchiolar monocytic infiltration dominated with eosinophils. Finally, at least 10^4 $TCID_{50}$ of RSV per gram lung

was recovered [5,6]. However, reexamination of the autopsy samples by Prince et al. (2001) revealed new insight: the majority of the peribronchial infiltrates were comprised of lymphocytes along with some neutrophils and macrophages [10]. Moreover, the bronchial exudate contained mostly neutrophils accompanied by macrophages and lymphocytes. Only 1-2% of the cell infiltrate population was identified to be eosinophils in both subjects [10]. The results from the reexamination of specimens from deceased subjects are not in agreement to those obtained in 1960s in terms of the types of cells infiltrated in the lung tissues. Interestingly, examination of the peripheral blood by Chin et al. (1969) showed that 56% of the vaccinees had eosinophils present [4], an observation which is apparently different from that in lung pathology made by Prince et al. (2001). Nevertheless, no in-depth immunological analyses were conducted, making it critical to dissect findings from animal studies.

The Lamb Model

Except cellular infiltrations in the lung tissues, results obtained in lamb model were starkly different from that obtained in human trial in FIRSV-induced neutralizing antibodies and clinical manifestations. Specifically, FIRSV-induced disease was recently investigated in perinatal lambs [11,12]. In these studies, colostrum-deprived lambs 3 to 5 days old were immunized with FIRSV (made with RSV-A2) followed by challenge with RSV Memphis 37. Compared to mock-immunization control, histological analysis on the lungs showed an increase in perivascular and peribronchiolar lymphocyte infiltration dominated by neutrophils. No prominent eosinophil infiltration was detected in any region of the lung. Furthermore, increased lymphocyte and plasma cell infiltration were detected in airways and blood vessels that were more expanded due to increased cellularity. Multifocal bronchioles

had mild to moderate infiltrates of lymphocytes, plasma cells and some macrophages in tunica adventitia. This was also seen in the lamina propria but to a lesser extent. However, fewer bronchiolar epithelial lesions were observed in the FIRSV immunized lambs than the mock-immunized lambs [12]. These pathological observations were similar to that obtained in humans. In contrast to human results, disease presentations in FIRSV group were not remarkable, with no differences observed in body weight, temperature, heart rate and respiratory rate between the FIRSV and mock-immunized lambs.

In contrast, FIRSV immunized lambs had higher neutralizing antibody titer in the serum compared to the mock immunized group [11,12], which correlated to better suppression of viral replication as demonstrated by decreased levels of RSV titer in the bronchoalveolar lavage (BAL) fluid and lung tissue as well as reduced amounts of viral mRNA and RSV antigen in bronchi/bronchioles and alveoli [12,13]. Taken together, the presence of elevated levels of neutralizing antibodies in the FIRSV immunized lamb sera resulted in more effective viral clearance, which in turn reduced the bronchiolar and alveolar lesions. These observations led Derscheid et al. (2013) to postulate that FIRSV directly affects viral load in a manner that triggers an "atypical immune response" [12]. Such "atypical immune response" seems beneficial as the lambs presented no marked symptoms compared to the mock control albeit quite significant inflammatory reactions in the lung tissue were observed.

Despite a lack of symptoms, the ovine model could be useful for preclinical assessment of RSV vaccines as perinatal lamb lungs are similar in size, structure and physiology to those of human infants. The susceptibility of lambs to RSV is evident by similar lesions observed in human infants. They are one of the few animals that can be used

preterm, which can be useful in assessing the role of maternal antibodies on FIRSV induced disease [13–17].

The Bovine Model

The bovine system is another useful model for RSV vaccine evaluation because bovines are naturally infected by bovine strains of RSV (bRSV) and FIRSV can induce moderate to severe disease upon subsequent exposure to bRSV [18–23]. Unlike the ovine model, bovines vaccinated with FIRSV display remarkable symptoms following RSV infection including an increase in rectal temperature, coughing, nasal discharge, sensitivity of larynx and trachea, lung sounds and severe dyspnea. Severe emphysema including pneumothorax can also be observed, similar to one of the infants who died in the human trial. Histological studies show bronchiolitis with epithelial necrosis and peribronchiolar interstitial mononuclear cell infiltration [5,6,18,19,21]. While alveolitis detected in calves was also seen in humans, conflicting results were reported on eosinophil infiltration in the bovine model. Gershwin et al. (1998) observed a mild neutrophilic alveolitisin calves without eosinophil infiltration whereas other groups reported the presence of eosinophils, but with an absence of neutrophils [18,19,21]. Such discrepancy in results is yet to be understood although the age of the calves used is different, with the calves in the former study being at least 2 months younger at necropsy than those in the latter studies.

The difference in the bovine studies is also apparent in their presentations. West et al. (1999) compared the FIRSV immunized group with modified live virus and mock control; they observed an early disease onset with a quicker attenuation of symptoms such as cough and wheezes [19]. Antonis et al. (2003) did not see the same pattern [21]. The difference between these results is not understood while it is noted that the time interval between RSV

infection and necropsy differs, i.e., 8 days in the West et al. study and 10 days in the Antonis et al. study.

Along with the differences in pathological and symptomatic findings reported in the bovine model studies, the immunological analyses were also interesting. Specifically, while higher lymphocyte proliferative responses to the bRSV antigen were found in the FIRSV immunization group, similar to that observed in the human study, cytotoxic activity of bronchoalveolar lavage (BAL) cells were low when compared to those from the mock-immunized group [9,19]. Moreover, higher IgG and IgE titers in the serum were detected in FIRSV immunized calves as compared to naïve animals, mock immunized and live virus groups upon subsequent bRSV infection. Yet, virus neutralizing antibodies were less induced by FIRSV compared with that in the live virus immunized calves [18,21]. These data indicate that higher IgG titre does not translate into better neutralizing activities, underscoring the need to use standardized neutralization assay for vaccine efficacy assessment.

The role of non-protective antibodies in ERD development remains to be clarified. One study suggests that these antibodies may not be protective but may not exacerbate the disease either. Moreover, the role of IgE is also not fully understood although a high amount of IgE may be suggestive of deregulation in T-cell response [19]. Antonis et al. (2003) suggests that the presence of eosinophils and IgE are indicative of a Type I hypersensitivity reaction and may reflect a Th2-biased CD4 response in FIRSV immunized calves post-infection [21].

The FIRSV dosage and immunization schedule have also been found to affect ERD or immune response [22,23]. Interestingly, a lower dose of FIRSV in conjunction with longer time interval between initial immunization and subsequent RSV challenge selectively

induced IgE reactive to the nucleoprotein while a higher dose (10-fold higher) combined with shorter time interval preferentially increased IgG antibodies reactive to all major viral proteins; some IgE detected in the higher dose group was against the F_1 subunit of the RSV fusion protein. Furthermore, higher histological scores in the lower FIRSV group indicated severe ERD, suggesting that larger antigen loads may partially alleviate immunopathological damage to the lung tissue [22]. The type of immune response might also be altered. Specifically, after RSV challenge, serum IgG2 was higher in the higher-dose group than the lower dose group, revealing a stronger Th1 response which was additionally supported by increased IFN-γ production [22,24–26]. Compared with the low dose group, high-dose of FIRSV induced higher IgG1 with less severe ERD; yet the IgA level was also found to be low. Therefore, the authors postulate that IgG1, not IgA must have played an important role in curtailing early viral replication due to its mucosal location [23]. It would be interesting to see if these observations could be confirmed through passive IgG1 transfer.

In short, bovines, like humans, are natural hosts of RSV. ERD induced by FIRSV is also similar between bovine and human, which may be due to the fact that bovine and human RSV share high nucleic acid homology and antigenic cross reactivity [27,28].

Non-Human Primate Model

Bonnet monkeys (*Macaca radiata*) present another interesting model in FIRSV induced ERD. Monkeys vaccinated with FIRSV have been shown to develop inflammation in peribronchiolar, perivascular, interstitial sites and intra-alveolar sites. Lung infiltrates consist predominantly of macrophages, eosinophils, lymphocytes and multinucleate giant cells [29,30]. Furthermore, compared to mock immunized monkeys, the higher

histopathological score was found to be correlated with higher RSV titers in the lungs and BAL fluid, an observation different from that in calves and rodents [29,31].

Ponnuraj et al. (2001) postulated that the excess number of macrophages in the pulmonary infiltrates may promote enhanced viral replication and exacerbate the disease in the lungs following FIRSV immunization [29]. Since RSV has been shown to infect macrophages and that IgG1 levels are increased in bovine [22,23] and murine [32] models, the authors suggest that the macrophages are infected through antibody-mediated endocytosis thereby increasing lung viral load and exacerbating inflammation [29]. However, in the bovine and murine models, increasing levels of IgG1 are correlated to lower lung viral titers. Therefore, it remains unclear as to whether IgG1-mediated endocytosis of RSV into macrophages is species-specific. Despite the discrepancy in results from these different animal models, the studies with primates shed light on the potential disease enhancement caused by antibodies. While serum neutralizing antibodies were lower in the FIRSV group as compared to the live virus infection control, the disease enhancing antibody levels, were found to be higher [30]. These were determined by antibody-dependent enhancement indices. Further characterization shows that antibodies against the RSV fusion (F) and attachment (G) proteins had high enhancement indices whereas antibodies against RSV nucleoprotein (N) did not have any disease enhancing effects [30,33–35]. It appears that there is a direct relationship between disease enhancing antibody titers and clinical scores in the monkeys. Such antibodies may enhance disease by forming immune complexes, thereby facilitating entry of the RSV virus into macrophages. These antibodies may also activate the complement system [36] or leukotrienes [37–39], thus enhancing inflammatory reactions. However, the roles of these antigen-specific antibodies could be further confirmed through more in vivo experiments such as passive antigen-specific antibody transfer.

Different species of non-human primates and adaption of viruses in specific primates may also affect the immunological and pathological outcomes. The results from studies with FIRSV in cynomolgus macaques were different from those in bonnet monkeys discussed above and in African green monkeys. In macaques, FIRSV induced higher levels of RSV neutralizing antibodies in their serum compared to a FI-measles control group and stronger lymphoproliferative responses, accompanied with better inhibition of viral replication [29,31,40]. The differences seen in viral load and neutralizing antibodies between the bonnet monkeys and macaques may be due to the fact that the macaques were infected with a macaque-adapted wild-type RSV A strain whereas the bonnet and African green monkeys were infected with the human RSV long strain. Interestingly, FIRSV was also found to suppress virus replication in bovine lungs when infected with bovine RSV (bRSV) [19,21]. It remains unknown as to whether FIRSV really helps the hosts better defend species-adapted virus infection.

In addition to the analyses of antibody responses, some studies also observed FIRSV induced lung eosinophilia, IL-13 and IL-5 producing T cells (Th2) in the macaques post-infection [40]. In both macaques and bonnet monkeys [29], eosinophil count in the BAL fluid was high, unlike that observed in the lamb [12] and cotton rat [10] model. Notably, increased levels of lymphoproliferative responses and Th2 phenotype was accompanied with higher macaques fatalities as a result of pulmonary hyper-inflammation following RSV infection [40], an observation similar to that in humans [5,6].

The dose of FIRSV can affect the outcome of subsequent RSV challenge in primates but rather differently compared to that in the bovine system. Specifically, immunization with lower dose of FIRSV appears to be beneficial as demonstrated by less viral infection and weaker inflammation, accompanied by higher antibody levels and lymphocyte responses

compared to the higher dose group receiving 10-fold more FIRSV antigens [29]. These observations are in contrast to the bovine model since lower dosage of FIRSV resulted in a more pronounced Th2 response and higher histopathology scores in Holstein bull calves [22]. The discrepancies in results between bovines and primates in FIRSV-induced immunological and pathological responses provide another layer of complexity in relation to species differences.

The Cotton Rat Model

One of the rodent models frequently used for RSV vaccine evaluation is the cotton rat (*sigmodon hispidus*). Following FIRSV immunization and subsequent infection with RSV, they display no weight loss but show increased severity of peribronchiolitis consisting mainly of lymphocytes, bronchitis, neutrophilic alveolitis and interstitial pneumonitis compared to a mock-vaccinated group [10,41,42]. The presence of neutrophils is similar to that reported in lambs [12], but not mice [43] or non-human primates [29,40]. When compared to pathological examination of the human autopsies by Prince et al. (2001), the neutrophilic alveolitis is similar, albeit less severe, in cotton rats [10].

With respect to virus replication, a 90% decrease in lung and nasal viral titer can be observed post infection in FIRSV immunized cotton rats but the nasal viral titer is the same as that in mock-vaccinated controls. However, the rats with lower lung viral load actually had higher histological scores, implying that the pathological lesions are unlikely due to virus replication itself but an allergic sensitization-like reaction [10,41,42,44].

FIRSV was found to substantially alter immune responses, with a Th2 response predominantly observed in the lungs of FIRSV immunized cotton rats as demonstrated by

increased levels of characteristic Th2 cytokines such as IL-4, IL-5, IL-9, IL-10 and IL-13 and chemokines such as RANTES [42,44–46] while others observed signs of a Th2 response along with elevated release of Th1 cytokines like IL-2 and chemokines such as MIP-1a in the lung post-infection [44–46]. In contrast, Sawada et al. (2016) did not observe significant elevations of Th1 cytokines and chemokines, instead they detected increased viral replication in the lungs of FIRSV immunized cotton rats compared to the mock-immunized control group [42]. The discrepancy in results between the Sawada publication and earlier reports remains to be understood. It is likely, however, that the dose and immunization schedule might partially contribute to the difference in results. Specifically, previous studies [44–46] employed about half the dose of challenge RSV virus per cotton rat as the more recent study [42], and the animals were challenged one week sooner.

Interesting data have also been obtained with respect to the characteristics of the antibodies induced by FIRSV. RSV-specific neutralizing antibody levels in FIRSV immunized cotton rats was as low as the mock immunization group even though the total IgG titer was higher in the FIRSV group; those RSV-specific IgGs also have low avidity [41,42,47]. It is likely that formaldehyde inactivation damaged the neutralizing epitopes of the antigen [42,48]. Specifically, the denatured F protein may prevent its binding to the toll-like receptor 4 (TLR4), resulting in a deficiency in triggering type I interferon response and/or an inflammatory response through myeloid differentiation factor 88 pathway [42,49]. As a result, FIRSV immunization could generate weakly neutralizing antibodies and a Th2 skewed immune response [42].

Alternative method to inactivate the virus in vaccine preparation was also explored. Boukhvalova et al. (2010) used 2,2’-dithiodipyridine (AT-2) to inactivate RSV virus; the agent disrupts the intramolecular disulfide bond of the zinc-finger motif in RSV M2-1

protein, thereby inactivating the virus [50]. The AT-2 RSV vaccines were found to be as effective as FIRSV in reducing lung viral replication but did not cause ERD in cotton rats. Interestingly, AT-2 RSV in conjunction with an adjuvant (Ribi) elicited enhanced vaccine immunogenicity comparable to that induced by live RSV; however, AT-2 RSV/Ribi combination caused ERD in the animals. These observations indicate that alternative inactivation of the virus by targeting the interior viral proteins could potentially reduce ERD occurrence whereas different combinations of vaccine with adjuvant need to be independently scrutinized [50].

Sawada et al. (2016) injected FIRSV immunized cotton rats with palivizumab, a monoclonal antibody against the RSV fusion protein (F) currently available on the market as a prophylactic drug, prior to RSV challenge [42,51,52]. The palivizumab treatment induced higher levels of neutralizing antibodies, Th1 response and cytotoxic T lymphocyte (CTL) activity while suppressing viral replication and inflammatory reactions in the lungs. The authors suggest that CTL activity, which is induced by the Th1 response but absent during FIRSV immunization, contributes to protection through elimination of infected cells and reduction of excessive inflammatory reactions associated with FIRSV vaccination [42].

The lack of protection observed with inactivated RSV vaccines might also be due to the RSV F protein predominantly assuming its post-fusion form. Cullen et al. (2015) immunized cotton rats with virus-like particle comprised of Newcastle disease viral proteins and RSV F in its pre-fusion form (VLP-F) [53]. Compared to FIRSV, VLP-F significantly reduced ERD as demonstrated by lower levels of peribronchiolitis, interstitial pneumonia and alveolitis. VLP-F was also more effective in suppressing pulmonary viral replication than FIRSV, while inducing even higher levels of neutralizing antibodies and pre-fusion F specific IgGs than live RSV immunization [53]. With respect to the post-fusion RSV-F

specific antibodies, VLP-F and live RSV immunizations induced similar serum antibody levels. Interestingly, VLP-F, which was designed to express pre-fusion F, induced higher levels of antibodies against post-fusion F than those specific for pre-fusion F, an observation similar to that with live RSV immunization [53].

While some studies suggest formaldehyde-treated F protein may play a role in FIRSV-induced altered immune response, others suggest non-viral element such as impurities and adjuvants in the FIRSV preparation could also have contributed to ERD. Shaw et al. (2013) observed alveolitis in cotton rats immunized with a formaldehyde-inactivated vaccine without RSV antigen (FI-mock) even though more pronounced alveolitis was found in FIRSV immunized animals, suggesting impurities may also be partially responsible for the induction of ERD. In addition, they detected even higher levels of BSA-specific T cells and cytokines than those specific for RSV F protein in both FIRSV and FI-mock groups [47]. It is also likely that aluminum in FIRSV preparation skews immune response to Th2 [54]. Further studies should be conducted to determine whether different cell substrates in RSV vaccine preparations could contribute to the development of ERD [43,47,48].

In conclusion, cotton rats are useful for RSV vaccine evaluation because of their higher permissiveness to human RSV infection compared to other rodents [44]. Yet, the scarcity of reagents for in-depth mechanistic studies limits their application, making it worthwhile to explore the mouse models.

The Mouse Model

The mouse model is advantageous in many aspects including the low cost of the animals, availability of research reagents and a variety of genetically modified mouse strains

for extensive mechanistic investigation. Compared to the commonly used cotton rats, mice present pathological and symptomatic manifestations which are not completely the same in ERD studies. Specifically, in post-infection following FIRSV immunization studies, the mice were found to have 15% weight loss, pulmonary inflammation, mucus hypersecretion, airway obstruction, and lung eosinophilia [32,43], of which eosinophilia, mucus hypersecretion and weigh loss were not reported in cotton rats.

There have been various studies conducted in mice to determine the mechanisms underlying FIRSV-induced ERD [32,43,55–58]. In one study, formaldehyde and its derivative with reduced carbonyl groups were compared [55]. While FIRSV induced increased levels of Th2 cytokines such as IL-4, IL-5 and IL-13 in the BAL and lungs and pulmonary eosinophilia, none of those immunological reactions was observed in the reduced FIRSV group [40,55,58,59,60]. Furthermore, increased expression levels of RSV-specific IgG1 (Th2 response) was associated with FIRSV immunized mice while the reduced FIRSV predominantly induced IgG2a, signifying a skewed Th1 response [55,58,61]. Also of note is that mice immunized with FIRSV prepared with either formaldehyde or its reduced form elicited poorly neutralizing antibodies against RSV [55]. Interestingly, glycoaldehyde, another derivative of aldehyde, was also found to induce ERD. Therefore, it can be postulated that carbonyl groups may increase uptake of RSV proteins by macrophages thereby increasing inflammation [55,58,61,62].

The non-viral elements in FIRSV preparation was also investigated by several groups with conflicting results. Some groups reported that both FIRSV and FI-mock are associated with ERD whereas others showed that only FIRSV is associated with the enhanced disease as demonstrated by pulmonary eosinophilia [32,43,57]. Regardless, while FIRSV has been consistently found by all research groups to be associated with ERD, immunization with

purified RSV F protein without formaldehyde treatment was also reported to induce ERD related syndromes such as hyperresponsiveness and lung eosinophilia post-infection. This suggests mechanism(s) other than formaldehyde-mediated process being involved [32]. This type of study has not been conducted in other animal models.

Much more in-depth mechanistic studies on ERD have been carried out in the mouse model compared with other animal models. Data published previously indicate that affinity maturation of antibodies is essential for effective protection against RSV infection [32]. Specifically, serum IgG titer was found to be high as detected by ELISA in FIRSV immunized mice but both antibody avidity against protective epitopes and virus neutralizing capacity were relatively poor. When compared with a live RSV immunized group, dendritic cells collected from popliteal lymph nodes of FIRSV immunized mice lacked maturation markers as demonstrated by decreased expression levels of CD40, CD80 and CD86 [32]. This could in turn result in decreased CD4 T cell proliferation as evidenced by low expression levels of the activation markers and co-stimulatory molecules such as CD71 and CD40 ligand on the surface of CD4 T cells. Furthermore, decreased germinal center formation in the lymph nodes was clearly identified, revealing a deficiency in B cell isotype switching, which hinders antibody affinity maturation. Another mechanism underlying generation of lower affinity antibodies could be the ineffective stimulation of TLRs by FIRSV since stimulation of TLR activity was shown to protect mice from RSV challenge as well as attenuation of ERD [32]. The relationship between TLR activities and skewed Th2 response observed in FIRSV-induced ERD in the mouse model remains to be defined.

In addition to antibody responses induced by FIRSV, the roles of specific T cell subsets and their secreted cytokines in ERD development have also been investigated [43,57]. FIRSV immunization induced lower number of IFN-γ producing CD8 T cells when

compared with live RSV immunized animals. However, priming RSV-specific CD8 T cell responses prior to viral challenge could suppress lung eosinophilia and Th2 responses in FIRSV immunized mice, suggesting that early recall of CD8 T cell responses before RSV infection could prevent RSV infection without inducing ERD [57,63–65].

The potential role of eosinophils in ERD was also investigated. Although pulmonary infiltration of eosinophils and/or neutrophils has been consistently observed in FIRSV induced-ERD in all animal models and humans, Knudson et al. (2015) showed that eosinophils do not play any significant role in ERD induction as the CD4 T cells do with their secreted cytokines [43]. Specifically, FIRSV induces ERD in eosinophil-deficient mice with significant pulmonary infiltration of CD4 T cells producing IL-4, IL-13, IFN-γ or TNF-α as that in the wild type mice; moreover, no difference in the quantitation of Th1 and Th2 responses, and viral clearance rate was found in eosinophil-deficient mice and the wild type strain [43]. However, the role of eosinophils in viral clearance remains to be determined as Phipps et al. (2007) suggest that eosinophils might increase RSV clearance [66]. Such discrepancy in results might be due to the experimental systems as Phipps et al. used a hypereosinophilic mouse model that constitutively expressed IL-5, an eosinophil chemoattractant, resulting in a constant presence of eosinophils in the lungs [66–68].

The role of CD4 T cells has also been extensively studied in the mouse model. Depletion of CD4 T cells in FIRSV immunized mice resulted in significantly less ERD although no difference in antibody response was observed between the CD4 T cells depleted mice and untreated mice, suggesting that CD4 T cells could contribute to ERD development [43,69]. This notion was further supported by studies using STAT6-deficient mice. Specifically animals with a deficiency in differentiation of naïve CD4 T cells into Th2 cells demonstrated decreased levels of IL-4, IL-13, eosinophils, mucus hypersecretion, and

perivascular leukocyte aggregates even though airway obstruction and weight loss were not significantly affected [43]. Moreover, neutralization of IL-4, IL-10 and IL-13 (Th2 cytokines) activities by antibodies in these animals also reduces severity of FIRSV-induced pathological lesions [70–73]. These data collectively indicate that CD4 T cell response, especially Th2 response, may be involved in almost all aspects of FIRSV induced enhanced respiratory disease [43]. However, clinical scores such as airway obstruction and weight loss in the mice were unlikely to be related to elevated levels of Th2 cytokines but to IFN-γ and TNF-α. Knudson et al. (2015) immunized IFN-γ deficient mice with FIRSV in conjunction with TNF-α neutralizing antibody administration before RSV challenge. They observed decreased levels of airway obstruction, weight loss and eosinophil count in these mice as compared to the untreated controls even though similar histopathology scores and lung viral clearance was observed. The investigators therefore concluded that TNF-α was one of the major factors contributing to the development of airway obstruction and weight loss [43].

While many reported on the mechanistic studies of ERD, research work has also been conducted to investigate gene expression profile and identify potential biomarkers suggestive of ERD. Using systems biology, Schuurhof et al. (2010) showed that during the first two days following RSV infection, the profile of gene expression in FIRSV-immunized mice was similar to that in the unimmunized control group. However, five days after viral challenge the mRNA profile in the FIRSV group resembled that of a primary infection instead of a memory response, unlike a robust immune response [56]. In agreement with other studies, Th2 genes were upregulated while Th1 genes downregulated in the FIRSV group [57,74,75]. Moreover, potential biomarkers were also investigated with proteomics analyses. These mice were immunized with recombinant vaccinia virus expressing RSV G or F protein, and not

FIRSV [58]. Enhanced disease was only observed in mice immunized with recombinant vaccinia virus expressing RSV G protein but not F [57,76,77]. Following RSV challenge, elevated levels of the proteins related to the direct influx of eosinophils (eosinophil peroxidase [Epx]), and to chemotaxis and extravasation processes (Chil3) as well as to eosinophil and neutrophil homing signals to the lung (Itgam) were found [58]. These proteins are expressed by eosinophils, neutrophils, macrophages or type 2 innate lymphocytes and/or have a role in mediating influx of immune cells into the lungs or increasing airway hyperresponsiveness [57,74,75]. The data obtained from pulmonary proteomics analysis appear to be largely in agreement with findings from pathological and immunological investigations of FIRSV induced ERD in the mouse model. Clearly, identifying additional biomarkers with predictive value of ERD is urgently needed.

Table 1. Summary of Clinical Presentations and Laboratory Analyses of ERD in Different Animal Models

Parameter	Animal Model	Signs/Symptoms Following FIRSV Immunization Post RSV Infection
Pulmonary Histopathological/ Immunological Observations	Humans	• Longer persistence of pneumonia, mild rhinitis, pharyngitis, bronchitis [5,6] • Patchy atelectasis with emphysema and pneumothorax [5,6] • Peribronchiolar eosinophil infiltration [5,6] or lymphocytes with some neutrophil and macrophage infiltration [10]
	Lamb	• High perivascular and peribronchiolar lymphocyte infiltration, mostly neutrophils and no eosinophils [12] • Low number of bronchiolar epithelial lesions [12] • Low RSV titer in lung tissue with low RSV antigens in bronchi/bronchioles and alveoli [12,13]
	Bovine	• Severe emphysema, bronchiolitis, peribronchiolar interstitial mononuclear cell infiltration [18,19,21] • Neutrophilic alveolitis [18] or eosinophilic alveolitis [19,21] • No virus in lung tissue [21]

Non-Human Primates	• Develop inflammation in peribronchiolar, perivascular, interstitial and intra-alveolar sites [29] • Macrophage, eosinophil, lymphocyte and multinucleate giant cell infiltration [29,40] • High RSV titers in lung tissue in bonnet and African green monkeys [29,31] • High number of IL-13 producing T cells observed in macaques lungs [40]
Cotton Rats	• Increased severity of peribronchiolitis (with lymphocytes), bronchitis, neutrophilic alveolitis and interstitial pneumonitis [10,41,42] • 90% decrease in lung and nasal viral titre [10] • Increased levels of IL-4, IL-5, IL-9, IL-10 and IL-13 [42,44–46] and some Th1 cytokines and chemokines [44–46] • Large amounts of RSV antigens and increased viral replication in lungs [42]
Mice	• Increased pulmonary inflammation, mucus hypersecretion, airway obstruction, and lung eosinophilia [32,43] • Decreased lung viral load [43] • High levels of Th2 cytokines like IL-4, IL-5 and IL-13 [43,55,59]

		• Lower number of IFN-γ producing CD8 T cells in the lungs compared to live-RSV immunized C57BL/6 mice [56] • High number of IFN-γ and TNF-α producing CD4 T cells in lungs of BALB/c mice [43]
Serum Antibodies	Humans	• High RSV specific antibody titre [5,6] • Eosinophils in peripheral blood [4]
	Lamb	• Higher RSV neutralizing antibodies than mock-immunized [11,12]
	Bovine	• Higher IgG and IgE titers compared to naïve, mock and live-virus immunized but lower RSV neutralizing antibodies [18,21]
	Non-Human Primates	• Lower RSV neutralizing antibodies compared to live-virus immunized group in bonnet monkeys [29,30] but higher levels in cynomolgus macaques compared to FI-measles immunized group [40] • Higher levels of disease enhancing antibodies in bonnet monkeys [30]
	Cotton Rats	• Low RSV neutralizing antibody levels and low avidity RSV-specific IgGs but high total IgG titer [41,42,47]
	Mice	• High levels of RSV-specific IgG1 and low IgG2a [32,55]

		• High IgG content but low antibody avidity to RSV epitopes [32]
BAL Fluid Viral Titer and Antibodies	Lamb	• Low RSV titer with low viral mRNA [12,13]
	Bovine	• No viral RNA [21] • IgG1 levels in BAL fluid negatively correlate to severity of disease [23] • Low IgA levels [23]
	Non-Human Primates	• High RSV titers in BAL fluid in bonnet and African green monkeys [29,31] but low RSV titer in cynomolgus macaques [40] • Eosinophil count high [29,40]
	Mice	• High levels of Th2 cytokines like IL-4, IL-5 and IL-13 [43,55,59]
Other	Lamb	• No change in body weight, temperature, heart rate and respiratory rate [11,12]
	Bovine	• Increase in rectal temperature, coughing, nasal discharge, sensitivity of larynx and trachea, lung sounds, severe dyspnea [18,19,21]
	Cotton Rat	• No weight loss [10]
	Mice	• Up to 15% weight loss and airway hyperresponsiveness [32,43] • Dendritic cells from popliteal lymph nodes lacked maturation with decreased expression

	of CD40, CD80 and CD86 [32] • Low levels of germinal center formation and B cell isotype switching [32]

ERD: enhanced respiratory disease; RSV: Respiratory Syncytial Virus; FIRSV: formalin-inactivated RSV; BAL: bronchoalveolar lavage; Ig: immunoglobulin; IL: interleukin; Th: T helper cell

Expert Commentary and Five-Year View

There have been several excellent reviews on RSV vaccine development in recent years [44,59,78-80]. In this review, we intended to focus on ERD associated with RSV vaccine, particularly formaldehyde-inactivated RSV vaccine (FIRSV), given that formaldehyde is widely used in licensed human vaccines [81]. We also made efforts to dissect findings from a range of animal models commonly used for RSV vaccine evaluations.

While Table 1 summarizes some major findings in different animal models and humans, some critical issues are worthy of being emphasized. First, as FIRSV induced characteristic ERD, which is generally reproducible in preclinical studies, it would serve as a valuable control to determine if a new candidate vaccine could induce the same vaccine-associated disease. Second, the significance of pulmonary infiltration of eosinophils remains to be determined since eosinophils may not be involved in ERD development as demonstrated in eosinophil-deficient mice [43]. It is of note that autopsy examination of tissues of the deceased children in the failed clinical trial was inconclusive with regards to the exact cellular identity although marked peribronchiolar monocytic infiltration was observed [5,6,10]. Third, FIRSV-induced ERD has been consistently observed in all reported animal models. Other forms of vaccines, such as purified F protein [32] and vaccinia virus vectored RSV vaccines [57,76,77], have also been linked to ERD, suggesting multiple pathways could be involved [47,54,58]. Fourth, it is noted that some pulmonary proteins including those involved in influx of eosinophils and neutrophils, and chemotaxis processes have been linked to ERD in mice [56,57]. However, the feasibility and significance of quantitative analyses of these proteins in vaccine human clinical trials remains to be determined, given that these proteins are not ERD-specific but known to be involved in a

variety of immunological processes. Ideally, biomarkers pertinent to clinical evaluation and quantitatively detectable in readily available specimen such as blood or mucus secretion would be valuable tools for safety assessment of RSV vaccines in human trials.

Key Issues

- Formaldehyde-inactivated RSV vaccine (FIRSV) in the 1960s resulted in severe adverse reaction, which could be largely reproduced in all animal models studied so far.
- Marked differences in disease presentations and immonopathological findings observed between and within animal models, likely due to various factors including antigen dose, immunization/protection study schedule and the nature of the viral antigens in addition to genetic background.
- More studies are needed to fully elucidate the mechanisms underlying vaccine-associated adverse reactions as both viral and non-viral elements could be involved.
- Low affinity antibodies and biased Th2 immune response observed in some ERD animal studies, with antibodies contributing to ERD by altering innate immune response and facilitating RSV uptake by monocytic cells.
- Continued efforts need to be made to explore more biomarkers of vaccine associated enhanced disease and immunological correlates of protection

Financial Disclosure/Acknowledgements

There is no conflict of interest. The work was supported by Genomics Research and Development Initiative of Government of Canada. We wish to thank Dr. Michael Johnston and Dr. Richard Isbrucker for critical review of the manuscript. We greatly appreciate critical comments on the manuscript from Laura Durno, Dr. Dean Smith and Dr. Maria Baca-Estrada. We thank Louise Larocque and Marsha Russell for useful discussion.

References

* Of interest

** Of considerable interest

[1] WHO, "Status of vaccine research and development of vaccines for RSV," 2014.

[2] R. Lozano, M. Naghavi, K. Foreman, A. D. Lopez, and C. J. L. Murray, "Global and regional mortality from 235 causes of death for 20 age groups in 1990 and 2010: A systematic analysis for the Global Burden of Disease Study 2010," *Lancet*, vol. 380, no. 9859, pp. 2095–2128, 2012.

[3] L. J. Stockman, A. T. Curns, L. J. Anderson, and G. Fischer-Langley, "Respiratory Syncytial Virus-associated Hospitalizations Among Infants and Young Children in the United States, 1997–2006," *Pediatr. Infect. Dis. J.*, vol. 31, no. 1, pp. 5–9, 2012.

[4] J. Chin, R. L. Magoeetn, L. a N. N. Shearer, J. H. Schleble, and E. H. Lennette, "Field Evaluation of a Respiratory Syncytial Virus Vaccine and a Trivalent Parainfluenza Virus Vaccine in a Pediatric Population," *Am. J. Epidemiol.*, vol. 89, no. 4, pp. 449–463, 1969.

[5] H. W. Kim, J. G. Canchola, C. D. Brandt, G. Pyles, R. M. Chanock, K. Jensen, and R. H. Parrott, "Respiratory Syncytial Virus Disease in Infants Despite Prior Administration of Antigenic Inactivated Vaccine," *Am. J. Epidemiol.*, vol. 89, no. 4, pp. 422–434, 1969.
**** First instance of FIRSV induced enhanced disease in humans reported and autopsies analyzed.**

[6] A. Z. Kapikian, R. H. Mitchell, R. M. Chanock, R. A. Shvedoff, and C. E. Stewart, "Epidemiologic Study Of Altered Clinical Reactivity To Respiratory Syncytial (RS) Virus Infection In Children Previously Vaccinated With An Inactivated Rs Virus Vaccine," *Am. J. Epidemiol.*, vol. 88, no. 4, pp. 405–421, 1969.

[7] B. S. Graham, "Biological Challenges and Technological Opportunities for RSV Vaccine Development," *Immunol. Rev.*, vol. 239, no. 1, pp. 149–166, 2011.

[8] P. L. Collins and J. A. Melero, "Progress in understanding and controlling respiratory syncytial virus: Still crazy after all these years," *Virus Res.*, vol. 162, no. 1–2, pp. 80–99, 2011.

[9] H. W. Kim, S. L. Leikin, J. Arrobio, C. D. Brandt, R. M. Chanock, and R. H. Parrott, "Cell-mediated immunity to respiratory syncytial virus induced by inactivated vaccine or by infection," *Pediatr. Res.*, vol. 10, no. 1, pp. 75–78, 1976.

[10] G. A. Prince, S. J. Curtis, K. C. Yim, and D. D. Porter, "Vaccine-enhanced respiratory syncytial virus disease in cotton rats following immunization with Lot 100 or a newly prepared reference vaccine," *J. Gen. Virol.*, vol. 82, no. 12, pp. 2881–2888, 2001.
**** Reevaluation of human autopsy results and development of the cotton rat model.**

[11] M. R. Ackermann, "Lamb model of respiratory syncytial virus-associated lung disease: Insights to pathogenesis and novel treatments," *ILAR J.*, vol. 55, no. 1, pp. 4–15, 2014.

[12] R. J. Derscheid, J. M. Gallup, C. J. Knudson, S. M. Varga, W. Dregrosz, A. Van Geelen, S. J. Hostetter, and M. R. Ackermann, "Effects of formalin-inactivated Respiratory syncytial virus (FI-RSV) in the Perinatal lamb model of RSV," *PLoS One*, vol. 8, no. 12, 2013.

[13] D. K. Meyerholz, B. Grubor, S. J. Fach, R. E. Sacco, H. D. Lehmkuhl, J. M. Gallup, and M. R. Ackermann, "Reduced clearance of respiratory syncytial virus infection in a preterm lamb model," *Microbes Infect.*, vol. 6, no. 14, pp. 1312–1319, 2004.
[14] R. J. Derscheid and M. R. Ackermann, "Perinatal lamb model of respiratory syncytial virus (RSV) infection," *Viruses*, vol. 4, no. 10, pp. 2359–2378, 2012.
[15] A. Olivier, J. Gallup, M. M. M. A. De MacEdo, S. M. Varga, and M. Ackermann, "Human respiratory syncytial virus A2 strain replicates and induces innate immune responses by respiratory epithelia of neonatal lambs," *Int. J. Exp. Pathol.*, vol. 90, no. 4, pp. 431–438, 2009.
[16] A. K. Olivier, J. M. Gallup, A. van Geelen, and M. R. Ackermann, "Exogenous administration of vascular endothelial growth factor prior to human respiratory syncytial virus a2 infection reduces pulmonary pathology in neonatal lambs and alters epithelial innate immune responses," *Exp. Lung Res.*, vol. 37, no. 3, pp. 131–143, 2011.
[17] T. Lazic, T. A. Wyatt, M. Matic, D. K. Meyerholz, B. Grubor, J. M. Gallup, K. W. Kersting, P. M. Imerman, M. Almeida-De-Macedo, and M. R. Ackermann, "Maternal alcohol ingestion reduces surfactant protein A expression by preterm fetal lung epithelia," *Alcohol*, vol. 41, no. 5, pp. 347–355, 2007.
[18] L. J. Gershwin, E. S. Schelegle, R. A. Gunther, M. L. Anderson, A. R. Woolums, D. R. Larochelle, G. A. Boyle, K. E. Friebertshauser, and R. S. Singer, "A bovine model of vaccine enhanced respiratory syncytial virus pathophysiology," *Vaccine*, vol. 16, no. 11–12, pp. 1225–1236, 1998.
[19] K. West, L. Petrie, D. M. Haines, C. Konoby, E. G. Clark, K. Martin, and J. a Ellis, "The effect of formalin-inactivated vaccine on respiratory disease associated with bovine respiratory syncytial virus infection in calves," *Vaccine*, vol. 17, no. 7–8, pp. 809–820, 1999.
[20] P. Schreiber, J. P. Matheise, F. Dessy, M. Heimann, J. J. Letesson, P. Coppe, and A. Collard, "High mortality rate associated with Bovine Respiratory Syncytial Virus (BRSV) infection in Belgian White Blue calves previously vaccinated with an inactivated BRSV vaccine," *J. Vet. Med. Ser. B*, vol. 47, no. 7, pp. 535–550, 2000.
[21] A. F. G. Antonis, R. S. Schrijver, F. Daus, J. G. M. Steverink, N. Stockhofe, E. J. Hensen, J. P. M. Langedijk, R. G. Van Der Most, and P. J. G. M. Steverink, "Vaccine-Induced Immunopathology during Bovine Respiratory Syncytial Virus Infection : Exploring the Parameters of Pathogenesis," *J. Virol.*, vol. 77, no. 22, pp. 12067–12073, 2003.
[22] W. V. Kalina, A. R. Woolums, R. D. Berghaus, and L. J. Gershwin, "Formalin-inactivated bovine RSV vaccine enhances a Th2 mediated immune response in infected cattle," *Vaccine*, vol. 22, no. 11–12, pp. 1465–1474, 2004.
[23] W. V. Kalina, A. R. Woolums, and L. J. Gershwin, "Formalin-inactivated bovine RSV vaccine influences antibody levels in bronchoalveolar lavage fluid and disease outcome in experimentally infected calves," *Vaccine*, vol. 23, no. 37, pp. 4625–4630, 2005.
[24] T. Olchowy, T. Ames, and T. Molitor, "Interaction of bovine respiratory syncytial virus with bovine alveolar macrophages in vivo: Effects of virus infection upon selected cell functions," *Can J Vet Res*, vol. 58, no. 1, pp. 42–48, 1994.
[25] A. R. Woolums, R. S. Singer, G. A. Boyle, and L. J. Gershwin, "Interferon gamma production during bovine respiratory syncytial virus (BRSV) infection is diminished

in calves vaccinated with formalin-inactivated BRSV," *Vaccine*, vol. 17, no. 11–12, pp. 1293–1297, 1999.

[26] R. Wang, S. I. Abrams, D. Y. Loh, C.-S. Hsieh, K. M. Murphy, and J. H. Russell, "Separation of CD4+ Functional Responses by Peptide Dose in Th1 and Th2 Subsets Expressing the Same Transgenic Antigen Receptor," *Cell. Immunol.*, vol. 148, pp. 357–370, 1993.

[27] M. H. Smith, M. L. Frey, and R. Dierks, "Isolation, characterization, and pathogenicity studies of a bovine respiratory syncytial virus," *Arch. Virol.*, vol. 47, no. 3, pp. 237–247, 1975.

[28] J. C. Baker and M. L. Frey, "Bovine Respiratory Syncytial Virus," *Symp. Bov. Respir. Dis. Vet. Clin. North Am.*, vol. 1, no. 2, pp. 259–275.

[29] E. M. Ponnuraj, A. R. Hayward, A. Raj, H. Wilson, and E. A. F. Simoes, "Increased replication of respiratory syncytial virus (RSV) in pulmonary infiltrates is associated with enchanced histopathological disease in bonnet monkeys (Macaca radiata) pre-immunized with a formalin-inactivated RSV vaccine," *J. Gen. Virol.*, vol. 82, no. 11, pp. 2663–2674, 2001.

[30] E. M. Ponnuraj, J. Springer, A. R. Hayward, H. Wilson, and E. A. Simoes, "Antibody-dependent enhancement, a possible mechanism in augmented pulmonary disease of respiratory syncytial virus in the Bonnet monkey model," *J. Infect. Dis.*, vol. 187, no. 8, pp. 1257–1263, 2003.
*** Interesting mathematical procedure to determine disease enhancement property of antibodies.**

[31] T. J. Kakuk, K. Soike, R. J. Brideau, R. M. Zaya, S. L. Cole, J. Y. Zhang, E. D. Roberts, P. A. Wells, and M. W. Wathen, "A human respiratory syncytial virus (RSV) Primate model of enhanced pulmonary pathology induced with a formalin-inactivated RSV vaccine but not a recombinant FG subunit vaccine," *J. Infect. Dis.*, vol. 167, no. 3, pp. 553–561, 1993.

[32] M. F. Delgado, S. Coviello, A. C. Monsalvo, G. A. Melendi, J. Z. Hernandez, J. P. Batalle, L. Diaz, A. Trento, H.-Y. Chang, W. Mitzner, J. Ravetch, J. A. Melero, P. M. Irusta, and F. P. Polack, "Lack of antibody affinity maturation due to poor Toll-like receptor stimulation leads to enhanced respiratory syncytial virus disease.," *Nat. Med.*, vol. 15, no. 1, pp. 34–41, 2009.
*** Exploring an experimental approach to preventing vaccine-induced disease enhancement.**

[33] H. Gimenez, S. Chisholm, J. Doran, and P. Cash, "Neutralizing and enhancing activities of human respiratory syncytial virus–specific antibodies," *Clin Diagn Lab Immunol*, vol. 3, pp. 280–286, 1996.

[34] S. Techaarpornkul, P. L. Collins, and M. E. Peeples, "Respiratory syncytial virus with the fusion protein as its only viral glycoprotein is less dependent on cellular glycosaminoglycans for attachment than complete virus," *Virology*, vol. 294, pp. 296–304, 2002.

[35] L. R. Kirlov, L. J. Anderson, L. Marcoux, V. R. Bonagura, and J. F. Wedgwood, "Antibody-mediated enhancement of respiratory syncytial virus infection in two monocyte/macrophage cell lines," *J. Infect. Dis.*, vol. 160, pp. 777–782, 1989.

[36] F. P. Polack, M. N. Teng, P. L. Collins, G. a Prince, M. Exner, H. Regele, D. D. Lirman, R. Rabold, S. J. Hoffman, C. L. Karp, S. R. Kleeberger, M. Wills-Karp, and R. a Karron, "A role for immune complexes in enhanced respiratory syncytial virus

disease," *J. Exp. Med.*, vol. 196, no. 6, pp. 859–865, 2002.
[37] G. A. Ananaba and L. J. Anderson, "Antibody enhancement of respiratory syn- cytial virus stimulation of leukotriene production by a macrophage- like cell line," *J. Virol.*, vol. 65, pp. 5052–5060, 1991.
[38] B. Volovitz, R. C. Welliver, G. De Castro, D. A. Krystofik, and P. L. Ogra, "The release of leukotrienes in the respiratory tract during infection with respiratory syncytial virus: role in obstructive airway disease," *Pediatr. Res.*, vol. 24, pp. 504–507, 1988.
[39] K. Wedde-Beer, C. Hu, M. M. Rodriguez, and G. Piedimonte, "Leukotrienes mediate neurogenic inflammation in lungs of young rats infected with respiratory syncytial virus," *Am J Physiol Lung Cell Mol Physiol*, vol. 282, pp. 1143–1150, 2002.
[40] R. L. De Swart, T. Kuiken, H. H. Timmerman, G. van Amerongen, B. G. Van Den Hoogen, H. W. Vos, H. J. Neijens, A. C. Andeweg, and A. D. M. E. Osterhaus, "Immunization of macaques with formalin-inactivated respiratory syncytial virus (RSV) induces interleukin-13-associated hypersensitivity to subsequent RSV infection.," *J. Virol.*, vol. 76, no. 22, pp. 11561–11569, 2002.
*** Mechanistic analysis of the vaccine-induced enhanced disease in a non-human primate model; determination of the role of Th2 cytokines.**
[41] G. Taylor, M. Thom, S. Capone, A. Pierantoni, E. Guzman, R. Herbert, E. Scarselli, F. Napolitano, A. Giuliani, A. Folgori, S. Colloca, R. Cortese, A. Nicosia, and A. Vitelli, "Efficacy of a virus-vectored vaccine against human and bovine respiratory syncytial virus infections," *Sci Transl Med*, vol. 7, no. 300, pp. 1–13, 2015.
[42] A. Sawada and T. Nakayama, "Experimental animal model for analyzing immunobiological responses following vaccination with formalin-inactivated respiratory syncytial virus," *Microbiol. Immunol.*, vol. 60, no. 4, pp. 234–242, 2016.
[43] C. J. Knudson, S. M. Hartwig, D. K. Meyerholz, and S. M. Varga, "RSV Vaccine-Enhanced Disease Is Orchestrated by the Combined Actions of Distinct CD4 T Cell Subsets," *PLoS Pathog.*, vol. 11, no. 3, pp. 1–23, 2015.
**** In-depth analysis of the role of eosinophils, T cell subsets and cytokines in FIRSV pathogenesis in mice.**
[44] M. S. Boukhvalova, G. A. Prince, and J. C. G. Blanco, "The cotton rat model of respiratory viral infections.," *Biologicals*, vol. 37, no. 3, pp. 152–159, 2009.
[45] G. A. Prince, F. Denamur, M. Deschamps, N. Garçon, J. P. Prieels, M. Slaoui, C. Thiriart, and D. D. Porter, "Monophosphoryl lipid A adjuvant reverses a principal histologic parameter of formalin-inactivated respiratory syncytial virus vaccine-induced disease," *Vaccine*, vol. 19, no. 15–16, pp. 2048–2054, 2001.
[46] M. S. Boukhvalova, G. A. Prince, L. Soroush, D. C. Harrigan, S. N. Vogel, and J. C. G. Blanco, "The TLR4 agonist, monophosphoryl lipid A, attenuates the cytokine storm associated with respiratory syncytial virus vaccine-enhanced disease," *Vaccine*, vol. 24, no. 23, pp. 5027–5035, 2006.
[47] C. A. Shaw, J. R. Galarneau, K. E. Bowenkamp, K. A. Swanson, G. A. Palmer, G. Palladino, J. E. Markovits, N. M. Valiante, P. R. Dormitzer, and G. R. Otten, "The role of non-viral antigens in the cotton rat model of respiratory syncytial virus vaccine-enhanced disease," *Vaccine*, vol. 31, no. 2, pp. 306–312, 2013.
[48] Pedro Piedra et al., "Enhanced pulmonary pathology associated with the use of formalin-inactivated respiratory syncytial virus vaccine in cotton rats is not a uniqu viral phenomenon," Vaccine, vol. 11, no. 14, pp. 1415-1423, 1993.

[49] V. Hornung, J. Schlender, M. Guenthner-Biller, S. Rothenfusser, S. Endres, K. K. Conzelmann, and G. Hartman, “Replication-Dependent Potent IFN-alpha Induction in Human Plasmacytoid Dendritic Cells by a Single-Stranded RNA Virus,” *J. Immunol.*, vol. 173, pp. 5935–5943, 2004.
[50] Marina S Boukhvalova, Gregory A Prince, and Jorge CG Blanco, "Inactivation of respiratory syncytial virus by zinc finger reactive compounds," Virology, vol. 7, no. 20, pp. 1-10, 2010.
[51] J. Young, “Development of a potent respiratory syncytial virus specific monoclonal antibody for the prevention of serious lower respiratory tract disease in infants,” *Respir Med*, vol. 96, pp. S31–S35, 2002.
[52] The IMpact-RSV Study Group, “Palivizumab, a humanized respiratory syncytial virus monoclonal antibody, reduces hospitalization from re- spiratory syncytial virus infection in high risk infants,” *Pediatrics*, vol. 102, no. 531–537, 1998.
[53] Lori McGinnes Cullen, Jorge CG Blanco, and Trudy G Morrison, "Cotton rat immune responses to virus-like particles containing the pre-fusion form of respiratory syncytial virus fusion protein," Journal of Translation Medicine, vol. 13, no. 350, pp. 1-13, 2015.
[54] D. S. Wheeler, M. A. Chase, A. P. Senft, S. E. Poynter, H. R. Wong, and K. Page, “Extracellular Hsp72, an Endogenous DAMP, is Released by Virally Infected Airway Epithelial Cells and Activates Neutrophils via Toll-like Receptor (TLR)-4,” *Respir. Res.*, vol. 10, no. 1, p. 31, 2009.
[55] A. Moghaddam, W. Olszewska, B. Wang, J. S. Tregoning, R. Helson, Q. J. Sattentau, and P. J. Openshaw, “A potential molecular mechanism for hypersensitivity caused by formalin-inactivated vaccines,” *Nat Med*, vol. 12, no. 8, pp. 905–907, 2006.
[56] A. Schuurhof, L. Bont, J. L. A. Pennings, H. M. Hodemaekers, P. W. Wester, A. Buisman, L. C. G. H. de Rond, M. N. Widjojoatmodjo, W. Luytjes, J. L. L. Kimpen, and R. Janssen, “Gene expression differences in lungs of mice during secondary immune responses to respiratory syncytial virus infection,” *J. Virol.*, vol. 84, no. 18, pp. 9584–9594, 2010.
[57] D. Kruijsen, M. A. Schijf, M. V. Lukens, N. O. van Uden, J. L. Kimpen, F. E. Coenjaerts, and G. M. Van Bleek, “Local innate and adaptive immune responses regulate inflammatory cell influx into the lungs after vaccination with formalin inactivated RSV,” *Vaccine*, vol. 29, no. 15, pp. 2730–2741, 2011.
[58] A. van Diepen, H. K. Brand, L. de Waal, M. Bijl, V. L. Jong, T. Kuiken, G. van Amerongen, H. J. van den Ham, M. J. Eijkemans, A. Osterhaus, P. W. M. Hermans, and A. C. Andeweg, “Host Proteome Correlates of Vaccine-Mediated Enhanced Disease in a Mouse Model of Respiratory Syncytial Virus Infection,” *J. Virol.*, vol. 89, no. 9, pp. 5022–5031, 2015.
[59] P. J. Openshaw, F. J. Culley, and W. Olszewska, “Immunopathogenesis of vaccine-enhanced RSV disease.,” *Vaccine*, vol. 20, pp. S27–S31, 2002.
[60] B. R. Murphy and E. E. Walsh, “Formalin-inactivated respiratory syncytial virus vaccine induces antibodies to the fusion glycoprotein that are deficient in fusion-inhibiting activity,” *J. Clin. Microbiol.*, vol. 26, no. 8, pp. 1595–1597, 1988.
[61] M. E. D. Allison and D. T. Fearon, “Enhanced immunogenicity of aldehyde-bearing antigens: A possible link between innate and adaptive immunity,” *Eur. J. Immunol.*, vol. 30, no. 10, pp. 2881–2887, 2000.
[62] S. Horiuchi, M. Murakami, K. Takata, and Y. Morino, “Scavenger receptor for

aldehyde-modified proteins," *J. Biol. Chem.*, vol. 261, no. 11, pp. 4962–4966, 1986.
[63] M. Olson and S. Varga, "CD8 T cells inhibit respiratory syncytial virus (RSV) vaccine-enhanced disease," *J. Immunol.*, vol. 179, pp. 5415–5424, 2007.
[64] M. Olson, S. Hartwig, and S. Varga, "The number of respiratory syncytial virus (RSV)-specific memory CD8 T cells in the lung is critical for their ability to inhibit RSV vaccine-enhanced pulmonary eosinophilia," *J. Immunol.*, vol. 181, pp. 7958–7968, 2008.
[65] W. Stevens, J. Sun, J. Castillo, and T. Braciale, "Pulmonary eosinophilia is attenuated by early responding CD8(+) memory T cells in a murine model of RSV vaccine-enhanced disease," *Viral Immunol*, vol. 22, pp. 243–251, 2009.
[66] S. Phipps, C. E. Lam, S. Mahalingam, M. Newhouse, R. Ramirez, H. F. Rosenberg, P. S. Foster, and K. I. Matthaei, "Eosinophils contribute to innate antiviral immunity and promote clearance of respiratory syncytial virus," *Blood*, vol. 110, no. 5, pp. 1578–1586, 2007.
[67] E. M. Castilow, D. K. Meyerholz, and S. M. Varga, "IL-13 is required for eosinophil entry into the lung during respiratory syncytial virus vaccine-enhanced disease," *J. Immunol.*, vol. 180, no. 4, pp. 2376–2384, 2008.
[68] T. R. Johnson, M. E. Rothenberg, and B. S. Graham, "Pulmonary eosinophilia requires interleukin-5, eotaxin-1, and CD4+ T cells in mice immunized with respiratory syncytial virus G glycoprotein.," *J. Leukoc. Biol.*, vol. 84, no. 3, pp. 748–759, 2008.
[69] M. Connors, A. B. Kulkarni, C. Firestone, K. L. Holmes, H. C. M. Iii, A. V Sotnikov, and B. R. Murphy, "Pulmonary Histopathology Induced by Respiratory Syncytial Virus (RSV) Challenge of Formalin-Inactivated RSV-Immunized BALB/c Mice Is Abrogated by Depletion of CD4 + T Cells," *J. viro*, vol. 66, no. 12, pp. 7444–7451, 1992.
[70] M. Connors, N. Giese, A. Kulkarni, C. Firestone, H. Morse III, and B. Murphy, "Enhanced pulmonary histopathology induced by respiratory syncytial virus (RSV) challenge of formalin-inactivated RSV-immunized BALB/c mice is abrogated by depletion of interleukin-4 (IL-4) and IL-10," *J. Virol.*, vol. 68, pp. 5321–5325, 1994.
[71] T. Johnson and B. Graham, "Secreted respiratory syncytial virus G glycoprotein induces interleukin-5 (IL-5), IL-13, and eosinophilia by an IL-4-independent mechanism," *J. Virol.*, vol. 73, pp. 8485–8495, 1999.
[72] T. Johnson, R. Parker, J. Johnson, and B. Graham, "IL-13 is sufficient for respiratory syncytial virus G glycoprotein-induced eosinophilia after respiratory syncytial virus challenge," *J. Immunol.*, vol. 170, pp. 2037–2045, 2003.
[73] Y. Tang and B. Graham, "Anti-IL-4 treatment at immunization modulates cytokine expression, reduces illness, and increases cytotoxic T lymphocyte activity in mice challenged with respiratory syncytial virus," *J. Clin. Invest*, vol. 94, pp. 1953–1958, 1994.
[74] H. Iwashita, S. Morita, Y. Sagiya, and A. Nakanishi, "Role of eosinophil chemotactic factor by T lymphocytes on airway hyperresponsiveness in a murine model of allergic asthma," *Am. J. Respir. Cell Mol. Biol.*, vol. 35, no. 1, pp. 103–109, 2006.
[75] J. K. Bando, J. C. Nussbaum, H.-E. Liang, and R. M. Locksley, "Type 2 innate lymphoid cells constitutively express arginase-I in the naive and inflamed lung," *J. Leukoc. Biol.*, vol. 94, no. 5, pp. 877–84, 2013.
[76] R. A. Olmsted, N. Elango, G. A. Prince, B. R. Murphy, P. R. Johnson, B. Moss, R. M.

Chanock, and P. L. Collins, “Expression of the F glycoprotein of respiratory syncytial virus by a recombinant vaccinia virus: comparison of the individual contributions of the F and G glycoproteins to host immunity.,” *Proc. Natl. Acad. Sci. U. S. A.*, vol. 83, no. 19, pp. 7462–7466, 1986.

[77] P. Openshaw, S. Clarke, and F. Record, “Pulmonary eosinophilic response to respiratory syncytial virus infection in mice sensitized to the major surface glycoprotein G,” *Int Immunol*, vol. 4, pp. 493–500, 1992.

[78] L. G. Byrd and G. A. Prince, "Animal Models of Respiratory Syncytial Virus Infection," Clinical Infectious Diseases, vol. 25, pp. 1363-1368, 1997.

[79] P. J. M. Openshaw and J. S. Tregoning, "Immune Responses and Disease Enhancement during Respiratory Syncytial Virus Infection," Clinical Microbiology Reviews, vol. 18, no. 3, pp. 541-555, 2005.

[80] B. S. Graham, K. Modjarrad and J. S. McLellan, "Novel Antigens for RSV Vaccines," Current Opinion in Immunology, vol. 35, pp. 30-38, 2015.

[81] B. Sanders, M. Koldijk and H. Schuitemaker, "Inactivated Viral Vaccines," in Vaccine Analysis: Strategies, Principles, and Control, 2015, pp. 45-80.

Appendix B

Identification of Immunodominant CD8 Epitope in the Stalk Domain of Influenza B Viral Hemagglutinin

Abenaya Muralidharan[a, d], Caroline Gravel[a], Amparo Duran[a, d], Louise Larocque[a], Changgui Li[b], Adrian Zetner[c], Gary Van Domselaar[c], Lisheng Wang[d], Xuguang Li[a, d]

Published: ***Biochem Biophys Res Commun,*** **2018 Jul 12; 502(2):226-231**

[a]Centre for Biologics Evaluation, Biologics and Genetic Therapies Directorate, HPFB, Health Canada and WHO Collaborating Center for Standardization and Evaluation of Biologicals, Ottawa, ON, Canada.
[b]National Institute for Food and Drug Control and WHO Collaborating Center for Standardization and Evaluation of Biologicals, Beijing, China
[c]National Microbiology Laboratory, Public Health Agency of Canada, Winnipeg, MB, Canada
[d]Department of Biochemistry, Microbiology and Immunology, Faculty of Medicine, University of Ottawa, Ottawa, ON, Canada

*Corresponding author (XL): sean.li@hc-sc.gc.ca

Abstract

Human infections by type B influenza virus constitute about 25% of all influenza cases. The viral hemagglutinin is comprised of two subunits, HA1 and HA2. While HA1 is constantly evolving in an unpredictable fashion, the HA2 subunit is highly conserved, making it a potential candidate for a universal vaccine. However, immunodominant epitopes in the HA2 subunit remain largely unknown. To delineate MHC Class I epitopes, we first identified 9-mer H-2K^{d}-restricted CD8 T cell epitopes in the HA2 domain by *in silico* analyses, followed by evaluating the immunodominance of these peptides in mice challenged with the virus. Of three peptides selected through *in silico* analysis, the universally conserved peptide, YYSTAASSL (B/HA2-190), possessed the highest predicted binding affinity to MHC Class I and was most effective in inducing IL-2 and TNF-α in mouse splenocytes. Importantly, the peptide demonstrated best capability of stimulating peptide-specific *ex-vivo* cytotoxicity against target cells. Taken together, this finding would be of value for assessment of cell-mediated immune responses elicited by vaccines based on the highly conserved HA2 stalk domain.

Keywords: influenza, epitope prediction, vaccine evaluation, MHC Class I

Introduction

Influenza viruses include the genera of A, B and C. Type A and B influenza viruses are generally associated with more severe disease, while type C virus is not thought to cause influenza in humans. Influenza B virus (IBV) causes 20-30% of all influenza cases on average and can be the dominant strain in a given flu season [1] [2] [3] [4] [5]. Although influenza A virus (IAV) is generally thought to be more virulent than IBV, it is not uncommon to find more severe IBV infection. For example, IBV infections were reported to be more severe than pandemic H1N1 infections [6] [7] [8]. Of particular concern is the increasing influenza B-related mortality rate among infants and children under the age of 10 [9]. During the 2010-2011 epidemic, 25% of all influenza cases were caused by IBV, and as high as 38% of all pediatric deaths worldwide were attributed to infection by IBV [5] [10] [11] [12]. It is also of note that during the non-epidemic season of a year, the death rate in infants and children hospitalized with IBV influenza is 1.1% compared to 0.4% with IAV infection [13]. Furthermore, interim reports of the 2017-18 flu season indicate that 46.8% of all reported cases worldwide were positive for influenza A whereas 53.2% were positive for influenza B with more severe symptoms [14]. These data indicate that efforts should be strengthened to prevent and contain IBV infections.

The most effective means against influenza is annual vaccination of susceptible populations. The current seasonal influenza vaccines are produced using the strains recommended by the World Health Organization (WHO) 6–8 months ahead of the targeted season. These vaccines typically contain two subtypes of IAV and one or two of IBV derived from the strains predicted to circulate in the upcoming year [15]. However, there are inherent disadvantages associated with the preparation of conventional influenza vaccines such as the

uncertainty of the actual circulating strains, the need for annual updating of the manufacturing process and preparation of reagents for vaccine lot release. Furthermore, mismatches between the strains selected for vaccine preparation and the circulating viruses can cause a marked reduction in the efficacy of seasonal influenza vaccines. Indeed, the mismatch has been observed for both IAV and IBV vaccines [4] [16] [17].

IBV is broadly classified into two genetic lineages, ie. Victoria and Yamagata; these two antigenically different groups of virus are known to co-circulate within the human population [16] [6] [9] [18]. Although the quadrivalent vaccines consist of one IBV strain from each lineage, there may still be a mismatch with the circulating strains [15]. In fact, vaccine effectiveness in the 2017-18 flu season in the United States was estimated to be only 42% against influenza B viruses [19]. All these problems concerning the influenza vaccines are largely due to one single biological property of the influenza virus itself, i.e., the frequent mutations of the virus surface proteins, particularly the hemagglutinin (HA) [20]. The mutations often take place in the HA1 subunit of the HA protein in both IAV and IBV, resulting in highly variable antigenicity of the HA protein whereas the other subunit, HA2, is highly conserved among all strains analyzed [21].

Viral infection or vaccination is well known to induce antibodies predominantly targeting the variable HA1 subunit (head) whereas the HA2 subunit (stalk) is not the primary target of neutralizing antibodies, given that the latter is largely shielded by the head [22] [23]. Moreover, while antibodies targeting the stalk of HA can be broadly protective since it is highly conserved [1] [24], the role of cell mediated immune responses targeting the stalk region is not well studied, particularly in response to IBV infection or vaccination. Clearly, it would be of great interest to delineate, in the stalk region, immunodominant T cell epitopes so they could be employed to evaluate next generation of vaccines such as the stalk-based

universal vaccines. In this study, we used *in silico* analyses to predict candidate epitopes in the HA2 stalk region of IBV and subsequently validated their immunodominance using H-2K^d-restricted mice.

Materials and Methods

Bioinformatics and statistical analyses

H-2K^d-restricted MHC class I binding predictions was performed using syfpeithi.de [25], NeTMHC3.4, and Immune Epitope Database (IEDB) Analysis Resource [26] [27] [28] [29] [30]. Class I immunogenicity was predicted using IEDB [31]. The selected peptides were synthesized with over 95% purity (New England Peptides, Cambridge MA). Influenza B hemagglutinin sequences from 3488 strains in the Victoria lineage and 4572 strains in the Yamagata lineage deposited in public domains (NCBI Influenza Virus Resource Database) were retrieved for multiple gene alignment. They were aligned using Geneious 7.0.6 software to determine the universality of the selected peptides. For statistical analyses, all comparisons were conducted using one-way ANOVA with Bonferroni post-test. They were performed using GraphPad Prism 5.

Cell lines, virus and mice

Madin-Darby canine kidney (MDCK) cells for virus plaque assay and P815 mouse mastocytoma (H-2d) cells for CTL assay were grown in DMEM (Gibco) supplemented with 10% FBS and penicillin-streptomycin. B/Victoria/2/87 virus preparations were generated as follows. Virus was grown in 10-day-old embryonated chicken eggs (Canadian Food Inspection Agency) for 3 days at 33°C. Eggs were cooled down overnight to 4°C. Allantoic

fluid was harvested and centrifuged at 2,000 rpm for 10 min at 4°C. The virus titer in the supernatant was determined on monolayers of MDCK cells [1].

Twelve- to fourteen-week-old female DBA.2 mice (Jackson Laboratories) were intranasally infected with $1.5x10^4$ PFU (10x LD_{50}) in 25µl per mouse. Mice were weighed on a daily basis. Weight loss of >25%, or a combination of unresolved dehydration, marked respiratory distress, muscular atrophy, erratic feeding behavior, and low mobility for 72 hours were set as the endpoint and the mice were euthanized.

Lung and tracheal viral titer

Lungs and trachea from DBA.2 mice were collected and snap-frozen 3 days post infection. The tissues were weighed, crushed with a pistil, and centrifuged at 8,000 x g for 2 min at 4°C. The supernatant was then filtered using a 0.45-micron syringe filter for lungs and 0.22-micron for trachea prior to determining the viral titer. Plaque assay was done using MDCK cells as previously described [32]. Briefly, MDCK cells were seeded at a density of $4.5x10^4$ cells/ml. Four days later, cells were washed with PBS and 0.5ml of serially diluted supernatant from homogenized tissue was added. After incubation for two hours at 37°C, 2 ml of a 1:1 mixture of 2x DMEM media with 4µg/ml TPCK-treated trypsin and 1.6% agarose was added. Crystal violet staining was used for counting plaques after incubating the plates for 4 days at 35°C.

Histology

Lungs from DBA.2 mice 3 days post infection were formalin-fixed for pathological analysis. Sections from multiple lung lobes from each animal were trimmed and embedded

in paraffin. Five-micron sections were cut and stained with Hematoxylin and Eosin (H&E) for lung lesion classification. For each lesion, a numeric scoring was used to indicate severity, where 0 indicates lesion is within normal limits, with 1 for a minimal degree of severity, 2 mild, 3 moderate, 4 marked and 5 severe [33]. Cell infiltration refers to infiltrates of the predominant inflammatory cells in the perivascular stroma [34]. Bronchiolitis refers to inflammation of the bronchioles, the intrapulmonary airways and the terminal bronchioles. With bronchiolar epithelial necrosis, affected dead cells are often sloughing and have pyknotic or karyorrhectic nuclei with variable inflammation. The combination category, necrosis/apoptosis, is employed when either or both of these processes are identified or if the diagnosis is uncertain.

CD8+ T cell intracellular cytokine staining

CD8+ T cell IFN-γ, TNF-α, and IL-2 responses were evaluated 3 days post infection as previously described [32] in DBA.2 mice. In brief, splenocytes were cultured in RPMI 1640 medium with 10% FBS in the presence of 10 μg/ml synthetic H-2K^{d} MHC class I–restricted peptides for *ex vivo* restimulation for 6 hours. Stimulated cells ($2x10^{6}$) were stained with a fixable viability dye (eBiosciences) for 30 min followed by a Fc block (eBiosciences) for 5 min and then a FITC–conjugated anti-mouse CD8a (clone 53-6.7; BD biosciences) for 30 min. Cells were then permeabilized with Cytofix/Cytoperm (BD biosciences) for 20 min and then stained with BV786–conjugated anti-mouse IFN-γ (clone XMG1.2; BD biosciences), PE-conjugated anti-mouse TNF-α (clone MP6-XT22; BD biosciences), and BV421–conjugated anti-mouse IL-2 (clone JES6-5H4; BD biosciences). Results for IFN-γ, TNF-α, and IL-2 were calculated as a percentage of CD8+ T cells corrected using a control

without peptide. A BD LSRII flow cytometer was used for data acquisition, and analysis was completed with Flow Jo, Version 10 (Tree Star, Ashland, OR). Unstained cells and single-stained compensation beads (BD Biosciences, Mississauga, ON) were used as controls for background fluorescence and false-positives because of fluorochrome bleeding.

Cytotoxic T lymphocyte (CTL) assay

CTL assay was conducted using lactate dehydrogenase release assay as previously described [32]. In brief, $2x10^7$ splenocytes from infected DBA.2 mice were collected 3 days post infection. They were restimulated *ex vivo* with 1 μg/ml peptide to generate effector CTLs. Five days later, cytotoxic activity was measured by lactate dehydrogenase release using peptide-pulsed P815 targets (H-2d). The percentage of cytotoxicity was calculated as (experimental release - effector spontaneous release - target spontaneous release)/ (maximum release - target spontaneous release) x 100% and corrected with no peptide controls.

Results and Discussion

H-2K^d-restricted epitope prediction in silico

The highly conserved HA2 subunit of Influenza B/Victoria/2/87 was subjected to *in silico* analyses using three different online MHC class I binding prediction programs, NeTMHC3.4, syfpeithi.de and IEDB Analysis Resource (Supp Table S1) [35]. A snapshot of the outputs from each program consisting of 9mer peptides is summarized in Supp Table S1 in descending order of MHC I binding affinity. All three programs predicted the same two peptides to have the highest binding affinity to H-2K^d-restricted MHC Class I, YYSTAASSL (B/HA2-190) and VYMVSRDNV (B/HA2-209). Some variation in the ordering based on

binding affinity was observed between prediction tools from the third position (Supp Table S1).

We also used IEDB Analysis Resource to determine the immunogenicity of given peptides [31] [35]. The peptides predicted to have high affinity were analyzed. The strongest binding peptides were predicted not to have the highest immunogenicity (Supp Table S2). Specifically, the peptide with the highest binding affinity, B/HA2-190, had a low immunogenicity score. Therefore, for analysis of universality, two peptides predicted to have the highest binding affinity, B/HA2-190 and B/HA2-209, and 2 peptides predicted to have the highest immunogenicity, TFNAGEFSL (B/HA2-156) and STQEAINKI (B/HA2-40), were selected.

Three of the predicted epitopes are well conserved in majority of influenza B strains in both lineages

To determine if the selected peptides were universally conserved, hemagglutinin sequence from 3488 influenza B strains from the Victoria lineage and 4572 strains from the Yamagata lineage were analyzed. We found that all amino acids in peptides B/HA2-190, B/HA2-40 and B/HA2-209 are conserved in over 98% of strains from both genetic lineages (Figure 1). However, in B/HA2-156, all except one amino acid are conserved in above 99% of the strains. The amino acid in the third position, asparagine (N), is conserved in 99.4% of the Yamagata strains but only conserved in 2.1% of the Victoria strains (Figure S1). Therefore, B/HA2-156 was not validated further in the *in vivo* model.

Confirming in vivo model for IBV infection

As the *in silico* algorithms can vary in their accuracy and the degree to which the predictions translate to biological systems, it is necessary to validate the predicted peptides for their immunological activities by *in vitro* or *in vivo* experiments [35]. To this end, a previously established *in vivo* model of IBV infection was used [36]. 10 to 12-week-old DBA.2 mice were infected with $1.5x10^4$ PFU of B/Victoria/2/87 in 25µl per mouse corresponding to 10x LD_{50} as determined by Pica et al. [36]. Survival was observed for 14 days post intranasal infection (Figure 2A). After Day 6, mice were euthanized following 25% weight loss, which was set as one of the endpoints. The survival rate stabilized at 40% on Day 9 and the surviving mice began regaining the weight lost.

Three days post-infection, lungs and trachea were collected for determination of viral titer. Approximately 10^6 PFU per gram was detected in both tissues (Figure 2B). Lungs were also harvested at Day 3 for pathological analysis. They were H&E stained to determine the extent of virus-induced pulmonary lesion based on the degree of lymphoid and plasma cell infiltration, bronchiolitis, and bronchiolar epithelial lesions of necrosis and apoptosis. These parameters were scored and showed a high degree of tissue damage and cell infiltration accompanying the high viral titer in the lungs (Figure 2C). Representative images of the profound disease observed in the lungs of infected mice compared to naïve lungs are shown in Figure 2D. Overall, these results indicate that DBA.2 mice are susceptible to infection with B/Victoria/2/87 and display a wide range of symptoms that can be observed starting at Day 3 post-infection.

Validation of CD8 immunodominant epitopes in vivo following IBV infection

Using this established *in vivo* model, we validated the biological relevance of the three chosen predicted peptides: B/HA2-190, B/HA2-40 and B/HA2-209. For validation, the immunodominance was determined by assessing peptide-specific CD8 cytokine profile and cytotoxic T lymphocyte (CTL) activity following a B/Victoria/2/87 infection. To this end, DBA.2 mice were given $1.5x10^4$ PFU intranasally [36]. Three days post-infection, splenocytes were isolated from the infected mice and stimulated with the selected peptides along with a no peptide control. Following *ex vivo* stimulation, intracellular cytokine expression profile in CD8+ T cells was analyzed by flow cytometry.

Expression levels of IFN-γ in CD8+ cells were high but not significantly different compared to the no peptide control or between the three peptides (data not shown), which might be due to high background of IFN-γ expression as a result of high dose of IBV used for infection. However, the expression levels of IL-2 and TNF-α in CD8+ T cells were significantly higher when stimulated with B/HA2-190 compared to B/HA2-40 and B/HA2-209 (Figure 3A and 3B). This observation of increased IL-2 level as a result of B/HA2-190 peptide stimulation indicates that B/HA2-190 is an important viral epitope because IL-2 promotes the differentiation of naïve CD8+ T cells into effector and memory T cells. Specifically, IL-2 activates cytotoxic T lymphocyte differentiation by inducing eomesodermin and perforin expression while inhibiting expression of Bcl16 and IL-7Rα, thereby facilitating long-lived memory cells and secondary expansion of memory CD8+ T cells [37] [38] [39]. Moreover, B/HA2-190 better stimulates TNF-α expression than the other two selected peptides, further supporting the immunodominance of this peptide, given that TNF-α is known to play an important role in host defense against pathogens [40]. Specifically, treatment with TNF-α has been shown to inhibit virus replication during an

influenza infection, and such inhibitory effects might even be stronger than that of interferon α/γ for certain virus strains, suggesting that TNF-α may be the first line of defense against influenza [41] [42].

To further investigate the abilities of the selected peptides in inducing functional cytotoxic T cells, CTL assay was conducted with P815 target cells, where the ability of the stimulated splenocytes to induce antigenic peptide-specific P815 killing was determined. As shown in Figure 4, stimulation with B/HA2-190 resulted in significantly higher cytotoxic activity than B/HA2-40 and B/HA2-209. Taken together, these results indicate that B/HA2-190 is a potent immunodominant epitope involved in IBV specific cell-mediated immune response.

In short, the HA2 subunit of influenza virus is a potential candidate universal influenza vaccine, given that the stalk region is highly conserved. While many studies have been carried out to determine the interaction between the stalk and antibodies, little is known with regards to the immunodominant epitopes involved in cell mediated immune responses. This work is focused on the identification of critical epitopes triggering type I immune responses. The *in silico* prediction of the peptide epitopes were further validated using DBA.2 mice which are susceptible to IBV infection. It is of note that DBA.2 mice and BALB/c mice have the same MHC allele ($H\text{-}2K^d$); CD8 epitopes identified in DBA.2 mice can also be employed to study IBV infection of BALB/c. The peptide epitope we have identified here is conserved in over 98% of IBV strains reported so far. It could be of value for the assessment of universal vaccines based on the stalk of the viral HA proteins, particularly for cell-mediated immune responses.

Acknowledgements

We thank Dr. Jessie Lavoie and Dr. Michael Johnston for their critical review of the manuscript. We are indebted to Jun Gao (Health Canada) for statistical advice. The authors declare no conflict of interest. This work is funded by the Canadian Regulatory Strategy for Biotechnology:(XL), the Ministry of Science and Technology, PR China.

Tables and Figures

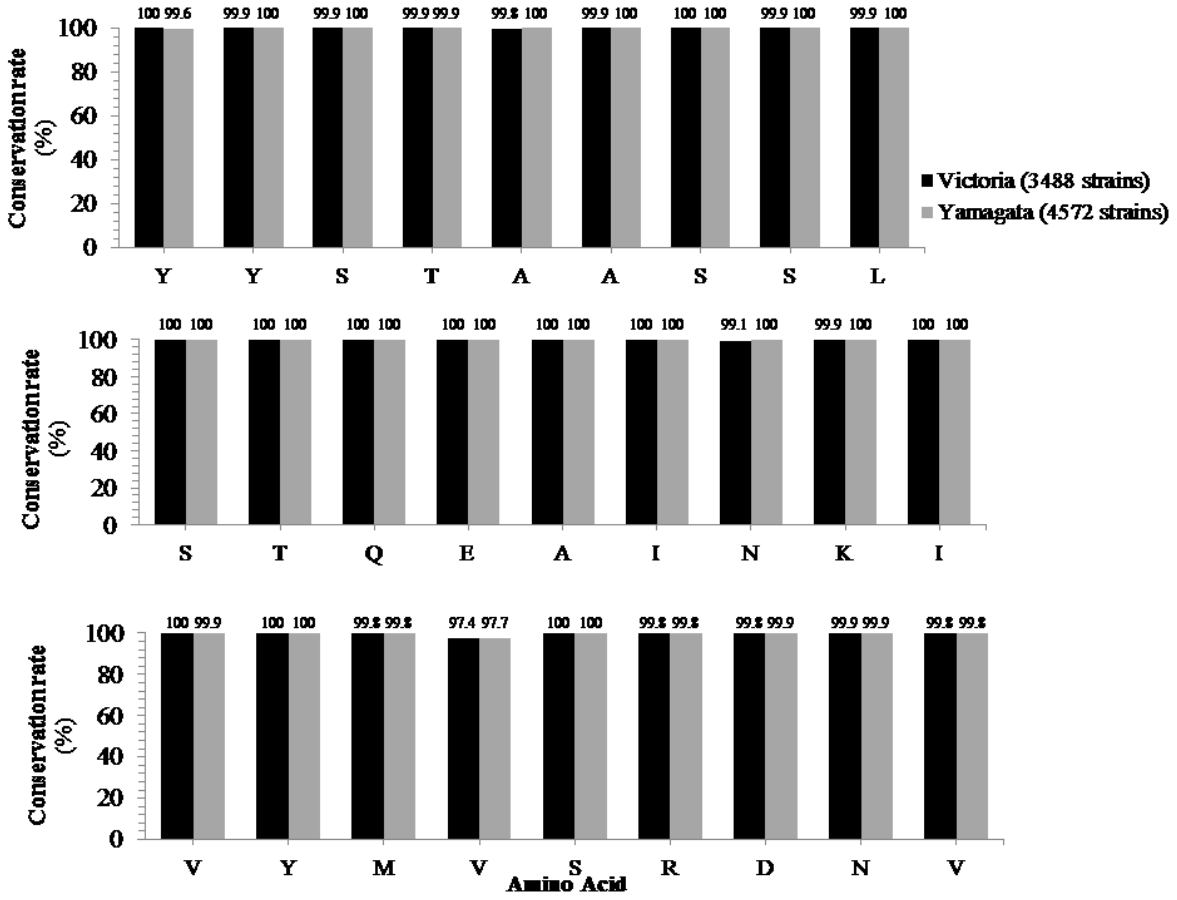

Figure 1: Conservation rate of each amino acid in multiple Influenza B strains. Sequences from 3488 strains in the Victoria lineage and 4572 strains in the Yamagata lineage in public domains (NCBI Influenza Virus Resource Database) were retrieved and analyzed using multiple alignment to determine the conservation rate of each amino acid in each peptide used.

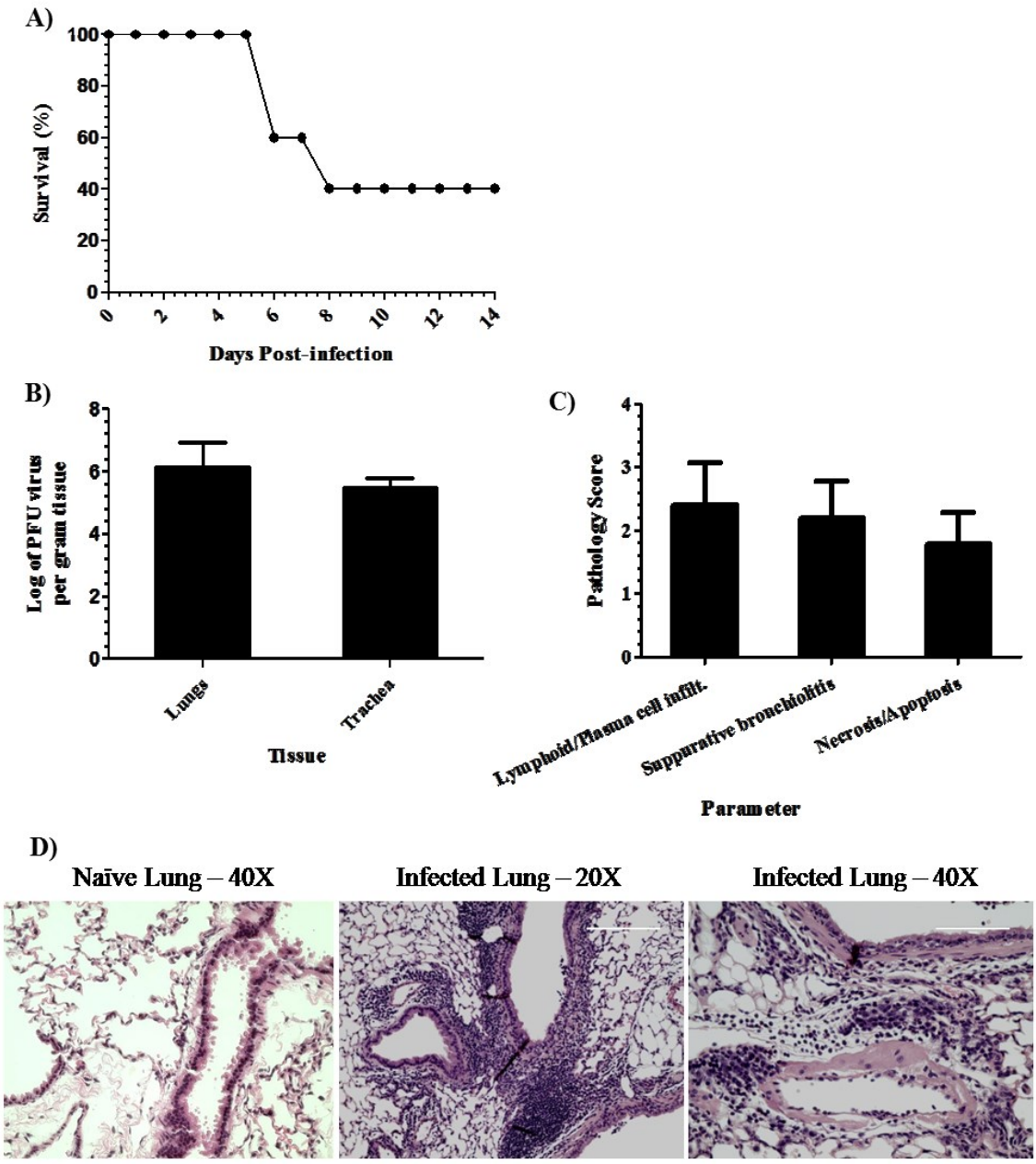

Figure 2: Confirming the *in vivo* model for Influenza B infection. 10 to 12-week-old DBA.2 mice were intranasally infected with $1.5x10^4$ PFU in 25µL per mouse**. A)** Survival of the mice was observed for 14 days following infection (n=5). Weight loss of 25% was set as the endpoint. **B)** Viral titre determined using plaque assay of lung and tracheal homogenates 3 days post infection (n=5) **C)** Pathological scoring of H&E stained slides of lung tissue. Perivascular infiltration of lymphoid/plasma cell, suppurative bronchiolitis, and bronchiolar epithelial lesions of necrosis/apoptosis was assessed on Day 3 following infection (n=5). **D)** Representative images of H&E stained infected lungs 3 days post infection. Data shown is mean ± s.e.m; PFU: Plaque Forming Unit

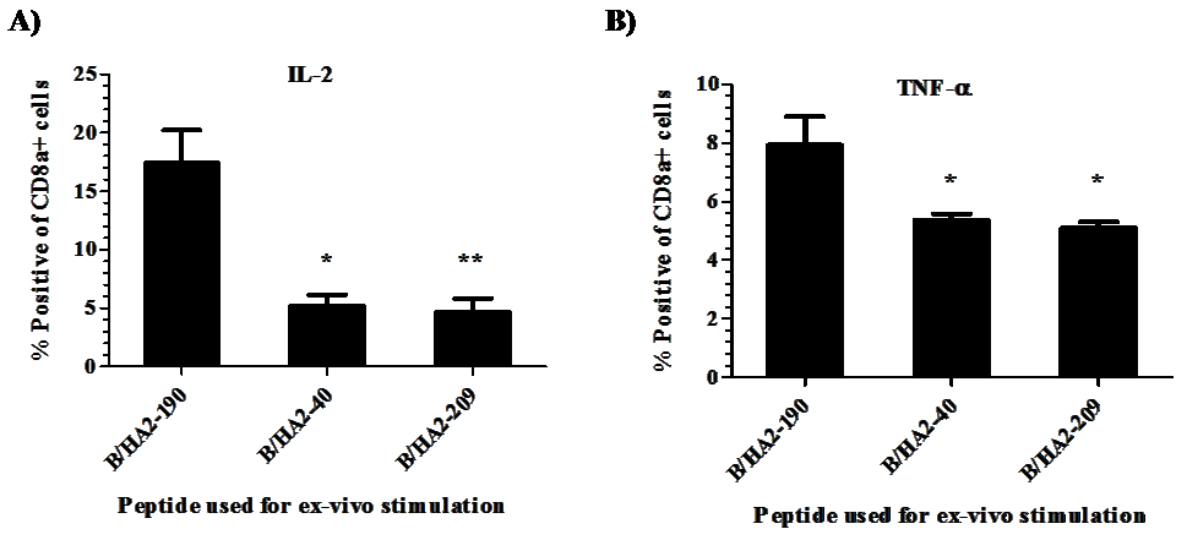

Figure 3: Cytokine expression induced by predicted epitopes. Splenocytes were isolated from DBA.2 mice 3 days post infection. Following stimulation with each peptide for 6 hours, the cells were stained with a viability dye, then a CD8a antibody, permeabilized and further stained with cytokine antibodies for analysis by flow cytometry. Significant differences were observed in expression of IL-2 (**A**) and TNF-α (**B**). Data shown is mean ± s.e.m; n=3 representative of 2 independent experiments; all groups compared to B/HA2-190; *$p < 0.05$, **$p<0.01$ (One way ANOVA with Bonferroni post-test); B/HA2-190: YYSTAASSL; B/HA2-40: STQEAINKI; B/HA2-209: VYMVSRDNV

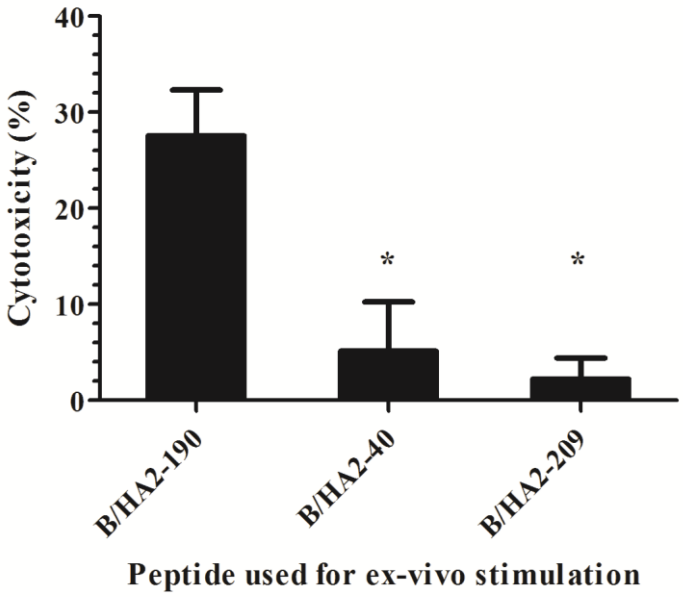

Figure 4: Cytotoxic T lymphocytes induced by predicted epitopes. Splenocytes were isolated from DBA.2 mice 3 days post infection. Following stimulation with each peptide for 5 days, splenocytes were incubated with P815 target cells at a 25:1 (effector: target) ratio. Percent peptide-specific cytotoxicity was determined using a LDH assay. Data shown is mean ± s.e.m; n=3 representative of 2 independent experiments; all groups compared to B/HA2-190; *$p < 0.05$ (One way ANOVA with Bonferroni post-test); B/HA2-190: YYSTAASSL; B/HA2-40: STQEAINKI; B/HA2-209: VYMVSRDNV

Supplementary Table S1: *In silico* prediction of H-2K^{d}-restricted MHC Class I peptide in HA2 subunit of B/Victoria/2/87. MHC I binding predictions from three online tools summarized in descending order of binding affinity. The HA2 portion of B/Victoria/2/87 was used as the input. The peptides chosen for further validation are highlighted in yellow.

B/Victoria/2/87 hemagglutinin Genbank Accession Number: M58428

Input sequence: HA2 stem domain

NeTMHC 3.4 http://www.cbs.dtu.dk/services/NetMHC-3.4/		Epitope prediction http://www.syfpeithi.de/bin/MHCServer.dll/EpitopePrediction.htm		IEDB Analysis Resource http://tools.iedb.org/mhci/	
Position	**Peptide**	**Position**	**Peptide**	**Position**	**Peptide**
189	YYSTAASSL	190	YYSTAASSL	190	YYSTAASSL
208	VYMVSRDNV	209	VYMVSRDNV	209	VYMVSRDNV
155	TFNAGEFSL	156	TFNAGEFSL	50	KNLNSLSEL
1	FFGAIAGFL	50	KNLNSLSEL	192	STAASSLAV
46	KITKNLNSL	162	FSLPTFDSL	196	SSLAVTLMI
49	KNLNSLSEL	2	FFGAIAGFL	189	LYYSTAASS
122	KKMLGPSAV	94	SQIELAVLL	47	KITKNLNSL
140	KHKCNQTCL	125	MLGPSAVEI	162	FSLPTFDSL
168	SLNITAASL	180	DGLDNHTIL	123	KKMLGPSAV
188	LYYSTAASS	196	SSLAVTLMI	213	SRDNVSCSI
195	SSLAVTLMI	40	STQEAINKI	144	CNQTCLDRI
98	AVLLSNEGI	141	KHKCNQTCL	156	TFNAGEFSL
39	STQEAINKI	166	TFDSLNITA	40	STQEAINKI
161	FSLPTFDSL	169	SLNITAASL	26	SHGAHGVAV
99	VLLSNEGII	189	LYYSTAASS	62	NLQRLSGAM
36	DLKSTQEAI	30	HGVAVAADL	94	SQIELAVLL
113	HLLALERKL	90	DTISSQIEL	99	AVLLSNEGI
212	SRDNVSCSI	213	SRDNVSCSI	2	FFGAIAGFL
68	AMDELHNEI	37	DLKSTQEAI	169	SLNITAASL
191	STAASSLAV	65	RLSGAMDEL	88	RADTISSQI
143	CNQTCLDRI	99	AVLLSNEGI	191	YSTAASSLA

Supplementary Table S2: *In silico* prediction of immunogenecity. The immunogenicity of the peptides predicted to have the highest MHC I binding affinity was determined using IEDB Class I immunogenicity analysis. The results are listed in descending order of predicted immunogenicity. The peptides chosen for further validation are highlighted in yellow.

IEDB Analysis Resource http://tools.iedb.org/immunogenicity/	
Peptide	**Score**
TFNAGEFSL	0.13366
STQEAINKI	0.05697
VYMVSRDNV	0.0482
CNQTCLDRI	0.03998
FSLPTFDSL	0.0175
SSLAVTLMI	-0.03965
STAASSLAV	-0.09016
KNLNSLSEL	-0.10167
LYYSTAASS	-0.19448
KKMLGPSAV	-0.19536
YYSTAASSL	-0.21409
SRDNVSCSI	-0.2972
KITKNLNSL	-0.31696

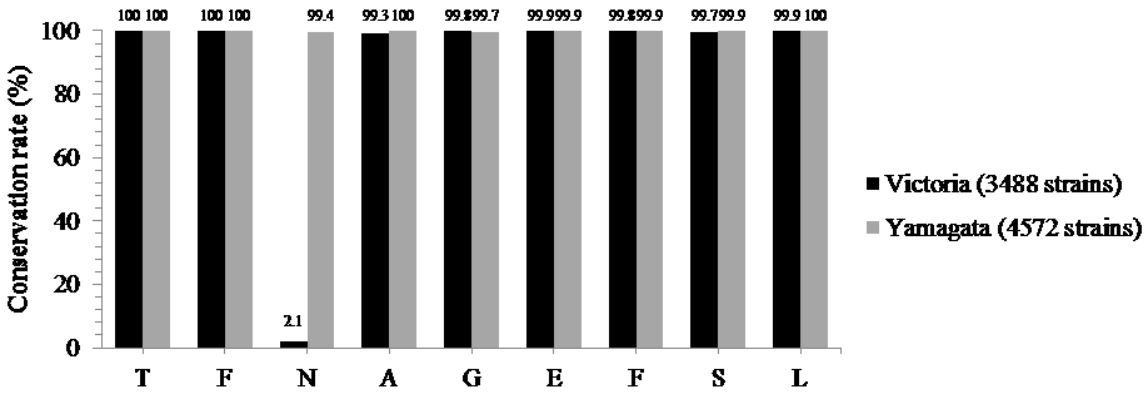

Supplementary Figure S1: Conservation rate of each amino acid in multiple Influenza B strains. Sequences from 3488 strains in the Victoria lineage and 4572 strains in the Yamagata lineage deposited in public domains (NCBI Influenza Virus Resource Database) were retrieved and analyzed using multiple alignment to determine the conservation rate of each amino acid. 97.9% of the strains in the Victoria lineage have a D in the third position.

References

[1] M. Ermler, E. Kirkpatrick , W. Sun, R. Hai, F. Amanat, V. Chromikova, P. Palese and F. Krammer, "Chimeric hemagglutinin constructs induce braod protection against influenza B virus challenge in mouse model," *J Virol,* vol. 91, no. 12, pp. 1-14, 2017.

[2] N. Molinari, I. Ortega-Sanchez, M. Messonier, W. Thompson, P. Wortley, E. Weintraub and C. Bridges, "The annual impact of seasonal influenza in the US: measuring disease burden and costs," *Vaccine,* vol. 25, pp. 5086-5096, 2007.

[3] F. Dijkstra, G. Donker, B. Wilbrink, A. Van Gageldonk-Lafeber and M. Van Der Sande, "Long time trends in influenza-like illness and associated determinants in The Netherlands," *Epidemol Infect,* vol. 137, pp. 473-479, 2009.

[4] T. Heikkinen, N. Ikonen and T. Ziegler, "Impact of influenza B lineage-level mismatch between trivalent seasonal influenza vaccines and circulating viruses, 1999-2012," *Clin Infect Dis,* vol. 59, pp. 1519-1524, 2014.

[5] E. Brottet, D. Vandroux, B. Gauzere, E. Antok, M. Jaffar-Bandjee , A. Michault and L. Filleul, "Influenza season in Reunion dominated by influenza B virus circulation asociated with numerous cases of severe disease, France 2014," *Euro Surveill,* vol. 19, no. 39, 2014.

[6] M. Koutsakos, T. Nguyen, W. Barclay and K. Kedzierska, "Knowns and unknowns of influenza B viruses," *Future Microbiol,* vol. 11, pp. 119-135, 2016.

[7] Y. Pan, Y. Zhang, P. Yang, H. Qian, W. Shi, S. Wu, S. Cui, D. Zhang and Q. Wang, "Epidemiological and phylogenetic characteristics of influenza B infection in severe acute respiratory infection cases in Beijing, 2014-2015," *Medicine,* vol. 94, 2015.

[8] W. Thompson, M. Moore, E. Weintraub, P. Cheng, X. Jin, C. Bridges, J. Bresee and D. Shay, "Estimating influenza-associated deaths in the United States," *Am J Public Health,* vol. 99, no. Suppl 2, pp. S225-S230, 2009.

[9] L. Jennings, Q. S. Huang, I. Barr, P.-I. Lee, W. J. Kim, P. Buchy, M. Sanicas, B. A. Mungall and J. Chen, "Literature review of the epidemiology of influenza B disease in 15 countries in the Asia-Pacific region," *Influenza Other Respi Viruses,* pp. 1-29, 2017.

[10] J. McCullers and F. Hayden, "Fatal influenza B infecitons: time to reexamine influenza research priorities," *J Infect Dis,* vol. 205, pp. 870-872, 2012.

[11] P. Chan, M. Chan, J. Cheung, N. Lee, T. Leung, A. Yeung, M. Wong, K. Ngai, E. Nelson and D. Hui, "Influenza B lineage circulation and hospitalization rates in the subtropical city, Hong Kong," *Clin Infect Dis,* vol. 56, pp. 677-684, 2013.

[12] H. Kosasih, Roselinda, Nurhayati, A. Klimov, X. Xiyan, S. Lindstrom, F. Mahoney, C. Beckett, T. Burgess, P. Blair, T. Uyeki and E. Sedyaningsih, "Surveillance of influenza in Indonesia, 2033-2007," *Influenza Other Respir Viruses,* vol. 7, pp. 312-320, 2013.

[13] D. Tran, W. Vaudry, D. Morre, J. Bettinger, S. Halperin, D. Scheifele, T. Jadvji, T. Lee, T. Mersereau and Canadian Immunization Monitoring Program Active, "Hospitalization for infliuenza A versus B," *Peadiatrics,* vol. 138, 2016.

[14] WHO, "Influenza Update N 312," WHO, 2018.

[15] M. Schotsaert and A. Garcia-Sastre, "Inactivated influenza virus vaccines: the future of TIV and QIV," *Curr Opin Virol,* vol. 23, pp. 102-106, 2017.

[16] C. Van de Sandt, R. Bodewes, G. Rimmelzwaan and R. de Vries, "Influenza B viruses: not to be discounted," *Future Microbiol,* vol. 10, pp. 1447-1465, 2015.

[17] M. Tafalla, M. Buijssen, R. Geets and M. Vonk Noordegraaf-Schouten, "A comprehensive review of the epidemiology and disease burden of influenza B in 9 European countries," *Hum Vaccin Immunother,* vol. 12, pp. 993-1002, 2016.

[18] P. Rota, T. Wallis, M. Harmon, J. Rota, A. Kendal and K. Nerome, "Cocirculation of two distinct evolutionary lineages of influenza type B virus since 1983," *Virology,* vol. 175, pp. 59-68, 1990.

[19] B. Flannery, J. Chung, E. Belongia and et al, "Interim estimates of 2017-18 seasonal influenza vaccine effectiveness-United States, February 2018," *Morb Mortal Wkly Rep,* vol. 67, pp. 180-185, 2018.

[20] C. Gerdil, "The annual production cycle for influenza vaccine," *Vaccine,* vol. 21, pp. 1776-1779, 2003.

[21] A. Hashem, T. Doyle, G. Van Domselaar, A. Farnsworth, C. Li, J. Wang, R. He and X. Li, "Recent developments in bioinformatics analyses of influenza A virus surface glycoproteins and their biological relevance," *Curr Bioinformatics,* vol. 6, no. 4, pp. 415-426, 2011.

[22] S. Andrews, Y. Huang, K. Kaur, L. Popova, I. Ho, N. Pauli, C. Henry Dunand, W. Taylor, S. Lim, M. Huang, X. Qu, J. Lee, M. Salgado-Ferrer, F. Krammer, P. Palese, J. Wrammert, R. Ahmed and P. Wilson, "Immune history profoundly affects broadly protective B cell responses to influenza," *Sci Transl Med,* vol. 7, 2015.

[23] R. Nachbagauer, A. Choi, R. Izikson, M. Cox, P. Palese and F. Krammer, "Age dependence and isotype specificity of influenza virus hemagglutinin stalk-reactive antibodies in humans," *mBio,* vol. 7, 2016.

[24] F. Krammer and P. Palese, "Influenza virus hemagglutinin stalk-based antibodies and vaccines," *Curr Opin Virol,* vol. 3, pp. 521-530, 2013.

[25] H.-G. Rammensee, J. Bachmann, N. N. Emmerich, O. A. Bachor and S. Stevanovic, "SYFPEITHI: database for MHC ligands and peptide motifs," *Immunogenetics,* vol. 50, pp. 213-219, 1999.

[26] Y. Kim, J. Ponomarenko, Z. Zhu, D. Tamang, P. Wang, J. Greenbaum, C. Lundegaard, A. Sette, O. Lund, P. Bourne, M. Nielsen and B. Peters, "Immune epitope database analysis reseource," *NAR,* 2012.

[27] M. Nielsen, C. Lundegaard, P. Worning, S. Lauemoller, K. Lamberth, S. Buus, S. Brunak and O. Lund, "Reliable prediction of T-cell epitopes using neural networks with novel sequence representations," *Protein Sci,* vol. 12, pp. 1007-1017, 2003.

[28] C. Lundegaard, K. Lamberth, M. Harndahl, S. Buus, O. Lund and M. Nielsen, "NetMHC-3.0: Accurate web accessible predictions of Human, Mouse, and Monkey MHC class I affinities for peptides of length 8-11," *NAR,* vol. 36, pp. W509-512, 2008.

[29] B. Peters and A. Sette, "Generating quantitative models describing the sequence specificity of biological processes with the stabilized matrix method," *BMC Bioinformatics,* vol. 6, no. 132, 2005.

[30] J. Sidney, E. Assarsson, C. Moore, S. Ngo, C. Pinilla, A. Sette and B. Peters, "Quantitative peptide binding motifs for 19 human and mouse MHC class I molecules derived using positional scanning combinatorial peptide libraries," *Immunome Res,* vol. 4, no. 2, 2008.

[31] J. Calis, M. Maybeno, J. Greenbaum, D. Weiskopf, A. De Silva, A. Sette, C. Kesmir and B. Peters, "Properties of MHC class I presented peptides that enhance immunogenicity," *PloS Comp Biol,* vol. 8, no. 1, p. 361, 2013.

[32] A. Hashem, C. Gravel, Z. Chen, Y. Yi, M. Tocchi, B. Jaentschke, X. Fan, C. Li, M. Rosu-Myles, A. Pereboev, R. He, J. Wang and X. Li, "CD40 ligand preferentially modulates immune response and enhances preotection against influenza virus," *J Immunol,* vol. 193, pp. 722-734, 2014.

[33] R. Renne, A. Brix, J. Harkema, R. Herbert, B. Kittel, D. Lewis, T. March, K. Nagano, M. Pino, S. Rittinghausen, M. Rosenbruch, P. Tellier and T. Wohrman, "Proliferative and non-proliferative lesions of the rat and mouse respiratory tract," *Toxicologic Pathology,* vol. 37, pp. 5S-73S, 2009.

[34] B. Berridge, V. Mowat, H. Nagai, A. Nyska, Y. Okazaki, P. Clements, M. Rinke, P. Snyder, M. Boyle and M. Wells, "Non-proliferative and proliferative lesions of the cardiovascular system of the rat and mouse," *J Toxicol Pathol,* vol. 29, no. 3 Supp, pp. 1S-47S, 2016.

[35] C. Lundegaard, O. Lund, S. Buus and M. Nielsen, "Major histocompatibility complex class I binding predictions as a tool in epitope discovery," *Immunology,* vol. 130, pp. 309-318, 2010.

[36] N. Pica, A. Iyer, I. Ramos, N. M. Bouvier, A. Fernandez-Sesma, A. Garcia-Sastre, A. C. Lowen, P. Palese and J. Steel, "The DBA.2 mouse is susceptible to disease following infection with a broad, but limited, range of influenza A and B viruses," *J Virol,* vol. 85, no. 23, pp. 12825-12-829, 2011.

[37] V. Kalia, S. Sarkar, S. Subramaniam, W. Haining, K. Smith and R. Ahmed, "Prolonged interleukin-2Ralpha expression on virus-specific CD8+ T cells favors terminal-effector differentiation in vivo," *Immunity,* vol. 32, pp. 91-103, 2010.

[38] M. Pipkin, J. Sacks, F. Cruz-Guilloty, M. Lichtenheld, M. Bevan and A. Rao, "Interleukin-2 and inflammation induce distinct transcriptional programs that promote the differentiation of effector cytolytic T cells," *Immunity,* vol. 32, pp. 79-90, 2010.

[39] M. Williams, A. Tyznik and M. Bevan, "Interleukin-2 signals during priming are required for secondary expansion of CD8+ memory T cells," *Nature,* vol. 441, pp. 890-893, 2006.

[40] A. Abbas, A. Lichtman and J. Pober, in *Cellular and molecular immunology*, 4 ed., Philadelphia, PA, W. B. Saunders Company, 1991, pp. 235-269.

[41] S. H. Seo and R. G. Webster, "Tumor necrosis factor alpha exerts powerful anti-influenza virus effects in lung epithelial cells," *J Virol,* vol. 76, no. 3, pp. 1071-1076, 2002.

[42] M. Shale, M. Czub, G. G. Kaplan, R. Panaccione and S. Ghosh, "Anti-tumour necrosis factor therapy and influenza: keeping it in perspective," *Therapeutic advances in gastroenterology,* vol. 3, no. 3, pp. 173-177, 2010.

Collaborators' Contributions

- Marybeth Creskey performed the Mass spectrometry analysis and protein identification (Chapter 3) in the laboratory of Dr. Terry Cyr (Biologics Directorate, Health Products Food Branch, Health Canada, Ottawa, ON, Canada)
- Bozena Jaentschke, Caroline Gravel, Marsha Russell and Louise Larocque helped with the animal experiments
- Michelle Lemieux helped perform all the sequencing of the plasmids generated
- Emily Dupuis from Health Canada (Ottawa, ON, Canada) and Emily Chomyshyn from BD Biosciences helped design the flow cytometry antibody panels
- Dr. Don Caldwell, veterinary pathologist at Health Canada, conducted expert analyses of the lung tissues. These observations were also confirmed by Dr. Wangxue Chen at Human Therapeutics Portfolio, National Research Council of Canada, Ottawa, ON, Canada
- Primers were synthesized by Bio S&T (Montreal, QC, Canada)

Education

MSc/PhD	January 2015 – present (Transferred from Masters to PhD in March 2016) Microbiology and Immunology, Faculty of Medicine, University of Ottawa, Ontario, Canada Research Supervisor: Dr. Sean Li, Centre for Biologics Evaluation, Health Canada Thesis Title: Towards better understanding of Respiratory Syncytial Virus (RSV) vaccine-induced enhanced disease
BSc	2009 – 2014 Honours Bachelor of Science with specialization in Biochemistry Graduated *Magna Cum Lade* University of Ottawa, Ontario, Canada
BASc	2009 – 2014 Bachelor of Applied Science in Chemical Engineering Graduated *Magna Cum Lade* University of Ottawa, Ontario, Canada

Work Experience

September 2014 – December 2014
Chemical Engineering Thesis, University of Ottawa, Ottawa, Ontario, Canada
- Working under the supervision of Dr. Xudong Cao on micro-detection of bacterial cells using microfluidic devices

May 2014 – August 2014
Research Assistant, Health Canada – Centre for Vaccine Evaluation, Ottawa, Ontario, Canada
- Working with the H7N9 influenza vaccine
- Finding various applications for the Uni-H7 monoclonal antibody by utilizing its specificity to the H7 hemagglutinin on influenza viruses

August 2013 – April 2014
Biochemistry Honours Project, Health Canada – Centre for Vaccine Evaluation, Ottawa, Ontario
- Working on a different potency assays for the MMRV live-virus vaccine
- Conducting research to find a cell line that can stably grow the quadrivalent form of the vaccine (MMRV)

January 2013 – April 2013
Research Assistant, CFIA Centre of Expertise for Rabies, Ottawa, Ontario, Canada
- Worked in a bio-containment Level 3 lab under minimal supervision
- Assisted in determining the potency of the ONRAB wildlife rabies vaccine baits in the field
- Conducted a study to determine the rabies virus distribution in various big brown bat tissues
- Repeated a virus typing study done in Nigeria on local rabies-infected dogs to confirm their results

May 2012 - August 2012
Biology Research Assistant, Spartan Bioscience Inc., Ottawa, Ontario, Canada
- Worked in the laboratory at the Biology Department under minimal supervision
- Developed an external control procedure for the Food and Drug Administration (FDA) approval of the point-of care DNA testing system designed by the company

July 2011 - August 2011
Biology Research Assistant, University of Ottawa, Ottawa, Ontario, Canada
- Worked in a laboratory at the Biology Department under the supervision of Dr. Douglas Johnson
- Project involved identifying molecular markers in various grains
- Worked on sequencing various *Triticum* species using PCR, gel electrophoresis, and plasmid
preparation and assembled the resulting sequence

Skills

Molecular Biology
Cloning
Sequencing
Protein Expression and Purification
SDS-PAGE, Western Blotting and Slot Blotting
DNA and RNA isolation
PCR, RT-PCR, Real-time PCR and gel electrophoresis

Immunology
ELISA
Multiplex Cytokines Analysis and Flow Cytometry
Antibody Designing
Virus Neutralization
ADCC
CTL assays
Separation of Blood Components
Immunoblotting, Immunohistochimstry and Immunofluorescence
Tissue Block Cutting

Virology
Cell Culture Maintenance and Preservation
Virus Isolation, Amplification, Purification and Titration
Inoculation
Recombinant Adenovirus Generation
Vaccines Testing
Vaccine Potency Assays
Working with Level 2 and Level 3 Pathogens

General Skills
Working in BSL-2 and BSL-3 Facilities
Planning, Organizing, Executing and Analyzing data from Animal Studies Involving Mice

Chemistry
Titrations, Distillations, Extractions and Purifications

Science Softwares/ Programming Languages
NCBI, BLAST and ExPasy
Pymol
Alphaview and ImageLab
FlowJo
Immune epitope databases to design MHC I and II immunodominant peptides
CombiStats and GraphPad Prism for statistical analysis
Completed an introductory course in engineering computation on C, Visual Basic and Java

Honors and Grants Awarded

Sep 2016 – Aug 2018	Ontario Graduate Scholarship (OGS) of $15,000
2015 – 2016	Canadian Institutes of Health Research (CIHR) Masters Award of $17,500
Sep 2015 – Apr 2019	University of Ottawa Excellence Scholarship for Graduate students of $6000
2009 – 2014	University of Ottawa's Admission Scholarship of $20,000 total
2009 – 2013	Queen Elizabeth II Aiming for the Top Scholarship of $3500 per year
May 2012 – August 2012	NSERC Undergraduate Student Research Award (USRA) of $4500
2010-2011, 2012-2014	Dean's Honour List

Students Supervised

2015 Vivek Parekh; 3rd Year Undergraduate Honors Student, University of Ottawa, Ontario, Canada

2016 – 2018 Amparo Duran; MSc Student, University of Ottawa, Ontario, Canada

Publications

Papers Published in Refereed Journals:

1. **Muralidharan A**, Russell M, Larocque L, Gravel C, Li C, Chen W, Cyr T, Lavoie JR, Farnsworth A, Rosu-Myles M, Wang L, Li X. Targeting CD40 enhances antibody- and CD8-mediated protection against respiratory syncytial virus infection. ***Sci Rep,*** 2018 Nov 9; 8(1).

2. Russell MS, **Muralidharan A**, Larocque L, Cao J, Deschambault Y, Varga J, Thulasi Raman SN, Li X. Identification and characterisation of the CD40-ligand of *Sigmodon hispidus*. ***PLoS One,*** 2018 Jul 27; 13(7).

3. **Muralidharan A**, Gravel C, Duran A, Larocque L, Li C, Zetner A, Van Domselaar G, Wang L, Li X. Identification of immunodominant CD8 epitope in the stalk domain of influenza B viral hemagglutinin. ***Biochem Biophys Res Commun,*** 2018 Jul 12; 502(2):226-231.

4. **Muralidharan A**, Li C, Wang L, Li X. Immunopathogenesis associated with formaldehyde-inactivated RSV vaccine in preclinical and clinical studies. ***Expert Rev Vaccines,*** 2017 Apr; 16(4):351-360.

5. Gravel C, Elmgren C, **Muralidharan A**, Hashem AM, Jaentschke B, Xu K, Widdison J, Arnold K, Farnsworth A, Rinfret A, Van Domselaar G, Wang J, Li C, Li X. Development and applications of universal H7 subtype-specific antibodies for the analysis of influenza H7N9 vaccines. ***Vaccine,*** 2015 Feb 25; 33(9):1129-34.

Submitted Manuscripts:

1. Marsha S Russell, Marybeth Creskey, **Abenaya Muralidharan**, Changgui Li, Jun Gao, Wangxue Chen, Louise Larocque, Jessie R Lavoie, Aaron Farnsworth, Michael Rosu-Myles, Carole L Yauk, Jingxin Cao, Gary Van Domselaar, Terry Cyr, Sean (Xuguang) Li. Unveiling integrated functional pathways leading to enhanced respiratory disease associated with inactivated respiratory syncytial viral vaccine. Submitted to ***Frontiers in Immunology***.

2. **Abenaya Muralidharan**, Louise Larocque, Marsha Russell, Marybeth Creskey, Changgui Li, Wangxue Chen, Gary Van Domselaar, Terry Cyr, Lisheng Wang, Xuguang Li. PD-1 of Sigmodon hispidus: Gene identification, characterization and expression in

inactivated RSV vaccine-induced enhanced respiratory disease. Submitted to ***Scientific Reports***.

3. **Abenaya Muralidharan**, Marsha S. Russell, Louise Larocque, Caroline Gravel, Simon Sauvé, Ze Chen, Changgui Li, Wangxue Chen, Terry Cyr, Michael Rosu-Myles, Lisheng Wang, Xuguang Li. Chitosan enhances inactivated vaccine elicited protection against respiratory syncytial virus. Submitted to ***Vaccine.***

Conferences

Accepted Abstracts:

1. **Muralidharan A**, Russell M, Larocque L, Gravel C, Li C, Chen W, Cyr T, Lavoie JR, Farnsworth A, Rosu-Myles M, Wang L, Li X. "Targeting CD40 Prevents Vaccine-Induced Enhanced Respiratory Disease Following RSV Infection". Health Canada Science Forum, Ottawa, Ontario, Canada, February 2017; ***Oral and Poster Presentation***.

2. Marsha S Russell, Marybeth Creskey, **Abenaya Muralidharan**, Changgui Li, Jun Gao, Wangxue Chen, Louise Larocque, Jessie R Lavoie, Aaron Farnsworth, Michael Rosu-Myles, Carole L Yauk, Jingxin Cao, Gary Van Domselaar, Terry Cyr, Sean (Xuguang) Li. "Unveiling integrated functional pathways leading to enhanced respiratory disease associated with inactivated respiratory syncytial viral vaccine". Health Canada Science Forum, Ottawa, Ontario, Canada, February 2017; ***Oral and Poster Presentation***.

Submitted Abstracts:

1. **Muralidharan A**, Russell M, Larocque L, Gravel C, Li C, Chen W, Cyr T, Lavoie JR, Farnsworth A, Rosu-Myles M, Wang L, Li X. "Targeting CD40 enhances antibody- and CD8-mediated protection against respiratory syncytial virus infection". Immunology 2019, San Diego, CA, USA, May 2019; ***Poster Presentation***.

2. **Muralidharan A**, Russell M, Larocque L, Gravel C, Li C, Chen W, Cyr T, Lavoie JR, Farnsworth A, Rosu-Myles M, Wang L, Li X. "Targeting CD40 enhances antibody- and CD8-mediated protection against respiratory syncytial virus infection". European Congress of Virology, Rotterdam, Netherlands, April 2019; ***Poster Presentation***.